
Facultad de Ciencias
Departamento de Física Teórica

# Phenomenology of a new Supersymmetric Standard Model, the $\mu\nu$SSM

Memoria de Tesis Doctoral presentada para optar
al grado de Doctor en Ciencias Físicas por
**Javier Fidalgo Prieto**

Tesis Doctoral dirigida por el
**Catedrático Carlos Muñoz López**
Miembro del Departamento de Física Teórica U.A.M.
y del Instituto de Física Teórica UAM/CSIC

Madrid, Noviembre 2011

*A mis padres.*
*A Itxaso.*

# Agradecimientos

Cuando terminé la carrera en Valladolid, tenía muy claro que quería hacer un doctorado en Física Teórica pero con el paso del tiempo me he dado cuenta de que realmente no sabía la razón. Me llamaba mucho la atención estudiar ramas de la física que casi no se estudian en la licenciatura pero que, intuitivamente resultan fascinantes. Si a uno le entretiene calcular el tiempo en el que cae un bloque con un cierto coeficiente de rozamiento por una pendiente de 50 grados, estudiar los ladrillos del mundo seguro que resultaría fascinante. Nunca antes había estudiado Física de Partículas, ahora me doy cuenta de que no sabía lo que era pero me llamaba poderosamente la atención. Ahora que ya he aprendido algo, no sé si mucho o poco, sólo sé que he disfrutado mucho aprendiendo.

El Doctorado no ha sido un periodo fácil. Siempre hay momentos de dudas, de muchas dudas, de bloqueos mentales, de desorientación y de angustia. Pero en este momento, terminando mi Tesis Doctoral, al final creo que ha valido la pena.

En primer lugar me gustaría agradecer al Profesor Carlos Muñoz, mi director de Tesis, todas las atenciones que ha tenido conmigo. He aprendido mucha física gracias a su experiencia y me ha apoyado siempre en cualquier cuestión logística, burocrática o académica. Además, el trato personal ha sido inmejorable. Muchas gracias Carlos.

En segundo lugar me gustaría mostrar mi agradecimiento a los dos investigadores con los que he trabajado más directamente, el Doctor Daniel López-Fogliani y el Doctor Roberto Ruiz de Austri. Sin su ayuda, no podría haber escrito esta Tesis. Ha sido un placer trabajar con vosotros, personalmente he estado muy a gusto y además me habeis enseñado el camino para llevar a cabo una investigación científica. Gracias a los dos.

En tercer lugar me gustaría agredecer a todos los miembros del Departamento de Física Teórica de la U.A.M. o del IFT con los que he interaccionado de alguna manera. La verdad es que en este departamento da gusto trabajar. Mención especial para los miembros de la "familia Muñoz", David García Cerdeño, Carlos Yaguna, Ki-Young Choi, Beatriz Cañadas, Nicolas Escudero (gracias por tu ayuda en los momentos difíciles), German Vargas, Miguel Peiró... A los compañeros de los cursos de doctorado y a los compañeros del despacho, Stephan, María, Enrique, Mari Angeles, Tobias (Specka!), Federico y demás, esos partidos de squash con Dani, las comidas con César, Fabrice.. Y sobre todo, de esta peña agradecerle a José Oñorbe su amistad para contarnos nuestras cosillas del día a día y por toda su ayuda cada vez que me atascaba con la informática. Estás tardando en dejar la física y meterte a hacker.

Fuera del microclima de Teórica quiero agredecer antes de nada a mis padres todo lo que me han enseñado, lo bien que me han guiado en la vida y sobre todo el cariño que me han dado. Gracias a ellos he podido terminar esta Tesis porque sabía que estaban ahí detrás, con su apoyo incondicional.

También quiero agredecer a Itxaso estar a mi lado estos años. Has sido mi luz y mi oscuridad a la vez. A ti no hace falta que te diga gran cosa en los agradecimientos porque has estado ahí, día a día.

Y por supuesto, al resto de mi familia. Y a todos los coleguitas que he ido haciendo en la vida, por cruzarnos en ella, codo con codo, cada uno a su manera. Ese Juanito en Madrid-Vichy (siento mucho la pérdida que has tenido en estos años de mi Tesis, hermano), Jaime y todos los demás. A todos los del colegio francés, la lista es larga y no quiero discriminar, nos hemos criado juntos, no hace falta decir más. Mox, Daniel-Guzman, Eli, Eva, Edu, Fraguel y todos los demás compis de pucela (y también en Madrid), aupa la intensidad revolucionaria! A los compis de fuera de Madrid en Madrid (ese Dani, Ivan y toda esa peña), a los compis de la UVA, a los compis de los viajes por el mundo y a todos los demás, vosotros sabeis quienes estais. Simplemente gracias por ser mis colegas y estar ahí.

Bueno pues eso, gracias a todos y allá vamos.

# Contents

# Chapter 1

# Introduction

## 1.1 Introduction

This Thesis is devoted to the study of the most relevant aspects of the phenomenology of a supersymmetric model proposed recently in the literature, the $\mu\nu$SSM [1, 2].

The starting of the Large Hadron Collider (LHC) at CERN represents one of the most historically interesting events in high energy physics, since the laws of nature at the TeV scale will be explored. It is expected that this huge accelerator will be able to verify the only sector of the Standard Model (SM) [3] that has not been already experimentally proven, the Higgs sector, that is reponsible of the generation of masses of the SM particles. In addition, it is also expected that the LHC could find new physics beyond the SM at the TeV scale. There are many reasons to believe that the SM is not the ultimate theory of nature and that physics beyond the SM must exist at some energy scale. One of the main reasons to believe that this new physics should be present at the TeV scale is the so called gauge hierarchy problem [4], a theoretical problem of the SM related to the large hierarchy of energy scales between the electroweak (EW) scale and the Planck scale. As the Higgs is a scalar field, its mass is not protected from quadratically divergent radiative corrections.

Different theories compete for being the new physics that describes nature at the TeV scale. The most popular theory among them is still Supersymmetry [5] (SUSY). Supersymmetry is a symmetry between bosons and fermions that has many interesting theoretical features and nice phenomenological implications. In the phenomenological side, the main feature of SUSY is that each of the SM particles has a supersymmetric partner (with the same quantum numbers but different spin). The addition of these new particles to the

spectrum produces a cancellation of the quadratic divergences of the Higgs mass and solves the gauge hierarchy problem.

Supposing that SUSY would be the correct theory at the TeV scale and that the LHC would detect supersymmetric particles, the next step would be to determine which supersymmetric model is the correct one among the different SUSY models that have been proposed. Thus, it is clear that, from a theoretical/phenomenological point of view, it is very interesting the following question. If Supersymmetry is the correct theory that describes nature at the TeV scale, which is the correct supersymmetric model that is realized in nature? For an interesting discussion about this question see for example [6].

The simplest SUSY model is the Minimal Supersymmetric Standard Model (MSSM) that consists of the direct supersymmetrization of the SM. For a phenomenological SUSY review where the MSSM is extensively treated, see for example [7]. The MSSM is the most studied SUSY model due to its simplicity but this model also presents some theoretical or phenomenological problems that other SUSY models try to solve.

In this Thesis we will study in detail the most relevant phenomenological aspects of a supersymmetric model proposed recently in the literature, the $\mu\nu$SSM [1], that tries to solve problems that are present in other SUSY models, such as the well known $\mu$-problem [8] or the non-implementation of the experimental evidence of neutrino masses [9]. The $\mu\nu$SSM solves these problems in an elegant and minimal way, without adding new particles to the spectrum. The master key of the $\mu\nu$SSM consits of considering right-handed neutrino superfields in the spectrum (that is justified by the experimental fact of non-zero neutrino masses) with a superpotential coupling $\lambda^i \hat{\nu}_i^c \hat{H}_1 \hat{H}_2$. In the EW breaking, the right-handed sneutrinos take Vacuum Expectation Values (VEVs) that generate an effective $\mu$ term naturally of the order of the EW scale solving the $\mu$-problem. This superpotential term is also responsible of the mixing between right-handed neutrinos and neutral Higgsinos. In addition, a neutrino Yukawa coupling in the superpotential is added, $Y_\nu^{ij} \hat{H}_2 \hat{L}_i \hat{\nu}_j^c$, mixing left-handed neutrinos with neutralinos and giving rise to a $10 \times 10$ neutralino mass matrix with an EW scale seesaw structure that, as we will show in this Thesis, is able to reproduce current experimental neutrino data.

The presence of both terms in the superpotential of the $\mu\nu$SSM implies an explicit breaking of R-parity [10] and as a consequence, the phenomenology of the model is very different from the one of the MSSM or other R-parity conserving models. R-parity violation strongly affects the phenomenology at colliders. For example, as the Lightest Supersymmetric Particle (LSP) is not longer stable, in an accelerator experiment it could decay within the detector and that implies that the typical missing-energy SUSY signals would

not longer take place. In addition, since the LSP is not stable, it will be no longer a Dark Matter (DM) candidate. Other DM candidates apart from the lightest neutralino should be analysed in the context of this model, for example the gravitino [11, 12].

In this Thesis we will try to cover an important part of the phenomenological issues of the $\mu\nu$SSM. We will analyse the vacuum structure of the model and the electroweak breaking, focusing our attention on an important and almost unique aspect of this model. The $\mu\nu$SSM opens the possibility of Spontaneous CP Violation (SCPV) at the tree-level.

We will also explore in detail the neutrino sector of the model including CP-violation, both theoretically and numerically in order to understand intuitively how the seesaw mechanism is realized in this model and in order to demonstrate that the $\mu\nu$SSM can accommodate perfectly current neutrino experimental data.

Also, we will study some relevant aspects of the collider phenomenology of the $\mu\nu$SSM in order to find characteristic signatures of the model that could serve to distinguish between the $\mu\nu$SSM and other SUSY models at the LHC. We will provide a general overview of the typical decays that take place in the Higgs sector of the $\mu\nu$SSM and we will find numerically benchmark points where decays that can be considered as genuine of the $\mu\nu$SSM take place.

Besides, we will study the possibility of using a $U(1)$ extension of the gauge group of the $\mu\nu$SSM in order to ensure the stability of the proton without having to appeal to string theory arguments or discrete symmetries. Moreover, this extension can also be used to forbid bilinear terms in the superpotential and to solve a cosmological domain wall problem.

In particular, in Chapter 2 we will explain the motivations of the $\mu\nu$SSM and the reasons to go from the accepted SM of particle physics to SUSY and, once in Supersymmetry, the reasons to go from the simplest SUSY model, the MSSM, to a more complicated one as the $\mu\nu$SSM. In this chapter we will also present the $\mu\nu$SSM and we will briefly explain the main characteristics of the model. We will also provide bibliography where other aspects of the phenomenology of the $\mu\nu$SSM that are not covered in this Thesis have been studied.

In Chapter 3 we will analyse the vacuum structure of the model in the most general case, with complex VEVs. The $\mu\nu$SSM has the nice and very rare feature that is able to break spontaneously CP at the tree-level. We will compute the neutral scalar potential and we will provide the minimization equations. We will find numerically global minima that break spontaneously CP. A complete study of the neutrino sector of the model at the tree-level, both numerically and analitically, is also performed in this chapter, including CP violation in the PMNS matrix [13]. We will explain intuitively how the

seesaw mechanism works in this model and we will show that current neutrino data can be accommodated in the $\mu\nu$SSM, even with a diagonal neutrino Yukawa coupling. This chapter is based on the results published in [14].

In Chapter 4 we will first describe the mixings in the Higgs sector of the $\mu\nu$SSM. Then, we will provide a general overview of the novelties concerning the decays of the Higgs sector of the model compared to other SUSY models. After that, the couplings of Higgses with the Z boson and the sum rules will be computed in order to explain LEP constraints in the context of this model. We will also briefly review the production mechanisms of a Higgs boson at colliders. Then, we will provide benchmark points that have been computed where genuine signals of the $\mu\nu$SSM are expected. Finally, we will comment on the role of the gravitino at colliders. This chapter is based on the results published in [15].

In Chapter 5 we will study the extension of the gauge group of the $\mu\nu$SSM with an extra $U(1)$ symmetry. We will explain in detail the motivations to such an extension. We will analyse the anomaly cancellation conditions in order to find extensions of the $\mu\nu$SSM with the desired features. Once a viable model will be found, we will study the parameter space where a correct electroweak symmetry breaking takes place and where the experimental constraints on the existence of a new gauge boson $Z'$ can be reproduced. This chapter is based on [16].

In Chapter 6 we will present the general conclusions of this work and we will explain the future work that has to be carried out in order to complete the study of such a complex model as the $\mu\nu$SSM.

In Appendix A we will provide the mass matrices of the $\mu\nu$SSM and in Appendix B some relevant Higgs sector couplings.

## 1.2 Introducción

En esta Tesis se van a estudiar los aspectos más relevantes de la fenomenología de un modelo supersimétrico propuesto recientemente en la literatura, el $\mu\nu$SSM [1, 2].

La puesta en marcha del Large Hadron Collider (LHC) en el CERN se puede considerar como uno de los momentos más importantes de la historia de la Física ya que se va a explorar por primera vez la escala de energías del TeV. Se espera que este gran acelerador sea capaz de verificar el único sector del Modelo Estándar (SM) [3] que todavía no ha sido comprobado experimentalmente, el sector de Higgs que es el responsable de la generación de las masas de las partículas del SM. También se espera que el LHC pueda encontrar nueva física más allá del SM a la escala del TeV. Hay muchos argumentos

que indican que el SM no puede ser la teoría última de la naturaleza y que debe haber nueva física más allá del SM en alguna escala de energía. Uno de los argumentos que indican que debe haber nueva física y que además debe aparecer a la escala del TeV es el problema de las jerarquías [4], un problema teórico que presenta el SM relacionado con la enorme distancia en energías entre la escala electrodébil y la escala de Planck. Debido a que el Higgs es un campo escalar, su masa no está protegida de las correcciones radiativas cuadráticamente divergentes.

Existen diversas teorías que compiten por ser la nueva física que describa la naturaleza a la escala del TeV. Probablemente la teoría más estudiada y prometedora sea Supersimetría [5] (SUSY). Supersimetría es una simetría entre bosones y fermiones que tiene muchas implicaciones interesantes tanto a nivel teórico como fenomenológico. Desde el punto de vista de la fenomenología, la principal implicación de SUSY consiste en que cada partícula del SM tiene una compañera supersimétrica (es decir, una partícula con los mismos números cuánticos pero con distinto espín). La inclusión de esas nuevas partículas en el espectro produce la cancelación de las divergencias cuadráticas a la masa del Higgs resolviendo de esta manera el problema de las jerarquías.

Suponiendo que SUSY fuera la teoría correcta a la escala del TeV y que el LHC descubriera partículas supersimétricas, el siguiente paso sería distinguir cuál es, de entre todos los modelos supersimétricos propuestos, el modelo supersimétrico correcto. Por tanto, es evidente que desde un punto de vista teórico y fenomenológico, la cuestión de saber qué modelo supersimétrico describe la realidad, si SUSY es la teoría correcta de la naturaleza a la escala del TeV, es muy importante. Para una interesante discusión sobre este tema se puede consultar por ejemplo [6].

El modelo supersimétrico más sencillo es el Modelo Estándar Supersimétrico Mínimo (MSSM) que consiste en una supersimetrización directa del SM. Para un review fenomenológico de SUSY en el que se trata extensamente el MSSM se puede consultar por ejemplo [7]. El MSSM es el modelo supersimétrico más estudiado debido a su simplicidad pero también presenta algunos problemas fenomenológicos o teóricos que otros modelos supersimétricos tratan de solucionar.

En esta Tesis se van a estudiar en detalle muchos de los aspectos más relevantes de la fenomenología de un modelo supersimétrico que ha sido propuesto recientemente, el $\mu\nu$SSM [1]. Este modelo resuelve dos problemas importantes que presentan otros modelos supersimétricos: el problema $\mu$ [8] y la no implementación de la evidencia experimental de la masa de los neutrinos [9]. El $\mu\nu$SSM resuelve estos dos problemas de una forma elegante y mínima, sin tener que añadir partículas adicionales al espectro aparte de los

supercampos de neutrinos dextrógiros. La clave del $\mu\nu$SSM consiste en añadir neutrinos dextrógiros al espectro (lo que está justificado por la evidencia experimental de la masa de los neutrinos) y un término en el superpotencial $\lambda^i \hat{\nu}_i^c \hat{H}_1 \hat{H}_2$. En la rotura de la simetría electrodébil, los sneutrinos dextrógiros toman Valores Esperados en el Vacío (VEVs) que generan un término $\mu$ efectivo del orden de la escala electrodébil, resolviendo así el problema $\mu$ del MSSM. Este término del superpotencial también produce la mezcla de los neutrinos dextrógiros con los Higgsinos neutros. Como además, en el $\mu\nu$SSM también se añade al superpotencial el acoplo de Yukawa de los neutrinos, $Y_\nu^{ij} \hat{H}_2 \hat{L}_i \hat{\nu}_j^c$, también los neutrinos levógiros se mezclan con los neutralinos de modo que en el $\mu\nu$SSM la matriz de masa de neutralinos es una matriz $10 \times 10$ con la que se puede generar un mecanismo del seesaw a escala EW que, como demostraremos en esta Tesis, puede reproducir todas las medidas experimentales del sector de neutrinos.

La presencia conjunta de ambos términos en el superpotencial del $\mu\nu$SSM viola la simetría R-parity [10] explícitamente por lo que la fenomenología del modelo va a ser muy diferente de la del MSSM u otros modelos con R-parity conservada. La rotura de R-parity puede modificar mucho las señales que se pueden esperar en aceleradores. Por ejemplo, como la LSP no es estable, en experimentos de aceleradores puede decaer dentro del detector por lo que las señales típicas de supersimetría consistentes en energía perdida no se producirían. Además, como la LSP no es estable en este modelo, no puede ser candidata a formar la materia oscura del universo. Por lo tanto, otras partículas que puedan ser candidatas a materia oscura deben ser estudiadas en el $\mu\nu$SSM como por ejemplo, el gravitino [11, 12].

En esta Tesis se tratará de cubrir una parte importante de las cuestiones fenomenológicas del $\mu\nu$SSM. Se analizará el vacío del modelo y la rotura electrodébil. Se estudiará una cuestión importante que distingue al $\mu\nu$SSM de otros modelos supersimétricos, la posibilidad de tener rotura espontánea de CP (SCPV) a nivel árbol.

También se explorará en detalle el sector de neutrinos, incluyendo violación de CP de forma analítica y numérica para entender intuitivamente cómo se realiza el mecanismo del seesaw y para demostrar que el $\mu\nu$SSM puede explicar todas las medidas experimentales del sector de neutrinos.

También se estudiarán algunos aspectos relevantes de la fenomenología del $\mu\nu$SSM en aceleradores para encontrar las señales características que dejaría el modelo en un acelerador de partículas como el LHC y poderlo distinguir de otros modelos supersimétricos. Se presentará una panorámica general de los decaimientos típicos que pueden producirse en el sector de Higgs del $\mu\nu$SSM y se encontrarán numéricamente puntos benchmark en los que se producen decaimientos genuinos del $\mu\nu$SSM.

Asimismo, sin olvidar que en este modelo R-parity está rota, se estudiará la posibilidad de extender el grupo gauge del $\mu\nu$SSM con un factor $U(1)$ para garantizar la estabilidad del protón sin tener que recurrir a argumentos de teoría de cuerdas o simetrías discretas. Además, esta extensión puede usarse para prohibir términos bilineales en el superpotencial y para resolver un problema cosmológico de paredes de dominio.

En concreto, en el Capítulo 2 se explicarán las motivaciones del $\mu\nu$SSM y las razones de pasar del SM a SUSY y una vez en SUSY, el por qué pasar del MSSM a un modelo más complicado como el $\mu\nu$SSM. En este capítulo también se presentará el $\mu\nu$SSM y se explicarán brevemente sus principales características. También se proporcionará bibliografía en la que se estudian aspectos fenomenológicos del $\mu\nu$SSM que no se cubren en esta Tesis.

En el Capítulo 3 se estudiará la estructura del vacío del modelo, en el caso más general, con VEVs complejos. El $\mu\nu$SSM tiene la peculiar característica consistente en que se puede romper espontáneamente CP en el vacío a nivel árbol. Se computará el potencial escalar neutro y las ecuaciones de minimización. Se encontrarán numéricamente soluciones de mínimo que rompan espontáneamente CP. También se realizará un estudio completo del sector de neutrinos a nivel árbol, numérica y analíticamente, incluyendo violación de CP en la matriz PMNS [13]. Se explicará intuitivamente cómo funciona el mecanismo del seesaw en este modelo y se demostrará que el $\mu\nu$SSM es capaz de reproducir los datos experimentales del sector de neutrinos, incluso con un acoplo de Yukawa de neutrinos diagonal mediante un extenso análisis numérico. Este capítulo está basado en los resultados publicados en [14].

En el Capítulo 4 primero se describirán las mezclas en el sector de Higgs del $\mu\nu$SSM. Se dará una visión general de las novedades de los decaimientos que se producen en el sector de Higgs con respecto a otros modelos supersimétricos. Se calcularán los acoplos de los Higgses con el bosón Z y las reglas de sumación para explicar las restricciones que impone LEP en el contexto de este modelo. Se repasarán brevemente los mecanismos de producción de Higgses en colisionadores. Después, se proporcionarán puntos en el espacio de parámetros que han sido calculados, donde se pueden esperar señales genuinas del $\mu\nu$SSM. Finalmente, se comentará el papel que juega el gravitino en aceleradores. Este capítulo está basado en los resultados publicados en [15].

En el Capítulo 5 se estudiará la extensión del grupo gauge del $\mu\nu$SSM con un factor $U(1)$ extra. Se explicarán las razones para extender el grupo gauge y se estudiarán las ecuaciones de cancelación de anomalías para encontrar algún modelo que extienda el $\mu\nu$SSM con las características requeridas. Una vez encontrado un modelo interesante se estudiará el espacio de parámetros de la extensión $U(1)_{\text{extra}}$ del $\mu\nu$SSM para demostrar que hay regiones en las

que se produce una rotura electrodébil correcta y en las que se cumplen las cotas experimentales sobre la existencia de un nuevo bosón gauge $Z'$. Este capítulo está basado en [16].

En el Capítulo 6 se presentarán las conclusiones generales de esta Tesis y se explicarán las líneas de investigación que quedan abiertas y el trabajo futuro para completar el estudio de un modelo tan complejo como el $\mu\nu$SSM.

Finalmente, en el Apéndice A se proporcionarán las matrices de masa del $\mu\nu$SSM y en el Apéndice B algunos acoplos del sector de Higgs relevantes.

# Chapter 2

# Motivations and basics of the $\mu\nu$SSM

In this chapter we will explain the motivations of the $\mu\nu$SSM and the basics of the model. We will also provide bibliography where the $\mu\nu$SSM is studied.

## 2.1 Motivations

In this section we will review the motivations of the $\mu\nu$SSM and the reasons to go from the SM of particle physics to SUSY and from the simplest SUSY model, the MSSM, to the $\mu\nu$SSM.

The SM of particle physics is one of the major successes in the history of physics since it can explain all the phenomena up to the highest energies reached by current accelerators with a huge precision. The SM is a renormalizable quantum field theory based on a gauge symmetry group $SU(3)_C \times SU(2)_L \times U(1)_Y$ that describes with a very high accuracy all the phenomena in an energy range between fractions of eV to about 100 GeV. In spite of the enormous success of the SM describing the sub-TeV physics, there are several arguments that suggest that the SM can not be the ultimate theory of nature. It seems to be an effective theory of other more fundamental theory.

In the simplest version of the SM, neutrinos are massless. However, there are experimental evidences of non-zero neutrino masses [9]. The simplest way to generate neutrino masses is to extend the SM with the addition of right-handed neutrinos to the spectrum with a neutrino Yukawa coupling, $Y_\nu$, of the order $10^{-13}$. However, the magnitude of this coupling seems very unnatural. The seesaw mechanism [17] is then the best motivated way to give masses to neutrinos in the SM. For example in Type I seesaw, right-

handed neutrinos are also added to the SM but not only with Dirac masses, also with Majorana masses. Note that neutrino physics is one of the main motivations for the $\mu\nu$SSM. On the other hand, the observations that lead to the existence of dark matter [18] can not be accounted for in the SM. There is not any particle that could be a candidate for constituing the DM of the universe in the SM and for this reason, it has to be extended.

There are also aesthetic reasons that suggest that the SM is an effective theory of other more fundamental theory. For example, the flavour problem, that means, the non-explanation in the SM of the very different orders of magnitude of the masses of the SM particles and their complicate pattern of mixings. Also, the SM can not explain by itself why the gauge group is $SU(3)_C \times SU(2)_L \times U(1)_Y$ or why the space-time is a 4-dimensional space.

In what concerns the theoretical reasons, the SM can not account for the gravitational force. At least at the Planck scale, where the gravitational effects become relevant, there should be a more fundamental theory to quantize the gravitational field. Moreover, the EW breaking is only explained in the SM through the Higgs mechanism with a potential introduced "by hand". Finally, the gauge hierarchy problem [4] does not only suggest that there should be new physics beyond the SM, but it also implies that new physics should exist at the TeV scale. Therefore, the perspectives of finding this new physics with the LHC are robust.

Different theories are candidates to extend the SM at the TeV scale (each one solves the gauge hierarchy problem in a different way) and could be found at the LHC such as technicolor [19], low energy extra dimensions [20], Little Higgs [21], SUSY... Since this Thesis is devoted to the study of the phenomenology of a SUSY model, we will introduce very briefly the theory of Supersymmetry. To study SUSY in depth, we refer the interested reader to [5].

Supersymmetry is a symmetry that relates bosons and fermions. It was discovered at the very end of the sixties [22] as an interesting mathematical construction but without expectations of applicability to particle physics. When it was proven to solve the gauge hierarchy problem [23], an explosion of interest on SUSY phenomenology begun.

A supersymmetric operator $Q$ is an anticonmuting spinor that converts a bosonic state into a fermionic state and viceversa. Each of the SM particles would have a supersymmetric partner [24] with the same properties (the same quantum numbers, the same mass etc...) but with a spin differing in 1/2. These new degrees of freedom are the responsible of cancelling the quadratic divergences of the Higgs mass and then, the gauge hierarchy problem is solved. Since no supersymmetric particle has been detected yet, supersymmetry has to be broken and SUSY particles should be heavier than

the SM particles. There is not a completed accepted theory of how SUSY is broken, but it has to be broken "softly" for solving the gauge hierarchy problem. Then, at the TeV scale the unknown mechanism that breaks SUSY can be parametrized with soft terms in the Lagrangian.

Supersymmetry has many nice features. First of all, it has been demonstrated that the most general symmetry of the S matrix is the direct product of the SUSY algebra times the internal symmetry group [25]. SUSY solves the gauge hierarchy problem. In contrast with other theories of physics beyond the SM at the TeV scale, SUSY can be extended to the Grand Unified Theory (GUT) scale or to the Planck scale without new physics at intermediate scales. SUSY can also have connections with gravity since promoting SUSY to be a local symmetry instead of a global one, one obtains a theory of gravity called supergravity (SUGRA) [26]. In a spacetime with four dimensions the supergravity theory is not renormalizable but the connection between SUSY and gravity is certainly very interesting. SUSY is also a fundamental ingredient of superstring theory. In addition, the unification of the gauge couplings is much more precise in the MSSM than in the SM. In supersymmetric models with conserved R-parity, the LSP is stable and it is usually the neutralino in most part of the parameter space. Since the neutralino is electrically neutral and colourless, it is an excellent DM candidate and the dark matter relic density can be reproduced [27]. Finally, SUSY provides a much better explanation of the EW breaking than the SM. In the SM, the Higgs potential $V = m^2 H^+ H + \lambda (H^+ H)^2$ (with the free parameter $m^2 < 0$) is introduced by hand. In SUSY, the parameters appearing in the Higgs potential are not free, they depend on the gauge couplings and in many SUSY models, the radiative corrections drive the mass squared parameter to be negative producing the correct EW breaking.

In spite of all these hints that suggest that SUSY could be the correct theory at the TeV scale, supersymmetric models are not free from drawbacks. Obviously, the first argument against SUSY is that no SUSY particle has been detected for the moment. Nevertheless, we hope that the LHC will find them in the near future. Then, if supersymmetry exists at all, it has to be a broken symmetry with SUSY particles heavier than the SM particles. The unknowledge of how SUSY is broken is parametrized at low energy as soft terms that are free parameters in the Lagrangian at the EW scale and represents an explicit breaking of SUSY: mass terms for gauginos and scalars and soft trilinear and bilinear terms. Roughly speaking, these soft terms have to be large enough for not having detected any SUSY particle but small enough to keep the solution of the gauge hierarchy problem. Then, the simplest SUSY model, the MSSM, has 124 free parameters. For reducing the number of free parameters of SUSY models, one can build a theory where SUSY is

broken spontaneously in a hidden sector, being communicated to the visible sector in different ways (gravity mediated SUSY breaking, gauge mediated SUSY breaking etc...) and generating the soft terms that are no longer free parameters. SUSY models suffer other problems such as the $\mu$ problem [8], the possible existence of both baryon and lepton number violating operators that lead to fast proton decay incompatible with the experimental bounds[1], the possible existence of colour or electric charge breaking minima [28], the little hierarchy problem that is other fine-tuning problem related to the LEP bound on the Higgs mass...

Actually, there are not so many supersymmetric standard models in the literature. On the one hand, there are models where R-parity is conserved, the most relevant ones being the MSSM , the NMSSM [2] [29] or the $U(1)$SSM [30, 31]. On the other hand, R-parity breaking models have been also proposed in the literature such as the Bilinear R-parity Violating model (BRpV) [32] or more recently, the $\mu\nu$SSM. If SUSY is discovered in future accelerators, it would be a crucial task to determine which of all the SUSY models is realized in nature.

Let us describe very briefly the simplest SUSY model, the MSSM and the reasons to go to the $\mu\nu$SSM. See for example [7] where the MSSM is extensively described . The MSSM consists of the direct supersymmetrization of the SM, each of the SM particles has a supersymmetric partner, the only exception is that there are two Higgs doublet superfields needed for cancelling the anomalies and for giving masses to all fermions. The superpotential of the MSSM is given by [3]:

$$W = \epsilon_{ab}(Y_u^{ij}\hat{H}_2^b\hat{Q}_i^a\hat{u}_j^c + Y_d^{ij}\hat{H}_1^a\hat{Q}_i^b\hat{d}_j^c + Y_e^{ij}\hat{H}_1^a\hat{L}_i^b\hat{e}_j^c) - \epsilon_{ab}\mu\hat{H}_1^a\hat{H}_2^b \qquad (2.1)$$

The Higgs sector of the MSSM after the EW symmetry breaking is composed of five physical degrees of freedom, two CP-even neutral Higgses $h^0$ and $H^0$, one neutral CP-odd Higgs $A^0$ and two charged Higgses. The other three degrees of freedom are Goldstone bosons that are "eaten" to provide the longitudinal components of the $W$ and $Z$ bosons. In the neutral fermion sector, there are four neutralino states that are the physical linear combinations (the mass eigenstates) of the electroweak neutral gauginos and the neutral Higgsinos. As R-parity is conserved, the LSP is stable. In most of the parameter space of the MSSM the LSP is the lightest neutralino and it is a good DM

[1] In Chapter 5 we present a complete discussion about proton decay in SUSY models since it will be one of the motivations to extend the gauge group of the $\mu\nu$SSM in that chapter.

[2] See Chapter 5 where the key features of the NMSSM are commented.

[3] See [5] for a description of the superfields formulation of SUSY.

candidate since it is electrically neutral and colourless. In addition, the relic density can be fitted in wide regions of the parameter space.

In spite of being the simplest SUSY model, the MSSM suffers from some phenomenological problems such as the $\mu$ problem [8], possible fast proton decay by B and L violating non-renormalizable operators that are not prohibited by R-parity, non-implementation of neutrino masses, the little hierarchy problem... Other SUSY models try to solve some of these problems. For example, the $\mu\nu$SSM solves the $\mu$ problem and accounts for neutrino masses in an elegant way. In addition, the tension with LEP data on Higgs searches is aliviated. In Chapter 5 the proton decay problem will be addressed in the context of the $\mu\nu$SSM introducing an extra $U(1)$ gauge symmetry.

We will also explain in detail the $\mu$ problem in Chapter 5. Very briefly, the last term in Eq. (2.1) is a bilinear term and the $\mu$ parameter has dimension of mass. On one hand this parameter is required by phenomenology to be of the order of the EW scale for the correct EW breaking. On the other hand, since it is a superpotential parameter, it should be of the order of the energy scale up to the theory is valid, for example, the GUT scale or the Planck scale. The $\mu\nu$SSM introduces an effective $\mu$ term with a trilinear superpotential operator $\lambda^i \hat{\nu}_i^c \hat{H}_1 \hat{H}_2$. In this way, there are not dimensional parameters in the superpotential and an effective $\mu$ term naturally of the order of the electroweak scale is generated when the sneutrinos get VEVs. Note that the $\mu\nu$SSM does not introduce extra singlets for this purpose as the NMSSM does. It uses the right-handed neutrino superfields that also serve to generate light neutrino masses.

As mentioned, other problem that suffers the MSSM and that the $\mu\nu$SSM solves is that the MSSM does not account for non-zero neutrino masses. Neutrino experiments [9] have confirmed that neutrinos are massive and for this reason, all models should account for this experimental fact. The trivial extension of the MSSM that accounts for neutrino masses consists of simply adding right-handed neutrinos to the spectrum and a superpotential coupling $Y_\nu^{ij} \hat{H}_2 \hat{L}_i \hat{\nu}_j^c$. The problem is that the neutrino Yukawa coupling should be of the order of $10^{-13}$ to generate light neutrino masses, many orders of magnitude smaller than the electron Yukawa of order $10^{-6}$ or the top Yukawa of order 1. That would complicate more the flavour puzzle. Apart from the trivial extension of the MSSM to give masses to neutrinos, there are at least two more ways in SUSY to generate neutrino masses.

There are models with violation of lepton number in two units $\delta L = 2$. This corresponds to the supersymmetrization [35] of the seesaw mechanism. Right-handed neutrino superfields and two superpotential terms Eq. (2.2) are added. One is a Dirac mass term and the other, a Majorana mass term that is a bilinear operator that conserves R-parity but breaks lepton number

in two units.

$$W_{neutrinos} = Y_\nu^{ij} \hat{H}_2 \hat{L}_i \hat{\nu}_j^c + m_M^{ij} \hat{\nu}_i^c \hat{\nu}_j^c \tag{2.2}$$

The Yukawa coupling determines the Dirac mass $m_D = Y_\nu v_2$. Then, in the interaction basis the neutrino mass matrix has the following block structure:

$$m_{(\nu_L,\nu_R)} = \begin{pmatrix} 0 & m_D \\ m_D & m_M \end{pmatrix}$$

If $m_D << m_M$, both contributions, Dirac and Majorana, induce light neutrino masses of the order $m_\nu \sim m_D^2/m_M$. For example, with a neutrino Yukawa coupling of the order of the top Yukawa coupling $\mathcal{O}(1)$ and a Majorana mass of the order of the GUT scale, that gives rise to neutrino masses of order $10^{-2}$ eV, compatible with the experimental bounds. With a TeV scale seesaw, taking a Majorana mass of order 1 TeV and a neutrino Yukawa coupling of the order of the one of the electron, $\mathcal{O}(10^{-6})$, one can also obtain light neutrino masses compatible with the experimental bounds.

The second way of generating neutrino masses in SUSY consits of allowing lepton number violation by one unit $\delta L = 1$. This way of generating neutrino masses is intrinsically supersymmetric and it is based on the breaking of R-parity. In this case, the relevant energy scale is the electroweak one and it is not necessary to add right-handed neutrinos to the spectrum in order to generate light neutrino masses. One example of this type of models is the BRpV model [32]. This interesting model is based in the addition to the superpotential of the MSSM, Eq. (2.1), a bilinear term $\mu'^i \hat{L}_i \hat{H}_2$. This term violates R-parity and lepton number by one unit. Neutrino masses are generated through the mixing of neutrinos with neutralinos. One mass is generated at the tree-level and the other two masses at the one-loop level [33, 34]. One potential problem of the BRpV model is that the $\mu$ problem is increased since there are three more bilinear terms in the superpotential and three new dimensional parameters $\mu'^i$. For phenomenological reasons they have to be of the order of the EW scale but, since they are superpotential couplings, they are expected to be of the order of the GUT or Planck scale.

As we will explain in detail in Chapter 3, the $\mu\nu$SSM generates neutrino masses in a hybrid way. On the one hand, the superpotential term of the $\mu\nu$SSM $\kappa^{ijk} \hat{\nu}_i^c \hat{\nu}_j^c \hat{\nu}_k^c$ is an effective Majorana mass term when the right-handed sneutrinos take VEVs. On the other hand the violation of R-parity induces the mixing of the left- and right-handed neutrinos with neutralinos and this also contributes to the neutrino masses.

Summarizing, in this section we have presented an overview for going from the SM of particle physics to SUSY. Many arguments suggest that the

SM can not be the ultimate theory of nature. Among these arguments, the hierarchy problem points out that new physics should exist at the TeV scale. Different theories compit to be this new physics accesible at LHC. Supersymmetry is probably the most promising among them. There are many different supersymmetric models and the question of which model is realized in nature if SUSY is the correct theory is highly relevant. The simplest SUSY model is the MSSM but this model presents some phenomenological problems that other models try to solve. The $\mu$ problem and neutrino physics are the main motivations for the $\mu\nu$SSM. Simply adding right-handed neutrinos to the spectrum and allowing the violation of R-parity, non-zero neutrino masses are generated and the $\mu$ problem is solved at the same time. Then, as it is a very well motivated and attractive model, the study of the phenomenology of the $\mu\nu$SSM is highly relevant.

In the rest of this chapter we will describe briefly the main features of the $\mu\nu$SSM before presenting a complete study of different phenomenological issues in the next chapters.

## 2.2 The $\mu\nu SSM$, an overview

In this section we will explain the basics of the SUSY model that we are going to study in detail in this Thesis, the $\mu\nu SSM$ [1]. The most relevant bibliography concerning this model will also be provided. In the following chapters we will treat in detail several phenomenological issues but before that, let us review the main features of the model.

Let us recall that the main motivation of this model is to solve the $\mu$ problem of the MSSM connecting it with neutrino physics. The fact that neutrinos are massive has been confirmed by neutrino experiments [9]. Then, all theoretical models should be extended to reproduce this experimental result.

It is then natural in the context of SUSY to add to the spectrum of the theoretical models, right-handed neutrino superfields $\hat{\nu}_i^c$, $i = 1, 2, 3$. Given the fact that sneutrinos are allowed to get VEVs, the $\mu\nu SSM$ model is based on adding the superpotential term $\lambda^i \hat{\nu}_i^c \hat{H}_1 \hat{H}_2$ in order to produce an effective $\mu$ term given by $\mu_{\text{eff}} \equiv \lambda^i \langle \tilde{\nu}_i^c \rangle$ naturally of the order of the EW scale once the electroweak symmetry is broken, solving the $\mu$ problem of SUSY [8] without adding an extra singlet superfield as in the case of the NMSSM [29]. Thus the "$\mu$ from $\nu$" Supersymmetric Standard Model solves the $\mu$ problem with natural particle content generating at the same time $\nu$ masses in a natural way as we will discuss below.

The superpotential is given by:

$$\begin{aligned} W &= \epsilon_{ab}\,(\,Y_u^{ij}\hat{H}_2^b\hat{Q}_i^a\hat{u}_j^c \;+\; Y_d^{ij}\hat{H}_1^a\hat{Q}_i^b\hat{d}_j^c \;+\; Y_e^{ij}\hat{H}_1^a\hat{L}_i^b\hat{e}_j^c \;+\; Y_\nu^{ij}\hat{H}_2^b\hat{L}_i^a\hat{\nu}_j^c\,) \\ &- \epsilon_{ab}\,\lambda^i\hat{\nu}_i^c\hat{H}_1^a\hat{H}_2^b \;+\; \frac{1}{3}\,\kappa^{ijk}\hat{\nu}_i^c\hat{\nu}_j^c\hat{\nu}_k^c \end{aligned} \tag{2.3}$$

where $\hat{H}_1^T = (\hat{H}_1^0, \hat{H}_1^-)$, $\hat{H}_2^T = (\hat{H}_2^+, \hat{H}_2^0)$, $\hat{Q}_i^T = (\hat{u}_i, \hat{d}_i)$, $\hat{L}_i^T = (\hat{\nu}_i, \hat{e}_i)$, $a, b$ and $i, j, k$ are respectively $SU(2)$ and family indices and $\epsilon_{12} = 1$. Note that in other chapters we will also use the notation $\hat{H}_1^T \equiv \hat{H}_d^T$ and $\hat{H}_2^T \equiv \hat{H}_u^T$. Only trilinear dimensionless terms are allowed in the superpotential. This could be explained with a $Z_3$ symmetry that forbids the bilinear $\mu$ term as is usually done in the NMSSM. Another explanation in favour of the absence of the explicit $\mu$ term arises from the low energy limit of string constructions where only trilinear terms are present in the superpotential. An effective $\mu$ term is generated in the EW breaking and the $\mu$ problem is solved.

The last type of terms in Eq. (2.3), allowed by all symmetries, avoids the presence of an unacceptable axion associated to a global $U(1)$ symmetry. This term also generates effective Majorana masses for neutrinos at the EW scale. In addition, the neutrino Yukawa term generates Dirac masses for neutrinos. Then, an EW-scale seesaw is present in the model and light neutrino masses arise as we will show in Chapter 3. The two last terms in Eq. (2.3) break *explicitly* lepton number and therefore, after spontaneous symmetry breaking, a massless Goldstone boson (Majoron) does not appear.

R-parity is also explicitly broken by these two terms. The size of the breaking can be easily understood realizing that in the limit where $Y_\nu$ are vanishing, the $\hat{\nu}^c$ are ordinary singlet superfields like the $\hat{S}$ of the NMSSM, without any connection with neutrinos, and R-parity is therefore conserved. Once $Y_\nu$ are switched on, the $\hat{\nu}^c$ become right-handed neutrinos, and, as a consequence, R-parity is broken. Thus the breaking is small because the EW-scale seesaw implies small values for $Y_\nu$.

Needless to say, the breaking of R-parity implies that the phenomenology of the model will be very different from the one of the MSSM. The supersymmetric particles have not to be produced in pairs and the LSP is not stable. This fact would produce very different signals of the $\mu\nu SSM$ with respect to models that conserve R-parity in accelerator experiments, avoiding typical missing energy signals of R-parity conserving models if the LSP has sufficiently small lifetime to decay within the detector. The extended Higgs sector of the $\mu\nu$SSM could also lead to different signals in accelerators respect to other SUSY models. These issues will be discussed in Chapter 4.

The lightest neutralino in the $\mu\nu$SSM is no longer a DM candidate but other candidates can be found in the literature such as the gravitino [36, 11],

the axion or other exotic particles [27]. It is also interesting to note that the Yukawa term producing Dirac masses for neutrinos, the fourth term in (2.3), generates three effective bilinear terms $\hat{H}_2\hat{L}_i$ after the electroweak breaking through the VEVs of right-handed sneutrinos and that is what characterizes the BRpV model. In a sense, the BRpV model is contained in the $\mu\nu$SSM. Note that the only scale present in this model is the soft supersymmetric breaking scale. Then, all the known particle physics phenomenology could be reproduced with the presence of only this scale in the Lagrangian.

As we have explained, the superpotential (2.3) has a $Z_3$ symmetry, just like in the NMSSM. We will see in Chapter 5 that one expects to have also a cosmological domain wall problem in this model [37]. Nevertheless, the usual solutions based on non-renormalizable operators [38] will also work. Moreover, we will see in Chapter 5 that other solution to this problem is possible extending the gauge group of the $\mu\nu SSM$ with an extra $U(1)$ symmetry.

Working in the framework of gravity-mediated supersymmetry breaking we will discuss briefly the most relevant aspects of the phenomenology of the $\mu\nu$SSM concerning the EW breaking and the neutralino sector of the model. The soft Lagrangian $\mathcal{L}_{\rm soft}$ is given by:

$$\begin{aligned}
-\mathcal{L}_{\rm soft} &= (m^2_{\tilde{Q}})^{ij}\,\tilde{Q}^{a^*}_i\,\tilde{Q}^a_j + (m^2_{\tilde{u}^c})^{ij}\,\tilde{u}^{c^*}_i\,\tilde{u}^c_j + (m^2_{\tilde{d}^c})^{ij}\,\tilde{d}^{c^*}_i\,\tilde{d}^c_j + (m^2_{\tilde{L}})^{ij}\,\tilde{L}^{a^*}_i\,\tilde{L}^a_j \\
&+ (m^2_{\tilde{e}^c})^{ij}\,\tilde{e}^{c^*}_i\,\tilde{e}^c_j + m^2_{H_1}\,H^{a*}_1\,H^a_1 + m^2_{H_2}\,H^{a*}_2 H^a_2 + (m^2_{\tilde{\nu}^c})^{ij}\,\tilde{\nu}^{c^*}_i\tilde{\nu}^c_j \\
&+ \epsilon_{ab}\Big[(A_uY_u)^{ij}\,H^b_2\,\tilde{Q}^a_i\,\tilde{u}^c_j + (A_dY_d)^{ij}\,H^a_1\,\tilde{Q}^b_i\,\tilde{d}^c_j + (A_eY_e)^{ij}\,H^a_1\,\tilde{L}^b_i\,\tilde{e}^c_j \\
&+ (A_\nu Y_\nu)^{ij}\,H^b_2\,\tilde{L}^a_i\,\tilde{\nu}^c_j + \text{H.c.}\Big] \\
&+ \left[-\epsilon_{ab}(A_\lambda\lambda)^i\,\tilde{\nu}^c_i\,H^a_1H^b_2 + \frac{1}{3}(A_\kappa\kappa)^{ijk}\tilde{\nu}^c_i\tilde{\nu}^c_j\tilde{\nu}^c_k \;+ \text{H.c.}\right] \\
&- \frac{1}{2}\left(M_3\,\tilde{\lambda}_3\,\tilde{\lambda}_3 + M_2\,\tilde{\lambda}_2\,\tilde{\lambda}_2 + M_1\,\tilde{\lambda}_1\,\tilde{\lambda}_1 + \text{H.c.}\right). \qquad (2.4)
\end{aligned}$$

Apart the terms coming from $\mathcal{L}_{\rm soft}$, the tree-level neutral scalar potential receives the usual D and F term contributions. Once the EW symmetry is spontaneously broken, the neutral scalars develop the following VEVs that we take here for simplicity as real:

$$\langle H^0_1\rangle = v_1\,, \quad \langle H^0_2\rangle = v_2\,, \quad \langle\tilde{\nu}_i\rangle = \nu_i\,, \quad \langle\tilde{\nu}^c_i\rangle = \nu^c_i\,. \qquad (2.5)$$

For the moment we only want to demonstrate that the $\mu\nu$SSM can present a correct EW symmetry breaking. As a consequence, for our purposes it is enough to neglect mixing between generations in (2.3) and (2.4), and to assume that only one generation of sneutrinos gets VEVs, $\nu$ and $\nu^c$. The

extension of the analysis to all generations is straightforward and the conclusions are similar. In Chapter 3 we will study in detail the EW breaking of the model in the general case of complex VEVs with all generations.

With this approach, the neutral scalar potential is given by:

$$\begin{aligned}
\langle V_{\rm neutral}\rangle &= \frac{g_1^2+g_2^2}{8}\left(|\nu|^2+|v_1|^2-|v_2|^2\right)^2 \\
&+ |\lambda|^2\left(|\nu^c|^2|v_1|^2+|\nu^c|^2|v_2|^2+|v_1|^2|v_2|^2\right)+|\kappa|^2|\nu^c|^4 \\
&+ |Y_\nu|^2\left(|\nu^c|^2|v_2|^2+|\nu^c|^2|\nu|^2+|\nu|^2|v_2|^2\right) \\
&+ m_{H_1}^2|v_1|^2+m_{H_2}^2|v_2|^2+m_{\tilde{\nu}^c}^2|\nu^c|^2+m_{\tilde{\nu}}^2|\nu|^2 \\
&+ \Big(-\lambda\kappa^* v_1 v_2\nu^{c*2}-\lambda Y_\nu^*|\nu^c|^2 v_1\nu^*-\lambda Y_\nu^*|v_2|^2 v_1\nu^*+kY_\nu^* v_2^*\nu^*\nu^{c2} \\
&- \lambda A_\lambda\nu^c v_1 v_2+Y_\nu A_\nu\nu^c\nu v_2+\frac{1}{3}\kappa A_\kappa\nu^{c3}+\text{H.c.}\Big)\,. \qquad (2.6)
\end{aligned}$$

In the following, we also assume for simplicity that all the parameters appearing in the scalar potential are real. The four minimization conditions with respect to the VEVs $v_1$, $v_2$, $\nu^c$ and $\nu$ can be written as:

$$\begin{aligned}
&\frac{1}{4}(g_1^2+g_2^2)(\nu^2+v_1^2-v_2^2)v_1+\lambda^2 v_1\left(\nu^{c2}+v_2^2\right)+m_{H_1}^2 v_1 \\
-\;&\lambda\nu^c v_2\left(\kappa\nu^c+A_\lambda\right)-\lambda Y_\nu\nu\left(\nu^{c2}+v_2^2\right)=0\,, \\
-\;&\frac{1}{4}(g_1^2+g_2^2)(\nu^2+v_1^2-v_2^2)v_2+\lambda^2 v_2\left(\nu^{c2}+v_1^2\right)-\lambda\nu^c v_1\left(\kappa\nu^c+A_\lambda\right) \\
+\;&m_{H_2}^2 v_2+Y_\nu^2 v_2\left(\nu^{c2}+\nu^2\right)+Y_\nu\nu\left(-2\lambda v_1 v_2+\kappa\nu^{c2}+A_\nu\nu^c\right)=0\,, \\
&\lambda^2\left(v_1^2+v_2^2\right)\nu^c+2\kappa^2\nu^{c3}+m_{\tilde{\nu}^c}^2\nu^c-2\lambda\kappa v_1 v_2\nu^c-\lambda A_\lambda v_1 v_2+\kappa A_\kappa\nu^{c2} \\
+\;&Y_\nu^2\nu^c\left(v_2^2+\nu^2\right)+Y_\nu\nu\left(-2\lambda\nu^c v_1+2\kappa v_2\nu^c+A_\nu v_2\right)=0\,, \\
&\frac{1}{4}(g_1^2+g_2^2)(\nu^2+v_1^2-v_2^2)\nu+m_{\tilde{\nu}}^2\nu \\
+\;&Y_\nu^2\nu\left(v_2^2+\nu^{c2}\right)+Y_\nu\left(-\lambda\nu^{c2}v_1-\lambda v_2^2 v_1+\kappa v_2\nu^{c2}+A_\nu\nu^c v_2\right)=0\,. \qquad (2.7)
\end{aligned}$$

As we will see in Chapter 3 where we study in detail the neutrino sector of this model, the VEV of the left-handed sneutrino $\nu$ is in general small to reproduce the small neutrino masses. This fact has also been discussed in the context of R-parity breaking models with extra singlets [39]. Notice that in the last equation in (2.7) when $Y_\nu \to 0$ it happens that $\nu \to 0$, and since the Yukawa coupling $Y_\nu$ determines the Dirac mass for the neutrinos ($m_D \equiv Y_\nu v_2$), it has to be very small and as a consequence, also $\nu$ has to be very small. This also implies that we can approximate the other three

minimization equations as follows:

$$\begin{aligned}
&\frac{1}{2}M_Z^2\cos 2\beta+\lambda^2\left(\nu^{c2}+v^2\sin^2\beta\right)+m_{H_1}^2-\lambda\nu^c\tan\beta\left(\kappa\nu^c+A_\lambda\right)=0\,,\\
&-\frac{1}{2}M_Z^2\cos 2\beta+\lambda^2\left(\nu^{c2}+v^2\cos^2\beta\right)+m_{H_2}^2-\lambda\nu^c\cot\beta\left(\kappa\nu^c+A_\lambda\right)=0\,,\\
&\lambda^2v^2+2\kappa^2\nu^{c2}+m_{\tilde{\nu}^c}^2-\lambda\kappa v^2\sin 2\beta-\frac{\lambda A_\lambda v^2}{2\nu^c}\sin 2\beta+\kappa A_\kappa\nu^c\ =0\,,
\end{aligned}\tag{2.8}$$

where $\tan\beta\equiv v_2/v_1$, $2M_W^2/g_2^2=v_1^2+v_2^2+\nu^2\approx v_1^2+v_2^2\equiv v^2$, and we have neglected terms proportional to $Y_\nu$. The equations in (2.8) are identical to the minimization conditions of the NMSSM with the substitution $\nu^c\leftrightarrow s$. As it is well known, the NMSSM presents a correct EW breaking and many solutions of the minimization equations can be found in the parameter space. Then, we can conclude that the $\mu\nu$SSM also presents a correct EW symmetry breaking in a significant region of the parameter space

Once we know that solutions of the minimization equations are available, we turn our attention to the neutralino sector. This sector is highly relevant in the $\mu\nu$SSM since neutrino physics arises from it as we will show in detail in Chapter 3. The breaking of R-parity produces new mixings between particles. In particular, concerning the neutral fermion sector, neutral gauginos and Higgsinos are mixed with left- [4] and right-handed neutrinos [5]. Then, the four neutralino states of the MSSM are augmented with the six new states of left- and right-handed neutrinos giving rise to a $10\times 10$ neutralino mass matrix. As we will explain in detail in Chapter 3, three of the ten eigenstates of the neutralino mass matrix can be very light and the masses can be compatible with current neutrino experimental data. The other seven eigenstates are heavy and mainly composed of the four neutralinos of the MSSM and the three right-handed neutrinos. In order to explain intuitively this fact, we come back to the approximation of only one generation of sneutrinos taking VEVs and no mixing between generations. In this approximation, the neutralino mass matrix would be a $6\times 6$ mass matrix and one has to ensure that one eigenvalue has to be very light. In the weak interaction basis defined by ${\Psi^0}^T\equiv\left(\tilde{B}^0=-i\tilde{\lambda}',\tilde{W}_3^0=-i\tilde{\lambda}_3,\tilde{H}_1^0,\tilde{H}_2^0,\nu^c,\nu\right)$, the neutral fermion mass terms in the Lagrangian are $\mathcal{L}_{\rm neutral}^{\rm mass}=-\frac{1}{2}(\Psi^0)^T\mathcal{M}_{\rm n}\Psi^0+{\rm H.c.}$, with $\mathcal{M}_n$ given

[4] From the superpotential term $Y_\nu^{ij}\hat{H}_2^b\hat{L}_i^a\hat{\nu}_j^c$, when the right-handed sneutrinos take VEVs, effective bilinear terms as the ones of the BRpV are generated and produce the mixing of left-handed neutrinos with Higgsinos.

[5] From the superpotential term $\lambda_i\hat{\nu}_i^c\hat{H}_1^a\hat{H}_2^b$, right-handed neutrinos mix with the MSSM neutralinos in the same way as the singlino of the NMSSM mix with the MSSM neutralinos.

by:

$$\mathcal{M}_{\rm n} = \begin{pmatrix} M & m \\ m^T & 0 \end{pmatrix}, \tag{2.9}$$

where

$$M = \begin{pmatrix} M_1 & 0 & -M_Z \sin\theta_W \cos\beta & M_Z \sin\theta_W \sin\beta & 0 \\ 0 & M_2 & M_Z \cos\theta_W \cos\beta & -M_Z \cos\theta_W \sin\beta & 0 \\ -M_Z \sin\theta_W \cos\beta & M_Z \cos\theta_W \cos\beta & 0 & -\lambda\nu^c & -\lambda v_2 \\ M_Z \sin\theta_W \sin\beta & -M_Z \cos\theta_W \sin\beta & -\lambda\nu^c & 0 & -\lambda v_1 + Y_\nu \nu \\ 0 & 0 & -\lambda v_2 & -\lambda v_1 + Y_\nu \nu & 2\kappa\nu^c \end{pmatrix}. \tag{2.10}$$

Note that $M$ is very similar to the neutralino mass matrix of the NMSSM (substituting $\nu^c \leftrightarrow s$ and neglecting the small contributions $Y_\nu \nu$), and $m$ is given by:

$$m^T = \begin{pmatrix} -\frac{g_1 \nu}{\sqrt{2}} & \frac{g_2 \nu}{\sqrt{2}} & 0 & Y_\nu \nu^c & Y_\nu v_2 \end{pmatrix}. \tag{2.11}$$

Matrix (2.9) is a matrix of the seesaw type that gives rise to a very light eigenvalue if the entries of the matrix $M$ are much larger than the entries of the matrix $m$. This is the case since the entries of the matrix $M$ are of the order of the EW scale, but the entries of $m$ are much smaller since they are proportional either to $\nu$ or to $Y_\nu$. It can be checked numerically that using typical EW scale values for the entries of $M$ and a Dirac mass $Y_\nu v_2 \simeq 10^{-4}$ GeV one obtains that the lightest eigenvalue of (2.9) is of order $10^{-2}$ eV. Thus, it is clear with these intuitive and rough arguments that the $\mu\nu$SSM is able to generate light neutrino masses. The complete discussion where we analyse numerically the full $10 \times 10$ neutralino mass matrix (taking into account all three generations of neutrinos) is placed in Chapter 3 where we show that current experimental neutrino data can be accommodated in a wide portion of the parameter space of the $\mu\nu$SSM, even with a diagonal neutrino Yukawa coupling. Also in this chapter we will provide a complete explanation of how the seesaw mechanism works in this model, including also phases coming from complex VEVs and studying CP-violation in the lepton sector.

The breaking of R-parity in this model does not affect only to the neutralino sector but also to the chargino sector or to the scalar sector.

As it can be checked in [40], the MSSM charginos mix with the charged leptons giving rise to a $5 \times 5$ chargino mass matrix. In a basis where $\Psi^{+T} = (-i\tilde{\lambda}^+, \tilde{H}_u^+, e_R^+, \mu_R^+, \tau_R^+)$ and $\Psi^{-T} = (-i\tilde{\lambda}^-, \tilde{H}_d^-, e_L^-, \mu_L^-, \tau_L^-)$, one obtains the matrix

$$-\frac{1}{2}(\psi^{+T}, \psi^{-T}) \begin{pmatrix} 0 & M_C^T \\ M_C & 0 \end{pmatrix} \begin{pmatrix} \psi^{+T} \\ \psi^{-T} \end{pmatrix}, \tag{2.12}$$

where

$$M_C = \begin{pmatrix} M_2 & g_2 v_u & 0 & 0 & 0 \\ g_2 v_d & \lambda_i \nu_i^c & -Y_{e_{i1}} \nu_i & -Y_{e_{i2}} \nu_i & -Y_{e_{i3}} \nu_i \\ g_2 \nu_1 & -Y_{\nu_{1i}} \nu_i^c & Y_{e_{11}} v_d & Y_{e_{12}} v_d & Y_{e_{13}} v_d \\ g_2 \nu_2 & -Y_{\nu_{2i}} \nu_i^c & Y_{e_{21}} v_d & Y_{e_{22}} v_d & Y_{e_{23}} v_d \\ g_2 \nu_3 & -Y_{\nu_{3i}} \nu_i^c & Y_{e_{31}} v_d & Y_{e_{32}} v_d & Y_{e_{33}} v_d \end{pmatrix} . \tag{2.13}$$

Anyway, the mixing between the $2 \times 2$ block relative to the MSSM charginos and the $3 \times 3$ block of the SM leptons is small since the off-diagonal blocks are proportional to either $\nu$ or to $Y_\nu$ that are much smaller than the electroweak entries of the diagonal blocks. For this reason, this mixing can be safely neglected for practical purposes.

The Higgs sector is also extended in the $\mu\nu$SSM because of the breaking of R-parity that gives rise to the mixing of the neutral Higgses with the sneutrinos and to the mixing of the charged Higgses with the charged sleptons. The complete full mass matrices of the CP-even neutral scalars, CP-odd neutral scalars, charged scalars and squarks can be checked in [40] or in Appendix A of this Thesis. The Higgs sector will be studied in detail in Chapter 4 . Here, let us only mention that in the $\mu\nu$SSM, there are eight CP-even neutral scalar states, seven (once the Goldstone boson is rotated away) CP-odd neutral scalar states and seven charged scalar states. As we will see in Chapter 4, such an extended Higgs sector could lead to characteristic signals of the $\mu\nu$SSM [15], different from other SUSY model signals in Higgs searches at colliders.

We refer to the interested reader to [40] for checking the Renormalization Group Equations (RGEs) of the superpotential couplings and VEVs. Other relevant phenomenological issues about the $\mu\nu$SSM can be found in [40], such as the relevant couplings involved in the computation of the one-loop radiative corrections to the scalar potential tadpoles and to the CP-even scalar masses. The parameter space of the $\mu\nu$SSM is also studied there in order to find regions avoiding the existence of false minima and tachyons as well as imposing the perturbativity (Landau pole condition) on the couplings of the model. This study of the correct electroweak symmetry breaking with real VEVs as well as the Landau pole conditions allows to put constraints in the parameter space of the model. For example, assuming a GUT in a typical scale of $10^{16}$ GeV, the perturbativity of the couplings imposes that $\lambda_i \leq 0.4$ and if the tensor $\kappa_{ijk}$ is taken diagonal and universal with $\kappa_{iii} \simeq \kappa$, there is a bound $\kappa \leq 0.6$. These bounds based on the Landau pole constraints do not differ significantly from the NMSSM ones. The upper bound on the lightest Higgs mass is also discussed in [40]. Taking into account the one-loop corrections to the lightest Higgs mass, the upper bound in the $\mu\nu$SSM, similarly

to the NMSSM [41, 42], is around 140 GeV for $\tan\beta = 2$. We will treat with more detail this subject of the bound on the lightest Higgs mass in Chapter 5.

In the following, relevant bibliography concerning the $\mu\nu$SSM will be provided.

The original paper that proposes the $\mu\nu$SSM in the literature as a solution of the $\mu$ problem, taking into account neutrino masses at the same time, can be found in [1]. From then on, several phenomenological studies of this model have been performed.

In [40] the parameter space of the $\mu\nu$SSM is extensively analysed putting special attention on constraints arising from the correct electroweak symmetry breaking, avoiding false minima, tachyonic states and Landau poles in the parameters. The structure of the mass matrices and the associated particle spectrum were also computed mainly focusing on the mass of the lightest Higgs boson. Other interesting issues as the RGEs of the superpotential couplings and of the VEVs are also discussed.

In [43] the neutrino sector of the model is explored at the tree-level. Neutrino masses and mixing angles are discussed and it is shown that the $\mu\nu$SSM can reproduce the experimental neutrino data even with diagonal neutrino Yukawa couplings in a significant region of the parameter space. Also, the decays of the lightest neutralino to two body (W-lepton) final states are studied. The correlations of the decay branching ratios of the LSP with the neutrino mixing angles were studied as another possible test of the $\mu\nu$SSM at the LHC.

The phenomenology of the neutrino sector of the $\mu\nu$SSM and the decays of the lightest neutralino were also studied in [44, 45], particularized for the case of only one and two generations of right-handed neutrino superfields and taking into account all possible final states when studying the decays of the lightest neutralino. Possible signatures that might allow to distinguish experimentally this model from other R-parity breaking models were briefly discussed in [43, 44].

In [14] the analysis of the vacua of the $\mu\nu$SSM presented in [40] is completed, studying Spontaneous CP Violation (SCPV) of the tree-level neutral scalar potential and demonstrating that in general, the minimum of the scalar potential with real parameters has complex VEV solutions. In particular, CP violation in the leptonic sector is explored and it is shown how phases for the tree-level PMNS matrix [13] may arise due to the phases of the complex VEVs. The neutrino sector is also analysed at the tree-level both analitically and numerically and the seesaw mechanism in the $\mu\nu$SSM is discussed in an intuitive way, including also phases. In Chapter 3 we will present the results of this paper in order to study in detail the neutrino sector of the $\mu\nu$SSM

and its vacua.

The full effect of one-loop contributions to the neutrino mass matrix in the $\mu\nu$SSM has been analysed in [46], showing that current three flavour global neutrino data for both the tree-level and the one-loop corrected analysis can be accommodated in the $\mu\nu$SSM.

In [15] the Higgs sector of the $\mu\nu$SSM has been analysed in detail, with special emphasis in possible signals at colliders. The mixings of the Higgs sector and mechanisms to suppress them have been described. After a general overview of the production and decays of the Higgses, decays that are genuine of the $\mu\nu$SSM and could serve to distinguish this model from other SUSY models have been studied. Viable benchmark points for LHC searches have been provided. In Chapter 4 we will present the results of this paper in order to study in detail the Higgs sector of the model and possible signals at colliders. Also in [47] the collider phenomenology of the Higgs sector of the $\mu\nu$SSM has been studied predicting an unusual signal.

In [16] the extension of the gauge group of the $\mu\nu$SSM with an extra $U(1)$ factor is studied. In Chapter 5 we will present the results.

Let us also mention that superpotential terms of the $\mu\nu$SSM such as $\hat{\nu}^c\hat{H}_d\hat{H}_u$ and $\hat{\nu}^c\hat{\nu}^c\hat{\nu}^c$ were also analysed as sources of the observed Baryon Asymmetry of the Universe (BAU) [48] and of neutrino masses and tribimaximal mixing [49] respectively.

In [11, 12] the implications of gravitino dark matter in the $\mu\nu$SSM have been studied. Since the lifetime of the gravitino in this model becomes much longer than the age of the universe, it is a natural candidate for DM. In these works the prospects for detecting gamma rays from decaying gravitinos in the galactic halo and extragalactic objects such as the Virgo cluster are analysed. In particular, the Fermi-LAT telescope could detect monochromatic gamma-ray lines produced in a two-body decay of gravitinos. It is found that a gravitino with a mass range of $0.6 - 2$ GeV, and with a lifetime range of about $3 \times 10^{27} - 2 \times 10^{28}$ $s$ would be detectable by the Fermi-LAT with a signal-to-noise ratio larger than $3\sigma$. It is also obtained that gravitino masses larger than about 4 GeV are already excluded in the $\mu\nu$SSM by Fermi-LAT data of the galactic halo.

In [50] it is pointed out that the $\mu\nu$SSM does not allow a conventional thermal leptogenesis mechanism due to the low-energy scale seesaw present in the model. Then, it is shown that electroweak baryogenesis may be a promising way to create the observed BAU. A region of the parameter space of the $\mu\nu$SSM where the electroweak phase transition is sufficiently strongly first order to realize electroweak baryogenesis is identified. Given the fact that the $\mu\nu$SSM is one of the few supersymmetric models with a TeV scale seesaw mechanism accesible at present and future colliders, it is encouraging

that the model has a good chance at being consistent with the observed BAU.

Finally, for a recent general review of the $\mu\nu$SSM, the interested reader can see [51].

Summarizing, in this Chapter we have explained the motivations for going from the SM of particle physics to the $\mu\nu$SSM. We have also introduced the $\mu\nu$SSM and we have reviewed the basics of the model. From now on we will begin to study in detail the most relevant aspects of the phenomenology.

# Chapter 3

# Neutrino physics and SCPV in the $\mu\nu$SSM

In this chapter we will study the vacuum of the $\mu\nu$SSM in the general case, with complex VEVs, and the neutrino sector. It is based on the results published in [14]. We want to prove that in this model it is possible to break CP spontaneously (SCPV) at the tree-level and that the vacuum of this model is in general complex. We also want to discuss the neutrino sector of the model in the general case of CP-violation in the lepton sector. We will show how complex vacua can generate CP violating phases in the PMNS matrix.

First of all, in Section 3.1 we will describe the motivations and the most relevant features of breaking CP spontaneously. After this, in Section 3.2 we will prove intuitively that the $\mu\nu SSM$ can break CP spontaneously and we will calculate the scalar potential and minimization equations with complex VEVs of the $\mu\nu SSM$. In Section 3.3 we will examine the seesaw mechanism as the origin of neutrino masses and mixing angles in the model. We will prove that current experimental neutrino data can be fitted even with a diagonal neutrino Yukawa matrix. We will provide an intuitive explanation of how the seesaw mechanism works in this model and we will present analytical approximate formulas of the effective neutrino mass matrix. In Section 3.4 we will present our numerical results. Within the parameter space of the model, we will search numerically for global minima of the $\mu\nu SSM$ that break CP spontaneously. Using these CP violating minima we will analyse numerically the neutrino sector of the model ensuring that the experimental constraints on the neutrino sector are accomplished. As a consequence of SCPV, we will show that the PMNS matrix is in general complex with non-zero Dirac and Majorana CP phases. Note that the analysis of the neutrino sector is general, the case with real VEVs being a particular case of the general one

with complex VEVs. Finally, in Section 3.5 we will present some relevant comments and in Section 3.6 the conclusions of this chapter.

## 3.1 Motivations

We have already discussed that one of the main motivations of the $\mu\nu$SSM is to account for the experimental evidence of non-zero neutrino masses. The explicit breaking of R-parity in this model produces the mixing of neutralinos with left- and right-handed neutrinos. As a consequence, a generalized matrix of the seesaw type arises and gives rise at the tree-level to three light eigenvalues corresponding to neutrino masses. We will show that in the neutrino sector, the experimental constraints can be reproduced even with a diagonal neutrino Yukawa coupling. The neutrino sector of the $\mu\nu$SSM has been analysed in several works [43, 44, 14, 46]. In this chapter we want to analyse in detail the neutrino sector of the model following the guide of the work performed in [14].

On the other hand, we want to prove that in general, the vacuum of the $\mu\nu$SSM is complex, completing the analysis of the vacuum started in [40]. With these complex vacua we will analyse the neutrino sector of the model and show how CP violation in the leptonic sector arises as a consequence of SCPV. The analysis of the neutrino sector is general, the real vacuum case being a particular case of the complex one.

Let us recall that, although there is evidence for CP violation in the quark sector of the SM, there are not experimental traces of it in the leptonic part. CP can be explicitly broken through complex parameters in the Lagrangian or it can be broken spontaneously in a CP conserving Lagrangian (e.g. with all the parameters being real) through complex VEVs in what is called SCPV. Although the SM as well as the MSSM do not allow for SCPV, in more complicated models both sources of CP violation, complex parameters and complex VEVs, could be present.

Concerning the quark sector, a recent study argues that the Cabibbo-Kobayashi-Maskawa (CKM) matrix is likely complex [52]. This conclusion is supported by the measurement of the unitarity triangle angle $\gamma$ by BaBar and Belle collaborations [53, 54]. This evidence of a complex CKM matrix has ruled out NMSSM-like models with SCPV (see e.g. [55]) for being the entire source of CP violation in the quark sector, since the CKM matrix in such models is real. Thus complex parameters are necessary in the quark sector. Given the structure of the $\mu\nu$SSM, this fact also holds for this model. On the other hand, for the lepton sector, we will show that CP violating phases for the PMNS matrix could arise through SCPV in the $\mu\nu$SSM.

One argument in favor of the presence of SCPV at the Lagrangian level is that, if the determinant of the quark mass matrix is real, it leads to a solution to the strong CP problem [56]. Extensions of the MSSM having this property, have been extensively studied in the literature (see e.g. [57]). In those scenarios, the quark sector of the model is extended in such a way that the effective $3 \times 3$ CKM matrix is complex whereas the determinant of the quark mass matrix is real.

Other works have extended the Higgs sector of the models, leading to SCPV with a complex CKM matrix [58]. Last but not least, in supersymmetric models with both CP and Peccei-Quinn symmetries, SCPV can be used as a solution to the SUSY phase problem [59].

Regarding extensions of the $\mu\nu$SSM, the SCPV scenario with a complex CKM matrix can be accomplished by adding two more families of Higgs doublets. In this case the model would contain three families of matter and Higgs fields. This possibility is well motivated phenomenologically, since the potential problem of flavour changing neutral currents can be avoided [60]. In addition, having three Higgs families is favored in some string scenarios [61]. Indeed, extensions of the quark sector of the model can also be studied, without altering the results here presented. In Chapter 5 we will present a $U(1)_{extra}$ extension of the $\mu\nu$SSM with exotic quarks added to the spectrum for cancelling the anomaly equations associated to the $U(1)_{extra}$. These exotic quarks couple with the SM quarks and could transmit the CP violating phases of the VEVs to the CKM matrix. This model could serve as a starting point to obtain a SUSY model with SCPV and with a complex CKM matrix. For more details, see Subsection 5.2.1.

In this work we just want to point out that SCPV is possible at the tree-level in the simplest version of the $\mu\nu$SSM, i.e. with only one family of Higgs doublets, and therefore it is worth studying its consequences.

## 3.2 Complex VEVs in the $\mu\nu SSM$

Let us remember the superpotential of the $\mu\nu SSM$. The notation and the description of the various terms has already been introduced in Chapter 2.

$$\begin{aligned} W = & \sum_{a,b} \sum_{i,j} \left[ \epsilon_{ab} \left( Y_{u_{ij}} \hat{H}_u^b \hat{Q}_i^a \hat{u}_j^c + Y_{d_{ij}} \hat{H}_d^a \hat{Q}_i^b \hat{d}_j^c + Y_{e_{ij}} \hat{H}_d^a \hat{L}_i^b \hat{e}_j^c + Y_{\nu_{ij}} \hat{H}_u^b \hat{L}_i^a \hat{\nu}_j^c \right) \right] \\ & - \sum_{a,b} \sum_{i} \epsilon_{ab} \lambda_i \hat{\nu}_i^c \hat{H}_d^a \hat{H}_u^b + \sum_{i,j,k} \frac{1}{3} \kappa_{ijk} \hat{\nu}_i^c \hat{\nu}_j^c \hat{\nu}_k^c \,, \end{aligned} \tag{3.1}$$

It consists of Yukawa terms, including the one for neutrinos, an effective $\mu$ term with the dimensionless vector coupling $\lambda$ and an effective Majorana mass term for neutrinos with the totally symmetric tensor $\kappa$. Working in the framework of gravity mediated supersymmetry breaking, the soft terms appearing in the Lagrangian $\mathcal{L}_{soft}$ are given by:

$$\begin{aligned}
-\mathcal{L}_{\text{soft}} &= \sum_{i,j}\left[\sum_a m^2_{\tilde{Q}_{ij}}\,\tilde{Q}^{a\,*}_i\,\tilde{Q}^a_j + m^2_{\tilde{u}^c_{ij}}\,\tilde{u}^{c\,*}_i\,\tilde{u}^c_j + m^2_{\tilde{d}^c_{ij}}\,\tilde{d}^{c\,*}_i\,\tilde{d}^c_j + \sum_a m^2_{\tilde{L}_{ij}}\,\tilde{L}^{a\,*}_i\,\tilde{L}^a_j\right.\\
&+ \left. m^2_{\tilde{e}^c_{ij}}\,\tilde{e}^{c\,*}_i\,\tilde{e}^c_j + m^2_{\tilde{\nu}^c_{ij}}\,\tilde{\nu}^{c\,*}_i\tilde{\nu}^c_j\right]\\
&+ \sum_a\left[m^2_{H_d}\,H^{a*}_d\,H^a_d + m^2_{H_u}\,H^{a*}_u H^a_u\right]\\
&+ \sum_{a,b}\sum_{i,j}\epsilon_{ab}\left[(A_uY_u)_{ij}\,H^b_u\,\tilde{Q}^a_i\,\tilde{u}^c_j + (A_dY_d)_{ij}\,H^a_d\,\tilde{Q}^b_i\,\tilde{d}^c_j\right.\\
&+ \left.(A_eY_e)_{ij}\,H^a_d\,\tilde{L}^b_i\,\tilde{e}^c_j + (A_\nu Y_\nu)_{ij}\,H^b_u\,\tilde{L}^a_i\,\tilde{\nu}^c_j + \text{c.c.}\right]\\
&+ \left[-\sum_{a,b}\sum_i\epsilon_{ab}(A_\lambda\lambda)_i\,\tilde{\nu}^c_i\,H^a_dH^b_u + \sum_{ijk}\frac{1}{3}(A_\kappa\kappa)_{ijk}\,\tilde{\nu}^c_i\tilde{\nu}^c_j\tilde{\nu}^c_k\ + \text{c.c.}\right]\\
&- \frac{1}{2}\left(M_3\,\tilde{\lambda}_3\,\tilde{\lambda}_3 + M_2\,\tilde{\lambda}_2\,\tilde{\lambda}_2 + M_1\,\tilde{\lambda}_1\,\tilde{\lambda}_1 + \text{c.c.}\right). \qquad (3.2)
\end{aligned}$$

In the following we will suppose that CP is a good symmetry of the model, taking all the parameters in the neutral scalar potential real and assuming that CP is only violated by the complex VEVs of the scalar fields. Then, once the electroweak symmetry is spontaneously broken, the neutral scalars develop in general the following complex VEVs:

$$\langle H^0_d\rangle = e^{i\varphi_{v_d}}\,v_d\,,\quad \langle H^0_u\rangle = e^{i\varphi_{v_u}}\,v_u\,,\quad \langle\tilde{\nu}_i\rangle = e^{\varphi_{\nu_i}}\,\nu_i\,,\quad \langle\tilde{\nu}^c_i\rangle = e^{\varphi_{\nu^c_i}}\,\nu^c_i\,. \quad (3.3)$$

There are eight complex VEVs but only seven independent physical phases since the phase of $\langle H^0_d\rangle$ can always be rotated away. We define the seven physical phases as:

$$\varphi_v = \varphi_{v_u} + \varphi_{v_d}\ ,\ \chi_i = \varphi_{\nu_i} + \varphi_{v_u}\ ,\ \varphi_{\nu^c_i}. \qquad (3.4)$$

First of all, we want to calculate the tree-level neutral scalar potential of the $\mu\nu SSM$ with complex VEVs.

Let us remind that the scalar potential is the sum of three contributions, F-terms, D-terms and soft terms:

$$V^0 = V_F + V_D + V_{\text{soft}}. \qquad (3.5)$$

All these contributions have been computed in [14]. The part coming from soft terms can be calculated from the expression of the soft Lagrangian (3.2) replacing the fields by the VEVs, using tensor algebra and is given by:

$$\begin{aligned} V_{\rm soft} &= m_{H_d}^2 v_d v_d + m_{H_u}^2 v_u v_u + \sum_{i,j} m_{\tilde{L}_{ij}}^2 \,\nu_i\,\nu_j \cos(\chi_i - \chi_j) \\ &+ \sum_{i,j} m_{\tilde{\nu}_{ij}^c}^2 \nu_i^c \nu_j^c \cos(\varphi_{\nu_i^c} - \varphi_{\nu_j^c}) - 2\sum_i (A_\lambda \lambda)_i \nu_i^c v_d v_u \cos(\varphi_v + \varphi_{\nu_i^c}) \\ &+ \sum_{i,j,k} \frac{2}{3} (A_\kappa \kappa)_{ijk} \nu_i^c \nu_j^c \nu_k^c \cos(\varphi_{\nu_i^c} + \varphi_{\nu_j^c} + \varphi_{\nu_k^c}) \\ &+ 2\sum_{i,j} (A_\nu Y_\nu)_{ij} v_u \nu_i \nu_j^c \cos(\chi_i + \varphi_{\nu_j^c}). \end{aligned} \tag{3.6}$$

The D-term contribution to the scalar potential of a supersymmetric theory is the following: $V_D = \frac{1}{2} D^a D^a$ where

$$D^a = -g^2 \sum_{i=1}^{n} \rho_i^* T_i^a \rho_i \tag{3.7}$$

and the sum is over all the superfields of the model, $\rho_i$ are the scalar components of these superfields and $T_i^a$ are the generators of the gauge group.

If we proceed with the computation of $V_D$ in this model and with the help of tensor algebra we find the following contribution to the neutral scalar potential:

$$V_D = \frac{G^2}{8} \left( \sum_i \nu_i \nu_i + v_d v_d - v_u v_u \right)^2, \tag{3.8}$$

with $G^2 \equiv g_1^2 + g_2^2$.

Finally, the contribution of F-terms to the scalar potential of a supersymmetric theory is given by the general formula $V_F = \sum_{i=1}^{n} \mid F_i \mid^2$ where $F_i$ are the auxiliary components of the superfields and the sum extends over all the superfields of the model considered. Computing this for the $\mu\nu SSM$ with the help of tensor algebra, we find the following contribution to the neutral

scalar potential:

$$
\begin{aligned}
V_F &= \sum_i (\lambda_i)^2 v_d^2 v_u^2 + \\
&+ \sum_{i,j} \lambda_i \lambda_j v_d^2 \nu_i^c \nu_j^c \cos(\varphi_{\nu_i^c} - \varphi_{\nu_j^c}) + \sum_{i,j} \lambda_i \lambda_j v_u^2 \nu_i^c \nu_j^c \cos(\varphi_{\nu_i^c} - \varphi_{\nu_j^c}) \\
&+ \sum_{i,j,k,l} \sum_m \kappa_{imk} \kappa_{lmj} \nu_i^c \nu_j^c \nu_k^c \nu_l^c \cos(\varphi_{\nu_i^c} + \varphi_{\nu_j^c} - \varphi_{\nu_k^c} - \varphi_{\nu_l^c}) \\
&+ 2[- \sum_{i,j} \sum_k \kappa_{ikj} \lambda_k v_d v_u \nu_i^c \nu_j^c \cos(\varphi_{\nu_i^c} + \varphi_{\nu_j^c} - \varphi_v) \\
&+ \sum_{i,j,k} \sum_l Y_{\nu_{jl}} \kappa_{ilk} v_u \nu_j \nu_i^c \nu_k^c \cos(\varphi_{\nu_i^c} + \varphi_{\nu_k^c} - \chi_j) \\
&- \sum_{i,j,k} Y_{\nu_{ij}} \lambda_k v_d \nu_i \nu_j^c \nu_k^c \cos(\chi_i + \varphi_{\nu_j^c} - \varphi_{\nu_k^c} - \varphi_v) \\
&- \sum_{i} \sum_j Y_{\nu_{ij}} \lambda_j v_d v_u^2 \nu_i \cos(\varphi_v - \chi_i)] \\
&+ \sum_{i,j,k,l} Y_{\nu_{ij}} Y_{\nu_{kl}} \nu_i \nu_j^c \nu_k \nu_l^c \cos(\chi_i - \chi_k + \varphi_{\nu_j^c} - \varphi_{\nu_l^c}) \\
&+ \sum_{i,j} \sum_k Y_{\nu_{ik}} Y_{\nu_{jk}} v_u^2 \nu_i \nu_j \cos(\chi_i - \chi_j) \\
&+ \sum_{i,j} \sum_k Y_{\nu_{ki}} Y_{\nu_{kj}} v_u^2 \nu_i^c \nu_j^c \cos(\varphi_{\nu_i^c} - \varphi_{\nu_j^c}). \qquad (3.9)
\end{aligned}
$$

The neutral scalar potential is a function of fifteen variables, the eight modulus of the VEVs and the seven independent phases appearing in (3.3). In addition, it also depends on a large number of parameters whose values are unknown at the electroweak scale and hence, we take them as free parameters.

Now we can derive the fifteen minimization conditions of this potential with respect to the moduli $v_d,\ v_u,\ \nu_i^c,\ \nu_i$ and phases $\varphi_v,\ \chi_i,\ \varphi_{\nu_i^c}$. In the following, we present the eight minimization equations with respect to the modulus of the VEVs.

$$\begin{aligned}
\frac{\partial V}{\partial v_d} &= \frac{1}{4}G^2\left(\sum_i \nu_i\nu_i + v_d^2 - v_u^2\right)v_d + m_{H_d}^2 v_d + v_d v_u^2 \sum_i (\lambda_i)^2 \\
&- \sum_i (A_\lambda \lambda)_i \nu_i^c v_u \cos(\varphi_v + \varphi_{\nu_i^c}) + \sum_{i,j} v_d \lambda_i \lambda_j \nu_i^c \nu_j^c \cos(\varphi_{\nu_i^c} - \varphi_{\nu_j^c}) \\
&- \sum_{i,j,k} \kappa_{ikj}\lambda_k v_u \nu_i^c \nu_j^c \cos(\varphi_{\nu_i^c} + \varphi_{\nu_j^c} - \varphi_v) \\
&- \sum_{i,j,k} Y_{\nu_{ij}} \lambda_k \nu_i \nu_j^c \nu_k^c \cos(\chi_i + \varphi_{\nu_j^c} - \varphi_{\nu_k^c} - \varphi_v) \\
&- \sum_i \sum_j Y_{\nu_{ij}} \lambda_j v_u^2 \nu_i \cos(\varphi_v - \chi_i) = 0,
\end{aligned} \tag{3.10}$$

$$\begin{aligned}
\frac{\partial V}{\partial v_u} &= -\frac{1}{4}G^2\left(\sum_i \nu_i\nu_i + v_d^2 - v_u^2\right)v_u + m_{H_u}^2 v_u + v_u v_d^2 \sum_i (\lambda_i)^2 \\
&+ \sum_{i,j} (A_\nu Y_\nu)_{ij} \nu_i \nu_j^c \cos(\chi_i + \varphi_{\nu_j^c}) - \sum_i (A_\lambda \lambda)_i \nu_i^c v_d \cos(\varphi_v + \varphi_{\nu_i^c}) \\
&+ \sum_{i,j} \lambda_i \lambda_j v_u \nu_i^c \nu_j^c \cos(\varphi_{\nu_i^c} - \varphi_{\nu_j^c}) \\
&- \sum_{i,j} \sum_k \kappa_{ijk}\lambda_k v_d \nu_i^c \nu_j^c \cos(\varphi_{\nu_i^c} + \varphi_{\nu_j^c} - \varphi_v) \\
&+ \sum_{i,j,k} \sum_l Y_{\nu_{jl}} \kappa_{ilk} \nu_j \nu_i^c \nu_k^c \cos(\varphi_{\nu_i^c} + \varphi_{\nu_k^c} - \chi_j) \\
&- \sum_i \sum_j 2 Y_{\nu_{ij}} \lambda_j v_d v_u \nu_i \cos(\varphi_v - \chi_i) \\
&+ \sum_{i,j} \sum_k Y_{\nu_{ik}} Y_{\nu_{jk}} v_u \nu_i \nu_j \cos(\chi_i - \chi_j) \\
&+ \sum_{i,j} \sum_k Y_{\nu_{ki}} Y_{\nu_{kj}} v_u \nu_i^c \nu_j^c \cos(\varphi_{\nu_i^c} - \varphi_{\nu_j^c}) = 0,
\end{aligned} \tag{3.11}$$

$$\frac{\partial V}{\partial \nu_i^c} = \sum_j m^2_{\tilde{\nu}^c_{ij}} \nu_j^c \cos(\varphi_{\nu_i^c} - \varphi_{\nu_j^c}) - (A_\lambda \lambda)_i v_u v_d \cos(\varphi_v + \varphi_{\nu_i^c})$$
$$+ \sum_j (A_\nu Y_\nu)_{ji} \nu_j v_u \cos(\chi_j + \varphi_{\nu_i^c})$$
$$+ \sum_{j,k} (A_\kappa \kappa)_{ijk} \nu_j^c \nu_k^c \cos(\varphi_{\nu_i^c} + \varphi_{\nu_j^c} + \varphi_{\nu_k^c}) + \sum_j \lambda_i \lambda_j v_d^2 \nu_j^c \cos(\varphi_{\nu_i^c} - \varphi_{\nu_j^c})$$
$$+ \sum_j \lambda_i \lambda_j \nu_j^c v_u^2 \cos(\varphi_{\nu_i^c} - \varphi_{\nu_j^c})$$
$$+ \sum_{j,k,l} \sum_m 2\kappa_{imk} \kappa_{lmj} \nu_j^c \nu_k^c \nu_l^c \cos(\varphi_{\nu_i^c} + \varphi_{\nu_j^c} - \varphi_{\nu_k^c} - \varphi_{\nu_l^c})$$
$$- \sum_j \sum_k 2\kappa_{ijk} \lambda_k v_d v_u \nu_j^c \cos(\varphi_{\nu_i^c} + \varphi_{\nu_j^c} - \varphi_v)$$
$$+ \sum_{j,k} \sum_l 2 Y_{\nu_{jl}} \kappa_{ikl} v_u \nu_j \nu_k^c \cos(\varphi_{\nu_i^c} + \varphi_{\nu_k^c} - \chi_j)$$
$$- \sum_{j,k} Y_{\nu_{ji}} \lambda_k v_d \nu_j \nu_k^c \cos(\chi_j + \varphi_{\nu_i^c} - \varphi_{\nu_k^c} - \varphi_v)$$
$$- \sum_{j,k} Y_{\nu_{kj}} \lambda_i v_d \nu_k \nu_j^c \cos(\chi_k + \varphi_{\nu_j^c} - \varphi_{\nu_i^c} - \varphi_v)$$
$$+ \sum_{j,k,l} Y_{\nu_{ji}} Y_{\nu_{lk}} \nu_j \nu_l \nu_k^c \cos(\chi_j - \chi_k + \varphi_{\nu_i^c} - \varphi_{\nu_l^c})$$
$$+ \sum_j \sum_k Y_{\nu_{ki}} Y_{\nu_{kj}} v_u^2 \nu_j^c \cos(\varphi_{\nu_i^c} - \varphi_{\nu_j^c}) = 0, \tag{3.12}$$

$$\frac{\partial V}{\partial \nu_i} = \frac{1}{4} G^2 (\sum_j \nu_j \nu_j + v_d^2 - v_u^2) \nu_i + \sum_j m^2_{\tilde{L}_{ij}} \nu_j \cos(\chi_i - \chi_j)$$
$$+ \sum_j (A_\nu Y_\nu)_{ij} \nu_j^c v_u \cos(\chi_i + \varphi_{\nu_j^c})$$
$$+ \sum_{j,k} \sum_l Y_{\nu_{il}} \kappa_{jlk} v_u \nu_j^c \nu_k^c \cos(\varphi_{\nu_j^c} + \varphi_{\nu_k^c} - \chi_i)$$
$$- \sum_{j,k} Y_{\nu_{ij}} \lambda_k v_d \nu_j^c \nu_k^c \cos(\chi_i + \varphi_{\nu_j^c} - \varphi_{\nu_k^c} - \varphi_v) - \sum_j Y_{\nu_{ij}} \lambda_j v_d v_u^2 \cos(\varphi_v - \chi_i)$$
$$+ \sum_{j,k,l} Y_{\nu_{ij}} Y_{\nu_{kl}} \nu_j^c \nu_k \nu_l^c \cos(\chi_i - \chi_k + \varphi_{\nu_j^c} - \varphi_{\nu_l^c})$$
$$+ \sum_j \sum_k Y_{\nu_{ik}} Y_{\nu_{jk}} v_u^2 \nu_j \cos(\chi_i - \chi_j) = 0. \tag{3.13}$$

Here we present the seven minimization equations with respect to the independent phases of the VEVs:

$$\begin{aligned}
\frac{\partial V}{\partial \varphi_v} &= -\sum_{i,j}\sum_{k} 2\kappa_{ijk}\lambda_k v_d v_u \nu_i^c \nu_j^c \sin(\varphi_{\nu_i^c} + \varphi_{\nu_j^c} - \varphi_v) \\
&- 2[\sum_{i,j,k} Y_{\nu_{ij}}\lambda_k v_d \nu_i \nu_j^c \nu_k^c \sin(\chi_i + \varphi_{\nu_j^c} - \varphi_{\nu_k^c} - \varphi_v) \\
&- \sum_{i}\sum_{j} Y_{\nu_{ij}}\lambda_j v_d v_u^2 \nu_i \sin(\varphi_v - \chi_i)] \\
&+ 2\sum_{i}(A_\lambda \lambda)_i \nu_i^c v_d v_u \sin(\varphi_v + \varphi_{\nu_i^c}) = 0,
\end{aligned} \tag{3.14}$$

$$\begin{aligned}
\frac{\partial V}{\partial \varphi_{\nu_i^c}} &= -\sum_{j} m^2_{\tilde{\nu}^c_{ij}} \nu_i^c \nu_j^c \sin(\varphi_{\nu_i^c} - \varphi_{\nu_j^c}) \\
&- \sum_{j}\lambda_i\lambda_j v_d^2 \nu_i^c \nu_j^c \sin(\varphi_{\nu_i^c} - \varphi_{\nu_j^c}) - \sum_{j}\lambda_i\lambda_j v_u^2 \nu_i^c \nu_j^c \sin(\varphi_{\nu_i^c} - \varphi_{\nu_j^c}) \\
&- 2\sum_{j,k,l}\sum_{m}\kappa_{imk}\kappa_{lmj}\nu_i^c\nu_j^c\nu_k^c\nu_l^c \sin(\varphi_{\nu_i^c} + \varphi_{\nu_j^c} - \varphi_{\nu_k^c} - \varphi_{\nu_l^c}) \\
&+ 2\sum_{j,k}\kappa_{ikj}\lambda_k v_d v_u \nu_i^c \nu_j^c \sin(\varphi_{\nu_i^c} + \varphi_{\nu_j^c} - \varphi_v) \\
&- 2\sum_{j,k}\sum_{l} Y_{\nu_{jl}}\kappa_{ilk} v_u \nu_j \nu_i^c \nu_k^c \sin(\varphi_{\nu_i^c} + \varphi_{\nu_k^c} - \chi_j) \\
&+ \sum_{j,k} Y_{\nu_{ji}}\lambda_k v_d \nu_j \nu_i^c \nu_k^c \sin(\chi_j + \varphi_{\nu_i^c} - \varphi_{\nu_k^c} - \varphi_v) \\
&- \sum_{j,k} Y_{\nu_{kj}}\lambda_i v_d \nu_k \nu_j^c \nu_i^c \sin(\chi_k + \varphi_{\nu_j^c} - \varphi_{\nu_i^c} - \varphi_v) \\
&- \sum_{j,k,l} Y_{\nu_{ji}} Y_{\nu_{kl}} \nu_j \nu_i^c \nu_k \nu_l^c \sin(\chi_j - \chi_k + \varphi_{\nu_i^c} - \varphi_{\nu_l^c}) \\
&- \sum_{j}\sum_{k} Y_{\nu_{ki}} Y_{\nu_{kj}} v_u^2 \nu_i^c \nu_j^c \sin(\varphi_{\nu_i^c} - \varphi_{\nu_j^c}) \\
&+ (A_\lambda\lambda)_i \nu_i^c v_d v_u \sin(\varphi_v + \varphi_{\nu_i^c}) - \sum_{j,k}(A_\kappa \kappa)_{ijk}\nu_i^c\nu_j^c\nu_k^c \sin(\varphi_{\nu_i^c} + \varphi_{\nu_j^c} + \varphi_{\nu_k^c}) \\
&- \sum_{j}(A_\nu Y_\nu)_{ji} v_u \nu_j \nu_i^c \sin(\chi_j + \varphi_{\nu_i^c}) = 0,
\end{aligned} \tag{3.15}$$

$$
\begin{aligned}
\frac{\partial V}{\partial \chi_i} = & -\sum_j m^2_{\tilde{L}_{ij}}\, \nu_i\, \nu_j \sin(\chi_i - \chi_j) \\
& + \sum_{j,k} \sum_l Y_{\nu_{il}} \kappa_{jlk} v_u \nu_i \nu^c_j \nu^c_k \sin(\varphi_{\nu^c_j} + \varphi_{\nu^c_k} - \chi_i) \\
& + \sum_{j,k} Y_{\nu_{ij}} \lambda_k v_d \nu_i \nu^c_j \nu^c_k \sin(\chi_i + \varphi_{\nu^c_j} - \varphi_{\nu^c_k} - \varphi_v) \\
& - \sum_j Y_{\nu_{ij}} \lambda_j v_d v_u^2 \nu_i \sin(\varphi_v - \chi_i) \\
& - \sum_{j,k,l} Y_{\nu_{ij}} Y_{\nu_{kl}} \nu_i \nu^c_j \nu_k \nu^c_l \sin(\chi_i - \chi_k + \varphi_{\nu^c_j} - \varphi_{\nu^c_l}) \\
& - \sum_j \sum_k Y_{\nu_{ik}} Y_{\nu_{jk}} v_u^2 \nu_i \nu_j \sin(\chi_i - \chi_j) \\
& - \sum_j (A_\nu Y_\nu)_{ij} v_u \nu_i \nu^c_j \sin(\chi_i + \varphi_{\nu^c_j}) = 0.
\end{aligned} \tag{3.16}
$$

Finding minima requires the solution of equations (3.10-3.16). A standard way to obtain this is to give the values of the cosines of the phases in terms of the moduli, using the triangle method [62, 63, 64] for the equations of the phases, and then substitute the expressions in the minimum equations for the moduli, solving them numerically. This method allows to demonstrate the existence of only real minima at tree-level in several models. This is for example the case of the NMSSM [65], and the MSSM with extra doublets. The latter result has been proved for the MSSM with an extra pair of Higgs doublets [63] (the so called 4D model), the bilinear R-parity violating model (analogous to a 5D model because of the VEVs of the left-handed sneutrinos), and the MSSM with two extra pairs of Higgs doublets (6D model) [64].

Another way of finding minima consists of using as inputs the moduli and phases and solve the fifteen equations to fix the parameters that are linear in these equations, as it is the case of some of the soft terms. This is the procedure that we will follow.

In Section 3.4 we will find numerically global minima that break spontaneously CP. Before doing it, we would like to present an intuitive proof of the existence of SCPV minima in the $\mu\nu SSM$ using the results of Ref. [64], where the authors prove that SUSY scenarios for SCPV at the tree-level require singlets. In particular, they found that, if the singlets do not introduce dimensional parameters in the superpotential (i.e. no linear or bilinear terms), the MSSM extended with two gauge singlets (let us call it (M+2)SSM) would be the minimal SUSY model where CP violation can be generated spontaneously at the tree-level. Since that model

is a limiting case of the $\mu\nu$SSM with vanishing neutrino Yukawa couplings $Y_{\nu_{ij}} = 0$, $\lambda_3 = 0$, and $\kappa_{333} = \kappa_{322} = \kappa_{332} = \kappa_{311} = \kappa_{331} = \kappa_{123} = 0$, this proves that the $\mu\nu$SSM can break CP spontaneously. Let us remark that, since in the $\mu\nu$SSM one is using a seesaw at the electroweak scale, the Yukawa coupling $Y_{\nu_{ij}}$ has to be very small compared with the other parameters [1, 14], and as a consequence, the neutral scalar potential can be understood as a small deformation of the MSSM extended with three gauge singlets (let us call it (M+3)SSM)). Although there is no literature about general solutions that break CP spontaneously in the (M+3)SSM, it is obvious that this model contains the (M+2)SSM as a limiting case when $\kappa_{333} = \kappa_{322} = \kappa_{332} = \kappa_{311} = \kappa_{331} = \kappa_{123} = 0$, and $\lambda_3 = 0$. As already mentioned, SCPV solutions are well known in this case [64, 66]. Thus one could argue that a subset of solutions with neutrino masses different from zero could be obtained deforming the scalar potential of the MSSM extended with three singlets[1] through non-zero $Y_{\nu_{ij}}$.

In Section 3.4 we will do a thorough numerical analysis showing explicitly how SCPV is realizable in the $\mu\nu$SSM and we will show how this CP violation is translated to the leptonic sector. Nevertheless, it is worth pointing out here that to find complex solutions is a highly non-trivial task compared to the search of real ones. As we will show, the key of SCPV is on the $(A_\kappa \kappa)_{ijk}$ terms used as inputs. In order to fulfill the minimization equations, the basic requirement is that entries different from $(A_\kappa \kappa)_{iii}$ must be allowed. In addition, these parameters have to be chosen carefully to obtain global minima that break CP spontaneously.

In the next section the seesaw mechanism as the origin of neutrino masses and mixing angles in this model will be studied.

## 3.3 The neutrino sector of the $\mu\nu$SSM

In this section we will study the neutrino sector of the $\mu\nu$SSM following the guide of [14]. We will show how to extract the effective neutrino mass matrix from the neutralino mass matrix. We will give approximate analytical formulas for this effective neutrino mass matrix in the general case with complex VEVs and we will explain how the seesaw mechanism works in this model in an intuitive way. It is worth to mention that this analysis is general

[1] Since only mass differences for neutrino masses have been measured, in principle two right-handed neutrino supermultiplets are enough to give two tree-level masses and also break CP spontaneously. Thus a version of the $\mu\nu$SSM with only two right-handed neutrinos instead of three could be formulated. Nevertheless, we will follow the philosophy that the existence of three generations of all kind of leptons is more natural.

with the real VEVs case being a particular case of the complex VEVs one.

In the $\mu\nu$SSM the MSSM neutralinos mix with the left- and right-handed neutrinos as a consequence of R-parity violation. Therefore the right-handed neutrinos behave as singlino components of the neutralinos. In the basis $\chi^{0^T} = (\tilde{B}^0, \tilde{W}^0, \tilde{H}_d, \tilde{H}_u, \nu_{R_i}, \nu_{L_i})$ the neutralino-neutrino mass matrix is given in [14] and is written as:

$$\mathcal{M}_n = \begin{pmatrix} M & m \\ m^T & 0_{3\times 3} \end{pmatrix}, \tag{3.17}$$

where the neutralino mass matrix, $M$, is

$$\begin{pmatrix} M_1 & 0 & -A\langle H_d^0\rangle^* & A\langle H_u^0\rangle^* & 0 & 0 & 0 \\ 0 & M_2 & B\langle H_d^0\rangle^* & -B\langle H_u^0\rangle^* & 0 & 0 & 0 \\ -A\langle H_d^0\rangle^* & B\langle H_d^0\rangle^* & 0 & -\lambda_i\langle\tilde{\nu}_i^c\rangle & -\lambda_1\langle H_u^0\rangle & -\lambda_2\langle H_u^0\rangle & -\lambda_3\langle H_u^0\rangle \\ A\langle H_u^0\rangle^* & -B\langle H_u^0\rangle^* & -\lambda_i\langle\tilde{\nu}_i^c\rangle & 0 & -\lambda_1\langle H_d^0\rangle + Y_{\nu_{i1}}\langle\tilde{\nu}_i\rangle & -\lambda_2\langle H_d^0\rangle + Y_{\nu_{i2}}\langle\tilde{\nu}_i\rangle & -\lambda_3\langle H_d^0\rangle + Y_{\nu_{i3}}\langle\tilde{\nu}_i\rangle \\ 0 & 0 & -\lambda_1\langle H_u^0\rangle & -\lambda_1\langle H_d^0\rangle + Y_{\nu_{i1}}\langle\tilde{\nu}_i\rangle & 2\kappa_{11j}\langle\tilde{\nu}_j^c\rangle & 2\kappa_{12j}\langle\tilde{\nu}_j^c\rangle & 2\kappa_{13j}\langle\tilde{\nu}_j^c\rangle \\ 0 & 0 & -\lambda_2\langle H_u^0\rangle & -\lambda_2\langle H_d^0\rangle + Y_{\nu_{i2}}\langle\tilde{\nu}_i\rangle & 2\kappa_{21j}\langle\tilde{\nu}_j^c\rangle & 2\kappa_{22j}\langle\tilde{\nu}_j^c\rangle & 2\kappa_{23j}\langle\tilde{\nu}_j^c\rangle \\ 0 & 0 & -\lambda_3\langle H_u^0\rangle & -\lambda_3\langle H_d^0\rangle + Y_{\nu_{i3}}\langle\tilde{\nu}_i\rangle & 2\kappa_{31j}\langle\tilde{\nu}_j^c\rangle & 2\kappa_{32j}\langle\tilde{\nu}_j^c\rangle & 2\kappa_{33j}\langle\tilde{\nu}_j^c\rangle \end{pmatrix}, \tag{3.18}$$

with $A = \frac{G}{\sqrt{2}}\sin\theta_W$, $B = \frac{G}{\sqrt{2}}\cos\theta_W$, and

$$m^T = \begin{pmatrix} -\frac{g_1}{\sqrt{2}}\langle\tilde{\nu}_1\rangle^* & \frac{g_2}{\sqrt{2}}\langle\tilde{\nu}_1\rangle^* & 0 & Y_{\nu_{1i}}\langle\tilde{\nu}_i^c\rangle & Y_{\nu_{11}}\langle H_u^0\rangle & Y_{\nu_{12}}\langle H_u^0\rangle & Y_{\nu_{13}}\langle H_u^0\rangle \\ -\frac{g_1}{\sqrt{2}}\langle\tilde{\nu}_2\rangle^* & \frac{g_2}{\sqrt{2}}\langle\tilde{\nu}_2\rangle^* & 0 & Y_{\nu_{2i}}\langle\tilde{\nu}_i^c\rangle & Y_{\nu_{21}}\langle H_u^0\rangle & Y_{\nu_{22}}\langle H_u^0\rangle & Y_{\nu_{23}}\langle H_u^0\rangle \\ -\frac{g_1}{\sqrt{2}}\langle\tilde{\nu}_3\rangle^* & \frac{g_2}{\sqrt{2}}\langle\tilde{\nu}_3\rangle^* & 0 & Y_{\nu_{3i}}\langle\tilde{\nu}_i^c\rangle & Y_{\nu_{31}}\langle H_u^0\rangle & Y_{\nu_{32}}\langle H_u^0\rangle & Y_{\nu_{33}}\langle H_u^0\rangle \end{pmatrix}. \tag{3.19}$$

The above matrix (3.17) is of the seesaw type giving rise to neutrino masses which have to be very small for being in the experimental allowed range. This is the case since the entries of the matrix $M$ (3.18) are much larger than the ones in the matrix $m$ (3.19). Notice in this respect that the entries of $M$ are of the order of the electroweak scale while the ones in $m$ are of the order of the Dirac masses for the neutrinos [1, 40, 14]. Therefore in a first approximation the effective neutrino mass matrix can be written as

$$m_{eff} = -m^T \cdot M^{-1} \cdot m. \tag{3.20}$$

Because $m_{eff}$ is a complex symmetric matrix and $m_{eff}^\dagger m_{eff}$ is Hermitian, one can diagonalize them by a unitary transformation

$$U_{MNS}^T m_{eff} U_{MNS} = diag(m_{\nu_1}, m_{\nu_2}, m_{\nu_3}), \tag{3.21}$$

$$U_{MNS}^\dagger m_{eff}^\dagger m_{eff} U_{MNS} = diag(m_{\nu_1}^2, m_{\nu_2}^2, m_{\nu_3}^2). \tag{3.22}$$

Summarazing, we have explained how in the $\mu\nu$SSM, since R-parity is broken, left- and right-handed neutrinos are mixed with the MSSM neutralinos giving

rise to a $10 \times 10$ mass matrix. In the seesaw approximation, we have seen how to extract the effective light neutrino mass matrix. This matrix has to be diagonalized to find the eigenvalues (the neutrino masses) and the eigenvectors which will provide the mixing angles of the PMNS matrix. In the following we will obtain approximate analytical formulas for the effective neutrino mass matrix in order to discuss certain interesting limits that will explain intuitively how the seesaw mechanism works in this model.

The formula presented here is obtained from Eq. (3.20) neglecting terms proportional to $Y_\nu^2\nu^2$, $Y_\nu^3\nu$ and $Y_\nu\nu^3$ (that are negligibly small compared to other terms). This formula has been deduced for the case of complex VEVs but can be particularized to the real VEVs case setting the phases to zero. In addition, this formula has been particularized to a simplified structure of the phases and parameters of the Lagrangian. In Section 3.4 we will see that for simplicity and for not having a very large number of input parameters we have taken a common value of couplings $\lambda_i \equiv \lambda$, a tensor $\kappa$ with terms $\kappa_{iii} \equiv \kappa_i \equiv \kappa$ and vanishing otherwise, diagonal Yukawa couplings $Y_{\nu_{ii}} \equiv Y_{\nu_i}$, and a common value of the VEVs of the right-handed sneutrinos $\nu_i^c \equiv \nu^c$. The phase structure of the global minimum that will be discussed in Section 3.4 for analysing the neutrino sector has also been used in the computation $\varphi_{\nu_1^c} = -\varphi_{\nu_2^c} = -\varphi_{\nu_3^c} \equiv \varphi_{\nu^c}$ and $\varphi_{\nu_1} = -\varphi_{\nu_2} = -\varphi_{\nu_3} \equiv \varphi_\nu$.

The expression of the effective neutrino mass matrix obtained with the help of Eq. (3.20) using the assumptions described before is given by:

$$(m_{eff})_{ij} \simeq \frac{X_{ij}}{\Delta} + \frac{T_{ij}}{Z}\,\frac{a_i a_j}{2\kappa\nu^c}, \tag{3.23}$$

where the parameters appearing in (3.23) have been defined as

$$\begin{aligned}
a_i &= Y_{\nu_i} v_u, \\
\Delta &= (e^{i\varphi_{\nu^c}} + 2e^{i3\varphi_{\nu^c}})\lambda^2(v_u^2+v_d^2)^2 + (8e^{i\varphi_{\nu^c}} + 4e^{i3\varphi_{\nu^c}})\lambda\kappa\nu^{c2} v_d v_u e^{-i\varphi_v} \\
&- (16 + 16e^{i2\varphi_{\nu^c}} + 4e^{i4\varphi_{\nu^c}})M\lambda^2\kappa\nu^{c3} \\
&- (8 + 20e^{i2\varphi_{\nu^c}} + 8e^{i4\varphi_{\nu^c}})M\lambda^3\nu^c v_d v_u e^{i\varphi_v}, \\
Z &= e^{i\varphi_{\nu^c}}[-4e^{i\varphi_{\nu^c}}(2 + e^{i2\varphi_{\nu^c}})\kappa\nu^{c2} v_d v_u + e^{i\varphi_v}\lambda(4M(2+e^{i2\varphi_{\nu^c}})^2\kappa\nu^{c3} \\
&- e^{i\varphi_{\nu^c}}(1 + 2e^{i2\varphi_{\nu^c}})(v_d^2+v_u^2)^2) + 4e^{i2(\varphi_{\nu^c}+\varphi_v)}\lambda^2 M\nu^c v_d v_u(5 + 4\cos 2\varphi_{\nu^c})],
\end{aligned} \tag{3.24}$$

with $\frac{1}{M} = \frac{g_1^2}{M_1} + \frac{g_2^2}{M_2}$,

$$
\begin{aligned}
T_{11} &= 2e^{i2\varphi_v}[-4e^{i2(\varphi_{\nu^c}+\varphi_v)}(2+e^{i2\varphi_{\nu^c}})M\lambda^2\nu^c v_d v_u \\
&+ 4e^{i\varphi_{\nu^c}}\kappa{\nu^c}^2 v_d v_u \\
&+ e^{i\varphi_v}\lambda(-4(2+e^{i6\varphi_{\nu^c}})M\kappa{\nu^c}^3 + e^{i3\varphi_{\nu^c}}(v_u^2+v_d^2)^2)], \\
T_{22} &= T_{33} = 2e^{i(\varphi_{\nu^c}+2\varphi_v)}[-4e^{i2(\varphi_{\nu^c}+\varphi_v)}(2+e^{i2\varphi_{\nu^c}})M\lambda^2\nu^c v_d v_u \\
&+ 4e^{i3\varphi_{\nu^c}}\kappa{\nu^c}^2 v_d v_u \\
&+ e^{i\varphi_v}\lambda(-4(1+e^{i2\varphi_{\nu^c}}+e^{i4\varphi_{\nu^c}})M\kappa{\nu^c}^3 + e^{i3\varphi_{\nu^c}}(v_u^2+v_d^2)^2)], \\
T_{12} &= T_{13} = -e^{i2\varphi_v}[-4e^{i2(\varphi_{\nu^c}+\varphi_v)}(2+e^{i2\varphi_{\nu^c}})M\lambda^2\nu^c v_d v_u \\
&+ 4e^{i3\varphi_{\nu^c}}\kappa{\nu^c}^2 v_d v_u\cos(2\varphi_{\nu^c}) \\
&+ e^{i(3\varphi_{\nu^c}+\varphi_v)}\lambda(4(-3\cos(3\varphi_{\nu^c}) \\
&+ i\sin(3\varphi_{\nu^c}))M\kappa{\nu^c}^3 + (v_u^2+v_d^2)^2)], \\
T_{23} &= -e^{i2\varphi_v}[-4e^{i2(2\varphi_{\nu^c}+\varphi_v)}(2+e^{i2\varphi_{\nu^c}})M\lambda^2\nu^c v_d v_u \\
&+ 4e^{i3\varphi_{\nu^c}}\kappa{\nu^c}^2 v_d v_u \\
&+ e^{i\varphi_v}\lambda(-4(-1+4e^{i3\varphi_{\nu^c}}\cos(\varphi_{\nu^c}))M\kappa{\nu^c}^3 \\
&+ e^{i5\varphi_{\nu^c}}(v_u^2+v_d^2)^2)],
\end{aligned}
\tag{3.25}
$$

and

$$
\begin{aligned}
X_{11} &= 2\kappa{\nu^c}^3(b_{11})^2 + 2\lambda\nu^c v_d v_u e^{i\varphi_v}(b'_{11})^2 + \epsilon_{11}, \\
X_{22} &= 2\kappa{\nu^c}^3(b_{22})^2 + 2\lambda\nu^c v_d v_u e^{i\varphi_v}(b'_{22})^2 + \epsilon_{22}, \\
X_{33} &= 2\kappa{\nu^c}^3(b_{33})^2 + 2\lambda\nu^c v_d v_u e^{i\varphi_v}(b'_{33})^2 + \epsilon_{33}, \\
X_{12} &= 2\kappa{\nu^c}^3(b_{11})(b_{22}) + 2\lambda\nu^c v_d v_u e^{i\varphi_v}(b'_{12})^2 + \epsilon_{12}, \\
X_{13} &= 2\kappa{\nu^c}^3(b_{11})(b_{33}) + 2\lambda\nu^c v_d v_u e^{i\varphi_v}(b'_{13})^2 + \epsilon_{13}, \\
X_{23} &= 2\kappa{\nu^c}^3(b_{22})(b_{33}) + 2\lambda\nu^c v_d v_u e^{i\varphi_v}(b'_{23})^2 + \epsilon_{23},
\end{aligned}
\tag{3.26}
$$

with

$$\begin{aligned}
(b_{11}) &= (2+e^{i2\varphi_{\nu^c}})\lambda e^{-i\varphi_\nu}\nu_1 + e^{i2\varphi_{\nu^c}} v_d Y_{\nu_1},\\
(b_{22}) &= (2+e^{i2\varphi_{\nu^c}})\lambda e^{i\varphi_\nu}\nu_2 + v_d Y_{\nu_2},\\
(b_{33}) &= (2+e^{i2\varphi_{\nu^c}})\lambda e^{i\varphi_\nu}\nu_3 + v_d Y_{\nu_3},\\
(b'_{11})^2 &= (2+5e^{i2\varphi_{\nu^c}}+2e^{i4\varphi_{\nu^c}})\lambda^2 e^{-i2\varphi_\nu}\nu_1^2\\
&+ (2+2e^{i2\varphi_{\nu^c}}+2e^{i4\varphi_{\nu^c}})\lambda v_d e^{-i\varphi_\nu}\nu_1 Y_{\nu_1} + e^{i2\varphi_{\nu^c}} v_d^2 Y_{\nu_1}^2,\\
(b'_{22})^2 &= (2+5e^{i2\varphi_{\nu^c}}+2e^{i4\varphi_{\nu^c}})\lambda^2 e^{i2\varphi_\nu}\nu_2^2\\
&+ (1+4e^{i2\varphi_{\nu^c}}+e^{i4\varphi_{\nu^c}})\lambda v_d e^{i\varphi_\nu}\nu_2 Y_{\nu_2} + e^{i2\varphi_{\nu^c}} v_d^2 Y_{\nu_2}^2,\\
(b'_{33})^2 &= (2+5e^{i2\varphi_{\nu^c}}+2e^{i4\varphi_{\nu^c}})\lambda^2 e^{i2\varphi_\nu}\nu_3^2\\
&+ (1+4e^{i2\varphi_{\nu^c}}+e^{i4\varphi_{\nu^c}})\lambda v_d e^{i\varphi_\nu}\nu_3 Y_{\nu_3} + e^{i2\varphi_{\nu^c}} v_d^2 Y_{\nu_3}^2,\\
(b'_{12})^2 &= (2+5e^{i2\varphi_{\nu^c}}+2e^{i4\varphi_{\nu^c}})\lambda^2\nu_1\nu_2 + (1+e^{i2\varphi_{\nu^c}}+e^{i4\varphi_{\nu^c}})\lambda v_d e^{i\varphi_\nu}\nu_2 Y_{\nu_1}\\
&+ ((1/2)+2e^{i2\varphi_{\nu^c}}+(1/2)e^{i4\varphi_{\nu^c}})\lambda v_d e^{-i\varphi_\nu}\nu_1 Y_{\nu_2}\\
&+ (1/2)(1+e^{i4\varphi_{\nu^c}})v_d^2 Y_{\nu_1} Y_{\nu_2},\\
(b'_{13})^2 &= (2+5e^{i2\varphi_{\nu^c}}+2e^{i4\varphi_{\nu^c}})\lambda^2\nu_1\nu_3 + (1+e^{i2\varphi_{\nu^c}}+e^{i4\varphi_{\nu^c}})\lambda v_d e^{i\varphi_\nu}\nu_3 Y_{\nu_1}\\
&+ ((1/2)+2e^{i2\varphi_{\nu^c}}+(1/2)e^{i4\varphi_{\nu^c}})\lambda v_d e^{-i\varphi_\nu}\nu_1 Y_{\nu_3}\\
&+ (1/2)(1+e^{i4\varphi_{\nu^c}})v_d^2 Y_{\nu_1} Y_{\nu_3},\\
(b'_{23})^2 &= (2+5e^{i2\varphi_{\nu^c}}+2e^{i4\varphi_{\nu^c}})\lambda^2 e^{i2\varphi_\nu}\nu_2\nu_3\\
&+ ((1/2)+2e^{i2\varphi_{\nu^c}}+(1/2)e^{i4\varphi_{\nu^c}})\lambda v_d e^{i\varphi_\nu}(\nu_3 Y_{\nu_2}+\nu_2 Y_{\nu_3})\\
&+ e^{i2\varphi_{\nu^c}} v_d^2 Y_{\nu_2} Y_{\nu_3}
\end{aligned} \tag{3.27}$$

and

$$\begin{aligned}
\epsilon_{11} &= (4e^{i4\varphi_{\nu^c}}-4)\lambda^2\nu^c v_u^3 e^{i\varphi_v} e^{-i\varphi_\nu}\nu_1 Y_{\nu_1},\\
\epsilon_{22} &= (2-2e^{i4\varphi_{\nu^c}})\lambda^2\nu^c v_u^3 e^{i\varphi_v} e^{i\varphi_\nu}\nu_2 Y_{\nu_2},\\
\epsilon_{33} &= (2-2e^{i4\varphi_{\nu^c}})\lambda^2\nu^c v_u^3 e^{i\varphi_v} e^{i\varphi_\nu}\nu_3 Y_{\nu_3},\\
\epsilon_{12} &= (2e^{i4\varphi_{\nu^c}}-2)\lambda^2\nu^c v_u^3 e^{i\varphi_v} e^{i\varphi_\nu}\nu_2 Y_{\nu_1} + (1-e^{i4\varphi_{\nu^c}})\lambda^2\nu^c v_u^3 e^{i\varphi_v} e^{-i\varphi_\nu}\nu_1 Y_{\nu_2},\\
\epsilon_{13} &= (2e^{i4\varphi_{\nu^c}}-2)\lambda^2\nu^c v_u^3 e^{i\varphi_v} e^{i\varphi_\nu}\nu_3 Y_{\nu_1} + (1-e^{i4\varphi_{\nu^c}})\lambda^2\nu^c v_u^3 e^{i\varphi_v} e^{-i\varphi_\nu}\nu_1 Y_{\nu_3},\\
\epsilon_{23} &= (1-e^{i4\varphi_{\nu^c}})\lambda^2\nu^c v_u^3 e^{i\varphi_v} e^{i\varphi_\nu}(\nu_3 Y_{\nu_2}+\nu_2 Y_{\nu_3}).
\end{aligned} \tag{3.28}$$

Two interesting limits of Eq. (3.23) where the formula becomes simple are the following. In the limit $M \to \infty$ and $v_d \to 0$ we obtain

$$(m_{eff})_{ij} \simeq F_{ij}\,\frac{a_i a_j}{2\kappa\nu^c}, \tag{3.29}$$

where

$$\begin{aligned}
F_{11} &= -2e^{i(2\varphi_v-\varphi_{\nu^c})}(2+e^{i6\varphi_{\nu^c}})\left(2+e^{2i\varphi_{\nu^c}}\right)^{-2},\\
F_{22} &= F_{33} = -2e^{i(2\varphi_v-\varphi_{\nu^c})}(1+e^{i2\varphi_{\nu^c}}+e^{i4\varphi_{\nu^c}})\left(2+e^{2i\varphi_{\nu^c}}\right)^{-2},\\
F_{12} &= F_{13} = e^{i2(\varphi_{\nu^c}+\varphi_v)}(3\cos(3\varphi_{\nu^c})-i\sin(3\varphi_{\nu^c}))\left(2+e^{2i\varphi_{\nu^c}}\right)^{-2},\\
F_{23} &= e^{i(2\varphi_v-\varphi_{\nu^c})}(4e^{i3\varphi_{\nu^c}}\cos(\varphi_{\nu^c})-1)\left(2+e^{2i\varphi_{\nu^c}}\right)^{-2}. \qquad (3.30)
\end{aligned}$$

Another interesting limit is the situation with vanishing phases i.e. real VEVs (no SCPV), we obtain

$$\begin{aligned}
(m_{eff|real})_{ij} &\simeq \frac{2}{3}\frac{(\kappa{\nu^c}^2+\lambda v_u v_d)\nu^c}{\lambda^2(v_u^2+v_d^2)^2+4\lambda\kappa{\nu^c}^2 v_u v_d-12M\lambda(\kappa{\nu^c}^2+\lambda v_u v_d)\lambda\nu^c}\; b_i b_j\\
&+ \frac{1}{6\kappa\nu^c}(1-3\delta_{ij})a_i a_j, \qquad (3.31)
\end{aligned}$$

where we have defined

$$b_i = Y_{\nu_i} v_d + 3\lambda\nu_i. \qquad (3.32)$$

Regarding the previous parameters we note that for the real case

$$\begin{aligned}
b_i = b_{ii} = b'_{ii},\\
b'^2_{ij} = b_{ii}b_{jj} = b_i b_j,\\
\epsilon_{ij} = 0. \qquad (3.33)
\end{aligned}$$

As we have already said, the analytical approximate effective neutrino mass matrix in the case with complex VEVs (3.23) is reduced in the limit of vanishing phases to (3.31).

In the following we will discuss certain interesting limits of the effective neutrino mass matrix with real VEVs (3.31) in order to have a qualitative idea of how the seesaw mechanism works in this model. For our purposes of explaining the seesaw mechanism in the model it is preferable to ignore the complicated phases-dependent factors moving to the limit of vanishing phases.

Let us first rewrite the expression (3.31) in the following form:

$$(m_{eff|real})_{ij} \simeq \tfrac{v_u^2}{6\kappa\nu^c}Y_{\nu_i}Y_{\nu_j}\,(1-3\,\delta_{ij}) \quad -\frac{1}{2M_{eff}}\left[\nu_i\nu_j+\frac{v_d\left(Y_{\nu_i}\nu_j+Y_{\nu_j}\nu_i\right)}{3\lambda}+\frac{Y_{\nu_i}Y_{\nu_j}v_d^2}{9\lambda^2}\right], \qquad (3.34)$$

with

$$M_{eff} \equiv M\left[1-\frac{v^2}{2M\left(\kappa{\nu^c}^2+\lambda v_u v_d\right)\;3\lambda\nu^c}\left(2\kappa{\nu^c}^2\frac{v_u v_d}{v^2}+\frac{\lambda v^2}{2}\right)\right], \qquad (3.35)$$

These expressions deduced in [14] coincide with the results in [43], where the possibility of obtaining an adequate seesaw with diagonal Yukawa couplings was also pointed out. Here $v^2 = v_u^2 + v_d^2 + \sum_i \nu_i^2 \approx v_u^2 + v_d^2$ with $v \approx 174$ GeV has been used, since $\nu_i << v_u, v_d$ [1], and let us recall that $\frac{1}{M} = \frac{g_1^2}{M_1} + \frac{g_2^2}{M_2}$.

In the limit where gauginos are very heavy and decouple (i.e. $M \to \infty$), Eq. (3.34) reduces to

$$(m_{eff|real})_{ij} \simeq \frac{v_u^2}{6\,\kappa\nu^c} Y_{\nu_i} Y_{\nu_j} \left(1 - 3\,\delta_{ij}\right). \tag{3.36}$$

It is interesting to note that in contrast with the ordinary seesaw (i.e. generated only through the mixing between left- and right-handed neutrinos), where the case of diagonal Yukawas would give rise to a diagonal mass matrix of the form

$$(m_{eff|ordinary\ seesaw})_{ij} \simeq \frac{-v_u^2 Y_{\nu_i} Y_{\nu_j} \delta_{ij}}{2\,\kappa\nu^c}, \tag{3.37}$$

in this case we have an extra contribution given by the first term of Eq. (3.36). This is due to the effective mixing of the right-handed neutrinos and Higgsinos in this limit, and produces off-diagonal entries in the mass matrix. Besides, when right-handed neutrinos are also decoupled (i.e. $\nu^c \to \infty$), the neutrino masses are zero as corresponds to the case of a seesaw with only Higgsinos.

Another observation is that, independently on the nature of the lightest neutralino, Higgsino-like or $\nu^c$-like or even a mixture of them (recall that the $\nu^c$ can be interpreted also as the singlino component of the neutralino since R-parity is broken), the form of the effective neutrino mass matrix is the same when the gauginos are decoupled, as given by (3.36).

Another limit which is worth discussing is $\nu^c \to \infty$. Then, Eq. (3.34) reduces to the form

$$(m_{eff|real})_{ij} \simeq -\frac{1}{2M}\left[\nu_i\nu_j + \frac{v_d(Y_{\nu_i}\nu_j + Y_{\nu_j}\nu_i)}{3\lambda} + \frac{Y_{\nu_i}Y_{\nu_j}v_d^2}{9\lambda^2}\right]. \tag{3.38}$$

We can also see that for $v_d \to 0$ (i.e. $\tan\beta = \frac{v_u}{v_d} \to \infty$) one obtains from (3.38) the following expression:

$$(m_{eff|real})_{ij} \simeq -\frac{\nu_i\nu_j}{2M}. \tag{3.39}$$

Note that this result can actually be obtained if $\nu_i >> \frac{Y_{\nu_i} v_d}{3\lambda}$, and that this relation can be fulfilled with $v_d \sim v_u \sim 174$ GeV for suitable values of $\lambda$. It means that decoupling right-handed neutrinos/singlinos and Higgsinos, the seesaw mechanism is generated through the mixing of left-handed neutrinos

| $\Delta m^2_{sol}/10^{-5}$ eV$^2$ | $\sin^2\theta_{12}$ | $\sin^2\theta_{13}$ | $\sin^2\theta_{23}$ | $\Delta m^2_{atm}/10^{-3}$ eV$^2$ |
|---|---|---|---|---|
| 7.14-8.19 | 0.263-0.375 | $< 0.046$ | 0.331-0.644 | 2.06-2.81 |

Table 3.1: Allowed $3\sigma$ ranges for the neutrino masses and mixings as discussed in [67].

with gauginos. This is a characteristic feature of the seesaw in the well-known bilinear R-parity violating model (BRpV) [33].

The seesaw in the $\mu\nu$SSM comes, in general, from the interplay of the above two limits. Namely, the limit where we suppress only certain Higgsino and gaugino mixings. Hence, taking $v_d \to 0$ in Eq. (3.34), which means quite pure gauginos but Higgsinos mixed with right-handed neutrinos, we obtain

$$(m_{eff|real})_{ij} \simeq \frac{v_u^2}{6\kappa\nu^c} Y_{\nu_i} Y_{\nu_j}(1-3\delta_{ij}) - \frac{1}{2\,M_{\rm eff}}\nu_i\nu_j \ . \tag{3.40}$$

As above, we remark that actually this result can be obtained if $\nu_i >> \frac{Y_{\nu_i} v_d}{3\lambda}$. The effective mass $M_{eff} = M(1 - \frac{v^4}{12\kappa M\nu^{c^3}})$ represents the mixing between gauginos and Higgsinos-$\nu^c$ that is not completely suppressed in this limit. Expression (3.40) is more general than the other two limits studied above. On the other hand, for typical values of the parameters involved in the seesaw, $M_{eff} \approx M$, and therefore we get a simple formula that can be used to understand the seesaw mechanism in this model in a qualitative way, that is

$$(m_{eff|real})_{ij} \simeq \frac{v_u^2}{6\kappa\nu^c} Y_{\nu_i} Y_{\nu_j}(1-3\delta_{ij}) - \frac{1}{2M}\nu_i\nu_j. \tag{3.41}$$

The simplicity of Eq. (3.41), in contrast with the full formula given by Eq. (3.34), comes from the fact that the mixing between gauginos and Higgsinos-$\nu^c$ is neglected.

To continue the discussion of the seesaw in the $\mu\nu$SSM, let us remind that two mass differences and mixing angles have been measured experimentally in the neutrino sector. The allowed $3\,\sigma$ ranges for these parameters are shown in Table 3.1. We also show the compositions of the mass eigenstates in Fig. 3.1 for the normal and inverted hierarchy cases. For the discussion, hereafter we will use indistinctly the subindices $(1,2,3) \equiv (e,\mu,\tau)$.

Due to the fact that the mass eigenstates have, in a good approximation, the same composition of $\nu_\mu$ and $\nu_\tau$ (see Fig. 3.1) we start considering $Y_{\nu_2} = Y_{\nu_3}$ and $\nu_2 = \nu_3$, and therefore Eq. (3.41) takes the form

$$m_{eff} = \begin{pmatrix} d & c & c \\ c & A & B \\ c & B & A \end{pmatrix}, \tag{3.42}$$

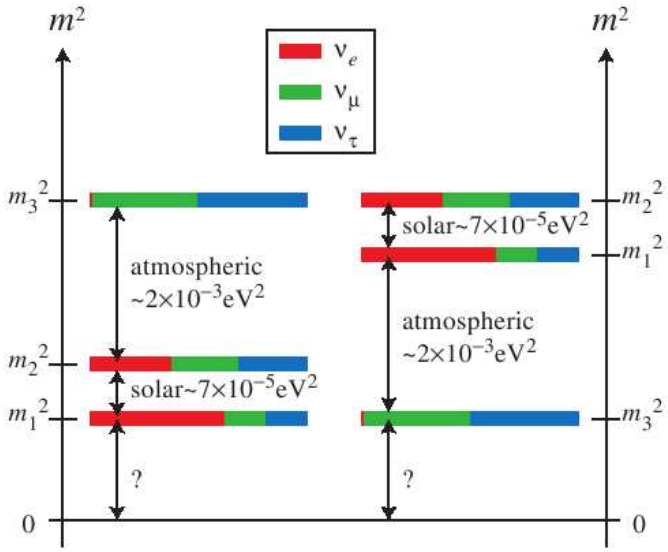


Figure 3.1: The two possible hierarchies of neutrino masses as shown in [68]. The pattern on the left side corresponds to the normal hierarchy and is characterized by one heavy state with a very little electron neutrino component, and two almost degenerated light states with a mass difference which is the solar mass difference. The pattern on the right side corresponds to the inverted hierarchy and is characterized by two almost degenerated heavy states with a mass difference that is the solar mass difference, and a light state which has very little electron neutrino component. In both cases the mass difference between the heaviest/lightest eigenstate and the almost degenerated eigenstates is the atmospheric scale.

where

$$\begin{aligned} d &= -\frac{v_u^2}{3\kappa\nu^c}Y_{\nu_1}^2 - \frac{1}{2M}\nu_1^2, \\ c &= \frac{v_u^2}{6\kappa\nu^c}Y_{\nu_1}Y_{\nu_2} - \frac{1}{2M}\nu_1\nu_2, \\ A &= -\frac{v_u^2}{3\kappa\nu^c}Y_{\nu_2}^2 - \frac{1}{2M}\nu_2^2, \\ B &= \frac{v_u^2}{6\kappa\nu^c}Y_{\nu_2}^2 - \frac{1}{2M}\nu_2^2. \end{aligned} \tag{3.43}$$

The eigenvalues of matrix (3.42) are the following:

$$\begin{aligned} &\tfrac{1}{2}\left(A+B-\sqrt{8c^2+(A+B-d)^2}+d\right), \\ &\tfrac{1}{2}\left(A+B+\sqrt{8c^2+(A+B-d)^2}+d\right), \\ &\qquad A-B\ , \end{aligned} \tag{3.44}$$

and the corresponding eigenvectors (for simplicity they are not normalised) are:

$$\begin{aligned} &\left(-\tfrac{A+B+\sqrt{8c^2+(A+B-d)^2}-d}{2}, c, c\right), \\ &\left(\tfrac{-A-B+\sqrt{8c^2+(A+B-d)^2}+d}{2c}, 1, 1\right), \\ &\qquad (0,-1,1)\,. \end{aligned} \tag{3.45}$$

We have ordered the eigenvalues in such a way that it is clear how to obtain the normal hierarchy for the $\nu_\mu - \nu_\tau$ degenerated case. Then we see that $\sin^2\theta_{13} = 0$ and $\sin^2\theta_{23} = \frac{1}{2}$, as in the tri-bimaximal mixing regime. Also we have enough freedom to fix the parameters in such a way that the experimental values for the mass differences and the remaining angle $\theta_{12}$ can be reproduced. It is important to mention that the above two values of the angles are a consequence of considering the example with $\nu_\mu - \nu_\tau$ degeneration, and therefore valid even if we use the general formula (3.34) instead of the simplified expression (3.41). Notice that Eqs. (3.42), (3.44) and (3.45) would be the same but with the corresponding values of $A, B, c$ and $d$.

Let us remark that the fact that to obtain the correct neutrino angles is easy in this kind of seesaw is due to the following characteristics: R-parity is broken and the relevant scale is the electroweak one. In a sense we are giving an explanation to the question why the mixing angles are so different in the quark and lepton sectors.

To show qualitatively how we can obtain an adequate seesaw with diagonal neutrino Yukawa couplings, let us first consider the limit [2] $c \to 0$. In this limit the electron neutrino is the lightest neutrino, and is completely decoupled from the rest. The second eigenvector has no $\nu_e$ composition ($\sin\theta_{12} \to 0$), and it is half $\nu_\mu$ and half $\nu_\tau$. Understood this case, we can easily generalize the situation to the case $\sin\theta_{12} \neq 0$, switching on the parameter

[2] Actually this limit can be obtained taking $Y_{\nu_1} \to 0$, $\nu_1 \to 0$, implying $c \to 0$, and also $d \to 0$, and leading to similar conclusions. This limit means that the electron neutrino is decoupled from the other two neutrinos, having a negligible mass.

$d$. The eigenvalues in this limit are

$$d\ ,\ A+B,\ A-B, \tag{3.46}$$

where

$$\begin{aligned} |d| &= \left|\frac{v_u^2}{3\kappa\nu^c}Y_{\nu_1}^2+\frac{1}{2M}\nu_1^2\right|, \\ |A+B| &= \left|\frac{v_u^2}{6\kappa\nu^c}Y_{\nu_2}^2+\frac{1}{M}\nu_2^2\right|, \\ |A-B| &= \frac{v_u^2}{2\kappa\nu^c}Y_{\nu_2}^2. \end{aligned} \tag{3.47}$$

We can see that $\Delta m^2_{atm}\sim|4AB|=\left|4(\frac{v_u^4Y_{\nu_2}^4}{18\kappa^2\nu^{c2}}-\frac{1}{4M^2}\nu_2^4-\frac{v_u^2Y_{\nu_2}^2\nu_2^2}{12M\kappa\nu^c})\right|$ and $\Delta m^2_{sol}\sim|(A+B)^2-d^2|=\left|(\frac{v_u^2}{6\kappa\nu^c}Y_{\nu_2}^2+\frac{1}{M}\nu_2^2)^2-(\frac{v_u^2}{3\kappa\nu^c}Y_{\nu_1}^2+\frac{1}{2M}\nu_1^2)^2\right|$.

It is important to note that we need $|A-B|>|A+B|$ for the normal hierarchy case, otherwise the $\theta_{12}$ angle is zero even when $c$ is not neglected. This is easy to obtain for $M>>2\kappa\nu^c$. If $M\sim2\kappa\nu^c$, using different signs for the effective Majorana and gaugino masses helps to fulfill the above inequality. For this to hold with our convention, one must take $M<0$.

In the inverted hierarchy scenario, $|A-B|>|A+B|$ leads the angle $\theta_{12}$ to zero also with $c\neq0$ which is not phenomenologically viable. Then we impose $|A-B|<|A+B|$. Note that when $c$ is switched on, the parameter $d$ has to be large enough for having the associated neutrino with an intermediate mass, as corresponds to the inverted hierarchy scenario. Therefore in this case we can also have easily the bilarge mixing regime for $M<<2\kappa\nu^c$. When $M\sim2\kappa\nu^c$, having $M>0$ helps to fulfill the above condition.

Let us finally remark that we can get the complete tri-bimaximal mixing regime $\sin^2\theta_{13}=0$, $\sin^2\theta_{23}=1/2$ and $\sin^2\theta_{12}=1/3$ fixing in Eq. (3.42) $c=A+B-d$. In this way we obtain the eigenvalues

$$-(A+B)+2d\ ,\ 2(A+B)-d,\ A-B, \tag{3.48}$$

and from Eq. (3.45), after normalization, we arrive to $\sin^2\theta_{12}=1/3$.

Breaking the degeneracy between the $Y_\nu$ and $\nu$ of the muon and tau neutrinos, it is possible to find more general solutions in the normal and inverted hierarchy cases. We will show this with numerical examples in Section 3.4, working always in the case $M\sim2\kappa\nu^c$. Note also that in the case of degenerate $\nu_\mu-\nu_\tau$ parameters, as the Dirac CP phase always appears in the PMNS matrix in the form $\sin\theta_{13}e^{i\delta}$ (see Eq. (3.52) below), the SCPV effect

is suppressed since $\sin\theta_{13}$ is negligible. This is not the case if we break the degeneration between $\nu_\mu$ and $\nu_\tau$.

When the vacuum is non CP-conserving the situation is much more complicated since new relative phases are present, but the idea still holds. In Section 3.4 we will use the above results to find numerical examples in the general case where also phases are generated through complex vacua. Examples are given where changing the sign of $M$ the second and third eigenvalue are interchanged and the behaviour is similar to the one described in this section.

## 3.4 Numerical results

In Section 3.2 we have already demonstrated in an intuitive way with a simple argument that the $\mu\nu SSM$ can violate CP spontaneously. In Section 3.3 we have described the seesaw mechanism in the $\mu\nu$SSM and we have discussed how to obtain correct neutrino masses and mixing angles in this model, compatible with the experimental results.

In this section we will sketch the numerical method used for the search of global minima of the $\mu\nu$SSM with SCPV, giving rise also to an effective neutrino mass matrix that reproduces correctly the phenomenology of the neutrino sector according to observations. We will also give several numerical examples.

Thus, the principal task in this section is to find numerical examples of global minima of the scalar potential of the $\mu\nu SSM$ with non-trivial phases of the VEVs. Using these SCPV minima we will study numerically the neutrino sector of the model and we will present and discuss different plots of the evolution of the neutrino sector parameters (mass differences, mixing angles and CP phases) with the inputs. We will find SCPV global minima which in addition, could reproduce the phenomenology on the neutrino sector obtaining an effective neutrino mass matrix compatible with the experimental constraints on the mass differences and mixing angles.

We will not study the complete vacuum structure of the model since it is a highly non-trivial task to find CP-violating global minima and we will only present several examples of global minima that break CP spontaneously. We do this because our principal goal is to demonstrate that the $\mu\nu SSM$ can violate CP spontaneously finding numerically some CP-violating global minima. Note that with a slightly change on the values of the phases, the behaviour of the neutral scalar potential changes strongly. This is the main reason, together with the elevate number of parameters and minimization equations of the model, why it would be really hard to study the complete

vacuum structure of the model with complex VEVs.

We also want to prove that it is possible to reproduce the experimental constraints in the neutrino sector with the spontaneous CP-violating $\mu\nu SSM$ model with all the parameters in the Lagrangian being real and with a diagonal neutrino Yukawa coupling. It will be also interesting to study how the CP violation that arises spontaneously from the Higgs sector is transmitted to the leptonic sector resulting in non trivial CP violating phases in the PMNS matrix.

Let us recall that, for simplicity, in order to avoid the presence of an excessive number of parameters in the numerical study of the neutral scalar potential of the model, we will assume that all the parameters appearing in this neutral scalar potential are diagonal in flavour space at the electroweak scale. The only exception will be the trilinear $(A_\kappa \kappa)_{ijk}$ terms whose entries different from the diagonal entries $(A_\kappa \kappa)_{iii}$ are crucial to break CP spontaneously.

As a consequence, for the rest of this chapter, we will introduce the following notation for the flavour diagonal free parameters of the neutral scalar potential:

$$\begin{aligned} &\kappa_{iii} \equiv \kappa_i \ , \ Y_{\nu_{ii}} \equiv Y_{\nu_i} \ , \ (A_\nu Y_\nu)_{ii} \equiv (A_\nu Y_\nu)_i \ , \\ &m^2_{\tilde{L}_{ii}} \equiv m^2_{\tilde{L}_i} \ , \ m^2_{\tilde{\nu}^c_{ii}} \equiv m^2_{\tilde{\nu}^c_i}, \end{aligned} \tag{3.49}$$

with $i = 1, 2, 3$ being flavour indices.

Then, under this assumption, the neutral scalar potential (3.5) is obviously simplified. As a consequence, also the fifteen minimization conditions (3.10-3.16) of the neutral scalar potential are also simplified under this assumption of diagonal flavour structure of the parameters.

Thus, the neutral scalar potential is a function of 15 variables (8 modulus and 7 phases of the VEVs). It also depends on a large number of parameters whose numerical values are unknown at the electroweak scale. We take them as free parameters: $\lambda_i$, $\kappa_i$, $Y_{\nu_i}$, $A_{\kappa_{ijk}}$, $A_{\lambda_i}$, $A_{\nu_i}$, $m_{H_d}$, $m_{H_u}$, $m_{\tilde{\nu}^c_i}$, $m_{\tilde{L}_i}$.

The expression of the simplified neutral scalar potential is given by the following equation:

$$
\begin{aligned}
V &= \frac{G^2}{8}(\sum_i \nu_i\nu_i + v_d v_d - v_u v_u)^2 + m^2_{H_d} v_d v_d + m^2_{H_u} v_u v_u + \sum_i m^2_{\tilde{L}_i}\nu_i\nu_i \\
&+ \sum_i m^2_{\tilde{\nu}^c_i}\nu^c_i\nu^c_i - 2\sum_i \lambda_i A_{\lambda_i}\nu^c_i v_u v_d \cos(\varphi_v + \varphi_{\nu^c_i}) \\
&+ \sum_{i,j,k} \frac{2}{3}\kappa_{ijk}A_{\kappa_{ijk}}\nu^c_i\nu^c_j\nu^c_k \cos(\varphi_{\nu^c_i} + \varphi_{\nu^c_j} + \varphi_{\nu^c_k}) \\
&+ 2\sum_i Y_{\nu_i} A_{\nu_i} v_u \nu_i \nu^c_i \cos(\chi_i + \varphi_{\nu^c_i}) + \sum_i (\lambda_i)^2 v_d^2 v_u^2 \\
&+ \sum_{i,j} \lambda_i\lambda_j v_d^2 \nu^c_i\nu^c_j \cos(\varphi_{\nu^c_i} - \varphi_{\nu^c_j}) \\
&+ \sum_{i,j} \lambda_i\lambda_j v_u^2 \nu^c_i\nu^c_j \cos(\varphi_{\nu^c_i} - \varphi_{\nu^c_j}) + \sum_i \kappa_i\kappa_i\nu^c_i\nu^c_i\nu^c_i\nu^c_i \\
&+ 2[-\sum_i \kappa_i\lambda_i v_d v_u \nu^c_i\nu^c_i \cos(2\varphi_{\nu^c_i} - \varphi_v) \\
&+ \sum_i Y_{\nu_i}\kappa_i v_u \nu_i \nu^c_i\nu^c_i \cos(2\varphi_{\nu^c_i} - \chi_i) \\
&- \sum_{i,k} Y_{\nu_i}\lambda_k v_d \nu_i \nu^c_i\nu^c_k \cos(\chi_i + \varphi_{\nu^c_i} - \varphi_{\nu^c_k} - \varphi_v) \\
&- \sum_i Y_{\nu_i}\lambda_i v_d v_u^2 \nu_i \cos(\varphi_v - \chi_i)] \\
&+ \sum_{i,k} Y_{\nu_i}Y_{\nu_k}\nu_i\nu^c_i\nu_k\nu^c_k \cos(\chi_i - \chi_k + \varphi_{\nu^c_i} - \varphi_{\nu^c_k}) \\
&+ \sum_i Y_{\nu_i}Y_{\nu_i} v_u^2 \nu_i\nu_i + \sum_i Y_{\nu_i}Y_{\nu_i} v_u^2 \nu^c_i\nu^c_i
\end{aligned}
\tag{3.50}
$$

The strategy followed to find global minima of the model consists of solving the minimization equations in terms of the soft parameters that are linear in those equations. Then, we proceed a numerical study varying the values of the inputs: the VEVs (modulus and phases) and the soft terms that are not given by the minimization equations. Once we obtain the numerical values of the soft terms solved in the minimization equations, we ensure that the local minimum found is a global one with a numerical procedure based on global optimisation.

More precisely, the three minimization equations (3.16), corresponding to $\frac{\partial V}{\partial \chi_i} = 0$, are used to solve the values of $(A_\nu Y_\nu)_i$ only in terms of the inputs. Using this result, the equations (3.15) for $i = 2, 3$, corresponding to

$\frac{\partial V}{\partial \varphi^c_{\nu_{2,3}}} = 0$, after substituting the values of $(A_\nu Y_\nu)_i$ obtained before, are used to solve $(A_\lambda \lambda)_{2,3}$ in terms of the inputs. Repeating the procedure using the equation (3.14), $\frac{\partial V}{\partial \varphi_v} = 0$, one obtains $(A_\lambda \lambda)_1$ in terms of the inputs. Finally, Eq. (3.15) for $i = 1$ is used to get $(A_\kappa \kappa)_{111}$. With the minimization equations with respect to the moduli of the VEVs (3.10-3.13), substituting the values of the soft trilinear terms obtained before, we can solve the squared soft masses in terms of the inputs.

Then, with this procedure, given the numerical values of the inputs (that are varied in the numerical method), we are able to obtain the values of the soft masses $m^2_{H_d}$, $m^2_{H_u}$, $m^2_{\tilde{\nu}^c_i}$, $m^2_{\tilde{L}_i}$ and the trilinear soft terms $(A_\lambda \lambda)_i$, $(A_\nu Y_\nu)_i$,$(A_\kappa \kappa)_{111}$ required for being in a local minimum. Then, we check numerically if this local minimum is really a global one and we only store the global minima found. As discussed in [14, 40], one has to check in particular that the minimum found is deeper than the local minima with some or all the VEVs vanishing.

To accomplish the numerical task of finding global minima, the inputs needed are the eight moduli and seven phases of the VEVs, the superpotential couplings $\lambda_i$, $\kappa_i$ and $Y_{\nu_i}$ and the soft trilinear terms not determined by the minimization equations $(A_\kappa \kappa)_{ijk}$ with $(i, j, k) \neq (1, 1, 1)$. For simplicity, we assume a special structure for the latter: $(A_\kappa \kappa)_{222} = (A_\kappa \kappa)_{333}$, a common value for $(A_\kappa \kappa)_{ijk}$ with $i, j, k \neq 1$ and another common value for $(A_\kappa \kappa)_{ijk}$ with one or two indices equal to 1. Let us remind that $(A_\kappa \kappa)_{111}$ is given by the minimization equations. Moreover, let us recall that the modulus of the SUSY Higgs VEVs, can be determined from $v^2 = v_d^2 + v_u^2 + \sum_i \nu_i^2 \approx v_d^2 + v_u^2$ with $v \approx 174$ GeV, and the value of $\tan\beta$ is defined as usual: $\tan\beta = \frac{v_u}{v_d}$.

One interesting thing to note is that our method of solving the minimization equations explained before is only valid if the following constraints are accomplished:

$$\sin(\chi_i + \varphi_{\nu^c_i}) \neq 0 \ , \ \sin(\varphi_v + \varphi_{\nu^c_i}) \neq 0 \ , \ \sin(3\varphi_{\nu^c_1}) \neq 0.$$

Note that the behaviour of the potential strongly depends on the values of the phases of the VEVs since the sign of the terms in the potential can change varying them so it is difficult to predict the general behaviour.

Let us now describe the details on how we proceed with the numerical analysis of the neutrino sector of the model. First, we assume for simplicity the GUT inspired relation between the gaugino masses $M_1$ and $M_2$, $M_1 = \frac{\alpha_1^2}{\alpha_2^2} M_2$, implying $M_2 \simeq 2M_1$ at low energy. As discussed in Section 3.3, one has to diagonalize the neutrino effective mass matrix, $m_{eff} = -m^T \cdot M^{-1} \cdot m$. Since it is a complex symmetric matrix, it can be diagonalized with an unitary

transformation, as it is shown in Eqs. (3.21) and (3.22). For the PMNS matrix we follow the standard parametrization

$$U_{MNS} = \mathrm{diag}(e^{i\delta_e}, e^{i\delta_\mu}, e^{i\delta_\tau}) \cdot V \cdot \mathrm{diag}(e^{-i\phi_1/2}, e^{-i\phi_2/2}, 1), \tag{3.51}$$

where $\phi_1$ and $\phi_2$ are the Majorana phases and $V$ is given by

$$V = \begin{pmatrix} c_{12}c_{13} & s_{12}c_{13} & s_{13}e^{-i\delta} \\ -c_{23}s_{12} - s_{23}s_{13}c_{12}e^{i\delta} & c_{23}c_{12} - s_{23}s_{13}s_{12}e^{i\delta} & s_{23}c_{13} \\ s_{23}s_{12} - c_{23}s_{13}c_{12}e^{i\delta} & -s_{23}c_{12} - c_{23}s_{13}s_{12}e^{i\delta} & c_{23}c_{13} \end{pmatrix}. \tag{3.52}$$

Here $c_{ij} \equiv \cos\theta_{ij}$ and $s_{ij} \equiv \sin\theta_{ij}$ whereas $\delta$ is the Dirac CP violating phase. The conventions used for extracting the mixing angles and the Majorana and Dirac phases from (3.51) and (3.52) are outlined in Ref. [69].

Let us also recall that the smallness of $Y_{\nu_i}$ and $\nu_i$ for reproducing the light neutrino masses implies that the neutral scalar potential of the $\mu\nu$SSM can be viewed as a small deformation of the one for the NMSSM with three generations of singlets. The neutrino sector parameters $Y_{\nu_i}$ and $\nu_i$ and the gaugino mass parameter $M_1$ can be varied without altering the condition of global minimum. Thus, our strategy will consist of finding global minima of the $\mu\nu$SSM with SCPV and then we will vary the neutrino sector parameters and the gaugino mass for studying the neutrino sector of the model. With this, we will find points on the parameter space of the $\mu\nu$SSM that corresponds to CP violating global minima of the potential of the model and that reproduce current neutrino data.

Taking all the above into account, we show in Table 3.2 the parameters that characterize an example of a global minimum that breaks CP spontaneously. The values of the soft parameters not determined by the minimization equations have been chosen to be $(A_\kappa\kappa)_{iii} = 280$ GeV for $i \neq 1$, $(A_\kappa\kappa)_{ijk} = -40$ GeV for $i, j, k \neq 1$, and $(A_\kappa\kappa)_{ijk} = -120$ GeV for one or two indices equal to 1. In Table 3.3 we show the neutrino/neutralino inputs used in order to obtain a $\nu_\mu$-$\nu_\tau$ degenerated case with normal hierarchy, producing values of masses and mixing angles within the ranges of Table 3.1. In particular, we obtain $\sin^2\theta_{13} \sim 0$ and $\sin^2\theta_{23} = 0.5$, as expected from the discussion in Section 3.3, $\sin^2\theta_{12} = 0.323$, and neutrino masses $m_1 = 0.00305$ eV, $m_2 = 0.00949$ eV and $m_3 = 0.05091$ eV, producing $\Delta m^2_{solar} = 8.08\times10^{-5}$ eV$^2$ and $\Delta m^2_{atm} = 2.50\times10^{-3}$ eV$^2$. The corresponding values of the soft terms calculated with the minimization equations are presented in Table 3.4.

It is worth noticing that for this solution, the soft masses of the left-handed sneutrinos, $m_{\tilde{L}_i}$, do not need to be very different, and, actually, in this case they are almost degenerated $\sim 3700$ GeV. This can be understood

| | | |
|---|---|---|
| $\lambda_i = 0.13$ | $\kappa_i = 0.55$ | $\nu_i^c = 1000$ GeV |
| $\tan\beta = 29$ | $\varphi_v = -\pi$ | $\varphi_{\nu_1^c} = \frac{\pi}{7}$ |
| $\varphi_{\nu_2^c} = \varphi_{\nu_3^c} = -\frac{\pi}{7}$ | $\chi_1 = -\frac{\pi}{6}$ | $\chi_2 = \chi_3 = \frac{\pi}{6}$ |

Table 3.2: Numerical values of the relevant input parameters for a global minimum that breaks CP spontaneously.

| | | |
|---|---|---|
| $Y_{\nu_1} = 4.25 \times 10^{-7}$ | $Y_{\nu_2} = Y_{\nu_3} = 1.36 \times 10^{-6}$ | $M_1 = -340$ GeV |
| $\nu_1 = 3.88 \times 10^{-5}$ GeV | $\nu_2 = \nu_3 = 1.24 \times 10^{-4}$ GeV | |

Table 3.3: Numerical values of the neutrino/neutralino inputs that reproduce the neutrino experimental constraints, and correspond to the normal hierarchy scenario.

using the minimization equations (3.13), neglecting the terms with products of Yukawas. When $\frac{Y_{\nu_i}}{\nu_i} = \frac{Y_{\nu_j}}{\nu_j}$, $\forall\ i,j$, one obtains $m^2_{\tilde{L}_i} = m^2_{\tilde{L}_j}$. However, we have to point out that the values obtained for other soft parameters are not so natural in a SUSY framework. Notice for example that $A_\nu \sim -7$ TeV, $A_{\lambda_1} \sim -11$ TeV, whereas $A_{\kappa_{111}} \sim -0.5$ GeV. Indeed, this is a consequence of the particular solution shown in Table 3.2.

Although it is non-trivial to find realistic solutions, since many minima which apparently are acceptable, at the end of the day turn out to be false minima, we have been able to find more sensible solutions. This is the case of the one shown in Table 3.5, with the values of the input soft parameters $(A_\kappa\kappa)_{iii} = -150$ GeV for $i \neq 1$, $(A_\kappa\kappa)_{ijk} = 75$ GeV for $i,j,k \neq 1$ and $(A_\kappa\kappa)_{ijk} = -50$ GeV for one or two indices equal to 1. For example, lowering the values of $\nu^c$ one is able to lower the trilinear terms $A_\nu \sim -3$ TeV in order to fulfill Eqs. (3.16) (also lowering $\kappa$ contributes to this result), and also to lower the soft masses $m_{\tilde{L}_i} \sim 2.8$ TeV, as shown in Table 3.7. Lowering $\lambda$ one is able to lower the trilinears $A_{\lambda_1} \sim -1.5$ TeV, $A_{\lambda_{2,3}} \sim -840$ GeV, in order to fulfill Eqs. (3.14) and (3.15). Notice finally that the use of non-degenerated $\nu_i^c$ allows to increase the trilinear $A_{\kappa_{111}} \sim 36$ GeV. In Table 3.6 we show the corresponding neutrino/neutralino inputs producing values of masses and mixing angles within the ranges of Table 3.1.

Modifying the values of the phases we can also obtain other interesting solutions. See for example the one shown in Tables 3.8, 3.9, and 3.10. In this case the values of the input soft parameters are chosen to be $(A_\kappa\kappa)_{iii} = -200$ GeV for $i \neq 1$, $(A_\kappa\kappa)_{ijk} = 125$ GeV for $i,j,k \neq 1$ and $(A_\kappa\kappa)_{ijk} = -75$ GeV for one or two indices equal to 1. Notice that now the values obtained for the soft

| | | |
|---|---|---|
| $(A_\nu Y_\nu)_1 \simeq -0.0031$ GeV | $(A_\nu Y_\nu)_2 \simeq -0.010$ GeV | $(A_\nu Y_\nu)_3 \simeq -0.010$ GeV |
| $(A_\lambda \lambda)_1 \simeq -1487$ GeV | $(A_\lambda \lambda)_2 \simeq -679$ GeV | $(A_\lambda \lambda)_3 \simeq -679$ GeV |
| $(A_\kappa \kappa)_{111} \simeq -0.25$ GeV | $m^2_{H_d} \simeq 7.0325 \times 10^7$ GeV$^2$ | $m^2_{H_u} \simeq -47200$ GeV$^2$ |
| $m^2_{\tilde{\nu}^c_1} \simeq 260140$ GeV$^2$ | $m^2_{\tilde{\nu}^c_2} \simeq -100820$ GeV$^2$ | $m^2_{\tilde{\nu}^c_3} \simeq -100820$ GeV$^2$ |
| $m^2_{\tilde{L}_1} \simeq m^2_{\tilde{L}_2} = m^2_{\tilde{L}_3} = 1.37 \times 10^7$ GeV$^2$ | | |

Table 3.4: Values of the soft terms calculated with the minimization equations for the global minimum associated to the parameters shown in Table 3.2.

| | | |
|---|---|---|
| $\lambda_i = 0.10$ | $\kappa_i = 0.35$ | $\nu^c_1 = 835$ GeV , $\nu^c_2 = \nu^c_3 = 685$ GeV |
| $\tan\beta = 29$ | $\varphi_v = -\pi$ | $\varphi_{\nu^c_1} = \frac{\pi}{7}$ |
| $\varphi_{\nu^c_2} = \varphi_{\nu^c_3} = -\frac{\pi}{7}$ | $\chi_1 = -\frac{\pi}{6}$ | $\chi_2 = \chi_3 = \frac{\pi}{6}$ |

Table 3.5: Numerical values of the relevant inputs for the second global minimum discussed in the text, that breaks CP spontaneously.

terms are also of this order. In particular, the trilinears are $A_{\nu_1} \sim -657$ GeV, $A_{\nu_{2,3}} \sim -429$ GeV, $A_{\lambda_1} \sim -990$ GeV, $A_{\lambda_{2,3}} \sim -830$ GeV, and $A_{\kappa_{111}} \sim 100$ GeV. For the soft masses we obtain $m_{\tilde{L}_1} \sim 628$ GeV, $m_{\tilde{L}_{2,3}} \sim 950$ GeV.

A general analysis of the parameter space, finding many other interesting complex vacua, is obviously extremely complicated given the large number of parameters involved, and beyond the scope of this work. Nevertheless, we have checked that other sensible solutions can indeed be obtained modifying adequately the parameters. In the following we will work for the analysis of the neutrino sector with the solution associated to the parameters of Table 3.2, since the discussion below is essentially valid for other solutions. Our strategy will consist of varying the neutrino/neutralino inputs $Y_{\nu_i}$, $\nu_i$ and $M_1$ in such a way that the derived neutrino mass differences and mixing angles are within the ranges of Table 3.1. As mentioned above, this procedure will not alter the vacuum structure found. Notice in this respect that gaugino masses do not contribute to the minimization equations, and that the values of $Y_{\nu_i}$ and $\nu_i$ are very small and they do not affect to the global condition of the minimum. Let us also mention that this strategy can indeed be applied to the much more simple issue of analysing real vacua. In particular, it was shown in [40] that many global minima with real VEVs can be found. For them neutrino/neutralino inputs $Y_{\nu_i}$, $\nu_i$, $M_1$, similar to those studied here are also valid.

As noted in Sect. 3.3 we have chosen $M_1 < 0$ in order to guarantee

| | | |
|---|---|---|
| $Y_{\nu_1} = 5.4 \times 10^{-7}$ | $Y_{\nu_2} = Y_{\nu_3} = 9.2 \times 10^{-7}$ | $M_1 = -340$ GeV |
| $\nu_1 = 3.7 \times 10^{-5}$ GeV | $\nu_2 = \nu_3 = 8.8 \times 10^{-5}$ GeV | |

Table 3.6: Numerical values of the neutrino/neutralino inputs for the second global minimum discussed in the text, that reproduce the neutrino experimental constraints and correspond to the normal hierarchy scenario.

| | | |
|---|---|---|
| $(A_\nu Y_\nu)_1 \simeq -0.00209$ GeV | $(A_\nu Y_\nu)_2 \simeq -0.00294$ GeV | $(A_\nu Y_\nu)_3 \simeq -0.00294$ GeV |
| $(A_\lambda \lambda)_1 \simeq -156$ GeV | $(A_\lambda \lambda)_2 \simeq -84$ GeV | $(A_\lambda \lambda)_3 \simeq -84$ GeV |
| $(A_\kappa \kappa)_{111} \simeq 12.7$ GeV | $m^2_{H_d} \simeq 5.36 \times 10^6$ GeV$^2$ | $m^2_{H_u} \simeq -37910$ GeV$^2$ |
| $m^2_{\tilde{\nu}^c_1} \simeq 51035$ GeV$^2$ | $m^2_{\tilde{\nu}^c_2} \simeq 69155$ GeV$^2$ | $m^2_{\tilde{\nu}^c_3} \simeq 69155$ GeV$^2$ |
| $m^2_{\tilde{L}_1} \simeq 8.07 \times 10^6$ GeV$^2$ | $m^2_{\tilde{L}_2} \simeq 3.92 \times 10^6$ GeV$^2$ | $m^2_{\tilde{L}_3} \simeq 3.92 \times 10^6$ GeV$^2$ |

Table 3.7: Values of the soft terms calculated with the minimization equations for the second global minimum discussed in the text, associated to the parameters shown in Table 3.5.

a viable $\theta_{12}$ angle. It is worth pointing out here that a redefinition of the parameters leaving the Lagrangian invariant can be made, in such a way that $M_1$ becomes positive and other parameters such as the VEVs become negative, describing indeed the same physics. In our convention the VEVs, $v_d$, $v_u$, $\nu^c_i$, $\nu_i$ are always taken positive.

We would also like to stress that all the numerical results have been obtained without any approximation, that is, with the exact expression of the $10 \times 10$ neutralino mass matrix, calculating numerically the effective neutrino mass matrix and diagonalizing it. The analytical approximate formulas for the effective neutrino mass matrix presented in Sect. 3.3 have been deduced with the purpose of explaining intuitively how the seesaw mechanism works in this model but all the results presented in the following have been derived numerically using the exact $10 \times 10$ neutralino mass matrix.

Let us first study how the neutrino mass differences depend on the inputs. In Sect. 3.3 we showed that in this scenario there are two different contributions to the seesaw mechanism; the one involving right-handed neutrinos (and Higgsinos) given by $\frac{(Y_{\nu_i} v_u)^2}{2\kappa\nu^c}$, where the Dirac and Majorana masses are parameterized by $Y_{\nu_i} v_u$ and $2\kappa\nu^c$, respectively, and the contribution coming from the gaugino seesaw given by $\frac{(g_1 \nu_i)^2}{M_1} + \frac{(g_2 \nu_i)^2}{M_2}$, where the Dirac and Majorana masses are parameterized by $g_\alpha \nu_i$ and $M_\alpha$, respectively, with $\alpha = 1, 2$.

Figs. 3.2a and 3.2b show that the heaviest eigenvalue (dashed line) has

| | | |
|---|---|---|
| $\lambda_i = 0.10$ | $\kappa_i = 0.42$ | $\nu_1^c = 850$ GeV , $\nu_2^c = \nu_3^c = 550$ GeV |
| $\tan\beta = 29$ | $\varphi_v = -\pi$ | $\varphi_{\nu_1^c} = \frac{\pi}{5}$ |
| $\varphi_{\nu_2^c} = \varphi_{\nu_3^c} = -\frac{\pi}{5}$ | $\chi_1 = -\frac{\pi}{3}$ | $\chi_2 = \chi_3 = \frac{\pi}{3}$ |

Table 3.8: Numerical values of the relevant inputs for the third global minimum discussed in the text, that breaks CP spontaneously.

| | | |
|---|---|---|
| $Y_{\nu_1} = 1.9 \times 10^{-7}$ | $Y_{\nu_2} = Y_{\nu_3} = 8.5 \times 10^{-7}$ | $M_1 = -100$ GeV |
| $\nu_1 = 6 \times 10^{-5}$ GeV | $\nu_2 = \nu_3 = 4.9 \times 10^{-5}$ GeV | |

Table 3.9: Numerical values of the neutrino/neutralino inputs for the third global minimum discussed in the text, that reproduce the neutrino experimental constraints and correspond to the normal hierarchy scenario.

very little electron-neutrino component, as expected in the normal hierarchy scenario (see Fig. 3.1), and therefore it does not depend on $(Y_{\nu_1} v_u)^2/(2\kappa\nu^c)$, whereas the intermediate (solid line) and lightest (dotted line) eigenvalues, that have sizeable electron-neutrino components, grow with this term. As a consequence of the latter, the squared solar mass difference (i.e. mass squared difference between the intermediate and the lightest eigenvalues) grows as well. On the other hand, following the arguments related to Eq. (3.41), we can see in Figs. 3.2c and 3.2d that the heaviest eigenvalue is controlled by the contribution of the seesaw with right-handed neutrinos having an important muon/tau neutrino composition, thus we observe how the heaviest eigenvalue grows with $(Y_{\nu_2} v_u)^2/(2\kappa\nu^c)$ and, as a consequence, the squared atmospheric mass difference (i.e. mass square difference between the heaviest and the intermediate eigenvalues) grows accordingly. The variation with $(Y_{\nu_3} v_u)^2/(2\kappa\nu^c)$ is analogue.

Fig. 3.3 is analogous to Fig. 3.2 but showing the squared neutrino mass differences dependence on the gaugino seesaw component. In this case, because the heaviest eigenstate (dashed line) practically does not mix with the electron neutrino we can see that it does not vary with $((g_1\nu_i)^2/M_1 + (g_2\nu_i)^2/M_2)^2$ for $i = 1, 2, 3$. On the other hand, the intermediate eigenstate grows with the mixing with the gauginos, as explained in Sect. 3.3 with $M_1 < 0$, therefore the squared solar mass difference also grows.

Let us now discuss the mixing angles of the neutrino sector. Note that in the $\nu_\mu$-$\nu_\tau$ degenerated case with normal hierarchy and $M_1 < 0$ we have obtained $\sin^2\theta_{13} = 0$ and $\sin^2\theta_{23} = \frac{1}{2}$. In Fig. 3.4 we present the variation

| | | |
|---|---|---|
| $(A_\nu Y_\nu)_1 \simeq -0.000125$ GeV | $(A_\nu Y_\nu)_2 \simeq -0.000365$ GeV | $(A_\nu Y_\nu)_3 \simeq -0.000365$ GeV |
| $(A_\lambda \lambda)_1 \simeq -99$ GeV | $(A_\lambda \lambda)_2 \simeq -83$ GeV | $(A_\lambda \lambda)_3 \simeq -83$ GeV |
| $(A_\kappa \kappa)_{111} \simeq 41.9$ GeV | $m^2_{H_d} \simeq 3.6 \times 10^6$ GeV$^2$ | $m^2_{H_u} \simeq -25118$ GeV$^2$ |
| $m^2_{\tilde{\nu}^c_1} \simeq -24393$ GeV$^2$ | $m^2_{\tilde{\nu}^c_2} \simeq 208377$ GeV$^2$ | $m^2_{\tilde{\nu}^c_3} \simeq 208377$ GeV$^2$ |
| $m^2_{\tilde{L}_1} \simeq 394777$ GeV$^2$ | $m^2_{\tilde{L}_2} \simeq 903528$ GeV$^2$ | $m^2_{\tilde{L}_3} \simeq 903528$ GeV$^2$ |

Table 3.10: Values of the soft terms calculated with the minimization equations for the third global minimum discussed in the text, associated to the parameters shown in Table 3.8.

of $\sin^2\theta_{12}$ with the ratio of the parameters that control the gaugino seesaw, $b_e^2/b_\mu^2$, where for the sake of simplicity we take $b_i = Y_{\nu_i} v_d + 3\lambda\nu_i$ and we do not consider the complicated factors containing phases in Eqs. (3.27).

To obtain results different from $\sin^2\theta_{23} \sim \frac{1}{2}$ and $\sin^2\theta_{13} \sim 0$, in the following we consider the possibility of breaking the degeneracy between $\mu$ and $\tau$ neutrinos, that is having different values for the $Y_\nu$ and $\nu$ parameters for $\mu$ and $\tau$ neutrinos. We show in Fig. 3.5a $\sin^2\theta_{23}$ as a function of the ratio of the term that controls the Higgsino-$\nu^c$ seesaw, $a_\mu^2/a_\tau^2$. When $a_\mu/a_\tau$ goes to 1, the $\nu_\mu$-$\nu_\tau$ degeneracy is recovered and $\sin^2\theta_{23}$ goes to 1/2 as expected. In Fig. 3.5b we show $\sin^2\theta_{13}$ as a function of $\frac{4a_\mu a_\tau}{(a_\mu+a_\tau)^2}$ that is a good measure of the degeneration in this case. Note that when $4a_\mu a_\tau/(a_\mu + a_\tau)^2 \to 1$ the degeneracy is recovered and $\sin^2\theta_{13} \to 0$ as expected. The parameters $a_i$ have been defined in Eq. (3.24). Let us point out that $\sin^2\theta_{13} < 10^{-3}$ since we are breaking the degeneration between $\mu$ and $\tau$ neutrinos but the term that controls the Higgsino-$\nu^c$ seesaw for the first family is very small compared to the other two families.

As mentioned previously, the $\mu\nu$SSM with SCPV also predicts non-zero CP phases in the PMNS matrix. We have checked numerically that for each of the experimentally allowed regions found, the two Majorana CP phases and the Dirac CP phase are different from zero. This fact is reflected in Fig. 3.6 where we present two plots in the $\delta - \phi_1$ and $\delta - \phi_2$ planes (Dirac-Majorana CP phases) constructed varying all the inputs in the neutrino sector. However, it is fair to say that due to the smallness of $\sin^2\theta_{13} \sim 10^{-3}$ in this region, the CP violation effects of the phases of the VEVs turn out to be suppressed in the PMNS matrix because the Dirac CP phase always appears in the form $\sin\theta_{13} e^{i\delta}$ as can be seen in (3.52).

Notice that in all the plots of the evolution of mass squared differences, mixing angles or CP phases, all the points plotted belong to the experimental allowed region.

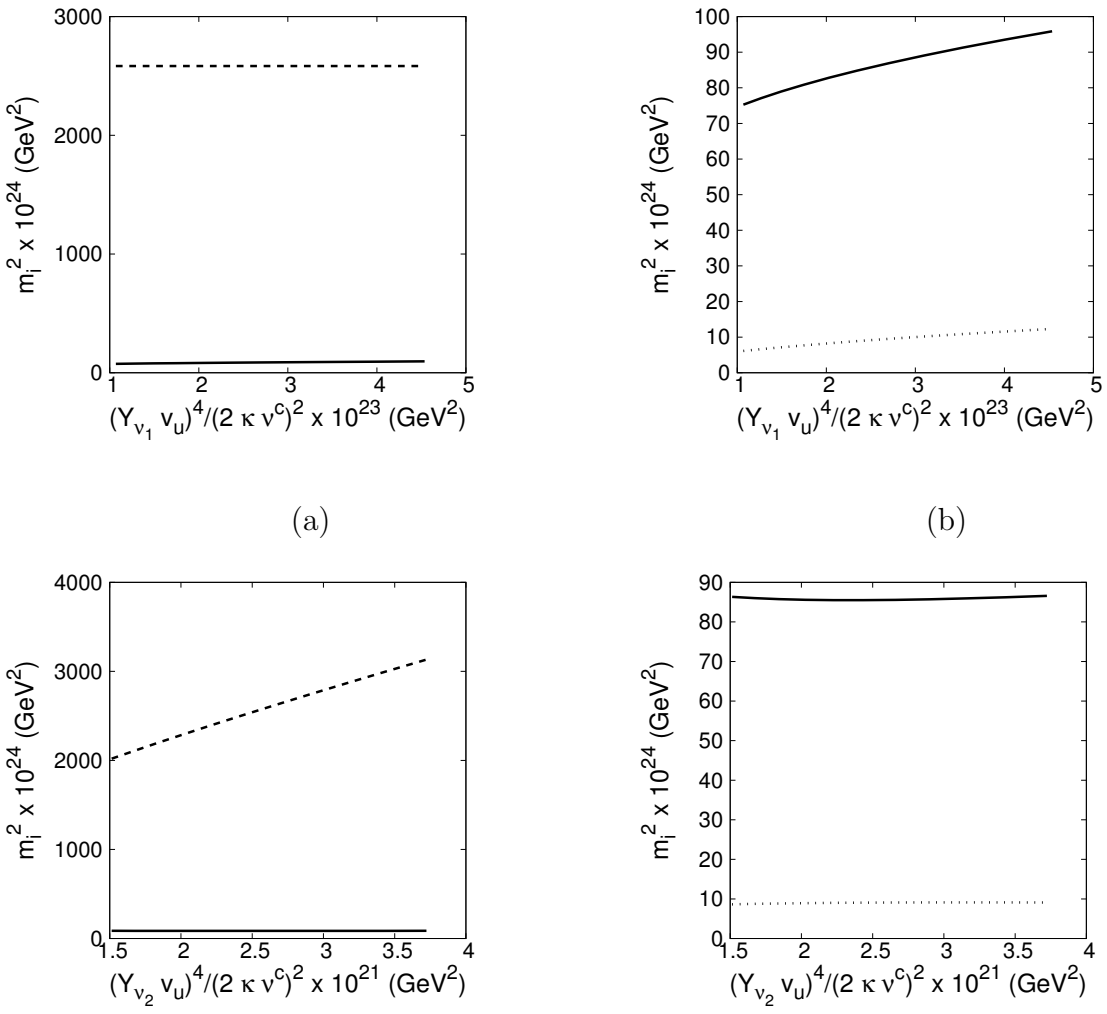


Figure 3.2: Squared neutrino masses versus $(Y_{\nu_i} v_u)^4/(2\kappa\nu^c)^2$. (a) and (b) show for $i = 1$ the two heaviest and lightest neutrinos, respectively. The same for (c) and (d) but for $i = 2$.

In order to complete the discussion about the neutrino sector in this scenario, we will consider the possibility $M_1 > 0$ instead of $M_1 < 0$ . In Sect. 3.3 we have seen that with $M_1 > 0$ it is more complicated to have a degeneracy between muon and tau neutrinos because it is easy to obtain $\sin^2\theta_{12} \sim 0$, in contradiction with the data (see Table 3.1). Thus we will show

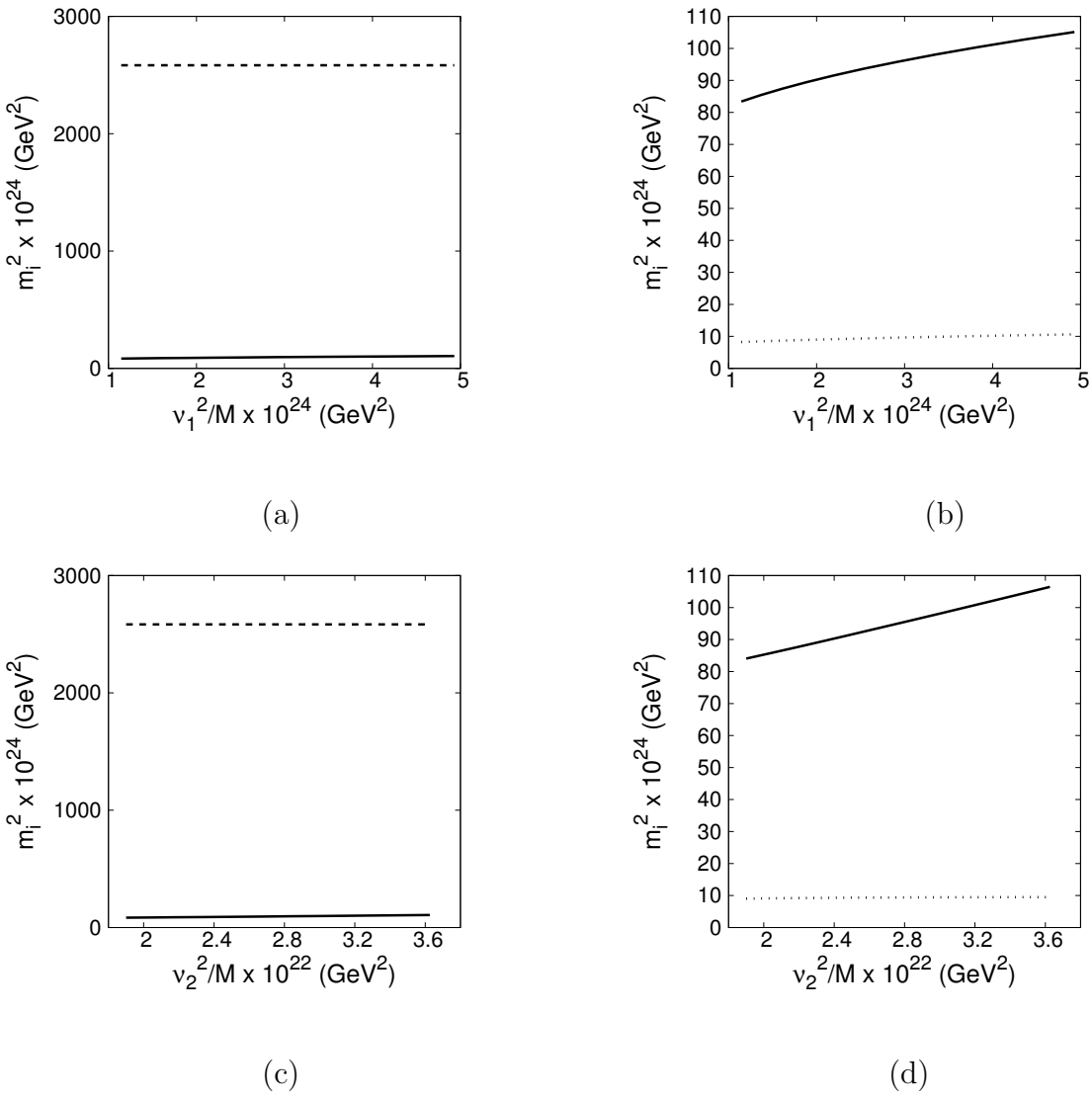


Figure 3.3: The same as in Fig. 3.2 but for the squared neutrino masses versus $[(g_1\nu_i)^2/M_1 + (g_2\nu_i)^2/M_2]^2$.

a region where breaking the degeneracy $\nu_\mu$-$\nu_\tau$ a normal hierarchy is obtained with $M_1 > 0$. This region is around the point of the parameter space shown in Table 3.11. In this example the angle $\sin^2\theta_{13}$ can easily be made small as required by the data, but it is not necessarily negligible. Thus the CP violating effects would be more present in the PMNS matrix. Besides, we can roughly say that $\sin^2\theta_{13}$ and $\sin^2\theta_{12}$ are interchanged with respect

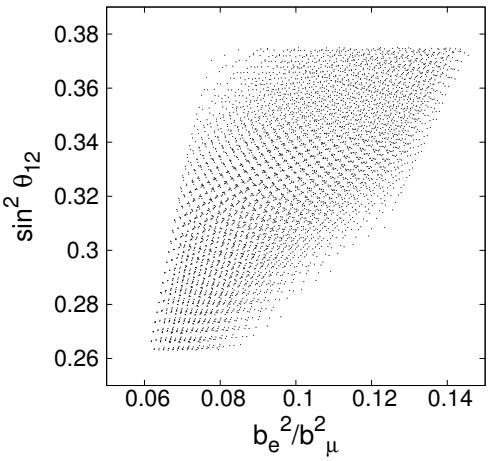


Figure 3.4: Variation of the solar mixing angle with respect to the relevant term that controls its evolution, $b_e^2/b_\mu^2$.

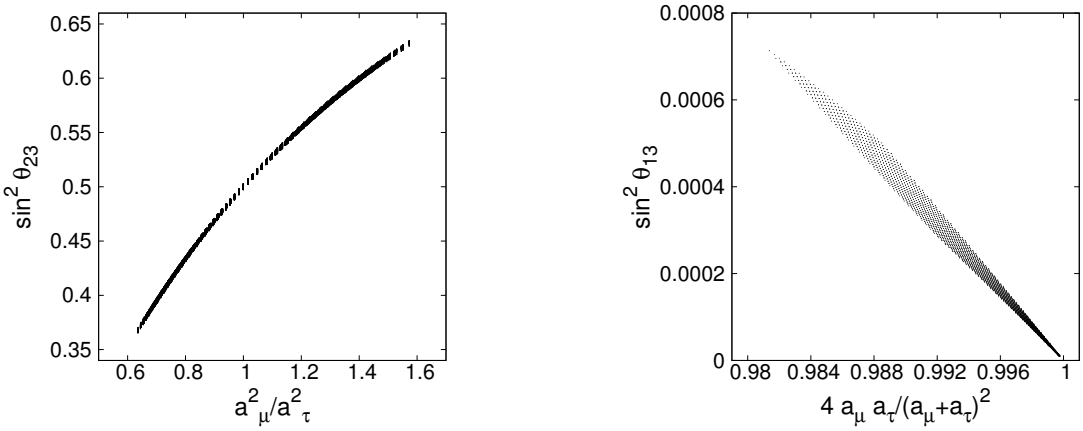


(a) (b)

Figure 3.5: (a) The variation of $\sin^2\theta_{23}$ with respect to the relevant term that controls its evolution, $a_\mu^2/a_\tau^2$. (b) The variation of $\sin^2\theta_{13}$ with respect to the term that measures the $\nu_\mu$-$\nu_\tau$ degeneracy.

to the case discussed above with $M_1 < 0$. For completeness, in Fig. 3.7a we show the variation of $\sin^2\theta_{13}$ with respect to the term that controls the gaugino seesaw relevant in this case, namely $b_e^2/(b_\mu^2+b_\tau^2)$. We also plot in Fig. 3.7b $\sin^2\theta_{12}$ as a function of the relevant term that controls the Higgsino-$\nu^c$ seesaw $\frac{4a_\mu a_\tau}{(a_\mu+a_\tau)^2}$. As mentioned above, an interesting feature of this region of

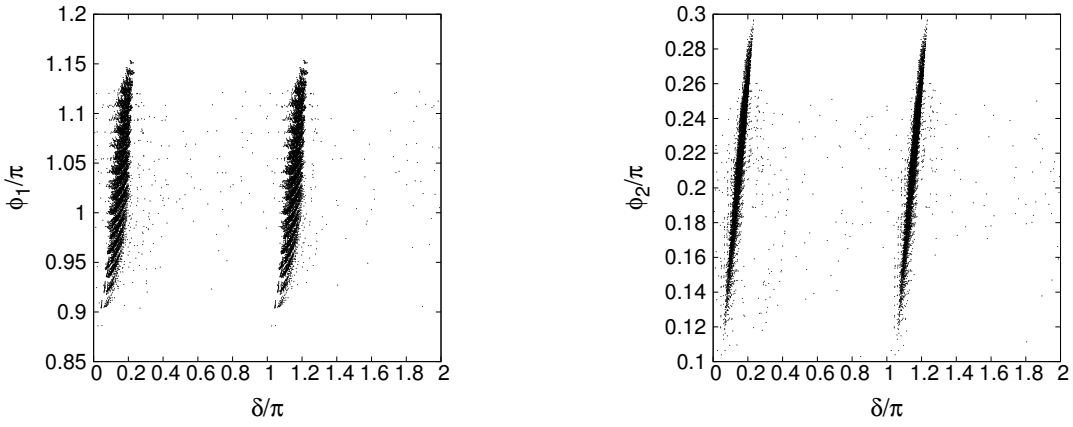


(a) (b)

Figure 3.6: $\delta - \phi_1$ plane (a) and $\delta - \phi_2$ plane (b) for the scenario with normal hierarchy and negative gaugino masses $M < 0$, varying simultaneously $Y_{\nu_i}, \nu_i, M_1$.

the parameter space is that the effect of the Dirac CP phase in the PMNS matrix is not removed, since the value of $\sin\theta_{13}$ is not negligible. Fig. 3.8 shows the derived CP phases of the PMNS matrix.

For the sake of completeness, we show in Table 3.12 an example where the inverse hierarchy scenario is achieved.

At this point it is clear that there are many regions in the parameter space with different characteristics, different compositions for the lightest neutralino or regions close to the tri-bimaximal mixing regime for normal or inverted hierarchy that can be found with different neutrino parameters. Furthermore, we have seen that the $\mu\nu$SSM with SCPV predicts non-zero CP-violating phases in the neutrino sector. We must say that none of these

| | | |
|---|---|---|
| $Y_{\nu_1} = 9.54 \times 10^{-7}$ | $Y_{\nu_2} = 9.47 \times 10^{-7}$ | $Y_{\nu_3} = 2.31 \times 10^{-7}$ |
| $\nu_1 = 8.59 \times 10^{-5}$ GeV | $\nu_2 = 2.25 \times 10^{-4}$ GeV | $\nu_3 = 2.29 \times 10^{-4}$ GeV |
| | $M_1 = 350$ GeV | |

Table 3.11: Numerical values of the relevant neutrino/neutralino-sector inputs that reproduce the neutrino experimental constraints, and correspond to the normal hierarchy scenario with $M_1 > 0$.

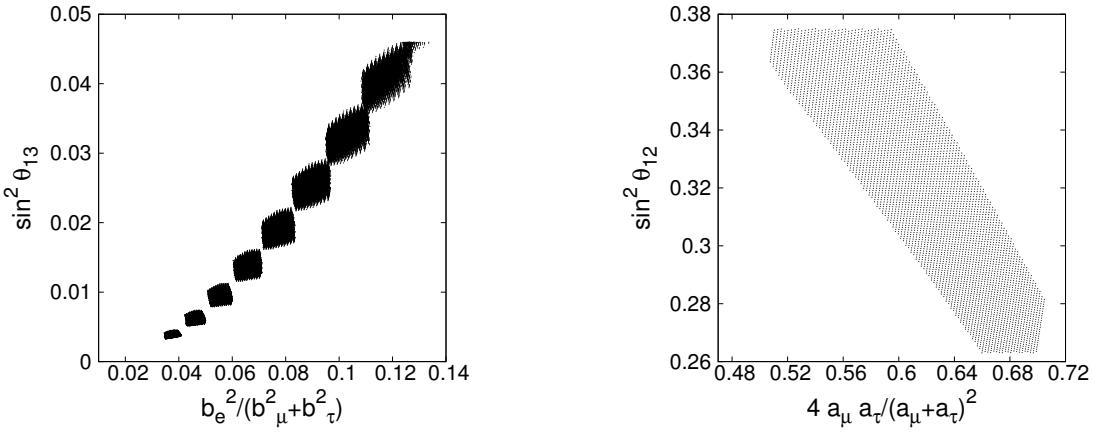


(a) (b)

Figure 3.7: (a) The variation of $\sin^2\theta_{13}$ with respect to the relevant term that controls its evolution. (b) The variation of $\sin^2\theta_{12}$ with respect to the relevant term $4a_\mu a_\tau/(a_\mu+a_\tau)^2$.

| | | |
|---|---|---|
| $Y_{\nu_1} = 5.98\times10^{-7}$ | $Y_{\nu_2} = 1.32\times10^{-6}$ | $Y_{\nu_3} = 1.40\times10^{-6}$ |
| $\nu_1 = 3.276\times10^{-4}$ GeV | $\nu_2 = 6.20\times10^{-5}$ GeV | $\nu_3 = 6.56\times10^{-5}$ GeV |
| | $M_1 = 340$ GeV | |

Table 3.12: Numerical values of the relevant neutrino/neutralino inputs that reproduce the neutrino experimental constraints, and correspond to the inverted hierarchy scenario.

phases have been measured already so it is not clear that CP violation occurs in the leptonic sector and the CP phases could, in principle, be zero. If in the future a non-zero CP violating phase in the lepton sector is measured, SCPV as the one analysed here could be a possible source.

## 3.5 Comments on CP phases and EDMs

Before presenting the conclusions of this chapter we would like to comment two relevant issues, the measurability of the CP-violating phases of the neutrino sector in neutrino experiments and the Electric Dipole Moments (EDMs) constraints.

Let us first comment the possibility of measuring the Dirac and Majorana

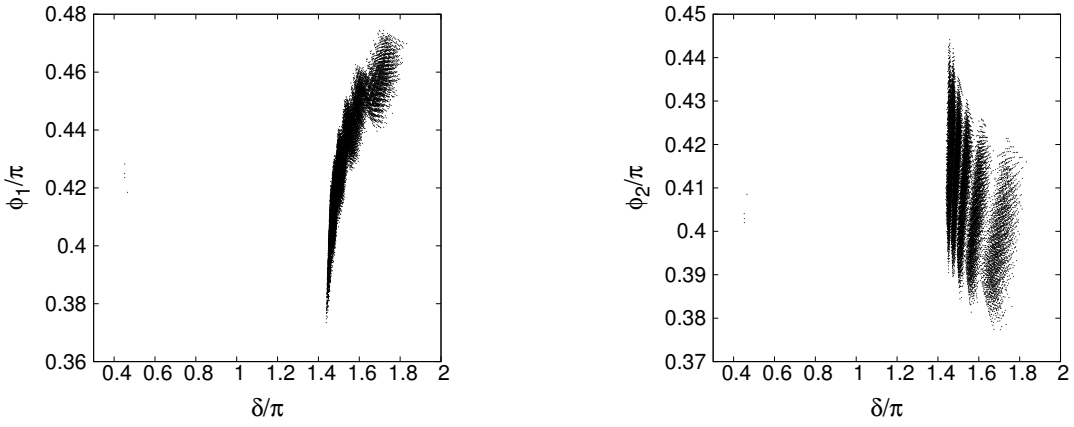


(a) (b)

Figure 3.8: $\delta - \phi_1$ plane (a) and $\delta - \phi_2$ plane (b) for the scenario with normal hierarchy and positive gaugino masses $M > 0$, varying simultaneously $Y_{\nu_i}, \nu_i, M_1$.

CP phases of the PMNS matrix in neutrino experiments. Neutrino oscillation experiments are sensitive only to the Dirac CP phase and insensitive to the Majorana phases. Let us briefly comment about the possible determination of $\delta$ in future neutrino experiments. The conservation of CP implies $P(\nu_\alpha \to \nu_\beta) = P(\bar{\nu}_\alpha \to \bar{\nu}_\beta)$. If CP is not conserved, we would have [70]

$$P(\nu_\mu \to \nu_e) - P(\bar{\nu}_\mu \to \bar{\nu}_e) = -16J \sin\left(\frac{\Delta m^2_{12} L}{4E}\right) \sin\left(\frac{\Delta m^2_{13} L}{4E}\right) \sin\left(\frac{\Delta m^2_{23} L}{4E}\right), \tag{3.53}$$

where $L$ is the oscillation length, $E$ is the neutrino beam energy and $J$ is the Jarlskog invariant for the neutrino mass matrix which is given by $J = s_{12}c_{12}s_{23}c_{23}s_{13}c^2_{13}\sin\delta$. There is only an upper experimental limit for $J$, $J < 0.04$. The reason is that $J$ depends on $\theta_{13}$ and $\delta$, which are currently unknown. If $\theta_{13}$ vanishes (recall the experimental bound $\sin^2\theta_{13} < 0.046$) $J$ vanishes and the effect of CP violation via (3.53) would be unobservable. The same occurs if there was a degeneracy in the neutrino masses. In spite of these extreme situations the process (3.53) implies that long baseline experiments allow the observation of CP violation due to the Dirac phase $\delta$ in the neutrino sector. Two experiments are designed for this purpose: NO$\nu$A [71] and the T2KK detector [72].

On the other hand, although Majorana phases affect neutrinoless double beta decay $0\nu\beta\beta$ [73], their determination turns out to be difficult.

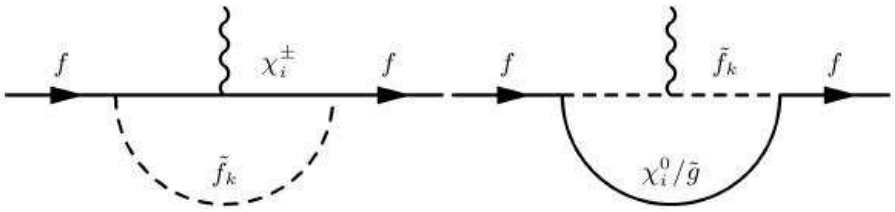


Figure 3.9: Loop contributions to fermion EDMs.

We want also to briefly discuss the issue of EDMs in our model. As it is well known, EDMs represent a serious challenge for supersymmetric theories in what is called the SUSY CP problem. The MSSM (with explicit CP violation in the soft Lagrangian) predicts EDMs about three orders of magnitude larger than the experimental bounds for the EDM of the electron and neutron if the SUSY CP violating phases are $\mathcal{O}(1)$ and the SUSY particles have masses near their current experimental bounds $\mathcal{O}(100)$ GeV [74]. There are usually three kind of solutions to this problem in supersymmetric theories. First, if the SUSY CP violating phases are unnaturally small, of order $\mathcal{O}(10^{-2} - 10^{-3})$ the EDM bounds can be easily satisfied [74]. Second, if the SUSY scalar particles are decoupled with masses larger than about 3 TeV and thus out of reach of the LHC but not spoiling the solution of SUSY to the hierarchy problem, the EDM bounds could also be accomplished [75]. Third, there can be internal cancellations between the different contributions to the EDMs [76].

The EDMs in our model arise at the loop level (see Figure 3.9). The definition of the EDM $d_f$ for a spin-$\frac{1}{2}$ particle is

$$\mathcal{L}_I = -\sum_{\mu\nu} \frac{i}{2} d_f \bar{\Psi} \sigma_{\mu\nu} \gamma_5 \Psi F^{\mu\nu}, \tag{3.54}$$

and the general interaction Lagrangian between two fermions $(\bar{\Psi}, \Psi)$ and a scalar $(\chi)$ containing CP violation is

$$-\mathcal{L}_{int} = \sum_{ik} \bar{\Psi}_f (K_{ik} \frac{1-\gamma_5}{2} + L_{ik} \frac{1+\gamma_5}{2}) \Psi_i \chi_k + h.c.. \tag{3.55}$$

Thus we can obtain the one loop EDM as

$$d_f = \sum_{ik} \frac{m_i}{(4\pi)^2 m_k^2} \mathrm{Im}(K_{ik} L_{ik}^*) \left[ Q_i A(\frac{m_i^2}{m_k^2}) + Q_k B(\frac{m_i^2}{m_k^2}) \right], \tag{3.56}$$

where $A$ and $B$ are loop functions that are given by $A(r) = \frac{1}{2(1-r)^2}(3 - r + \frac{2\log r}{1-r})$ and $B(r) = \frac{1}{2(1-r)^2}(1 + r + \frac{2r\log r}{1-r})$. $Q_i$, $Q_k$ are the charges and $m_i$,$m_k$ are the masses of the fermion and scalar respectively. Clearly CP violation is needed $\mathrm{Im}(K_{ik}L^*_{ik}) \neq 0$ for having a non-zero contribution to the EDMs. There are three different contributions depending on which particles are running in the loop: neutralino, chargino or gluino. As mentioned above, small EDMs compatible with the experimental bounds are achieved if these contributions cancel out. From (3.56) we can also see that if the CP phases are small or the scalar masses are heavy (thus respectively $\mathrm{Im}(K_{ik}L^*_{ik}) \to 0$ or $m_k \to \infty$ in (3.56)) both yield small EDMs.

We would like to point out that the $\mu\nu$SSM with SCPV could implement these three kind of solutions for the SUSY CP problem. First of all, the possibility of small CP phases is obviously present in our model. There are spontaneous CP violating global minima with small CP phases $\mathcal{O}(10^{-2}-10^{-3})$ that would imply values of the EDMs compatible with the experimental bounds. For example let us present a global minimum that break CP spontaneously with $\mathcal{O}(10^{-2})$ CP phases. We have also found global minima with $\mathcal{O}(10^{-3})$ phases.

The values of the soft-terms not determined by the minimization equations are chosen to be $A_{\kappa_{iii}}\kappa_{iii} = -175$ GeV for $i \neq 1$, $A_{\kappa_{ijk}}\kappa_{ijk} = 100$ GeV for $i,j,k \neq 1$ and $A_{\kappa_{ijk}}\kappa_{ijk} = -100$ GeV for one or two indices equal to 1. The numerical values of the phases and the rest of input parameters are presented in Tables 3.13 and 3.14.

Note that in a model with SCPV small phases are not unnatural. In the case of explicit CP violation, small CP phases in the soft Lagrangian sector are in principle unnatural because they are free parameters at the electroweak scale and it is difficult to realize why the breaking of supersymmetry could give rise to such unnatural small phases. On the contrary, small phases through VEVs are not unnatural, they are just a consequence of the minimization equations. The free parameters in a model with SCPV are the real soft parameters, the phases of the VEVs being determined with the minimization equations. Thus, for natural values of the real soft parameters

| | | |
|---|---|---|
| $\lambda_i = 0.13$ *for i=1,2,3* | $\kappa_i = 0.55$ *for i=1,2,3* | $\nu^c_1 = 900 GeV, \nu^c_2 = \nu^c_3 = 600 GeV$ |
| $\tan\beta = 29$ | $\varphi_v = 0$ | $\varphi_{\nu^c_1} = \frac{\pi}{100}$ |
| $\varphi_{\nu^c_2} = \varphi_{\nu^c_3} = -\frac{\pi}{100}$ | $\chi_1 = -\frac{\pi}{90}$ | $\chi_2 = \chi_3 = \frac{\pi}{90}$ |

Table 3.13: Numerical values of the relevant inputs of a global minimum that breaks CP spontaneously with small $\mathcal{O}(10^{-2})$ phases.

| | | |
|---|---|---|
| $Y_{\nu_1} = 1.9 \times 10^{-7}$ | $Y_{\nu_2} = Y_{\nu_3} = 1.06 \times 10^{-6}$ | $M_1 = 300$ GeV |
| $\nu_1 = 1.54 \times 10^{-4}$ GeV | $\nu_2 = \nu_3 = 2.4 \times 10^{-5}$ GeV | |

Table 3.14: Numerical values of the neutrino/neutralino inputs that reproduce the neutrino experimental constraints with the global minimum with small phases.

in the $\mu\nu$SSM, small phases of the VEVs are natural because the minimization conditions determine that the global minimum for these soft parameters has small values of the phases and the SUSY CP problem is solved without fine-tuning. This seems an advantage of the SUSY theories with the possibility of SCPV compared to SUSY theories with only explicit CP violation. Note that in this work we have taken the phases of the VEVs as inputs for simplicity in the calculation, but this is only an artifact of the computation.

The other two solutions, heavy scalars and internal cancellations also can be easily implemented in our model. Let us recall that the following soft parameters remain free in our model because they do not enter in the neutral scalar potential neither in the neutrino sector: $(A_u Y_u)_{ij}$ , $m^2_{\tilde{u}^c_{ij}}$ , $M_3$, $(A_e Y_e)_{ij}$ , $m^2_{\tilde{e}^c_{ij}}$ . Thus, the solution of the SUSY CP problem with heavy scalars remains valid for scalar masses heavier than about 3 TeV. We also expect the internal cancellations solution to be valid in our model since these free parameters enter in the calculation of the EDMs and we would have enough freedom to find regions on the parameter space where such cancellations could be accomplished reproducing the EDMs bounds.

Note that this discussion is only referred to the SUSY CP phases. The CKM phase has been measured to be $\mathcal{O}(1)$ but its contribution to the EDMs has been proved to be several orders of magnitude smaller than the bounds. In our model we would have various possibilities to generate the CKM phase. For example having complex Yukawas (the origin of CP violation being a combination of spontaneous and explicit), it is easy to generate the large CKM phase reproducing at the same time the EDM bounds.

In any case, a full computation of the EDMs in this model is beyond the scope of this chapter but we only wanted to remark that the usual solutions to the SUSY CP problem remain valid in this model. For interested readers, a more detailed analysis of EDMs constraints in a supersymmetric model with SCPV is performed in [77].

## 3.6 Conclusions

In this chapter we have studied in detail the neutrino sector of the $\mu\nu$SSM at the tree-level. This analysis is highly relevant for this model because one of the main motivations of the $\mu\nu$SSM is neutrino physics. We have also shown that, even if all parameters in the scalar potential are real, SCPV is possible at tree-level, and we have used these complex vacua to show how a complex PMNS matrix can arise.

In particular, we have calculated first the scalar potential of the $\mu\nu$SSM with real parameters, assuming the most general situation where the VEVs of Higgses and sneutrinos can be complex. The minimization equations of the scalar potential have been derived. We have shown, using a simple argument, that CP can actually be spontaneously violated in this model.

Then we have discussed the neutralino-neutrino mass matrix. Although the discussion is general, we have applied it also to the particularly interesting case of real vacua. We have analysed how the electroweak seesaw mechanism works in the $\mu\nu$SSM using approximate analytical equations for the effective neutrino mass matrix, particularized for certain interesting limits that clarify the neutrino sector behavior of the model. In addition, we have shown with a toy model the qualitative idea of how to find regions in the parameter space of the $\mu\nu$SSM that satisfy the neutrino experimental constraints. Let us remark that these constraints can be fulfilled even with a diagonal neutrino Yukawa matrix, since this seesaw does not involve only the right-handed neutrinos but also the MSSM neutralinos. Actually, to obtain the correct neutrino mixing angles turns out to be easy due to the following characteristics of this seesaw: R-parity is broken and the relevant scale is the electroweak one. In a sense, this gives an answer to the question why the mixing angles are so different in the quark and lepton sectors.

Finally, we have presented our results describing the method to obtain numerically global minima with SCPV, and giving examples of such minima. Let us emphasize however that, unlike the case with real VEVs where many global minima can be found, for the case with complex VEVs such minima are not so easy to find. In particular, one has to choose carefully the parameters of the model. For the examples found we have shown the dependence of the neutrino mass differences (for both normal and inverted hierarchies), mixing angles, and CP phases of the PMNS matrix, in terms of the relevant neutrino inputs always being into the experimental allowed region. Last but not least, we have checked that different regions on the parameter space can reproduce the neutrino experimental constraints. In this context, future neutrino experiments could be able to measure a non-zero Dirac CP-violating phase, opening the possibility to SCPV in the $\mu\nu$SSM as the dominant source

of CP violation in the leptonic sector. We have also discussed qualitatively the SUSY phase problem in the context of the $\mu\nu$SSM with complex VEVs. The three typical solutions to this problem can be implemented in our model, small CP phases (with the advantage of being natural in the case of SCPV, on the contrary that in the case of explicit CP violation), large masses of scalar particles and internal cancellations. In any case, if a non-zero Dirac CP phase is measured in neutrino experiments, SUSY models with SCPV arises as good candidates to explain this CP assymetry and among them, the $\mu\nu$SSM is probably one of the best motivated.

In what concerns the topics treated in this chapter, some phenomenological work has still to be done. In the case of SCPV in the $\mu\nu$SSM, including 1-loop corrections to the study of the vacuum and the neutrino sector would be interesting. A complete study of the EDMs in the case of SCPV would also be very welcome. Also finding a model based on the $\mu\nu$SSM with SCPV having a complex CKM matrix would be important. In this respect we would like to point out that extending the quark sector could lead to an effective complex CKM matrix [57] and the model found in Subsection 5.2.1 could be an interesting starting point. This model extends the gauge group of the $\mu\nu$SSM with an extra $U(1)$ factor and exotic colour triplets have to be added to the spectrum to cancel anomalies. Extending the Higgs sector could also lead to a complex CKM matrix. All these issues are left for future works.

# Chapter 4

# Higgs sector and collider physics

## 4.1 Motivations

In this chapter we will provide an overview of the collider phenomenology of the Higgs sector of the $\mu\nu$SSM. It is based on the work published in [15]. We will explain the novel features in the decays of the Higgs sector of the $\mu\nu$SSM compared to R-parity conserving models such as the NMSSM or compared to R-parity breaking models without extra singlet superfields such as the BRpV model. There are two main features that could help to distinguish the $\mu\nu$SSM from other SUSY models at colliders. On the one hand, since the LSP is no longer stable due to the breaking of R-parity, not all SUSY chains must yield missing energy events. In [43, 44, 45] the decays of the lightest neutralino were discussed, as well as the correlations of the decay branching ratios with the neutrino mixing angles. On the other hand, the breaking of R-parity also generates a peculiar structure for the mass matrices. In particular, the presence of right and left-handed sneutrino VEVs leads to mixing of the neutral Higgses with the sneutrinos producing $8 \times 8$ neutral scalar mass matrices. This extended Higgs sector could be very helpful for testing the $\mu\nu$SSM. It is clear than once a new model in physics is proposed, one of the most important issues to study is how it can be proved experimentally and this is the main motivation for this chapter.

In Section 4.2 we will analyse the Higgs sector of the $\mu\nu$SSM. In particular, we will study first the Higgs sector mixings, and second the possible Higgs decays taking place once a Higgs particle is produced at colliders. Finally, we will discuss the LEP constraints. For that we will compute the couplings of the Higgses with the Z boson, and the sum rules. In Section 4.3 we will briefly

review the production mechanisms of Higgses at lepton and hadron colliders. In Section 4.4 we will concentrate on Higgs decays that are genuine of this model, and could therefore serve to distinguish it from other SUSY models in certain regions of the parameter space. We will present a sample of numerical examples of viable benchmark points for LHC searches. For that, we will focus first our attention on the decays of a MSSM-like Higgs with a sizeable branching ratio into two lightest neutralinos. These neutralinos could decay inside the detector leading to displaced vertices. This fact can be used to distinguish the $\mu\nu$SSM from R-parity conserving models. Also, the product of the decays can be used to distinguish it from other R-parity breaking models. Higgs-to-Higgs cascade decays will also be studied, and we will discuss an interesting benchmark point with similar signals to the NMSSM that could also serve to distinguish the $\mu\nu$SSM from other R-parity breaking models. For completeness, we will discuss in Section 4.5 the possibility that gravitino dark matter in this model might alter the collider phenomenology through the decay channel neutralino to gravitino-photon. We will see that this branching ratio turns out to be negligible. Finally, the conclusions of this chapter are left for Section 4.6.

## 4.2 Higgs sector and decays

In this section we will analyse the mixings in the scalar (Higgs) sector of the $\mu\nu$SSM, and we will also study the possible decay modes of Higgses once they are generated at colliders. We will focus our attention on the novelties that this extended Higgs sector introduces compared to Higgs sectors of other SUSY models, like e.g. the one of the NMSSM. Finally, we will discuss the LEP constraints in the context of this model. In the following we will assume for simplicity that all parameters in the potential or in the Lagrangian are real (see Section 2.2), as well as the VEVs, i.e. that CP is conserved. As a consequence, the neutral CP-even scalars are not mixed with the neutral CP-odd scalars. On the other hand, all neutral scalars of the model are mixed, and since all them get VEVs, we will call them Higgses throughout this chapter. To be more precise, we will use the term 'Higgses' for the mass eigenstates, and 'Higgs doublets' or 'singlets' for the neutral components of the Higgs doublets or for right-handed sneutrinos respectively in the interaction basis.

### 4.2.1 Higgs sector mixings

The presence of right- and left-handed sneutrino VEVs in the $\mu\nu$SSM leads to the mixing of the neutral components of the Higgs doublets with the sneutrinos producing the $8\times 8$ neutral scalar mass matrices for the CP-even and CP-odd states [40] that can be found in Appendix A.1-A.2, where we have defined as usual

$$H_u^0 = \frac{h_u + iP_u}{\sqrt{2}} + v_u \ , \quad H_d^0 = \frac{h_d + iP_d}{\sqrt{2}} + v_d,$$
$$\widetilde{\nu}_i^c = \frac{(\widetilde{\nu}_i^c)^R + i(\widetilde{\nu}_i^c)^I}{\sqrt{2}} + \nu_i^c \ , \quad \widetilde{\nu}_i = \frac{(\widetilde{\nu}_i)^R + i(\widetilde{\nu}_i)^I}{\sqrt{2}} + \nu_i \ . \tag{4.1}$$

Note that after rotating away the CP-odd would be Goldstone boson, we are left with seven states. It is also worth noticing here that in the CP-even sector, the $5\times 5$ Higgs doublets-right handed sneutrino submatrix is basically decoupled from the $3\times 3$ left-handed sneutrino submatrix, since the mixing occurs only through terms proportional to $\nu_i$ or $Y_{\nu_{ij}}$ in (A.7),(A.8) and (A.10). As discussed in precedent chapters, because of the contribution of the small couplings $Y_\nu \sim 10^{-6,-7}$ to the minimization conditions for the left-handed sneutrinos, their VEVs turn out to be small $\nu \sim 10^{-4,-5}$ GeV. Then, all terms containing $Y_\nu$ or $\nu$ are negligible compared to the rest of terms that are of the order of the EW scale. The same decoupling between Higgs doublets-right handed sneutrinos and left-handed sneutrinos is true for the CP-odd sector.

On the contrary, the mixing between Higgs doublets and right-handed sneutrinos is not necessarily small. In the CP-even sector this is given by (A.5) and (A.6):

$$M^2_{h_d(\widetilde{\nu}_i^c)^R} = -a_{\lambda_i} v_u + 2\lambda_i\lambda_j v_d \nu_j^c - 2\lambda_k \kappa_{ijk} v_u \nu_j^c - Y_{\nu_{ji}}\lambda_k \nu_j \nu_k^c - Y_{\nu_{jk}}\lambda_i \nu_j \nu_k^c \ , \tag{4.2}$$

$$M^2_{h_u(\widetilde{\nu}_i^c)^R} = -a_{\lambda_i} v_d + a_{\nu_{ji}}\nu_j + 2\lambda_i\lambda_j v_u \nu_j^c - 2\lambda_k\kappa_{ilk} v_d \nu_l^c + 2Y_{\nu_{jk}}\kappa_{ilk}\nu_j\nu_l^c + 2Y_{\nu_{jk}} Y_{\nu_{ji}} v_u \nu_k^c \ . \tag{4.3}$$

Neglecting terms proportional to $Y_{\nu_{ij}}$, $\nu_i$, using $a_{\lambda_i} = (A_\lambda \lambda)_i$, and defining $\mu \equiv \lambda_j \nu_j^c$, one can write the above equations as

$$M^2_{h_d(\widetilde{\nu}_i^c)^R} \approx 2\lambda_i \mu v_d - 2\lambda_k \kappa_{ijk} v_u \nu_j^c - v_u (A_\lambda \lambda)_i \ , \tag{4.4}$$

$$M^2_{h_u(\widetilde{\nu}_i^c)^R} \approx 2\lambda_i \mu v_u - 2\lambda_k \kappa_{ilk} v_d \nu_l^c - v_d (A_\lambda \lambda)_i \ . \tag{4.5}$$

Let us now discuss how to suppress these mixings following the guide of [15]. This can be used to have very light $\tilde{\nu}^c$-like Higgses avoiding collider

constraints, but also, as we will discuss below, to have a doublet-like Higgs as the lightest one being as heavy as possible. The simplest possibility to suppress the mixings is that Eqs. (4.4) and (4.5) vanish. Clearly, this can be obtained with $\lambda_i \to 0$. Another possibility is that the sum of the three terms in the above equations vanishes. To simplify this analysis let us start with only one generation of right-handed neutrinos. Then,

$$0 \approx 2\lambda\mu v_u - 2\lambda\kappa v_d \nu^c - v_d A_\lambda \lambda \ , \tag{4.6}$$

$$0 \approx 2\lambda\mu v_d - 2\lambda\kappa v_u \nu^c - v_u A_\lambda \lambda \ , \tag{4.7}$$

and after a rotation in the mass matrix we obtain the condition [40]

$$A_\lambda = \frac{2\mu}{\sin 2\beta} - 2\kappa\nu^c \ , \tag{4.8}$$

similar to the one of the NMSSM (with $\nu^c \to S$) [42].

Following the same arguments as above, in the CP-odd sector, and after a rotation in the mass-squared matrix to isolate the Goldstone boson, we obtain the condition,

$$\lambda(A_\lambda - 2\kappa\nu^c)v = 0 \ , \tag{4.9}$$

implying $\lambda \to 0$ or $A_\lambda = 2\kappa\nu^c$.

The generalization of these results to three generations of right-handed neutrinos is straightforward. In addition to the solution $\lambda_i \to 0$, we obtain

$$A_{\lambda_i} = \frac{2\mu}{\sin 2\beta} - \frac{2}{\lambda_i}\sum_{j,k} \kappa_{ijk}\lambda_j \nu^c_k \ , \tag{4.10}$$

$$A_{\lambda_i} = \frac{2}{\lambda_i}\sum_{j,k} \kappa_{ijk}\lambda_j \nu^c_k \ , \tag{4.11}$$

for the CP-even and CP-odd sectors, respectively.

Nevertheless, although the above conditions for the decoupling of Higgs doublets and right-handed sneutrinos can be used in general, they are sufficient but not necessary conditions. As was shown in [40], there are regions of the parameter space where the off-diagonal mixing terms of the neutral scalar mass matrices are smaller than the diagonal terms, and then quite pure singlets can be obtained. Actually, we will use this mechanism in Section 4.4 in order to obtain interesting signals at colliders.

Let us finally emphasize that some of these conditions can be applied not only to obtain a very light $\tilde{\nu}^c$-like lightest Higgs, as discussed above, but

also to have the lightest scalar as heavy as possible[1]. Clearly this lightest scalar, for being as heavy as possible, must be Higgs doublet-like, since the right- and left-handed sneutrinos can be as heavy as we want. Thus to have the lightest scalar as heavy as possible the contamination with right-handed sneutrinos should be small. For this to happen the right-handed sneutrinos must be very heavy and/or the mixing should be small. However, for the latter we can not use the solution $\lambda_i \to 0$, since $\lambda_i$ must be as large as possible to saturate the upper bound on the lightest Higgs boson mass [40].

Summarizing, we have discussed in this subsection the mixing in the Higgs sector of the $\mu\nu$SSM. In particular, we have learnt how to suppress the mixings between right-handed sneutrinos and Higgs doublets. This can be used to have very light $\tilde{\nu^c}$-like Higgses avoiding collider constraints, but also to have a doublet-like Higgs as the lightest one being as heavy as possible.

### 4.2.2 Decays

Here we will study possible decay modes of the Higgses in the $\mu\nu$SSM, pointing out novel features with respect to other SUSY models as the MSSM, NMSSM or the BRpV. The presence of new fields extending the Higgs sector, and the fact that R-parity is not a symmetry of the model, give rise to new decays, thus changing substantially the phenomenology.

First of all, the Higgs-to-Higgs cascade decays can be more complicated since more Higgses are present in this model compared to the NMSSM (or the BRpV model in the case of R-parity breaking). As discussed above, in the $\mu\nu$SSM there are eight CP-even and seven CP-odd Higgses, while in the NMSSM there are three CP-even and two CP-odd Higgses. The relevant couplings for Higgs-to-Higgs decays in the $\mu\nu$SSM were computed in [15] and are written in Appendix B. The Feynman diagrams of all possible tree-level decays of the Higgses are given in Figs. 4.1-4.4. In particular, for a CP-even (CP-odd) decaying scalar we can see in Fig. 4.2 that the Feynman diagrams **a** and **c** (**b**) are crucial to understand new decays with respect to the NMSSM ones. Note that the Feynman diagram **b** (**a** and **c**) in the figure are present only if a source of CP violation is taken into account [2].

Let us assume that we have enough energy to generate only one CP-even Higgs at a collider, i.e., only one Higgs $h_1$, has mass below the threshold energy. Then the following decay is possible:

[1]Notice that the upper bound on the lightest Higgs boson mass for the $\mu\nu$SSM turns out to be similar to the one of the NMSSM [40].

[2]In order to reduce the number of Feynman diagrams shown in the figure, we allow an abuse of notation in the diagrams, since if CP is violated, CP-even and CP-odd Higgses mix together and the notation ceases to make sense.

$$h_1 \to 2 \text{ Standard Model fermions} . \tag{4.12}$$

In case that the second lightest Higgs, $h_2$, can be generated, the following cascade decay is possible if kinematically allowed:

$$h_2 \to 2h_1 \to 4 \text{ Standard Model fermions} . \tag{4.13}$$

If the third lightest Higgs, $h_3$, can be generated, then we have the possibility (if kinematically allowed)

$$h_3 \to 2h_2 \to 4h_1 \to 8 \text{ Standard Model fermions} . \tag{4.14}$$

The situation turns out to be more complicated if we take into account the decays to scalars that are not the ones immediately below in mass. Also we have the possibility of having light pseudoscalars entering in the game. In the $\mu\nu$SSM we have three/two (six/five including left-handed sneutrinos) pseudoscalars more than in the MSSM/NMSSM case, and they could be very light. Thus we may need to include the following decays (if kinematically allowed) into the cascades:

$$h_\alpha \to h_\beta h_\gamma , \qquad h_\alpha \to P_{\beta'} P_{\gamma'} , \qquad P_{\alpha'} \to P_{\beta'} h_\gamma . \tag{4.15}$$

where $\alpha,\ \beta,\ \gamma = 1, ..., 8$ and $\alpha',\ \beta',\ \gamma' = 1, ..., 7$.

In benchmark point 7 of Section 4.4 we will study an example where these types of Higg-to-Higgs cascade decays are present. Working with a MSSM-like CP even Higgs, $h_{\rm MSSM}$, it will decay into $b\bar{b}$ or through the cascades typical of the NMSSM, $h_{MSSM} \to 2P \to 2b2\bar{b}$, $h_{MSSM} \to 2h \to 4P \to 4b4\bar{b}$. In benchmark point 8 we will see that $h_{MSSM}$ can decay with the following relevant cascades: $h_{MSSM} \to 2h_1 \to 4P_{1,2} \to 4\tau^+4\tau^-$ or $h_{MSSM} \to 2P_3 \to 2b2\bar{b}$, because for the singlet-like pseudoscalars $P_{1,2}$ the decay into $b\bar{b}$ is kinematically forbidden, whereas for $P_3$ it is allowed. This is a genuine signal of the $\mu\nu$SSM.

Another difference of the $\mu\nu$SSM compared to the NMSSM, that comes from the breaking of R-parity, is that a very light lightest Higgs with the decays into $b\bar{b}$ or $\tau^+\tau^-$ kinematically forbidden, could decay into two neutrinos $\nu_i\nu_j$ at the tree-level. This possibility is included in the Feynman diagram **c** of Fig. 4.1, due to the mixing of the MSSM neutralinos and neutrinos. This decay takes place due to the presence of the superpotential terms $Y_\nu \hat{H}_u \hat{L} \hat{\nu}^c$. A Higgs with $H_u$ composition can decay in this way because the light neutrinos, that are mainly left-handed, have small right-handed neutrino $\nu^c$ components. A Higgs with $\tilde{\nu}$ component can decay to two neutrinos because

the light neutrinos can have respectively $\tilde{H}_u$ and $\nu^c$ components. Of special interest is the fact that a Higgs with $\tilde{\nu^c}$ composition can also decay into $\nu_i\nu_j$ because the light neutrinos can have $\tilde{H}_u$ component, as mentioned above, or through the $\kappa\hat{\nu}_i^c\hat{\nu}_j^c\hat{\nu}_k^c$ terms in the superpotential, taking into account that left- and right-handed neutrinos mix together. However, since the neutrino Yukawa couplings are small, it is difficult to compete with the usual 1-loop decay into photons through the chargino loop process (see Fig. 4.5). Then, the usual constraints for very light Higgses annihilating to photons [78] still apply.

Also we must take into account that, unless they are not kinematically allowed, new decays to leptons are present, as can be deduced from the Feyman diagram **d** of Fig. 4.1, since the charged leptons are mixed with the MSSM charginos. Then, a singlet-like Higgs could decay to charged leptons through the $\lambda\hat{\nu}^c\hat{H}_u\hat{H}_d$ terms in the superpotential, due to the chargino composition. The mixing of charged leptons with charginos also affects the loop diagrams describing Higgs decaying into photons (Fig. 4.5) due to the contribution from charged leptons running in the loop, since the charginos are contaminated with them. Besides, a Higgs with $\tilde{\nu}$ component can also decay into charged leptons through the $Y_e\hat{H}_d\hat{L}\hat{e}^c$ term in the superpotential. Notice that it can also decay into two light neutrinos through the contamination with $\tilde{H}_u^0$ and $\nu^c$ in the Yukawa term $Y_\nu\hat{H}_u\hat{L}\hat{\nu}^c$. For example for the benchmark point 2 shown in Table 4.2 in Section 4.4, the light singlet-like pseudoscalars $P_{1,2,3}$ decay mainly into $\tau^+\tau^-$ because of the small contamination with doublets.

An interesting situation that we will study in detail in Section 4.4, occurs when a MSSM-like CP even Higgs, $h_{\rm MSSM}$, has a sizeable branching ratio to two light neutralinos $h_{\rm MSSM} \to \tilde{\chi}^0\tilde{\chi}^0$. Since $R$-parity is broken, neutralinos can decay into a Higgs and a neutrino inside the detector leading to displaced vertices. This possibility is included in the Feynman diagram **c** of Fig. 4.1, due to the mixing of the MSSM neutralinos and neutrinos. Thus working with light on-shell singlet-like pseudoscalars, cascades of the type $h_{MSSM} \to \tilde{\chi}^0\tilde{\chi}^0 \to 2P2\nu \to 2b2\bar{b}2\nu$, leading to the final state 4 $b$-jets plus missing energy, will be present. If the decay of the pseudoscalars into two $b$'s is kinematically forbidden, then they decay into $\tau^+\tau^-$ generating the following cascade: $h_{MSSM} \to \tilde{\chi}^0\tilde{\chi}^0 \to 2P2\nu \to 2\tau^+2\tau^-2\nu$. We will also see that the final state 8 $b$-jets plus missing energy is possible in situations where singlet-like scalars are produced by the decay of the neutralino, and they decay to pseudoscalars as shown in (4.15), $h_{MSSM} \to \tilde{\chi}^0\tilde{\chi}^0 \to 2h2\nu \to 4P2\nu \to 4b4\bar{b}2\nu$. As mentioned above, in benchmark point 8 of Section 4.4, for the singlet-like pseudoscalars $P_{1,2}$ the decay into $b\bar{b}$ is kinematically forbidden, whereas for $P_3$ it is allowed, thus the following relevant cascades can be produced: $h_4 \to \tilde{\chi}_4^0\tilde{\chi}_4^0 \to 2P_{1,2}2\nu \to 2\tau^+2\tau^-2\nu$, $h_4 \to \tilde{\chi}_4^0\tilde{\chi}_4^0 \to 2h_{1,2,3}2\nu \to$

$4P_{1,2}2\nu \to 4\tau^+4\tau^-2\nu$, $h_4 \to \tilde{\chi}_4^0\tilde{\chi}_4^0 \to 2P_3 2\nu \to 2b2\bar{b}2\nu$.

Displaced vertices are typical signals of $R$-parity violating models and could help to distinguish the $\mu\nu$SSM from the NMSSM. In addition, other R-parity breaking models such as the BRpV [79] do not have singlets in the spectrum, and, as a consequence, the above decays can be considered as genuine of the $\mu\nu$SSM. Note e.g. that in the BRpV, if the lightest neutralino is lighter than gauge bosons, only three-body processes are available for its decay.

Regarding the charged Higgses, as was discussed in [40], they are mixed with the sleptons opening the following possibility. As usual, a slepton can decay into a neutralino and a lepton as shown in Fig. 4.6**a**. In a $R$-parity conserving model, if the neutralino is heavier than the slepton the latter will be stable. However, when $R$-parity is broken, the left-handed neutrinos mix with the neutralinos, and then the slepton decays into a lepton and a light neutrino. Since the charged Higgses are mixed with the sleptons, they can also decay in this way.

It is worth noticing here that, similarly to a slepton, a squark can decay into a quark and a light neutrino. This can be deduced from Figs. 4.6**b** and 4.6**c** using again that neutrinos and neutralinos mix together. Let us also mention that, as usual in $R$-parity breaking models, the squarks or the sleptons can be the LSP[3] without conflict with experimental bounds. Whereas in the MSSM/NMSSM this would imply a stable charged particle incompatible with these bounds, in the $\mu\nu$SSM the LSP decays.

In the next subsection we will study the couplings of the Higgses with the $Z$ boson and the sum rules in the $\mu\nu$SSM, discussing also the LEP constraints.

### 4.2.3 Couplings with the Z boson and sum rules

In the following we will discuss the LEP constraints, especially the ones coming from the Higgs-strahlung process shown in Fig. 4.7. In the previous subsection we have discussed Higgs-to-Higgs decays in the $\mu\nu$SSM (see Eq.(4.15)). Thus a CP-even Higgs originated through a Higgs-strahlung could decay in that way.

Let us remember that LEP data can be used to set lower bounds on the lightest Higgs boson mass in non-standard models, as shown in Fig. 4.8 from [80]. In the ratio $\xi^2 = (g_{hZZ}/g_{hZZ}^{SM})^2$, $g_{hZZ}$ designates the non-standard $hZZ$

[3]In the following we will define the LSP as the lightest supersymmetric particle present in the Lagrangian when the neutrino Yukawas are set to zero. As usual in $R$-parity breaking models, the LSP is not really well defined. For example, the lightest scalar with a singlet sneutrino composition can be lighter than the lightest neutralino. Also the left-handed neutrinos are very light and are mixed with the MSSM neutralinos.

coupling and $g^{SM}_{hZZ}$ the same coupling in the Standard Model. Whereas in Fig. 4.8, the Higgs boson is assumed to decay into fermions and bosons according to the Standard Model, when $BR(h \to b\bar{b})$ differs from the Standard Model one, the parameter in Fig. 4.8, $\xi^2$, must be replaced by $\xi^2\ BR(h \to b\bar{b})/BR_{SM}(h \to b\bar{b})$.

For the $\mu\nu$SSM for each Higgs we can define the couplings $\xi_\alpha$, with $\alpha = 1, ..., 8$, given by

$$\xi_\alpha = [v_u S(u,\alpha) + v_d S(d,\alpha) + \nu_i S(L_i,\alpha)]/v\ , \tag{4.16}$$

where $S(u,\alpha)$, $S(d,\alpha)$, $S(L_i,\alpha)$ are the fraction composition of up-type Higgs doublet, down-type Higgs doublet and left-handed sneutrinos of the $h_\alpha$ neutral scalar mass eigenstate. A sum over $i = 1, 2, 3$ is assumed in the last term, and $v^2 = v_u^2 + v_d^2 + \nu_i\nu_i$.

If more than one Higgs with mass below 114 GeV are present but they are degenerated, we could define $\xi^2 = \xi_\alpha\xi_\alpha$, where the sum is over all Higgses below 114 GeV, and still use Fig. 4.8 for $\xi^2\ BR(h \to b\bar{b})/BR_{\rm SM}(h \to b\bar{b})$.

Also with more than one Higgs below 114 GeV with arbitrary masses, for each Higgs these constraints can be used for the coupling $\xi^2_\alpha BR(h_\alpha \to b\bar{b})/BR_{\rm SM}(h \to b\bar{b})$. Notice however that, given a value of $\xi^2_\alpha BR(h_\alpha \to b\bar{b})/BR_{\rm SM}(h \to b\bar{b})$, the corresponding lower bound on the Higgs mass is a necessary but not sufficient condition to fulfil the LEP bounds.

Obviously, if the Higgs is mostly $\tilde{\nu}^c$-like the coupling goes to zero, and we could have three very light Higgses avoiding the LEP constraints. From the above discussion we can see that another way to avoid them would be to make $BR(h \to b\bar{b})$ small.

However, in the general case a more involved analysis is necessary, since for example more than $2b$ in the final state are possible. Let us remember that searches for $h \to \Phi\Phi$ and $\Phi \to b\bar{b}$ (where $\Phi$ is a CP-odd or CP-even Higgs) by OPAL [81] and DELPHI [82] impose a strong constraint on the parameter space of the Standar Model. Once combined these analyses, one obtains $M_H > 110$ GeV for $\xi \sim 1$. Nevertheless, in models with more scalars and pseudoscalars it is possible to obtain a larger number of $b\bar{b}$, e.g. $h_3 \to 2h_2 \to 4P_1 \to 4b4\bar{b}$. It seems therefore that a re-analysis of the LEP data, to take into account this well motivated and complex phenomenology, would be interesting. Specially interesting would be to re-analyse the well-known $2.3\sigma$ excess in the $e^+e^- \to Z + b\bar{b}$ channel in the LEP data around 100 GeV. In the context of the NMSSM, the consistency of the excess with $h \to PP$ decays was discussed in [83].

Searches for $e^+e^- \to hZ$ independent of the decay mode of the Higss by OPAL [84], could also be important to exclude some regions of the parameter space.

Searches for $h \to \Phi\Phi$ and $\Phi \to gg$, $\Phi \to c\bar{c}$, $\Phi \to \tau^+\tau^-$ by OPAL [85], and the recent analysis of the Higgs decaying into four taus carried out in [86], must also be taken into account. Nevertheless, the $\mu\nu$SSM requires a more detailed analysis than the one available in the literature, since for instance a larger number of $\tau's$ in the final states is possible.

It is also worth mentioning that an on-shell or off-shell Z could decay into neutralinos, with the three lightest neutralinos being very light and mainly composed by left-handed neutrinos. The decay of the neutralinos $\tilde{\chi}_a^0$ with $a = 4, ..., 10$ was discussed in [43, 44]. Invisible Z width constraints [87] must be applied.

Let us finally discuss the sum rules. For the $\xi_\alpha$ defined in Eq. (4.16), one can obtain the following sum rule:

$$\sum_{\alpha=1}^{8} \xi_\alpha^2 = 1 \ . \tag{4.17}$$

Notice that for the three $\tilde{\nu}$-like Higgses the corresponding $\xi_\alpha$ can be neglected, and therefore one can write

$$\sum_{\phi=1}^{5} \xi_\phi^2 \approx 1 \ , \tag{4.18}$$

where

$$\xi_\phi \approx [\sin\beta \ S(u,\phi) + \cos\beta \ S(d,\phi)] \ , \tag{4.19}$$

with $\tan\beta = \frac{v_u}{v_d}$ defined as usual, since the VEVs $\nu_i$ are very small as discussed above.

Also another important sum rule, in analogy with the one discussed in [88], is valid:

$$\sum_{\alpha=1}^{8} \xi_\alpha^2 M_{h_\alpha}^2 = M_{max}^2 \ , \tag{4.20}$$

where, neglecting terms with $Y_\nu$ and $\nu$, $M_{\rm max}$ is the upper bound on the lightest Higgs mass studied in [40]

$$M_{max}^2 = M_Z^2 \left( \cos^2 2\beta + \frac{2\lambda_i \lambda_i \cos^2\theta_W}{g_2^2} \sin^2 2\beta \right) + rad. \ corr. \tag{4.21}$$

Using Eqs. (4.17) and (4.20) one can deduce, as in the case of the NMSSM [89], that

$$M_{h_2}^2 \leq \frac{1}{1-\xi_1^2}(M_{\rm max}^2 - \xi_1^2 M_{h_1}^2) \ , \tag{4.22}$$

where $h_1$ and $h_2$ are the lightest and next-to-lightest Higgses.

Finally let us mention that a simple way to avoid current collider constraints is to make the new Higgses very heavy, in such a way that the constraints apply only to the first one, as we will see in benchmark point 6 presented in Section 4.4. Then very interesting signals could be expected from the Higgs cascade decays in experiments like LHC.

## 4.3 Production mechanisms at colliders

In this section we will briefly discuss the production mechanisms of a Higgs at lepton and hadron colliders. Once produced, the Higgs can decay through the processes explained in the previous section.

### 4.3.1 Lepton colliders

Let us start with a brief description of the main processes at leptonic colliders regarding Higgs production.

**LEP I**

Running with centre of mass energies close to the mass of the Z, $\sqrt{s} \approx$ 90 GeV, the Bjorken process shown in Fig. 4.9 is in principle the most relevant one. Besides, in this model could be important an on-shell $Z$ going to two light Higgses also on-shell (one scalar and one pseudoscalar, as shown in Fig. 4.10), as discussed in [82].

**LEP II**

Running with centre of mass energies close to the mass of the Z + the mass of the Higgs, ($\sqrt{s} \approx 209$ GeV), the Higgs-strahlung process shown in Fig. 4.7 is in principle one of the most relevant ones. Also important is the vector boson fusion process shown in Fig. 4.11. But in principle these are not the only relevant processes for Higgs production, specially for this model. The off-shell $Z$ could give rise to two on-shell Higgses (one scalar and one pseudoscalar, as shown in Fig. 4.10). The Yukawa process shown in Fig. 4.12 could also be important, where the case where both fermions are ejecting a Higgs could be relevant.

**ILC**

In this case vector fusion is in principle the most relevant process. But this depends on the energy of the collider. The case of an off-shell Z giving on-shell Higsses could be very important if the centre of mass energy is close to the sum of the masses of the Higgses.

### 4.3.2 Hadron colliders

The larger phase space with respect to the one of the MSSM, for Higgs decays, gives a rich phenomenology that could in principle be detected at the LHC, although constraints from hadron colliders are more complicated to analyse because of the hadron behaviour.

The most important processes for hadron colliders are: the gluon gluon fusion shown in Fig. 4.13, the vector fusion, the Higgs-strahlung and the analog with the W boson, $W \to W\ h$, where the first vector is off-shell and the Higgs and the resulting W are on-shell.

The associated production with heavy quarks, this is $gg \to Q\bar{Q}\ h$ or $q\bar{q} \to Q\bar{Q}\ h$ can also be important (see for example Fig. 4.14). Also in hadron colliders there are several possibilities for Higgs pair production, this is $pp \to hh\ X$, but it is beyond the scope of this work to review in detail the Higgs production mechanisms. Nevertheless, in Section 4.4 we will briefly discuss about the dominant production process and the production cross sections for the benchmark points presented.

## 4.4 Signals at colliders

In the previous sections we have tried to provide a general overview of the production and decays of the Higgses of the $\mu\nu$SSM. In this section we will concentrate in decays that are genuine of this model, and could therefore serve to distinguish it from other SUSY models. For that, we will focus first our attention on the decays of a MSSM-like Higgs with a mass about 114 GeV (for being detectable in the near future), and with a sizeable branching ratio into two lightest neutralinos. These neutralinos could decay inside the detector leading to displaced vertices. This fact can be used to distinguish the $\mu\nu$SSM from R-parity conserving models such as the NMSSM. For example, as mentioned in subsection 4.2.2, the lightest neutralino[4] $\tilde{\chi}_4^0$'s can decay into an on-shell light singlet pseudoscalar (that subsequently decays into $b\bar{b}$) and a neutrino, and therefore the decay $h_{MSSM} \to \tilde{\chi}_4^0\tilde{\chi}_4^0 \to 2P2\nu \to 2b2\bar{b}2\nu$ is genuine of the $\mu\nu$SSM. In other R-parity breaking models such as the BRpV, there are no singlet Higgses and a lightest neutralino lighter than gauge bosons could decay only through three-body decay processes. However, we have to point out that since the final decay products could be the same in both models, this may be difficult to distinguish experimentally.

We will also discuss an example where the Higg-to-Higgs cascade decays

[4]In our convention, when we refer to 'neutralino', we are excluding the three light left-handed neutrinos $\tilde{\chi}_{1,2,3}^0$.

studied in subsection 4.2.2 are relevant to distinguish the $\mu\nu$SSM from other SUSY models.

Following the above strategy, in this section we will present a sample of numerical examples of viable benchmark points of interest for LHC searches. The study of the heavier doublet-like Higgs, where the cascades described in subsection 4.2.2 could also be relevant, is left for a future work.

Let us mention that for the computation we have used a spectrum generator for the $\mu\nu$SSM (see [40] for a description[5]), linked with modified subroutines for the model, based on the codes NMHdecay [90] and Spheno [91]. In particular, the modified subroutines based on the code NMHdecay are used to compute the two-body decays of all Higgses present in the $\mu\nu$SSM. We have also built a subroutine to compute the two-body decays of neutralinos. The modified subroutines based on the code Spheno are used to compute the three-body decays of neutralinos.

We have searched for points of the parameter space that are safe from exclusion by current collider constraints but that could be detected in the near future at LHC. Nevertheless, a full analysis of these points in the light of LEP and TEVATRON is beyond the scope of this work and then it is not possible to totally guarantee that all the points satisfy all experimental constraints. In any case, if any of the benchmark points provided here is not completely safe from experimental constraints, it would be in the border and with small variations of the values of the parameters could be driven to the allowed experimental region.

Below we give a list with all the constraints that we are imposing on the points analysed. Some of them have already been discussed in the previous sections.

First, all the points are true minima of the neutral scalar potential. We have checked that tachyons do not appear and that the couplings fulfil Landau pole constraints at the GUT scale.

We have verified that all the points satisfy $3\sigma$ neutrino sector constraints [67] shown in Table 3.1 from the previous chapter.

We have guaranteed that current limits on sparticle masses with R-parity conserved are satisfied, excluding points with charged Higgs/sleptons, charginos, squarks and gluinos too light [92, 93]. We are being conservative, since strictly speaking these limits apply only to R-parity conserving models.

In the neutral Higgs sector we have checked the constraints on the reduced couplings $\times$ branching ratios in terms of the masses, for all the CP-even and CP-odd scalars, in the following channels analysed at LEP:

[5] In this version we have included one-loop corrections to neutrino masses (in general to neutralinos). These corrections have been computed in [46].

1) For $e^+e^- \to hZ$ with the following decays of h,

- $h \to$ invisible [94, 95]. Here we are assuming as invisible, the light neutrinos. A more elaborated analysis requires a re-analysis of LEP data, taking into account for instance that neutralinos could partially contribute to the missing energy when the decay distance is comparable to the size of the detector. We have checked that in the points where the decay length of the lightest neutralino is considerably greater than $\mathcal{O}(1\text{ m})$, considering also the LSP as invisible, the constraint is satisfied.
- $h \to \gamma\gamma$, from LEP Higgs working group results [78].
- $h \to b\bar{b}$, from the LEP Higgs working group [80].
- $h$ to two jets, from OPAL and the LEP Higgs working group, both at LEP2 [96, 97].
- $h \to \tau^+\tau^-$, from the LEP Higgs working group [80].
- $h \to PP$ with $PP$ decaying to 4 jets, 2 jets + cc, 2 jets + $\tau^+\tau^-$, 4 $\tau' s$, cccc, $\tau\tau + cc$, from OPAL results [85].

2) For $e^+e^- \to hP$ with $hP$ decaying into $4\,b$, $4\,\tau$, and $PPP \to 6b$ studied by DELPHI [82].

3) For $e^+e^- \to hZ \to PPZ \to 4b + 2jets$ the DELPHI constraints [82].

4) For $e^+e^- \to hZ$ independent of $h$ decay mode, combining the results of ALEPH and OPAL collaborations [94, 80].

On the other hand, as discussed in detail in [40], using the eight minimization conditions for the neutral scalar potential we have solved the soft masses $m_{H_u}$, $m_{H_d}$, $m_{\tilde{L}_i}$ and $m_{\tilde{\nu}_i^c}$ in terms of $\tan\beta$, $\nu_i^c$, $\nu_i$, and we have used the fact that $\nu_i$ are very small in order to define $\tan\beta \approx \frac{v_u}{v_d}$ and $v^2 \approx v_u^2 + v_d^2$ as usual. For simplicity, to perform the numerical analysis we have assumed a diagonal structure of the parameters in flavour space. We have also assumed universality for most of the parameters. In the case of the neutrino parameters this is not possible, since we need at least two generations with different $Y_{\nu_i}$ and $\nu_i$ in order to guarantee the correct hierarchy of neutrino masses as shown in Chapter 3. Besides, an exact universality of the other parameters would produce degenerations in the spectrum. Since we are working with low-energy parameters, the presence of exact universality after the running from higher scales seems to be extremely unlikely. To avoid this artificial situation, but still maintaining the simplicity of using universal parameters in the computation, we have slightly broken the universality in the diagonal

entries of the $\kappa$ tensor. On the other hand, in the case of the trilinear terms we take all of them proportional to the corresponding Yukawa couplings.

To summarize, the independent low-energy free parameters that we are varying in our analysis are,

$$\lambda_i = \lambda,\ \tan\beta,\ \kappa_{iii},\ \nu_i^c = \nu^c,\ \nu_1,\ \nu_2 = \nu_3,\ Y_{\nu_1},\ Y_{\nu_2} = Y_{\nu_3},\ A_\lambda,\ A_\kappa,\ M_2, \tag{4.23}$$

where for $M_1$ and $M_3$ we are assuming a relation that mimics the one coming from unification at the GUT scale, $M_1 = \frac{\alpha_1^2}{\alpha_2^2} M_2$, $M_3 = \frac{\alpha_3^2}{\alpha_2^2} M_2$, implying $M_1 \approx 0.5 M_2$, $M_3 \approx 2.7\, M_2$. In addition we have fixed the following soft parameters as, $m_{\tilde{Q}} = 1000\text{GeV}$, $m_{\tilde{u}} = 1000\text{GeV}$, $m_{\tilde{d}} = 1000\text{GeV}$, $m_{\tilde{e}} = 1000\text{GeV}$, $A_e = 1000\text{GeV}$, $A_u = 2400\text{GeV}$, $A_d = 1000\text{GeV}$, $A_\nu = -1000\text{GeV}$. Let us remark, nevertheless, that we have varied the value of $A_u$ for certain points, since it is relevant for the 1-loop corrections to the mass of the Standard Model Higgs.

For the values of the parameters that we will use in the benchmark points below, it is possible to show [40] using Appendix A that the mixing between the Higgses and the right-handed sneutrinos is of the order of $a_{\lambda_i} v_u = A_\lambda \lambda v_u$, and therefore small compared with the relevant diagonal terms $\lambda_i \lambda_j \nu_i^c \nu_j^c = 9\lambda^2 (\nu^c)^2$. Thus the Higgs doublets are basically decoupled from the right-handed sneutrinos. Note also that the right-handed neutrino masses are given by a value that can be approximated as $2\kappa_{iii}\nu^c$ [40].

Taking all the above into account, let us discuss now eight interesting benchmark points for collider physics. For the first three points that we will consider, the lightest neutralino $\tilde{\chi}_4^0$, is mainly a right-handed neutrino, since we take the value of $2\kappa_{iii}\nu^c$ small compared to the soft gaugino mass $M_2$ and Higgsino masses $\mu = \lambda_i \nu_i^c$. This composition of the LSP is genuine of the $\mu\nu$SSM and hence, very interesting to study. In principle, in such a case the decay length is usually $\mathcal{O}(1\ m)$ in contrast with other R-parity violating models such as the BRpV model where the decay length of the LSP is $\mathcal{O}(1\ cm)$. The other right-handed neutrino-like neutralinos $\tilde{\chi}_{5,6}^0$ are slightly heavier than $\tilde{\chi}_4^0$, and once produced in the decay of a Higgs, they decay rapidly to $\tilde{\chi}_4^0$ through 3-body processes such as $\tilde{\chi}_{5,6}^0 \to \tilde{\chi}_4^0 q\bar{q}$ or $\tilde{\chi}_{5,6}^0 \to \tilde{\chi}_4^0 l\bar{l}$.

On the other hand, for benchmark points 4,5 and 6, the lightest neutralino $\tilde{\chi}_4^0$ is MSSM-like. For example, taking small enough values for $M_2$ one can have a MSSM lightest neutralino almost bino-like. The right-handed neutrino-like neutralinos $\tilde{\chi}_{5,6,7}^0$ also decay through three-body processes to the lightest one and quarks/leptons very promptly.

Thus, additional quarks or leptons are present in the cascades due to the decays of the right-handed neutrino-like neutralinos into the lightest one.

Finally, in benchmark points 7 and 8 we work again with the lightest neutralino as a right-handed neutrino, although for benchmark point 7 it does not play an important role in the Higgs cascades and only Higgs-to-Higgs cascade decays are relevant.

Let us also remark that for all the eight benchmark points, $A_\kappa$ is chosen small for having light pseudoscalars, since its contribution is the dominant one in the diagonal element of the mass matrix. In this way the neutralino can decay into a light pseudoscalar and a neutrino through two-body processes, producing a distinctive signal. Since we have light singlets, we are also choosing for simplicity small values of $\tan\beta$ in order to be able to fulfill LEP constraints more easily.

Benchmark point 1 is presented in Table 4.1. There we only show the relevant masses and branching ratios for our discussion. The masses of the heavier doublet-like Higgs and left-handed sneutrinos (both scalars or pseudoscalars) are larger than the ones shown, and we do not study the decays of such Higgses. Neither the heavier MSSM-like neutralinos $\tilde{\chi}^0_{7,8,9,10}$ play any role on our discussion. In this benchmark point a doublet-like Higgs with mass $m_{h_4} = 118.8$ GeV can decay into two neutralinos with masses $m_{\tilde{\chi}^0} \approx 34 - 42$ GeV, and with a branching ratio of 4%. The lightest neutralino can decay through a two-body decay process to a scalar/pseudoscalar and a neutrino. Note that the branching ratios of the decays of neutralinos are referred only to two-body processes, while the decay lengths shown in the tables take into account two- and three-body processes. The decay into a pseudoscalar $P_{1,2,3}$ and a neutrino takes place in 67% of the cases. These pseudoscalars are mainly decaying into $b\bar{b}$ and a displaced vertex could be detected since the decay length of the lightest neutralino is 23 cm. Besides the cascade $h_4 \to \tilde{\chi}^0\tilde{\chi}^0 \to 2P2\nu \to 2b2\bar{b}2\nu$, the lightest neutralino could also decay to a CP-even singlet and a neutrino in 33% of the cases, with the CP-even Higgs decaying into two pseudoscalars. Then, the following cascade is also relevant: $h_4 \to \tilde{\chi}^0\tilde{\chi}^0 \to 2h2\nu \to 4P2\nu \to 4b4\bar{b}2\nu$, leading to 8 $b$-jets plus missing energy with a displaced vertex.

Benchmark point 2 is given in Table 4.2. In this case the decay of the Standard Model Higgs with a mass $m_{h_4} = 116.2$ GeV into neutralinos is enhanced to a 12%, since neutralino masses are smaller than in benchmark point 1 due to the smaller value of $2\kappa_{iii}\nu^c$. Besides, the decay of the lightest neutralino into CP-even Higgses is kinematically forbidden. Notice also that in this case the decay of the pseudoscalars into two b's is kinematically forbidden and then they decay into $\tau^+\tau^-$. Summarizing, the following cascade leading to a displaced vertex takes place: $h_4 \to \tilde{\chi}^0\tilde{\chi}^0 \to 2P2\nu \to 2\tau^+2\tau^-2\nu$. Note that in this case the decay length of the lightest neutralino $\tilde{\chi}^0_4$ is increased to 1.89 m since the mass of the lightest neutralino is smaller than in

benchmark point 1.

Benchmark point 3 is given in Table 4.3. A doublet-like Higgs with mass $m_{h_4} = 116.6$ GeV can decay into two neutralinos with masses $m_{\tilde{\chi}^0} \approx 47 - 50$ GeV in an 0.5% of the cases, with the interesting cascade $h_4 \to \tilde{\chi}^0\tilde{\chi}^0 \to 2P2\nu \to 2b2\bar{b}2\nu$. The decay length of the lightest neutralino $\tilde{\chi}^0_4$ is 12 $cm$.

Let us finally remark that, as expected, we have observed that increasing the mass of the lightest neutralino, its decay length is reduced. On the other hand, reducing the mass of the light pseudoscalars a few GeV, the decay into two b's can be kinematically forbidden, producing a dominant decay to leptons. Also it is possible to decrease the mass of the Higgs to values about 100 GeV, and then have a Higgs scenario in the line of the work [83], escaping the large fine-tuning and little hierarchy problems. We would also like to point out that, as was shown in [40], modifying the value of $\lambda$, it is possible to increase the mass of the MSSM-like Higgs up to about 140 GeV.

The input parameters of the benchmark point 4, presented in Table 4.4, are similar to those of the benchmark point 3, except for the fact that we are decreasing the soft gaugino mass $M_2$, and therefore generating a MSSM-like lightest neutralino (almost bino-like). Thus the production through the Standard Model-like Higgs decay is increased to 42%. Notice that while in the previous benchmark points only three neutralinos $\tilde{\chi}^0_{4,5,6}$ have masses below half of the mass of the Standard Model Higgs $h_4$, here four neutralinos $\tilde{\chi}^0_{4,5,6,7}$ fulfill that condition. The lightest neutralino has a decay length of 1.65 $m$ and decays into a pseudoscalar $P_{1,2,3}$ and a neutrino, with the pseudoscalar decaying 93% of the cases into two $b$'s. In this case, the production of $b$'s described through the cascade decays of the Standard Model Higgs, leading to displaced vertices, $h_4 \to \tilde{\chi}^0\tilde{\chi}^0 \to 2P2\nu \to 2b2\bar{b}2\nu$, is very enhanced and competes with a similar branching ratio for the direct decay of the Standard Model Higgs to two $b$'s.

Benchmark point 5 is given in Table 4.5. It is very similar to benchmark point 4, but reducing the trilinear soft term $A_u$, that is important for the 1-loop corrections to the mass of the Higgs, we can decrease the Standard Model Higgs mass to $m_{h_4} \sim 112.8$ GeV. LEP constraints are still satisfied since the branching ratio of $h_4$ into two $b$'s is dramatically reduced in favour of the branching ratio into neutralinos. We have checked that in this case, the process $h_4 \to \tilde{\chi}^0\tilde{\chi}^0 \to 2P2\nu \to 2b2\bar{b}2\nu$ satisfies the $4b$'s LEP constraint. We have also checked that the invisible Higgs constraint is satisfied even if we consider the lightest neutralino as invisible. Nevertheless, a more involved analysis of LEP data would be necessary regarding this point, to take into account the missing energy carried by the neutrinos.

Benchmark point 6 is presented in Table 4.6. In this case, the spectrum is heavier, with all CP-even singlet scalars above 114 GeV, and with $h_1$

being the Standard Model Higgs. The pseudoscalars are also considerably heavier than in the other benchmark points. This case is similar to the usual ones of the MSSM. The small difference comes from the fact that the Standard Model Higgs would decay in a significant ratio of 2% into neutralinos leading to displaced vertices. The lightest neutralino, MSSM-like, will have two-body decays kinematically forbidden and will decay only through three-body processes with a decay length of 5.33 $m$. In Table 4.6 we show the branching ratios to the following decay products (with a notation neglecting the mixings): $\nu ll$, $lq\bar{q}$, $\nu q\bar{q}$, $3\nu$.

Benchmark point 7 is presented in Table 4.7. In this case, the universality assumption has been broken also for the $\lambda_i$ parameters in order to favour the decay of $h_4$ into two singlet-like scalars $h_1$. Now the neutralino does not play an important role in the cascade decays of the Higgs, since the branching ratio of $h_4$ into two neutralinos is very suppressed. This is due to the fact that the only kinematically allowed decay of Higgs to neutralinos is $h_4 \to \tilde{\chi}_4^0\chi_4^0$, and $\tilde{\chi}_4^0$ is quite pure right-handed neutrino-like. The MSSM-like Higgs with a mass $m_{h_4} = 119.6$ GeV will have the typical decay of the MSSM into $b\bar{b}$ or the typical cascades of the NMSSM, $h_4 \to 2P \to 2b2\bar{b}$, in most of the cases. The decay of the Higgs $h_4$ into two CP-even singlet-like Higgses, with a branching ratio of 4% is also possible. Thus the following cascade is relevant $h_4 \to 2h_1 \to 4P \to 4b4\bar{b}$. These cascades serve to distinguish the $\mu\nu$SSM from other R-parity violating models. Besides, once a SUSY particle is produced at the collider, decaying into the LSP, the displaced vertex will allow to distinguish the $\mu\nu$SSM from the NMSSM.

Finally, let us discuss benchmark point 8 shown in Table 4.8, where we work again with a right-handed neutrino-like lightest neutralino. The main feature of this case is that, whereas for the singlet-like pseudoscalars $P_{1,2}$ the decay into $b\bar{b}$ is kinematically forbidden, for $P_3$ it is allowed. Then, several cascade decays are expected. The MSSM-like Higgs, $h_4$, has a mass of 120.2 GeV. Apart from the typical decay of the MSSM, $h_4 \to b\bar{b}$, it can also decay without leading to displaced vertices with the following relevant cascades: $h_4 \to 2h_1 \to 4P_{1,2} \to 4\tau^+4\tau^-$ or $h_4 \to 2P_3 \to 2b2\bar{b}$. This is a genuine feature of the $\mu\nu$SSM. The MSSM-like Higgs can also decay into neutralinos in 6% of the cases leading to the following relevant cascades, where displaced vertices and missing energy are expected: $h_4 \to \tilde{\chi}_4^0\tilde{\chi}_4^0 \to 2P_{1,2}2\nu \to 2\tau^+2\tau^-2\nu$, $h_4 \to \tilde{\chi}_4^0\tilde{\chi}_4^0 \to 2h_{1,2,3}2\nu \to 4P_{1,2}2\nu \to 4\tau^+4\tau^-2\nu$ or $h_4 \to \tilde{\chi}_4^0\tilde{\chi}_4^0 \to 2P_32\nu \to 2b2\bar{b}2\nu$. This benchmark point shows how extremely characteristic signals could be expected in certain regions of the parameter space of the $\mu\nu$SSM.

Let us finally discuss in more detail the detectability of these signals at the LHC. For that we need to study first the production cross section of the Higgs in the context of the $\mu\nu$SSM. It is well known that gluon fusion and

| $\lambda$ | $\kappa_{111}$ | $\kappa_{222}$ | $\kappa_{333}$ | $A_\kappa$ (GeV) | $M_2$ (GeV) |
|---|---|---|---|---|---|
| $1.0 \times 10^{-1}$ | $2.1 \times 10^{-2}$ | $1.9 \times 10^{-2}$ | $1.7 \times 10^{-2}$ | -5.0 | $-1.7 \times 10^3$ |
| $\tan\beta$ | $A_\lambda$ (GeV) | $\nu_1$ (GeV) | $\nu_{2,3}$(GeV) | $Y_{\nu_1}$ | $Y_{\nu_{2,3}}$ |
| 3.9 | $1.0 \times 10^3$ | $2.61 \times 10^{-5}$ | $1.31 \times 10^{-4}$ | $5.56 \times 10^{-8}$ | $2.66 \times 10^{-7}$ |
| $\nu^c$ (GeV) | $m_{h_1}$ (GeV) | $m_{h_2}$ (GeV) | $m_{h_3}$ (GeV) | $m_{h_4}$ (GeV) | $m_{P_1}$ (GeV) |
| $1.0 \times 10^3$ | 27.9 | 33.3 | 37.9 | 118.8 | 12.2 |
| $m_{P_2}$ (GeV) | $m_{P_3}$ (GeV) | $m_{\tilde{\chi}_4^0}$ (GeV) | $m_{\tilde{\chi}_5^0}$ (GeV) | $m_{\tilde{\chi}_6^0}$ (GeV) | — |
| 13.8 | 20.3 | 34.4 | 38.4 | 42.5 | — |
| $BR(h_4 \to \sum_{i,j=4}^{6} \tilde{\chi}_i^0 \tilde{\chi}_j^0)$ | $BR(\tilde{\chi}_4^0 \to \sum_{i=1}^{3} P_i \nu)$ | $BR(\tilde{\chi}_4^0 \to h_1 \nu)$ | $BR(h_1 \to \sum_{i,j=1}^{3} P_i P_j)$ | $BR(P_{1,2,3}) \to b\bar{b}$ | $l_{\tilde{\chi}_4^0 \to}$ (cm) |
| 0.04 | 0.67 | 0.33 | 0.89 | 0.93 | 23 |

Table 4.1: Relevant input parameters, masses and branching ratios of benchmark point 1.

| $\lambda$ | $\kappa_{111}$ | $\kappa_{222}$ | $\kappa_{333}$ | $A_\kappa$ (GeV) | $M_2$ (GeV) |
|---|---|---|---|---|---|
| $1.0 \times 10^{-1}$ | $7.7 \times 10^{-3}$ | $7.5 \times 10^{-3}$ | $7.3 \times 10^{-3}$ | -1.0 | $-1.7 \times 10^3$ |
| $\tan\beta$ | $A_\lambda$ (GeV) | $\nu_1$ (GeV) | $\nu_{2,3}$(GeV) | $Y_{\nu_1}$ | $Y_{\nu_{2,3}}$ |
| 3.7 | $1.0 \times 10^3$ | $2.92 \times 10^{-5}$ | $1.46 \times 10^{-4}$ | $2.70 \times 10^{-8}$ | $1.51 \times 10^{-7}$ |
| $\nu^c$ (GeV) | $m_{h_1}$ (GeV) | $m_{h_2}$ (GeV) | $m_{h_3}$ (GeV) | $m_{h_4}$ (GeV) | $m_{P_1}$ (GeV) |
| $8.0 \times 10^2$ | 13.6 | 13.9 | 17.0 | 116.2 | 8.4 |
| $m_{P_2}$ (GeV) | $m_{P_3}$ (GeV) | $m_{\tilde{\chi}_4^0}$ (GeV) | $m_{\tilde{\chi}_5^0}$ (GeV) | $m_{\tilde{\chi}_6^0}$ (GeV) | — |
| 9.5 | 9.6 | 11.8 | 12.2 | 14.0 | — |
| $BR(h_4 \to \sum_{i,j=4}^{6} \tilde{\chi}_i^0 \tilde{\chi}_j^0)$ | $BR(\tilde{\chi}_4^0 \to \sum_{i=1}^{3} P_i \nu)$ | $BR(P_1 \to \tau^+\tau^-)$ | $BR(P_2 \to \tau^+\tau^-)$ | $BR(P_3 \to \tau^+\tau^-)$ | $l_{\tilde{\chi}_4^0 \to}$ (cm) |
| 0.12 | 1.0 | 0.89 | 0.83 | 0.82 | 189 |

Table 4.2: Relevant input parameters, masses and branching ratios of benchmark point 2.

$b$-quark fusion are the two main production processes of a Higgs at the LHC in the context of SUSY. Gluon fusion dominates over $b$-quark fusion in our benchmark points, as can be shown using the relevant equations [98]:

$$\sigma(gg \to h_4) = \sigma(gg \to H_{\rm SM}) \frac{\Gamma(h_4 \to gg)}{\Gamma(H_{\rm SM} \to gg)} \simeq \sigma(gg \to H_{\rm SM}) \ , \qquad (4.24)$$

$$\sigma(b\bar{b} \to h_4) = \sigma(b\bar{b} \to H_{\rm SM}) \left( \frac{Y_{bbh_4}}{Y_{bbH_{\rm SM}}} \right)^2 = \sigma(b\bar{b} \to H_{\rm SM}) \frac{S^2(d,4)}{\cos^2\beta} \ . (4.25)$$

We can see that for the case of $b$-quark fusion, the production cross section is reduced compared to the one of the Standard Model because in our benchmark points the value of $\tan\beta$ is low, and the main component of the Higgs is $H_u^0$. However, the production cross section for gluon fusion is very similar to the one of the Standard Model. Note that in all benchmark points studied, we were interested in the production of a doublet-like Higgs ($h_4$ in our notation, except for the benchmark point 6 where it is the lightest Higgs and therefore is denoted as $h_1$). In addition, our gluinos and squarks are heavy, and as a consequence the decay width into gluons is very similar to the one of the Standard Model.

| $\lambda$ | $\kappa_{111}$ | $\kappa_{222}$ | $\kappa_{333}$ | $A_\kappa$ (GeV) | $M_2$ (GeV) |
|---|---|---|---|---|---|
| $1.0 \times 10^{-1}$ | $3.1 \times 10^{-2}$ | $3.0 \times 10^{-2}$ | $2.9 \times 10^{-2}$ | -1.0 | $-1.7 \times 10^{3}$ |
| $\tan\beta$ | $A_\lambda$ (GeV) | $\nu_1$ (GeV) | $\nu_{2,3}$(GeV) | $Y_{\nu_1}$ | $Y_{\nu_{2,3}}$ |
| 3.7 | $1.0 \times 10^{3}$ | $3.04 \times 10^{-5}$ | $1.18 \times 10^{-4}$ | $5.10 \times 10^{-8}$ | $2.95 \times 10^{-7}$ |
| $\nu^c$ (GeV) | $m_{h_1}$ (GeV) | $m_{h_2}$ (GeV) | $m_{h_3}$ (GeV) | $m_{h_4}$ (GeV) | $m_{P_1}$ (GeV) |
| $8.0 \times 10^{2}$ | 46.0 | 47.9 | 49.5 | 116.6 | 14.6 |
| $m_{P_2}$ (GeV) | $m_{P_3}$ (GeV) | $m_{\tilde{\chi}_4^0}$ (GeV) | $m_{\tilde{\chi}_3^0}$ (GeV) | $m_{\tilde{\chi}_6^0}$ (GeV) | — |
| 14.8 | 16.6 | 46.7 | 48.4 | 50.3 | — |
| $BR(h_4 \to \sum_{i,j=4}^{6} \tilde{\chi}_i^0 \tilde{\chi}_j^0)$ | $BR(\tilde{\chi}_4^0 \to \sum_{i=1}^{3} P_i \nu)$ | $BR(P_{1,2,3} \to b\bar{b})$ | $l_{\tilde{\chi}_4^0 \to}$ (cm) | — | — |
| 0.005 | 1.0 | 0.93 | 12 | — | — |

Table 4.3: Relevant input parameters, masses and branching ratios of benchmark point 3.

| $\lambda$ | $\kappa_{111}$ | $\kappa_{222}$ | $\kappa_{333}$ | $A_\kappa$ (GeV) | $M_2$ (GeV) |
|---|---|---|---|---|---|
| $1.0 \times 10^{-1}$ | $3.6 \times 10^{-2}$ | $3.5 \times 10^{-2}$ | $3.4 \times 10^{-2}$ | -1.0 | $-1.0 \times 10^{2}$ |
| $\tan\beta$ | $A_\lambda$ (GeV) | $\nu_1$ (GeV) | $\nu_{2,3}$(GeV) | $Y_{\nu_1}$ | $Y_{\nu_{2,3}}$ |
| 3.7 | $1.0 \times 10^{3}$ | $4.11 \times 10^{-6}$ | $1.59 \times 10^{-5}$ | $4.89 \times 10^{-8}$ | $3.27 \times 10^{-7}$ |
| $\nu^c$ (GeV) | $m_{h_1}$ (GeV) | $m_{h_2}$ (GeV) | $m_{h_3}$ (GeV) | $m_{h_4}$ (GeV) | $m_{P_1}$ (GeV) |
| $8.0 \times 10^{2}$ | 53.7 | 55.7 | 57.4 | 119.7 | 15.5 |
| $m_{P_2}$ (GeV) | $m_{P_3}$ (GeV) | $m_{\tilde{\chi}_4^0}$ (GeV) | $m_{\tilde{\chi}_3^0}$ (GeV) | $m_{\tilde{\chi}_6^0}$ (GeV) | $m_{\tilde{\chi}_7^0}$ (GeV) |
| 15.7 | 17.9 | 51.8 | 54.8 | 56.6 | 58.9 |
| $BR(h_4 \to \sum_{i,j=4}^{7} \tilde{\chi}_i^0 \tilde{\chi}_j^0)$ | $BR(\tilde{\chi}_4^0 \to \sum_{i=1}^{3} P_i \nu)$ | $BR(P_{1,2,3} \to b\bar{b})$ | $l_{\tilde{\chi}_4^0 \to}$ (cm) | — | — |
| 0.42 | 1.0 | 0.93 | 165 | — | — |

Table 4.4: Relevant input parameters, masses and branching ratios of benchmark point 4.

We have used the code HIGLU [99] to compute explicitly the production cross section of a Standard Model Higgs and the decay widths into gluons for our benchmark points, finding that $0.75\ \sigma(gg \to H_{\rm SM}) \lesssim \sigma(gg \to h_4) \lesssim \sigma(gg \to H_{\rm SM})$. For a center of mass energy of 7 TeV we find that $\sigma(gg \to H_{\rm SM})$ is about $17-19.5$ pb and, as a consequence, we obtain production cross sections of about $\sigma(gg \to h_4) \simeq 15-19$ pb. Then, in principle we expect that the LHC could detect the signals described in this work except maybe for cascades with a very small branching ratio (see Table 4.9). For example, the cascade described above with the maximal product of the cross section times branching ratio is the one of the benchmark point 4, $h_4 \to \tilde{\chi}_4^0 \tilde{\chi}_4^0 \to 2P2\nu \to 2b2\bar{b}2\nu$, with a result of 5860 fb. The cascade with the minimum value of this product is the one of the benchmark point 8, $h_4 \to \chi_4^0 \tilde{\chi}_4^0 \to 2P_3 2\nu \to 2b2\bar{b}2\nu$, with a result of 20 fb. The study of the detectability of these signals at the LHC with an event generator is beyond the scope of this Thesis and is left for a future work.

## 4.5 Gravitino and colliders

As we have already mentioned, since $R$-parity is broken in the $\mu\nu$SSM, neutralinos or sneutrinos, with very short lifetimes, are no longer candidates for the dark matter of the Universe. Nevertheless, if the gravitino $\Psi_{3/2}$ is the LSP, it was shown in [11] that it could be a good candidate for dark matter, with a lifetime much longer than the age of the Universe. There, it was also shown that because the gravitino decays producing a monochromatic photon, the indirect detection of gravitinos in the *Fermi* satellite [100] with a mass range between 0.1-10 GeV is possible. Larger masses are disfavored by current *Fermi* measurements.

In this case of gravitino LSP, one should check whether or not the collider signals studied in the previous section, are altered. In particular, the neutralino partial decay length into gravitino and photon must be computed. For this computation we can use the expression of the decay length $\tilde{\chi}_4^0 \to \Psi_{3/2}\gamma$ [101]. One obtains:

$$c\,\tau_{\tilde{\chi}_4^0}^{3/2} \sim 80 \text{ km } \left(\frac{m_{3/2}}{10 \text{ keV}}\right)^2 \left(\frac{m_{\tilde{\chi}_4^0}}{50 \text{ GeV}}\right)^{-5}. \tag{4.26}$$

We can easily see that in order to have a significant decay to gravitinos, the mass of the gravitino must be very low, less than 10 keV. That is, for gravitino masses larger than 10 keV, the decay width of neutralino into gravitino and photon is much smaller than the decay widths into SM particles and then, the gravitino does not alter the collider phenomenology discussed.

Summarizing, we want to emphasize that in the $\mu\nu$SSM the gravitino could be a viable dark matter candidate, accessible to indirect detection experiments, and without altering the collider phenomenology described along this chapter.

## 4.6 Conclusions

In this chapter we have studied the Higgs sector of the $\mu\nu$SSM focusing our attention on collider physics. In large regions of the parameter space, the phenomenology of the Higgs sector in this model is very rich and different from other SUSY models. On the one hand, the Higgs sector is extended due to the presence of left- and right-handed sneutrinos mixing with the MSSM Higgses. On the other hand the breaking of R-parity, could lead to signatures different from the usual missing energy.

First, we have analized the mixings in the Higgs sector of the $\mu\nu$SSM. Assuming three families of right-handed neutrino superfields, one obtains

| $\lambda$ | $\kappa_{111}$ | $\kappa_{222}$ | $\kappa_{333}$ | $A_\kappa$ (GeV) | $M_2$ (GeV) |
|---|---|---|---|---|---|
| $1.0 \times 10^{-1}$ | $3.6 \times 10^{-2}$ | $3.5 \times 10^{-2}$ | $3.4 \times 10^{-2}$ | -1.0 | $-1.0 \times 10^{2}$ |
| $\tan\beta$ | $A_\lambda$ (GeV) | $\nu_1$ (GeV) | $\nu_{2,3}$(GeV) | $Y_{\nu_1}$ | $Y_{\nu_{2,3}}$ |
| 3.7 | $1.0 \times 10^{3}$ | $4.11 \times 10^{-6}$ | $1.59 \times 10^{-5}$ | $4.89 \times 10^{-8}$ | $3.27 \times 10^{-7}$ |
| $\nu^c$ (GeV) | $A_u$ (GeV) | $m_{h_1}$ (GeV) | $m_{h_2}$ (GeV) | $m_{h_3}$ (GeV) | $m_{h_4}$ (GeV) |
| $8.0 \times 10^{2}$ | $1.2 \times 10^{3}$ | 53.3 | 55.6 | 57.4 | 112.8 |
| $m_{P_1}$ (GeV) | $m_{P_2}$ (GeV) | $m_{P_3}$ (GeV) | $m_{\tilde{\chi}^0_4}$ (GeV) | $m_{\tilde{\chi}^0_5}$ (GeV) | $m_{\tilde{\chi}^0_6}$ (GeV) |
| 15.4 | 15.6 | 17.8 | 51.7 | 54.8 | 56.5 |
| $m_{\tilde{\chi}^0_7}$ (GeV) | $BR(h_4 \to \sum_{i,j=4}^{7} \tilde{\chi}^0_i \tilde{\chi}^0_j)$ | $BR(\tilde{\chi}^0_4 \to \sum_{i=1}^{3} P_i \nu)$ | $BR(P_{1,2,3} \to b\bar{b})$ | $l_{\tilde{\chi}^0_4 \to}$ (cm) | — |
| 58.9 | 0.30 | 1.0 | 0.93 | 164 | — |

Table 4.5: Relevant input parameters, masses and branching ratios of benchmark point 5.

eight CP-even and seven CP-odd Higgses in the model. Although the three left-handed sneutrinos are basically decoupled from the rest of the Higgses, the mixing between Higgs doublets and right-handed sneutrinos is not necessarily small. In this work we have deduced general conditions to suppress the latter. This can be useful to obtain very light singlets avoiding collider constraints, but also to have a doublet-like Higgs as the lightest one being as heavy as possible.

Then, we have provided an overview of new decays in the Higgs sector with respect to other SUSY models with extra singlets like the NMSSM. Due to the extended Higgs sector, Higgs-to-Higgs cascade decays could be more complicated, as shown in subsection 4.2.2. In addition, the breaking of R-parity gives rise to new decays.

LEP constraints have been discussed in the context of the $\mu\nu$SSM. For this, we have computed the couplings of the Higgses with Z bosons and the sum rules. Also the production mechanisms of Higgses at lepton and hadron colliders in this model have been briefly reviewed.

Finally, in Section 4.4 we have concentrated on Higgs decays that are genuine of the $\mu\nu$SSM, and could serve to distinguish it from other SUSY models. We have provided benchmark points that should pass current constraints and are interesting for LHC. In particular, we have focused first our attention on the decays of a MSSM-like light Higgs $h_{MSSM}$ with a sizeable branching ratio to two lightest neutralinos. These neutralinos could decay inside the detector leading to displaced vertices. This fact can be used to distinguish the $\mu\nu$SSM from R-parity conserving models such as the NMSSM/MSSM. However, let us remark that in models of gauge mediated SUSY breaking, where the gravitino is usually the LSP, a displaced vertex can also be obtained depending on the lifetime of the next-to-LSP, see [102] for a review.

Besides, the decays can be into a neutrino and an on-shell light singlet pseudoscalar $P$, that subsequently decays into $b\bar{b}$ (or if kinematically forbidden into $\tau^+\tau^-$), and therefore the decay $h_{MSSM} \to \tilde{\chi}^0\tilde{\chi}^0 \to 2P2\nu \to 2b2\bar{b}2\nu$

| $\lambda$ | $\kappa_{111}$ | $\kappa_{222}$ | $\kappa_{333}$ | $A_\kappa$ (GeV) | $M_2$ (GeV) |
|---|---|---|---|---|---|
| $1.12 \times 10^{-1}$ | $7.12 \times 10^{-2}$ | $7.11 \times 10^{-2}$ | $7.10 \times 10^{-2}$ | -18 | $-1.0 \times 10^2$ |
| $\tan\beta$ | $A_\lambda$ (GeV) | $\nu_1$ (GeV) | $\nu_{2,3}$(GeV) | $Y_{\nu_1}$ | $Y_{\nu_{2,3}}$ |
| 3.7 | $1.0 \times 10^3$ | $7.21 \times 10^{-7}$ | $1.04 \times 10^{-7}$ | $6.66 \times 10^{-8}$ | $4.53 \times 10^{-7}$ |
| $\nu^c$ (GeV) | $m_{h_1}$ (GeV) | $m_{h_2}$ (GeV) | $m_{h_3}$ (GeV) | $m_{h_4}$ (GeV) | $m_{P_1}$ (GeV) |
| $8.47 \times 10^2$ | 113.7 | 115.1 | 115.3 | 118.9 | 57.8 |
| $m_{P_2}$ (GeV) | $m_{P_3}$ (GeV) | $m_{\tilde{\chi}_4^0}$ (GeV) | $m_{\tilde{\chi}_3^0}$ (GeV) | $m_{\tilde{\chi}_2^0}$ (GeV) | $m_{\tilde{\chi}_1^0}$ (GeV) |
| 57.9 | 61.3 | 52.1 | 114.2 | 120.2 | 120.4 |
| $BR(h_1 \to \tilde{\chi}_4^0\tilde{\chi}_4^0)$ | $BR(\tilde{\chi}_4^0 \to lq\bar{q})$ | $BR(\tilde{\chi}_4^0 \to \nu ll)$ | $BR(\tilde{\chi}_4^0 \to \nu q\bar{q})$ | $BR(\tilde{\chi}_4^0 \to 3\nu)$ | $l_{\tilde{\chi}_4^0 \to}$ (cm) |
| 0.02 | 0.52 | 0.28 | 0.15 | 0.05 | 533 |

Table 4.6: Relevant input parameters, masses and branching ratios of benchmark point 6.

| $\lambda_{1,2}$ | $\lambda_3$ | $\tan\beta$ | $A_\lambda$ (GeV) | $A_\kappa$ (GeV) | $M_2$ (GeV) |
|---|---|---|---|---|---|
| $1.0 \times 10^{-2}$ | $2.8 \times 10^{-1}$ | 3.7 | $1.0 \times 10^3$ | -1 | $-5.88 \times 10^3$ |
| $\kappa_{111}$ | $\kappa_{222}$ | $\kappa_{333}$ | $Y_{\nu_1}$ | $Y_{\nu_2}$ | $Y_{\nu_3}$ |
| $7.12 \times 10^{-2}$ | $6.95 \times 10^{-2}$ | $3.15 \times 10^{-2}$ | $8.58 \times 10^{-8}$ | $2.42 \times 10^{-7}$ | $2.13 \times 10^{-6}$ |
| $\nu_1$ (GeV) | $\nu_2$ (GeV) | $\nu_3$ (GeV) | $\nu^c$ (GeV) | | — |
| $1.19 \times 10^{-4}$ | $1.71 \times 10^{-4}$ | $4.72 \times 10^{-7}$ | $8.0 \times 10^2$ | | — |
| $m_{h_1}$ (GeV) | $m_{h_2}$ (GeV) | $m_{h_3}$ (GeV) | $m_{h_4}$ (GeV) | $m_{P_{1,2}}$ (GeV) | $m_{P_3}$ (GeV) |
| 47.9 | 110.9 | 113.6 | 119.6 | 14.0 | 25.7 |
| $m_{\tilde{\chi}_4^0}$ (GeV) | $m_{\tilde{\chi}_5^0}$ (GeV) | $m_{\tilde{\chi}_{6,7}^0}$ (GeV) | — | — | — |
| 53.9 | 111.2 | 113.9 | — | — | — |
| $BR(h_4 \to h_1h_1)$ | $BR(h_1 \to \sum_{i,j=1}^3 P_iP_j)$ | $BR(P_i \to b\bar{b})$ | $BR(h_4 \to \sum_{i,j=1}^3 P_iP_j)$ | $BR(h_4 \to b\bar{b})$ | — |
| 0.04 | 0.97 | 0.93 | 0.39 | 0.40 | — |

Table 4.7: Relevant input parameters, masses and branching ratios of benchmark point 7.

is genuine of the $\mu\nu$SSM. For example, in other R-parity breaking models such as the BRpV, there are no singlet Higgses and a lightest neutralino lighter than gauge bosons could decay only through three-body decay processes. We have also seen that a final state with 8 $b$-jets plus missing energy is possible in situations where singlet-like scalars are produced first by the decay of the neutralino, and they decay into pseudoscalars, $h_{MSSM} \to \tilde{\chi}^0\tilde{\chi}^0 \to 2h2\nu \to 4P2\nu \to 4b4\bar{b}2\nu$.

We have also studied a case with an spectrum similar to the one of the MSSM, where all CP-even singlet scalars are above 114 GeV, and the pseudoscalars are heavier than the neutralinos. Then, the $h_{MSSM}$ will decay in a significant ratio to neutralinos, and these will decay only through three-body processes leading to displaced vertices.

In another case the neutralino does not play an important role and only Higg-to-Higgs cascade decays are relevant. Although displaced vertices are not expected, the decays $h_{MSSM} \to 2P \to 2b2\bar{b}$, $h_{MSSM} \to 2h \to 4P \to 4b4\bar{b}$ are possible, allowing to distinguish the $\mu\nu$SSM from other R-parity violating models. Besides, once a SUSY particle is produced at the collider, decaying into the LSP, the displaced vertex would allow to distinguish the $\mu\nu$SSM

| $\lambda$ | $\kappa_{111}$ | $\kappa_{222}$ | $\kappa_{333}$ | $A_\kappa$ (GeV) | $M_2$ (GeV) |
|---|---|---|---|---|---|
| $1.0 \times 10^{-1}$ | $1.66 \times 10^{-2}$ | $1.65 \times 10^{-2}$ | $1.64 \times 10^{-2}$ | -5.0 | $-1.7 \times 10^3$ |
| $\tan\beta$ | $A_\lambda$ (GeV) | $\nu_1$ (GeV) | $\nu_{2,3}$(GeV) | $Y_{\nu_1}$ | $Y_{\nu_{2,3}}$ |
| 4.9 | $1.0 \times 10^3$ | $5.84 \times 10^{-5}$ | $2.25 \times 10^{-4}$ | $1.25 \times 10^{-7}$ | $2.26 \times 10^{-7}$ |
| $\nu^c$ (GeV) | $m_{h_1}$ (GeV) | $m_{h_2}$ (GeV) | $m_{h_3}$ (GeV) | $m_{h_4}$ (GeV) | $m_{P_1}$ (GeV) |
| $8.0 \times 10^2$ | 19.8 | 21.6 | 21.8 | 120.2 | 8.8 |
| $m_{P_2}$ (GeV) | $m_{P_3}$ (GeV) | $m_{\tilde{\chi}^0_4}$ (GeV) | $m_{\tilde{\chi}^0_3}$ (GeV) | $m_{\tilde{\chi}^0_2}$ (GeV) | — |
| 8.9 | 16.9 | 26.3 | 26.5 | 27.8 | — |
| $BR(h_4 \to h_1 h_1)$ | $BR(h_4 \to P_3 P_3)$ | $BR(h_4 \to \sum_{i,j=4}^{6} \tilde{\chi}^0_i \tilde{\chi}^0_j)$ | $BR(h_4 \to b\bar{b})$ | $BR(h_1 \to \sum_{i,j=1}^{2} P_i P_j)$ | $BR(h_{2,3} \to \sum_{i,j=1}^{2} P_i P_j)$ |
| 0.05 | 0.12 | 0.06 | 0.55 | 0.98 | 1.0 |
| $BR(P_{1,2} \to \tau^+\tau^-)$ | $BR(P_3 \to b\bar{b})$ | $BR(\tilde{\chi}^0_4 \to \sum_{i=1}^{3} h_i \nu)$ | $BR(\tilde{\chi}^0_4 \to P_{1,2}\nu)$ | $BR(\tilde{\chi}^0_4 \to P_3\nu)$ | $l_{\tilde{\chi}^0_4}$ (cm) |
| 0.88 | 0.93 | 0.51 | 0.33 | 0.16 | 15 |

Table 4.8: Relevant input parameters, masses and branching ratios of benchmark point 8.

from the NMSSM.

Finally, we have studied a case where for singlet-like pseudoscalars $P_{1,2}$ the decay into $b\bar{b}$ is kinematically forbidden, but for $P_3$ is allowed. Then, several interesting cascade decays are expected without leading to displaced vertices: $h_{MSSM} \to 2h_1 \to 4P_{1,2} \to 4\tau^+4\tau^-$, $h_{MSSM} \to 2P_3 \to 2b2\bar{b}$. This is a genuine feature of the $\mu\nu$SSM. In addition, the following relevant cascades are possible, with displaced vertices and missing energy: $h_{MSSM} \to \tilde{\chi}^0_4\tilde{\chi}^0_4 \to 2P_{1,2}2\nu \to 2\tau^+2\tau^-2\nu$, $h_{MSSM} \to \tilde{\chi}^0_4\tilde{\chi}^0_4 \to 2h_{1,2,3}2\nu \to 4P_{1,2}2\nu \to 4\tau^+4\tau^-2\nu$ or $h_{MSSM} \to \tilde{\chi}^0_4\tilde{\chi}^0_4 \to 2P_3 2\nu \to 2b2\bar{b}2\nu$.

In conclusion, the above discussion gives us the idea that extremely characteristic signals could be expected in certain regions of the parameter space of the $\mu\nu$SSM.

We have also emphasized that in the $\mu\nu$SSM the gravitino could be a viable dark matter candidate, accessible to indirect detection experiments, and without altering the collider phenomenology described along this work. In particular, the branching ratio of neutralino to gravitino-photon turns out to be negligible.

Let us finally remark that the collider phenomenology of the $\mu\nu$SSM is very rich and peculiar, as shown here using several benchmark points, and, as a consequence, we still need to carry out much work in the future to cover all interesting aspects of the model.

For example, it would be interesting to study in the future the decays of the heavier Higgses where the Higgs-to-Higgs cascade decays would be relevant. In this work we have concentrated in the case where the lightest neutralino is the LSP. The situation having a squark, a sneutrino or a slepton LSP has not been analysed in the literature and it would be also very interesting to study in the context of the $\mu\nu$SSM. The analysis of these and other signals with an event generator will be performed in future works.

| Benchmark point | Cascade | $\sigma(gg \to h_4) \times BR_{\text{cascade}}$ (fb) |
|---|---|---|
| 1 | $h_4 \to \tilde{\chi}_4^0\tilde{\chi}_4^0 \to 2P2\nu \to 2b2\bar{b}2\nu$ | 270 |
| | $h_4 \to \tilde{\chi}_4^0\tilde{\chi}_4^0 \to 2h2\nu \to 4P2\nu \to 4b4b2\nu$ | 44 |
| 2 | $h_4 \to \tilde{\chi}_4^0\tilde{\chi}_4^0 \to 2P2\nu \to 2\tau^+2\tau^-2\nu$ | 1620 |
| 3 | $h_4 \to \tilde{\chi}_4^0\tilde{\chi}_4^0 \to 2P2\nu \to 2b2b2\nu$ | 70 |
| 4 | $h_4 \to \tilde{\chi}_4^0\tilde{\chi}_4^0 \to 2P2\nu \to 2b2\bar{b}2\nu$ | 5860 |
| 5 | $h_4 \to \tilde{\chi}_4^0\tilde{\chi}_4^0 \to 2P2\nu \to 2b2b2\nu$ | 4870 |
| 6 | $h_1 \to \tilde{\chi}_4^0\tilde{\chi}_4^0 \to 2l2q2\bar{q}$ | 150 |
| | $h_1 \to \tilde{\chi}_4^0\tilde{\chi}_4^0 \to 2\nu2l2l$ | 80 |
| | $h_1 \to \tilde{\chi}_4^0\tilde{\chi}_4^0 \to 2\nu2q2\bar{q}$ | 40 |
| | $h_1 \to \tilde{\chi}_4^0\tilde{\chi}_4^0 \to 6\nu$ | 15 |
| 7 | $h_4 \to 2P \to 2b2\bar{b}$ | 5450 |
| | $h_4 \to 2h_1 \to 4P \to 4b4b$ | 460 |
| 8 | $h_4 \to 2P_3 \to 2b2\bar{b}$ | 1660 |
| | $h_4 \to h_1h_1 \to 4P_{1,2} \to 4\tau^+4\tau^-$ | 460 |
| | $h_4 \to \tilde{\chi}_4^0\tilde{\chi}_4^0 \to 2P_{1,2}2\nu \to 2\tau^+2\tau^-2\nu$ | 80 |
| | $h_4 \to \tilde{\chi}_4^0\tilde{\chi}_4^0 \to 2h2\nu \to 4P_{1,2}2\nu \to 4\tau^+4\tau^-2\nu$ | 150 |
| | $h_4 \to \tilde{\chi}_4^0\tilde{\chi}_4^0 \to 2P_32\nu \to 2b2b2\nu$ | 20 |

Table 4.9: Production cross sections times branching ratios of the cascades for the benchmark points discussed in the text.

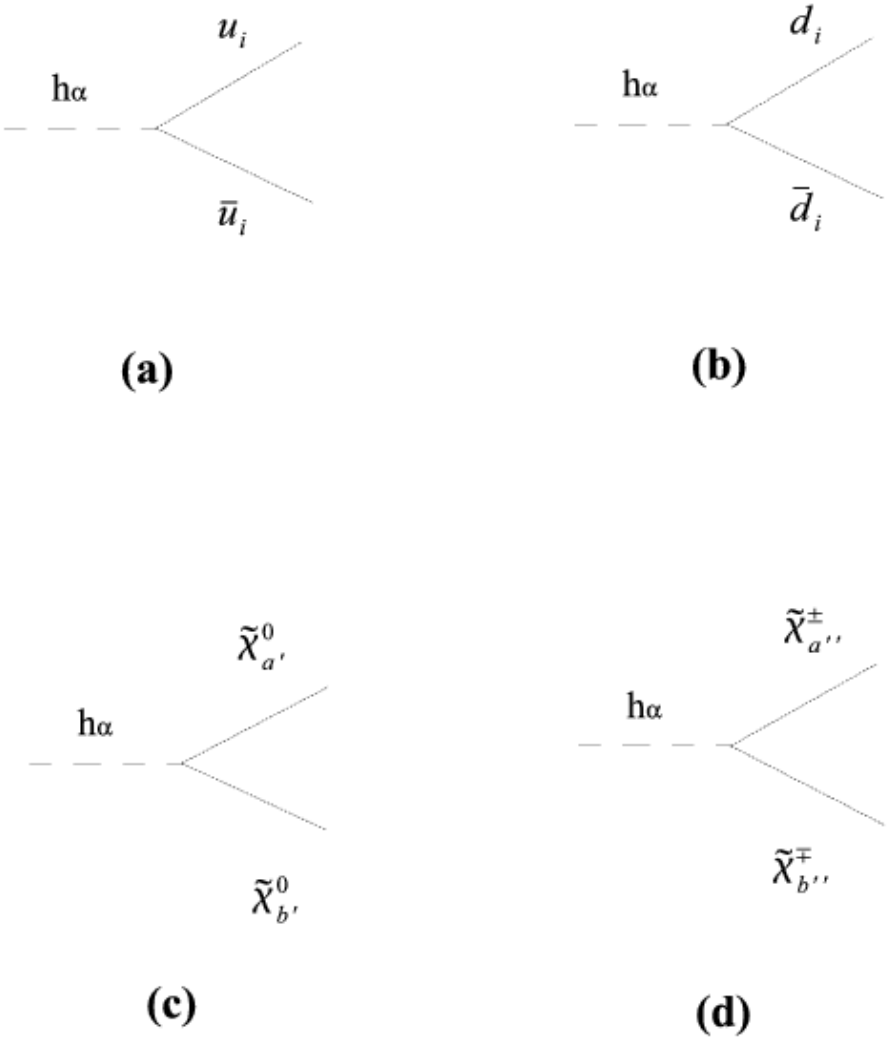


Figure 4.1: Feynman diagrams of Higgs decay to fermions, with $\alpha = 1, ..., 8$, $i = 1, 2, 3$, $a', b' = 1, ..., 10$, and $a'', b'' = 1, ..., 5$. Replacing the decaying $h_\alpha$ by a pseudoscalar $P_{\alpha'}$, with $\alpha' = 1, ..., 7$, all the Feynman diagrams are valid.

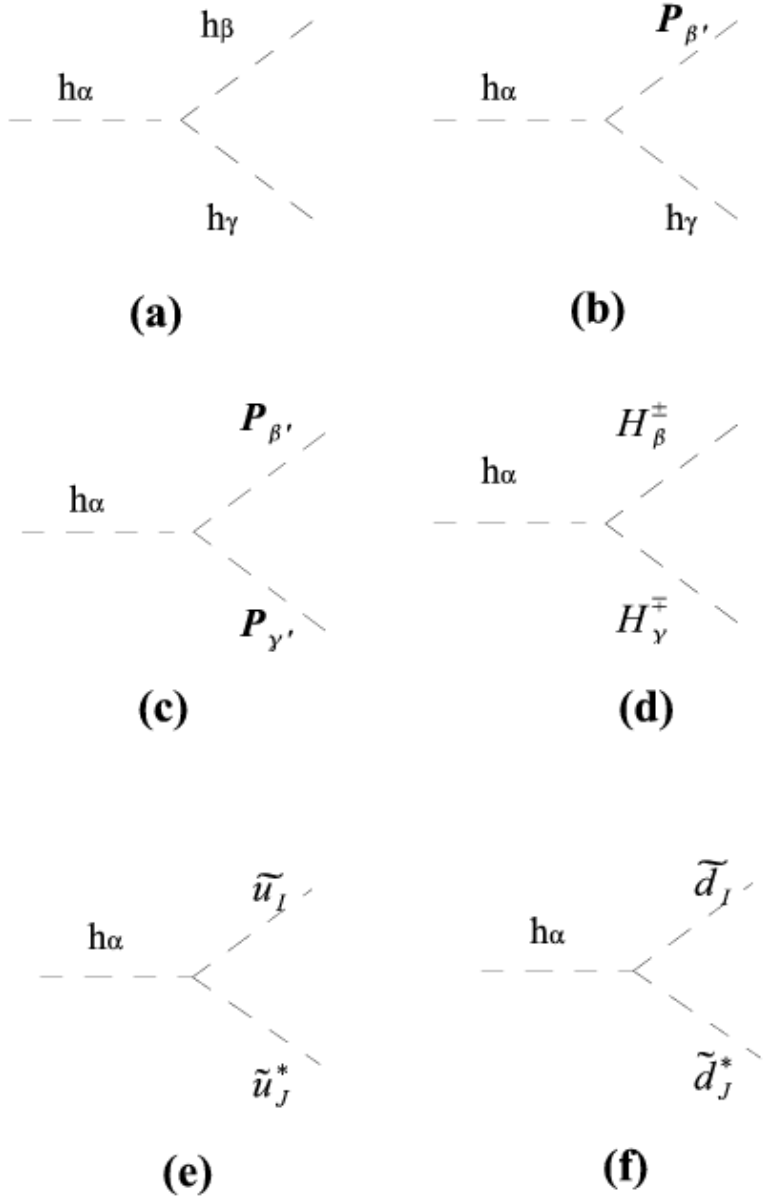


Figure 4.2: Feynman diagrams of Higgs decays to scalars (under Lorentz), with $I, J = 1..6$. Replacing the decaying $h_\alpha$ by a pseudoscalar $P_{\alpha'}$, all the Feynman diagrams are valid. The index convention is like in Fig. 4.1.

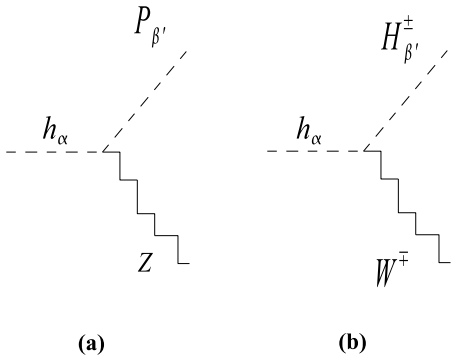


Figure 4.3: Feynman diagrams of Higgs decays to scalars and vectors (under Lorentz). Replacing the decaying $h_\alpha$ by a pseudoscalar $P_{\alpha'}$, all the Feynman diagrams are valid. The index convention is like in Fig. 4.1.

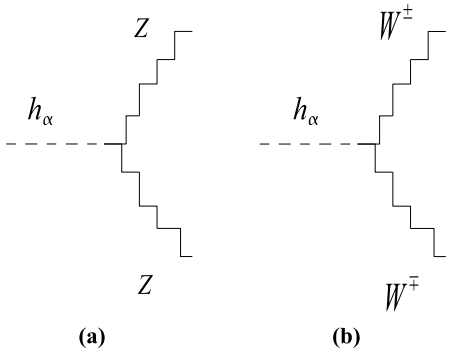


Figure 4.4: Feynman diagrams of Higgs decays to vectors (under Lorentz). The index convention is like in Fig. 4.1.

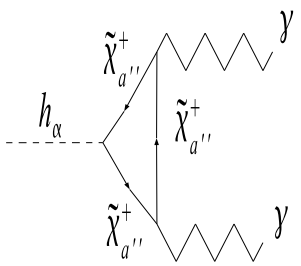


Figure 4.5: Di-photon Higgs decay. Replacing the decaying $h_\alpha$ by a pseudoscalar $P_{\alpha'}$, the Feynman diagram is valid. The index convention is like in Fig. 4.1.

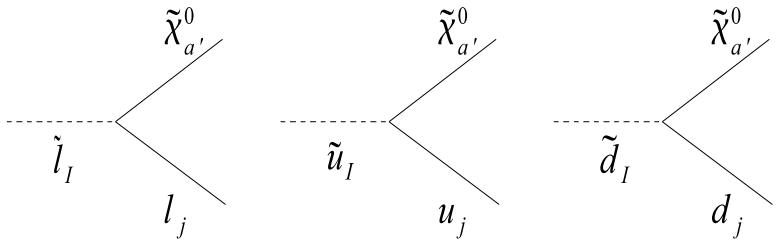


(a) (b) (c)

Figure 4.6: (a) Charged slepton decay. (b) Up squark decay. (c) Down squark decay. The index convention is like in Figs. 4.1 and 4.2.

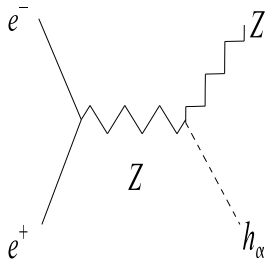


Figure 4.7: Higgs-strahlung. The index convention is like in Fig. 4.1.

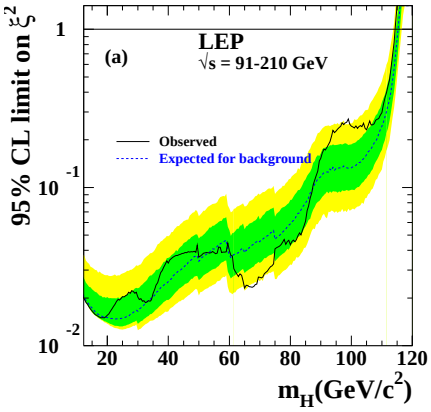


Figure 4.8: The 95% confidence level upper bound on the ratio $\xi^2 = (g_{hZZ}/g_{hZZ}^{SM})^2$ from [80]. The dark and light shaded bands around the median expected line correspond to the 68% and 95% probability bands. The horizontal line corresponds to the Standard Model coupling for Higgs boson decays predicted by the Standard Model.

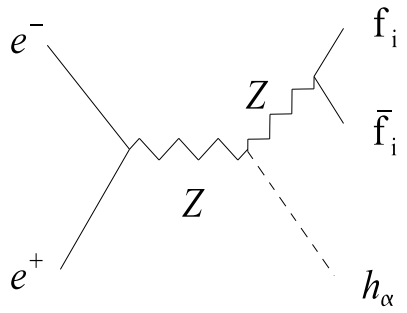


Figure 4.9: Bjorken process. The index convention is like in Fig. 4.1.

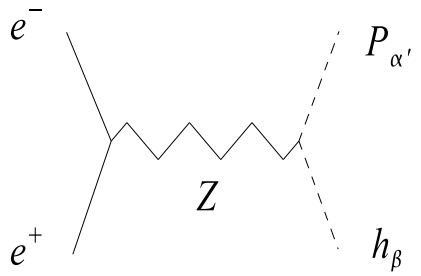


Figure 4.10: Pair production of a scalar and a pseudoscalar Higgs. The index convention is like in Fig. 4.1.

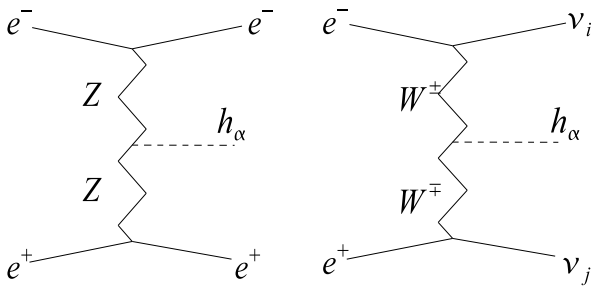


(a) (b)

Figure 4.11: (a) Vector (Z) boson fusion. (b) Vector (W) boson fusion. The index convention is like in Fig. 4.1.

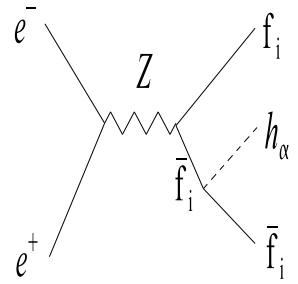


Figure 4.12: Yukawa process producing a Higgs. Replacing the $h_\alpha$ by a pseudoscalar $P_{\alpha'}$, the Feynman diagram is valid. The index convention is like in Fig. 4.1.

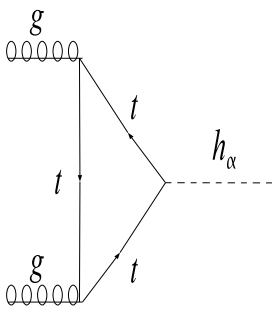


Figure 4.13: Gluon gluon fusion giving a Higgs. Replacing the $h_\alpha$ by a pseudoscalar $P_{\alpha'}$, the Feynman diagram is valid. The index convention is like in Fig. 4.1.

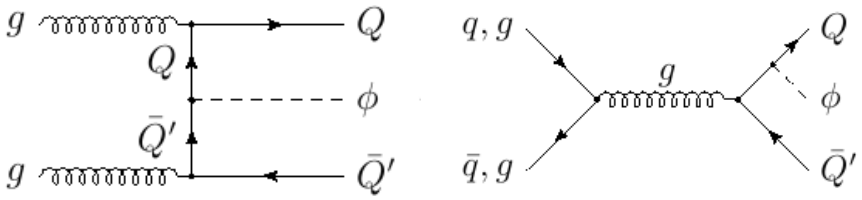


(a) (b)

Figure 4.14: Examples of associated production of a Higgs with heavy quarks where $\phi$ can be either a CP-even or a CP-odd Higgs.

# Chapter 5

# The $\mu\nu SSM$ with an extra $U(1)$

In this chapter we will analyse the possibility of extending the gauge group of the $\mu\nu$SSM with an extra U(1) factor. It is based on the results presented in [16].

Once R-parity is not a symmetry of the model, lepton and baryon number violating operators are allowed by gauge invariance in the superpotential. If stringent unnatural bounds are not imposed on certain combinations of the corresponding couplings, too fast proton decay occurs. There are several solutions to this problem such as discrete symmetries, like e.g. baryon triality [103], or arguments based on string theory. In string constructions, the matter superfields can be located in different sectors or have different extra $U(1)$ charges, in such a way that some R-parity breaking operators can be forbidden [104], but others can be allowed.

Another problem is related to the absence of both, an explicit $\mu$ term and an explicit Majorana mass term for neutrinos in the superpotential (2.3) of the $\mu\nu$SSM, since both type of bilinear terms are allowed by gauge invariance. Again, several solutions are available. The fact that only dimensionless trilinear terms are present can be explained invoking a $Z_3$ symmetry. Another solution comes from string constructions, where the low-energy limit is determined by the massless string modes. Since the massive modes are of the order of the string scale, only trilinear couplings are present in the low-energy superpotential.

Moreover, since the $\mu\nu$SSM superpotential contains only trilinear terms, it has a $Z_3$ symmetry, just like the NMSSM. Then, one expects to have also a cosmological domain wall problem [37]. Nevertheless, the usual solution [37, 38] based on non-renormalizable operators also works in this case.

The aim of this chapter is to solve these three problems adopting a different strategy. In particular, we will add an extra $U(1)$ gauge symmetry to the gauge group of the SM. In this way, and since all the fields can be

charged under the extra $U(1)$, all the dangerous operators could be forbidden without relying in string theory arguments, discrete symmetries or non-renormalizable operators. In a sense, we substitute the two discrete global symmetries (R-parity and $Z_3$) of the NMSSM by only one gauge symmetry.

In Section 5.1 we will explain in detail the motivations for extending the gauge group. In Subsection 5.1.1 we will discuss the proton decay problem in SUSY and the role of R-parity. In Subsection 5.1.2 we will explain the $\mu$ problem (related to the issue of bilinear terms in the superpotential) and the domain wall problem. In Section 5.2, we will use the $U(1)$ extra charges of the matter fields to allow the interesting operators, forbidding the dangerous ones. We will also impose the anomaly cancellation conditions associated with the extra $U(1)$ to constrain the values of the $U(1)$ charges. We will see that the introduction of extra matter is required. Once we have found consistent assignments of the extra charges (models), in Section 5.3 we will study their phenomenology concerning the electroweak symmetry breaking. We will also check for the different models the experimental constraints on an extra gauge boson and neutrino masses. We will also show how the upper bound on the lightest Higgs mass is improved in the extra $U(1)$ version of the $\mu\nu$SSM. Finally, the conclusions of this chapter are left for Section 5.4.

# 5.1 Motivations

## 5.1.1 Proton stability in SUSY models and R-parity

In this subsection we will explain the issue of proton decay in SUSY and the role of R-parity. Let us first focus our attention on the simplest SUSY extension of the SM, the MSSM (see [7] for a review). The superpotential is given by:

$$W = \epsilon_{ab}(Y_u^{ij}\hat{H}_2^b\hat{Q}_i^a\hat{u}_j^c + Y_d^{ij}\hat{H}_1^a\hat{Q}_i^b\hat{d}_j^c + Y_e^{ij}\hat{H}_1^a\hat{L}_i^b\hat{e}_j^c) - \epsilon_{ab}\ \mu\hat{H}_1^a\hat{H}_2^b. \quad (5.1)$$

It contains Yukawa terms for generating charged fermion masses and an explicit $\mu$ term required by phenomenology. There are also other renormalizable, gauge invariant terms allowed by SUSY that do not appear in (5.1). They violate either lepton or baryon number and are given by:

$$W_{\Delta L=1} = \epsilon_{ab}(\lambda^{'''ijk}\hat{L}_i^a\hat{L}_j^b\hat{e}_k^c + \lambda^{'ijk}\hat{L}_i^a\hat{Q}_j^b\hat{d}_k^c + \mu^i\hat{L}_i^a\hat{H}_2^b) \quad (5.2)$$

$$W_{\Delta B=1} = \lambda^{''ijk}\hat{u}_i^c\hat{d}_j^c\hat{d}_k^c \quad (5.3)$$

If both type of terms are allowed in the superpotential, a phenomenological problem arises since the L or B violating processes associated to these operators have not been detected in nature. The most strict restriction comes from

the non-observation of proton decay [105]. The experimental lower bound on its lifetime is $\tau_{proton} \geq 10^{32}$ *years*. Many other processes also give strong constraints on the violation of lepton and baryon numbers [106, 107]. For evading too fast proton decay mediated by the interchange of squarks with masses of the order of the EW scale (see for example Figure 5.1), very stringent bounds on certain combinations of the B or L violating couplings have to be imposed as e.g. $\lambda'_{112}\lambda''_{112} \leq 2 \times 10^{-27}$ [108]. As this seems unnatural, one usually forbids at least one type of the dangerous operators.

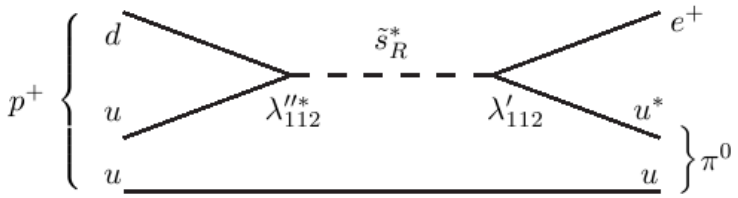


Figure 5.1: $p \to e^+\pi^0$ Other possible decay processes of the proton would be $p \to e^+K^0$ , $p \to \mu^+\pi^0$ , $p \to \mu^+K^0$ , $p \to \nu K^+$ , $p \to \nu\pi^+$ etc...

Note that in the SM, L and B are accidental anomalous global symmetries since the gauge symmetry does not allow for L- or B-violating terms in the Lagrangian. One of the goals of this chapter is to protect the proton of decaying in the $\mu\nu$SSM only with the gauge symmetry.

The most popular option in SUSY to protect the proton of decaying is to use a discrete symmetry called R-parity [10] ($R_p = (-1)^R$ with $R = 1$ for SM particles and $R = -1$ for SUSY particles) that forbids both L- and B-violating renormalizable operators at the same time. Nevertheless, in SUSY models with conserved R-parity there are dimension-five non-renormalizable operators of the type $QQQL$, $QQQH_1$, $Qu^ce^cH_1$ that violate L and/or B. They are suppressed by one power of the energy scale until the theory is valid (for example the GUT scale) but could induce too fast proton decay if the couplings are of order one. So, in this sense, the R-parity conserving models do not evade a certain fine-tuning to prevent fast proton decay [109]. The most important feature of R-parity is that in all vertex of a Feynman diagram, there have to be an even number of SUSY particles. Then, the LSP is stable and if it is electrically neutral and colourless, it is a good DM candidate.

In spite of these nice features, R-parity, as a discrete global symmetry, seems not to be a fundamental symmetry. Gauge symmetries have been

proved to be very useful, with the application of the gauge principle for explaining the distance forces and to build the SM of particle physics. Moreover, global symmetries can be violated by quantum gravitational effects [110].

Other discrete symmetries as lepton parity or baryon triality [103] can forbid proton decay allowing respectively B- or L-violating couplings. Therefore, R-parity is not an essential ingredient of low energy supersymmetry. In addition, R-parity is not a minimal approach to solve the proton decay problem since it forbids both L and B-violating operators at the same time.

As the $\mu\nu SSM$ violates R-parity and L-violating operators are required by phenomenology, the issue of proton stability should be addressed. Several solutions are available: discrete symmetries such as baryon triality, or string theory arguments. In string constructions, the matter superfields can be located in different sectors or have different extra $U(1)$ charges, in such a way that some R-parity breaking operators can be forbidden [104], but others can be allowed. In this chapter we will ensure proton stability in the context of quantum field theory without appealing to discrete symmetries. This will be accomplished adding an extra $U(1)$ gauge group that forbids all renormalizable B-violating operators. The proton is thus protected from decaying in the same way that in the SM, by the gauge symmetry. In addition, in the model found, all dimension-five B-violating operators are forbidden by the extra $U(1)$. The addition of an extra $U(1)$ gauge symmetry to SUSY models for addressing the proton stability problem has been extensively considered in the literature [30, 31].

### 5.1.2 Forbidding bilinear operators. The domain wall problem

Let us remind that the $\mu$ problem [8] of the MSSM, related to the presence of the bilinear term $\mu H_1 H_2$ in the superpotential (5.1), is one of the main motivations of the $\mu\nu$SSM. Being the only bilinear term appearing in (5.1), $\mu$ is the only superpotential parameter of the MSSM with mass dimension.

For phenomenological reasons concerning the correct EW breaking, the dimensionful parameter $\mu$ has to be of the order of the EW scale $\mathcal{O}(10^2$ GeV). On the other hand, being a superpotential term, there is not a reason for $\mu$ to be of this order of magnitude since in principle, a bare $\mu$ term is not linked to the SUSY or EW breaking scale. The natural value of $\mu$ would be the energy scale until the theory remains valid, e.g. the GUT scale $\mathcal{O}(10^{16}$ GeV) or the Planck scale $\mathcal{O}(10^{19}$ GeV). This apparent contradiction between the theoretical and the phenomenological expectations on the order of magnitude of the $\mu$ term is what is called the $\mu$ problem of SUSY. Note that the presence

of a $\mu$ term or a term playing a similar role on the superpotential of SUSY models is necessary for two phenomenological reasons. On one hand, if $\mu = 0$ the superpotential (5.1) would have a global $U(1)$ symmetry $H_{1,2} \rightarrow e^{i\alpha} H_{1,2}$ spontaneously broken by the VEVs of the Higgses giving rise to an undetected massless Goldstone boson. On the other hand, if the $\mu$ term would vanish, charginos would be lighter than current experimental bounds [111]. When minimizing the MSSM scalar potential the following equation arises:

$$\mu^2 = \frac{m_{H_d}^2 - m_{H_u}^2 \tan^2\beta}{\tan^2\beta - 1} - \frac{1}{2} m_Z^2. \tag{5.4}$$

We can see from (5.4) that $\mu$ has to be $\mathcal{O}(10^2$ GeV) since the terms on the right side are of the order of the EW scale (or soft SUSY breaking scale).

In general, the solutions to the $\mu$ problem appearing in the literature try to generate an effective $\mu$ term from the breaking of a symmetry for explaining the smallness of $\mu$. For example, it is usual to link the generation of the $\mu$ term with the breaking of SUSY, but this approach depends on the nature of the hidden sector and on the mechanism of transmission to the visible sector (see e.g. [112, 113]). Other solutions to the $\mu$ problem have been proposed at low energy, linking the generation of an effective $\mu$ term with the EW breaking. In this context, the NMSSM [29], suggests to extend the particle content of the MSSM with an extra gauge singlet superfield $\hat{S}$. The superpotential is given by the following expression (for simplicity we suppress color, family and $SU(2)$ indices):

$$W = Y_u \hat{H}_2 \hat{Q} \hat{u}^c + Y_d \hat{H}_1 \hat{Q} \hat{d}^c + Y_e \hat{H}_1 \hat{L} \hat{e}^c - \lambda \hat{S} \hat{H}_1 \hat{H}_2 + \frac{1}{3} \kappa \hat{S} \hat{S} \hat{S}. \tag{5.5}$$

The $\mu$ problem is solved since all the terms in (5.5) are trilinear. An effective $\mu$ term, $\mu_{eff} = \lambda \langle S \rangle$ arises when the scalar component of the singlet superfield takes a VEV in the EW breaking, naturally of the order of the EW scale as required by phenomenology. The last term in (5.5), allowed by all symmetries, is required by phenomenology since it evades the problem of an undetected Goldstone boson associated to a global $U(1)$ symmetry $H_1 H_2 \rightarrow e^{i\alpha} H_1 H_2$ , $S \rightarrow e^{-i\alpha} S$ that would be spontaneously broken by the VEVs of the Higgses. In the NMSSM, the absence of an explicit $\mu$ term is supported invoking a discrete $Z_3$ symmetry under which all the superfields transform as: $\hat{\phi} \rightarrow e^{i2\pi/3} \hat{\phi}$, only allowing trilinear terms.

Then, the NMSSM is expected to have a cosmological domain wall problem [37] since the $Z_3$ symmetry would be spontaneously broken during the EW phase transition in the primitive universe. Due to the existence of causal horizons in the universe in evolution, the formation of domains of different degenerate vacua separated by domain walls takes place. These walls would

have a surface energy density given by $\sigma \sim (\langle S \rangle)^3$, where $\langle S \rangle$ is of the order of the EW scale, that could dominate the energy density of the universe giving rise to large anisotropies in the cosmic microwave background incompatible with the observational results. There are solutions available to this problem in the NMSSM that can be applied in a similar way to the $\mu\nu$SSM since this model could also suffer from this problem. Non-renormalizable operators that break explicitly the dangerous $Z_3$ symmetry could be added to the superpotential [37, 38] lifting the degeneracy of the three original vacua. This can be done without reintroducing hierarchy problems and choosing these operators small enough as not to alter the low-energy phenomenology. Another option is to add an extra $U(1)$ factor to the gauge symmetry of the model that would embed the discrete $Z_3$ symmetry and prohibiting the dangerous term $\frac{1}{3}\kappa\hat{S}\hat{S}\hat{S}$ as well as the explicit $\mu$ term solving the domain wall problem. The Goldstone boson that would appear without the term $\frac{1}{3}\kappa\hat{S}\hat{S}\hat{S}$ is eaten by the $Z'$ in the EW breaking to provide its longitudinal component.

Concerning $U(1)$SSM like-models, there is a vast amount of literature [115]. In the $U(1)$SSM, the solution to the $\mu$ problem is similar to the one of the NMSSM in the sense that the effective $\mu$ term is also generated through the VEV of the scalar component of an extra singlet superfield. The difference between these two models consists of the symmetry that forbids the explicit $\mu$ term. In the $U(1)$SSM, instead of using a discrete $Z_3$ symmetry, an extra $U(1)$ gauge symmetry embedding $Z_3$ is used and the domain wall problem is solved. The anomaly cancellation conditions for the extra $U(1)$ usually imply the addition of exotic matter to the spectrum.

The $\mu\nu$SSM also solves the $\mu$ problem generating an effective $\mu$ term through the VEVs of gauge singlets, in this case, right-handed sneutrinos. A superpotential term $\lambda^i\hat{\nu}_i^c\hat{H}_1\hat{H}_2$ is used, neutrino data is reproduced, and no extra singlet superfields are added to the spectrum. As in the NMSSM, the symmetry invoked to forbid the explicit $\mu$ term is a $Z_3$ discrete symmetry and consequently, the $\mu\nu$SSM is expected to have the same domain wall problem. Nevertheless, the usual solution with non-renormalizable operators work in the same way that in the NMSSM. Anyway, it is also interesting to extend the gauge group of the $\mu\nu$SSM with an extra $U(1)$ factor for embedding the $Z_3$ symmetry and solve the domain wall problem.

Summarizing, we have interesting motivations for extending the gauge group of the $\mu\nu$SSM. In the following we will study the extension with a $U(1)$ factor for selecting the terms allowed in the superpotential. With the anomaly cancellation conditions we will determine the extra charges of the particles and we will see that exotic matter has to be added to the spectrum.

## 5.2 Anomaly cancellation conditions

The idea of extending the gauge group of the SM has been extensively analysed in the literature in many different frameworks (see [114] for early examples). In the context of SUSY, we have already mentioned $U(1)$SSM-type models [115]. There are restrictive experimental bounds to the extension with an extra $U(1)$ factor deduced from direct searches of a new gauge boson $Z'$ at Tevatron, precision indirect tests at the Z-pole performed in LEP2 or weak neutral current experiments. These bounds depend on the couplings of the $Z'$ of the specific model considered but, in general, the lower limit on the mass of the $Z'$ [116] and the upper limit to the mixing between the $Z$ and the $Z'$ [117] are usually estimated to be respectively $M_{Z'} > (500 - 800 \text{ GeV})$ and $R < \mathcal{O}(10^{-3})$.

In the following, we will work with the gauge group of the SM adding an extra U(1),

$$SU(3)_C \times SU(2)_L \times U(1)_Y \times U(1)_{\text{extra}}. \tag{5.6}$$

With this extra $U(1)$ we will select the terms that will be allowed in the superpotential and we will prohibit the terms that could lead to phenomenological problems as we have already explained in Section 5.1. We will see that, except in the case not considered here where certain superpotential couplings are prohibited at the tree-level [118], the cancellation of the gauge anomalies associated to the extra $U(1)$ forces the introduction of exotic matter to the spectrum. We will search for a model with minimal extra matter content that selects adequately all the terms allowed in the superpotential. With the anomaly cancellation conditions we will constrain the extra charges.

The matter content of the $\mu\nu$SSM with three families of quarks and leptons has the following representation under the gauge group (5.6):

$$\begin{gathered} Q(3,2,\frac{1}{6},Q_Q)\ ;\ u^c(\bar{3},1,-\frac{2}{3},Q_u)\ ;\ d^c(\bar{3},1,\frac{1}{3},Q_d)\ ;\ L(1,2,-\frac{1}{2},Q_L) \\ e^c(1,1,1,Q_e)\ ;\ \nu^c(1,1,0,Q_{\nu^c})\ ;\ H_1(1,2,-\frac{1}{2},Q_{H_1})\ ;\ H_2(1,2,\frac{1}{2},Q_{H_2}) \end{gathered} \tag{5.7}$$

where for simplicity we take the extra charges as family independent.

Now we ask the Yukawa terms $\hat{Q}\hat{H}_1\hat{d}^c$, $\hat{Q}\hat{H}_2\hat{u}^c$, $\hat{L}\hat{H}_1\hat{e}^c$, $\hat{L}\hat{H}_2\hat{\nu}^c$ (that give tree-level masses to all fermions) and the effective $\mu$ term $\hat{\nu}^c\hat{H}_1\hat{H}_2$ to be allowed in the superpotential. Since they have to be invariant under the $U(1)_{\text{extra}}$, we can obtain five equations for the extra $U(1)$ charges. Using

these equations we can express five charges in terms of the other three:

$$\begin{aligned} Q_u &= Q_{H_1} + Q_d - Q_{H_2} \\ Q_Q &= -Q_{H_1} - Q_d \\ Q_e &= -2Q_{H_1} \\ Q_L &= Q_{H_1} \\ Q_{\nu^c} &= -Q_{H_1} - Q_{H_2}. \end{aligned} \tag{5.8}$$

It is worth noticing here that equations (5.8) imply that the lepton number violating terms, $\hat{L}\hat{L}\hat{e}^c$ and $\hat{L}\hat{Q}\hat{d}^c$, are automatically allowed. Thus to avoid fast proton decay, the baryon number violating term, $\hat{u}^c\hat{d}^c\hat{d}^c$, should be forbidden and using (5.8) we obtain:

$$Q_{H_1} \neq Q_{H_2} - 3Q_d. \tag{5.9}$$

Besides, to forbid the bilinear $\mu$ term, $\mu\hat{H}_1\hat{H}_2$, one has to impose,

$$Q_{H_1} \neq -Q_{H_2}. \tag{5.10}$$

Given (5.8), this implies that the bilinear lepton number violating operator $\hat{L}\hat{H}_2$ is automatically forbidden. In addition, from (5.8) one obtains that $Q_{\nu^c} \neq 0$ and, as a consequence, the term that generates the cosmological domain wall problem, $\hat{\nu}^c\hat{\nu}^c\hat{\nu}^c$, is also automatically forbidden. It is worth noticing here that a Goldstone boson does not appear from the absence of this term in the superpotential, since the U(1) symmetry is gauged. As a consequence, the Goldstone boson is eaten by the Z' in the process of EW symmetry breaking. Although this effective Majorana mass term, typical of the $\mu\nu$SSM, is not present now, we will see in the next section that a generalized seesaw matrix mixing neutrinos with neutralinos can generate the correct neutrino masses.

Summarizing, selecting the terms allowed in the superpotential, the following conditions on the extra charges are obtained:

$$\begin{aligned} &Q_u = Q_{H_1} + Q_d - Q_{H_2} \\ &Q_Q = -Q_{H_1} - Q_d \\ &Q_e = -2Q_{H_1} \\ &Q_L = Q_{H_1} \\ &Q_{\nu^c} = -Q_{H_1} - Q_{H_2} \\ &Q_{H_1} \neq Q_{H_2} - 3Q_d \quad \text{to evade the proton decay problem.} \\ &Q_{H_1} \neq -Q_{H_2} \qquad \text{to forbid bilinear terms and domain walls.} \end{aligned} \tag{5.11}$$

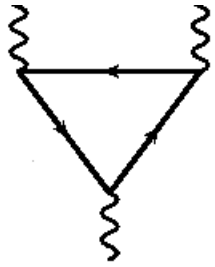

Figure 5.2: Feynman diagram of a triangular anomaly.

All realistic models on particle physics have to be free from gauge anomalies in order to satisfy important theoretical requirements as renormalizability and consistency. In Fig. 5.2 is represented the anomaly Feynman diagram. In the case of the SM, the values of the hypercharges lead to the cancellation of the gauge anomalies associated to $U(1)_Y$. In fact, this configuration of the hypercharges is the only possible one that cancels all the gauge anomalies of the SM (once we consider the gravitational anomaly). Therefore, we will use this powerful argument of the cancellation of gauge anomalies to determine the extra charges of the particles of the $\mu\nu$SSM. We will see that the addition of exotic matter is needed. This exotic matter should be sufficiently massive to have escaped detection and the hypercharges have to be chosen in a way not to spoil the SM anomaly cancellation.

We have six anomaly cancellation equations (see Table 5.1) to determine the extra charges of the model. Note that we take into account the gravi-

| | |
|---|---|
| $[SU(3)_C]^2 - U(1)_{extra}$ | $\sum Q_{\rm extra} = 0$ (color triplets only) |
| $[SU(2)_L]^2 - U(1)_{extra}$ | $\sum Q_{\rm extra} = 0$ (SU(2) doublet fermions only) |
| $[U(1)_Y]^2 - U(1)_{extra}$ | $\sum Q_{\rm extra} Y^2 = 0$ |
| $U(1)_Y - [U(1)_{extra}]^2$ | $\sum Y Q_{\rm extra}^2 = 0$ |
| $[U(1)_{extra}]^3$ | $\sum Q_{\rm extra}^3 = 0$ |
| $[Gravity]^2 - U(1)_{extra}$ | $\sum Q_{\rm extra} = 0$ |

Table 5.1: Anomaly cancellation equations (see e.g. [119]). The sum extends over all left-handed fermions and antifermions. $Q_{\rm extra}$ generically denotes the extra charges of the particles.

tational anomaly. We also want to stress that we take the number of Higgs families, $n_H$, as unknown to be determined with the anomaly conditions.

Let us analyse the anomaly equation $[SU(3)_C]^2U(1)_{\text{extra}}$ given in Table 5.1. In the corresponding Feynman diagram, see Fig. 5.2, only color triplets run in the loop. The anomaly equation reads: $3(2Q_Q + Q_u + Q_d) = 0$. Using (5.11) this equation is reduced to $Q_{H_1} = -Q_{H_2}$, which does not fulfill (5.10), thus the bilinear operators would be allowed in the superpotential, spoiling the solution of the $\mu\nu$SSM to the $\mu$ problem. Then, we conclude that exotic matter with color charge has to be added to the spectrum. On the other hand, in order not to alter the anomaly cancellation conditions associated to the SM gauge group, we assume that we have $n_q$ generations of exotics which are vector-like pairs of chiral superfields with opposite hypercharges, $\hat{q}(3, 1, Y_q, Q_q)$ and $\hat{q}^c(\bar{3}, 1, -Y_q, Q_{q^c})$. In addition, to avoid conflicts with experiments, the exotic quarks must be sufficiently heavy to not have been detected. Then, we add a trilinear effective mass term in the superpotential:

$$\lambda_q^{ijk}\hat{\nu}_i^c\hat{q}_j\hat{q}_k^c. \tag{5.12}$$

Requiring that this term is allowed by the $U(1)_{\text{extra}}$, i.e. $Q_{\nu^c} = -Q_q - Q_{q^c}$, and using (5.11), we obtain the relation:

$$Q_q + Q_{q^c} = Q_{H_1} + Q_{H_2} \tag{5.13}$$

Taking into account this relation together with the equation of cancellation of the $[SU(3)_C]^2U(1)_{\text{extra}}$ anomaly, we finally obtain $n_q = 3$.

The $[Gravity]^2U(1)_{\text{extra}}$ anomaly equation takes the form:

$$\begin{aligned} &3(6Q_Q + 3Q_u + 3Q_d + 2Q_L + Q_e + Q_{\nu^c}) + n_H(2Q_{H_1} + 2Q_{H_2}) \\ &+3(3Q_q + 3Q_{q^c}) = 0, \end{aligned} \tag{5.14}$$

and using (5.11) and (5.13) we arrive to $(2n_H - 3)(Q_{H_1} + Q_{H_2}) = 0$ which has no solution for $Q_{H_1} \neq -Q_{H_2}$ or an integer number of Higgs families. Then we conclude that we have to add more exotic matter to the spectrum to cancel the gravitational anomaly. Since we would like to extend the model with the minimal content of matter, the simplest option is to add a third degree of freedom on the extra charges, with $n_s$ generations of singlets under the SM gauge group, $\hat{s}(1, 1, 0, Q_s)$, in order not to alter the SM anomaly cancellation. Being a singlet under the SM gauge group, it would only interact through the gravitational interaction or through its extra $U(1)$ charge. As there is a high lower bound to the mass of the $Z'$ this extra singlet would have escaped experimental detection and no mass term is needed in the superpotential.

In the $[SU(2)_L]^2U(1)_{\text{extra}}$ anomaly equation, only $SU(2)_L$ doublets run in the loop and takes the form:

$$3(3Q_Q + Q_L) + n_H(Q_{H_1} + Q_{H_2}) = 0 \tag{5.15}$$

and using (5.11) we obtain $Q_d = \frac{n_H-6}{9}Q_{H_1} + \frac{n_H}{9}Q_{H_2}$. Note that in the case $n_H = 3$ we would have $Q_{H_1} = Q_{H_2} - 3Q_d$ that leads to B-violating operators in the superpotential. Therefore, the case $n_H = 3$ is excluded for solving the proton decay problem. The gravitational anomaly after using (5.11) gives the value of the extra charge of the extra singlets: $Q_s = \frac{3-2n_H}{n_s}(Q_{H_1} + Q_{H_2})$.

The anomaly $[U(1)_Y]^2U(1)_{\text{extra}}$ is given by:

$$\begin{aligned} &3(6Y_Q^2Q_Q + 3Y_u^2Q_u + 3Y_d^2Q_d + 2Y_L^2Q_L + Y_e^2Q_e + Y_\nu^2Q_{\nu^c}) \\ &+n_H(2Y_{H_1}^2Q_{H_1} + 2Y_{H_2}^2Q_{H_2}) + 3(3Y_q^2Q_q + 3Y_{q^c}^2Q_{q^c}) + n_sY_s^2Q_s = 0 \end{aligned} \tag{5.16}$$

and after using (5.11), (5.13), $Y_s = 0$ and $Y_{q^c} = -Y_q$ we finally obtain $(9Y_q^2+n_H-4)(Q_{H_1}+Q_{H_2}) = 0$. Taking into account $Q_{H_1} \neq -Q_{H_2}$ we obtain $Y_q = \frac{\sqrt{4-n_H}}{3}$. The cases $n_H = 1, 2$ are excluded since $Y_q$ takes irrational values. Values for $n_H > 4$ are also excluded since $Y_q$ would be complex. Finally, the case $n_H = 4$ is excluded since the anomaly equation $[U(1)_{\text{extra}}]^2U(1)_Y$ would automatically lead to $Q_{H_1} = -Q_{H_2}$. The only option left is $n_H = 3$ with $Y_q = \pm\frac{1}{3}$ but we have already seen that the $[SU(2)_L]^2U(1)_{\text{extra}}$ implies $n_H \neq 3$ for solving the proton decay problem.

We conclude that it is not possible to cancel all the anomalies with only three new degrees of freedom $(Q_q, Q_{q^c}, Q_s)$. Then, we are forced to introduce more exotic matter to the spectrum. Before carrying out that analysis in Subsection 5.2.2, let us suppose that the proton decay problem is solved with baryon triality or string theory arguments and then study the interesting solution with $n_H = 3$ and $Y_q = \pm\frac{1}{3}$ in the next subsection.

### 5.2.1 An $U(1)_{\text{extra}}$ extension with B-violating operators

In this subsection we will study an interesting model that consists of a $U(1)_{\text{extra}}$ extension of the $\mu\nu$SSM with B-violating operators allowed in the superpotential. This model solves the domain wall problem, forbids bilinear terms but does not address proton decay. Nevertheless, baryon triality or string theory arguments could guarantee the stability of the proton.

Let us recall that this model has $n_q = 3$ extra color triplets, vector-like under the SM gauge group $\hat{q}(3, 1, Y_q, Q_q)$ and $\hat{q}^c(\bar{3}, 1, -Y_q, Q_{q^c})$ with $Q_q + Q_{q^c} = Q_{H_1} + Q_{H_2}$ as well as $n_s$ generations of SM singlets. The anomaly equation $[U(1)_Y]^2U(1)_{\text{extra}}$ gives $n_H = 3$ and $Y_q = \pm\frac{1}{3}$. The $[SU(2)_L]^2U(1)_{\text{extra}}$ anomaly equation gives $Q_{H_1} = Q_{H_2} - 3Q_d$ and the gravitational anomaly leads to $Q_s = \frac{-3}{n_s}(Q_{H_1} + Q_{H_2})$. The $[U(1)_{\text{extra}}]^2U(1)_Y$ is quadratic on the

extra charges and is given by:

$$\begin{aligned}&3(6Y_Q Q_Q^2+3Y_u Q_u^2+3Y_d Q_d^2+2Y_L Q_L^2+Y_e Q_e^2+Y_\nu Q_{\nu^c}^2)\\&+3(2Y_{H_1}Q_{H_1}^2+2Y_{H_2}Q_{H_2}^2)+3(3Y_q Q_q^2+3Y_{q^c}Q_{q^c}^2)+n_s Y_s Q_s^2=0\end{aligned} \tag{5.17}$$

and after substituting all the variables known we would obtain a complicate expression for $Q_q$ in terms of $Q_{H_1}$ and $Q_{H_2}$ and using $Q_q+Q_{q^c}=Q_{H_1}+Q_{H_2}$ we would also obtain an expression for $Q_{q^c}$ as a function of $Q_{H_1}$ and $Q_{H_2}$. Finally, the anomaly equation $U(1)^3_{\text{extra}}$ is cubic in the extra charges:

$$\begin{aligned}&3(6Q_Q^3+3Q_u^3+3Q_d^3+2Q_L^3+Q_e^3+Q_{\nu^c}^3)+3(2Q_{H_1}^3+2Q_{H_2}^3)\\&+3(3Q_q^3+3Q_{q^c}^3)+n_s Q_s^3=0\end{aligned} \tag{5.18}$$

and after replacing all the variables known we obtain $\frac{3(27n_s^2+9(n_s^2-36))}{36n_s^2}(Q_{H_1}+Q_{H_2})^3=0$. The only way for solving this equation with $Q_{H_1}\neq -Q_{H_2}$ is to impose $n_s=3$. Note that with the six anomaly cancellation equations we have been able to solve all the extra charges in terms of two of them, $Q_{H_1}$ and $Q_{H_2}$. At the same time we have been able to determine the number of generations and hypercharges of the exotic matter in a unique way. For the complete determination of the extra charges, in this class of $U'(1)$ extensions of SUSY models, it is usual to impose additional conditions. The value of $Q_{H_2}$ in terms of $Q_{H_1}$ can be obtained imposing that the bases of the hypercharge and the extra charge have to be orthogonal, that is $Tr[YY']=0$. The normalization factor, that is, the numerical value of $Q_{H_1}$ can be obtained imposing $Tr[Y^2]=Tr[Y'^2]$. We will explain in more detail why to use such additional conditions in Subsection 5.2.2.

For definiteness, here we present the values of the extra charges up to the normalization factor for the case $Y_q=\frac{1}{3}$:

$$\begin{gathered}Q_{H_2}=4Q_{H_1}\ ,\ Q_Q=-2Q_{H_1}\ ,\ Q_u=-2Q_{H_1}\ ,\ Q_d=Q_{H_1}\ ,\ Q_L=Q_{H_1}\\Q_e=-2Q_{H_1}\ ,\ Q_{\nu^c}=-5Q_{H_1}\ ,\ Q_q=Q_{H_1}\ ,\ Q_{q^c}=4Q_{H_1}\ ,\ Q_s=-5Q_{H_1}\end{gathered} \tag{5.19}$$

This model is an interesting $U'(1)$ extension of the $\mu\nu$SSM since it has the minimal matter content and the solution is unique. It also has the nice feature of having three generations of Higgses as well as three generations of exotic matter. The superpotential of the model taking into account all renormalizable gauge invariant terms, neglecting generation, color and $SU(2)$ indices and omitting the corresponding couplings is given by:

$$\begin{aligned}W &= H_2Qu^c+H_1Qd^c+H_1Le^c+H_2L\nu^c+QLd^c+LLe^c\\&+ u^cd^cd^c+LH_2s+\nu^cH_1H_2+\nu^cqq^c+sH_1H_2+sqq^c\\&+ u^cq^cq^c+Qqq+QLq^c+QH_1q^c+\nu^cqd^c+sqd^c\end{aligned} \tag{5.20}$$

Let us briefly remark that, as the extra singlets have the same quantum numbers as the right-handed neutrinos and they couple in the same way in the superpotential, these three generations of exotic singlets are in fact three more generations of right-handed neutrinos. Nevertheless, one could imagine that those six generations are in fact $3+3$ generations that could be distinguished by some high-energy extra U(1) gauge group, perhaps coming from the compactification of a string model [104].

It is interesting to note that this model could serve as the starting point to construct a SUSY model with SCPV having a complex CKM matrix explaining the recent experimental results from BABAR [53] and BELLE [54] and being in agreement with the EDMs bounds and with the experiments with K mesons. As it is explained in Chapter 3, SCPV is an alternative to the usual CKM mechanism (that is, with explicit CP violation through complex Yukawas) for explaining the CP violation measured experimentally in the quark sector. In Chapter 3 it is demonstrated that the $\mu\nu$SSM can violate CP spontaneously at the tree-level. The main drawback of SUSY models with SCPV is that, in general, the CKM matrix is real since the complex phases of the VEVs are not transmitted to the quark sector due to the fact that these phases can be reasorbed. A real CKM matrix has been recently excluded in [52]. In [57] a SUSY model with SCPV where a complex CKM matrix arises is built adding to the spectrum exotic quarks vector-like under the SM gauge group that couple to the ordinary quarks of the SM. In principle, a similar study could be performed with the model presented here. This is out of the scope of this Thesis, but this analysis is left for a future work.

### 5.2.2 The $U(1)_{\mathbf{extra}}$ extension of the $\mu\nu$SSM

We have seen before Subsection 5.2.1 that with three extra degrees of freedom in the extra charges it is not possible to cancel all the anomalies prohibiting at the same time B-violating and bilinear operators. Then, we have to add more exotic matter. As we would like to find the model with minimal matter content, we have tried to find a model with four extra degrees of freedom in the extra charges. We have not found any viable model. Here we only summarise our results:

- Exotic matter: $n_{q_1}$ and $n_{q_2}$ generations of color triplets vector-like $\hat{q}_1(3,1,Y_1,Q_{q_1})$, $\hat{q}_1^c(\bar{3},1,-Y_1,Q_{q_1^c})$, $\hat{q}_2(3,1,Y_2,Q_{q_2})$ and $\hat{q}_2^c(\bar{3},1,-Y_2,Q_{q_2^c})$. In this model with two types of color triplets with effective mass terms in the superpotential $\hat{\nu}^c\hat{q}_1\hat{q}_1^c$ and $\hat{\nu}^c\hat{q}_2\hat{q}_2^c$, we have checked that it is not possible to cancel all the anomaly equations associated to the extra

$U(1)$ with $Q_{H_1} \neq -Q_{H_2}$.

- Exotic matter: $n_q$ generations of color triplets vector-like $\hat{q}(3,1,Y_q,Q_q)$ and $\hat{q}^c(\bar{3},1,-Y_q,Q_{q^c})$, $n_l$ and $n_s$ generations of $SU(2)_L$ doublets and singlets respectively $\hat{l}(1,2,0,Q_l)$ and $\hat{s}(1,1,0,Q_s)$ with vanishing hypercharge to not spoil the anomaly cancellation of the SM. It is possible to cancel all the anomaly equations with $Q_{H_1} \neq -Q_{H_2}$ but without a mass term in the superpotential for the extra doublets.

- Exotic matter: $n_q$ generations of color triplets vector-like $\hat{q}(3,1,Y_q,Q_q)$ and $\hat{q}^c(\bar{3},1,-Y_q,Q_{q^c})$ and $n_s$ generations of two types of singlets under $SU(3)_C \times SU(2)_L$ with non-vanishing and opposite hypercharge to not spoil the SM anomaly cancellation (for vanishing hypercharge it is impossible to cancel all the anomalies). As the singlets have non-zero hypercharge, they have to be sufficiently massive to have not been detected. If we impose to have an effective mass term in the superpotential of the type $\hat{\nu}^c\hat{s}_1\hat{s}_2$ we have checked that it is not possible to cancel all the anomaly equations with $Q_{H_1} \neq -Q_{H_2}$.

- Exotic matter: $n_q$ generations of color triplets vector-like $\hat{q}(3,1,Y_q,Q_q)$ and $\hat{q}^c(\bar{3},1,-Y_q,Q_{q^c})$ and $n_l$ generations of two type of $SU(2)_L$ doublets with opposite hypercharges to not spoil the SM anomaly cancellation $l(1,2,Y_l,Q_l)$ and $l^c(1,2,-Y_l,Q_{l^c})$ with effective mass terms in the superpotential $\hat{\nu}^c\hat{q}\hat{q}^c$ and $\hat{\nu}^c\hat{l}\hat{l}^c$. In this case the gravitational anomaly, after substitutions, takes the form $(2n_H+2n_l-3)(Q_{H_1}+Q_{H_2})=0$ and can not be satisfied for $Q_{H_1} \neq -Q_{H_2}$ and integer number of families.

We have demonstrated that with four extra variables in the extra charges, it is not possible to cancel all the anomalies selecting the adequate superpotential terms at the same time. Then, with five extra variables on the extra charges there are various possibilities. Here we only present the model that we consider the simplest $U(1)_{\rm extra}$ extension of the $\mu\nu$SSM with minimal exotic matter content. This model has the following extra matter: $n_q$ generations of color triplets vector-like under the SM gauge group

$$q(3,1,Y_q,Q_q)\ ,\ q^c(\bar{3},1,-Y_q,Q_{q^c}), \tag{5.21}$$

$n_l$ generations of $SU(2)_L$ doublets vector-like

$$l(1,2,Y_l,Q_l)\ ,\ l^c(1,2,-Y_l,Q_{l^c}) \tag{5.22}$$

and $n_s$ generations of singlets

$$s(1,1,0,Q_s). \tag{5.23}$$

As the exotic triplets and doublets have to be sufficiently massive to evade experimental detection, we include effective mass terms in the superpotential

$$\lambda_q \hat{\nu}^c \hat{q} \hat{q}^c + \lambda_l \hat{\nu}^c \hat{l} \hat{l}^c \tag{5.24}$$

giving rise to two additional equations:

$$\begin{aligned} &Q_q + Q_{q^c} = Q_{H_1} + Q_{H_2} \\ &Q_l + Q_{l^c} = Q_{H_1} + Q_{H_2}. \end{aligned} \tag{5.25}$$

We will see that the exotic singlets do not couple in the superpotential and do not play any role in the breaking of the EW symmetry. The presence of these extra singlets in the spectrum is not unexpected from a string theory point of view because, when string theory models are constructed for trying to reproduce the SM at low energies, extra singlets usually appear [120].

Now, we will follow the anomaly equations to determine the unknown extra charges, the numbers of generations and the hypercharges of the exotics. Let us remind that with the selection of the allowed terms in the superpotential we arrived to a system of equations for the extra charges of the particles of the spectrum (5.11). The five extra charges of the exotic matter add three more unknowns once we take into account the two equations for having effective mass terms in the superpotential (5.25). The number of Higgs families $n_H$ as well as the numbers of exotic matter generations are also taken as unknowns, the same as the hypercharges of the extra triplets and doublets. The $[SU(3)_C]^2 U(1)_{\text{extra}}$ anomaly equation gives

$$n_q = 3. \tag{5.26}$$

The $[SU(2)_L]^2 U(1)_{\text{extra}}$ anomaly equation, after using (5.11) and (5.25) leads to

$$Q_d = \frac{n_H + n_l - 6}{9} Q_{H_1} + \frac{n_H + n_l}{9} Q_{H_2}. \tag{5.27}$$

Note that the condition $Q_{H_1} \neq Q_{H_2} - 3Q_d$ to forbid B-violating operators gives a constraint for the numbers of generations $n_H + n_l \neq 3$. The gravitational anomaly after using (5.11), (5.25)-(5.27) gives:

$$Q_s = \frac{3 - 2n_H - 2n_l}{n_s} (Q_{H_1} + Q_{H_2}). \tag{5.28}$$

The $[U(1)_Y]^2 U(1)_{\text{extra}}$, after substitutions, leads to $(18Y_q^2 + 4n_l Y_l^2 + n_l + 2n_H - 8)(Q_{H_1} + Q_{H_2}) = 0$ giving the following restriction:

$$18Y_q^2 + 4n_l Y_l^2 = 8 - n_l - 2n_H. \tag{5.29}$$

| $n_H$ | 1 | 1 | 1 | 1 | 2 | 2 | 3 | 2 | 3 |
|---|---|---|---|---|---|---|---|---|---|
| $n_l$ | 3 | 3 | 4 | 4 | 2 | 2 | 1 | 2 | 1 |
| $Y_q$ | $\pm\frac{2}{5}$ | 0 | $\pm\frac{1}{3}$ | $\pm\frac{1}{9}$ | $\pm\frac{1}{5}$ | $\pm\frac{1}{3}$ | $\pm\frac{2}{9}$ | 0 | 0 |
| $Y_l$ | $\pm\frac{1}{10}$ | $\pm\frac{1}{2}$ | 0 | $\pm\frac{1}{3}$ | $\pm\frac{2}{5}$ | 0 | $\pm\frac{1}{6}$ | $\pm\frac{1}{2}$ | $\pm\frac{1}{2}$ |

Table 5.2: Number of generations of Higgses and extra doublets, and hypercharges that solve the $[U(1)_Y]^2 - U(1)_{extra}$ anomaly equation.

Note that the left-hand side of equation (5.29) is a sum of positive quantities and we can deduce an upper bound on the numbers of generations given by:

$$n_l + 2n_H \leq 8 \tag{5.30}$$

We can study (5.29) searching for reasonable rational values of the hypercharges. The solutions are presented in Table 5.2.

The $[U(1)_{\text{extra}}]^2U(1)_Y$ anomaly equation is quadratic in the extra charges: $3(6Y_QQ_Q^2 + 3Y_uQ_u^2 + 3Y_dQ_d^2 + 2Y_LQ_L^2 + Y_eQ_e^2 + Y_\nu Q_{\nu^c}^2) + n_H(2Y_{H_1}Q_{H_1}^2 + 2Y_{H_2}Q_{H_2}^2) + n_q(3Y_qQ_q^2 + 3Y_{q^c}Q_{q^c}^2) + n_l(2Y_lQ_l^2 + 2Y_{l^c}Q_{l^c}^2) + n_sY_sQ_s^2 = 0$. For each set of solutions appearing in Table 5.2 and using (5.11), (5.25)-(5.27), we can solve the value of $Q_q$ as a complicate function of $Q_{H_1}$, $Q_{H_2}$ and $Q_l$ and using (5.25) we can obtain $Q_{q^c}$ in terms of the same variables.

The $[U(1)_{\text{extra}}]^3$ anomaly equation is cubic in the extra charges: $3(6Q_Q^3 + 3Q_u^3 + 3Q_d^3 + 2Q_L^3 + Q_e^3 + Q_{\nu^c}^3) + 2n_H(Q_{H_1}^3 + Q_{H_2}^3) + 3n_q(Q_q^3 + Q_{q^c}^3) + 2n_l(Q_l^3 + Q_{l^c}^3) + n_sQ_s^3 = 0$. For each set of values $(n_H, n_l, Y_q, Y_l)$ that satisfies the $[U(1)_Y]^2U(1)_{\text{extra}}$ anomaly equation we obtain the value of $Q_l$ in terms of $Q_{H_1}$ and $Q_{H_2}$ and using (5.25) we obtain $Q_{l^c}$ in terms of $Q_{H_1}$ and $Q_{H_2}$. The only set of values $(n_H, n_l, Y_q, Y_l)$ in Table 5.2 that give rise to rational values for $Q_l$ and $Q_{l^c}$ are:

- $n_H = 1$, $n_l = 3$, $n_s = 6$, $Y_q = \pm\frac{2}{5}$, $Y_l = \frac{1}{10}$ with two distinct solutions for $Q_l$.
- $n_H = 1$, $n_l = 3$, $n_s = 6$, $Y_q = 0$, $Y_l = \pm\frac{1}{2}$ with two distinct solutions for $Q_q$.

It is worth noticing here that, although at the end we are left with the six different solutions (models) discussed above, we will see in the next section that all of them give rise to the same phenomenology at low energies. This is because the six models only differ in the extra charges and hypercharges of the exotic matter, and this matter does not play any role in the EW breaking.

We have then obtained all the extra charges in terms of two of them, $Q_{H_1}$ and $Q_{H_2}$. For rational values of $Q_{H_1}$ and $Q_{H_2}$ we obtain rational values for the

rest of extra charges. For definiteness, we add two additional conditions for the complete determination of the extra charges. First, we impose that the bases of the hypercharge and the extra charge are orthogonal. This means $Tr[YQ] = 0$. This condition gives us $Q_{H_2} = 6Q_{H_1}$. Second, we impose the normalization condition for the extra charges $Tr[Q^2] = Tr[Y^2]$ as is done in [31]. This condition is not physical since the relevant quantity is the product of the extra gauge coupling constant $g_1'$ times the normalization factor. The normalization factor is irrational but this is irrelevant. With this condition we obtain the numerical value of $Q_{H_1}$ and consequently, the numerical values of all the extra charges. We present these values in Tables 5.3 and 5.4, where the normalization factor is given by $N = \sqrt{\frac{3}{2426}}$.

| | | | | |
|---|---|---|---|---|
| $Q_{H_1} = 3\ N$ | $Q_{H_2} = 18\ N$ | $Q_Q = -\frac{31}{3}\ N$ | $Q_u = -\frac{23}{3} N$ | $Q_d = \frac{22}{3}\ N$ |
| $Q_L = 3\ N$ | $Q_e = -6\ N$ | $Q_{\nu^c} = -21\ N$ | $Q_s = -\frac{35}{2}\ N$ | |

Table 5.3: Values of the $U(1)_{\text{extra}}$ charges for the Standard Model content of the $\mu\nu$SSM and for the extra singlets.

| $Q_q$ | $Q_{q^c}$ | $Q_l$ | $Q_{l^c}$ | |
|---|---|---|---|---|
| $\frac{257}{30}N$ | $\frac{373}{30}N$ | $\frac{19}{15}N$ | $\frac{296}{15}N$ | Model 1: $Y_q = \frac{2}{5},\ Y_l = \frac{1}{10},\ Q_l = \frac{1}{45}(-5Q_{H_1} + 4Q_{H_2})$ |
| $\frac{173}{30}N$ | $\frac{457}{30}N$ | $\frac{271}{15}N$ | $\frac{44}{15}N$ | Model 2: $Y_q = \frac{2}{5},\ Y_l = \frac{1}{10},\ Q_l = \frac{1}{45}(31Q_{H_1} + 40Q_{H_2})$ |
| $\frac{373}{30}N$ | $\frac{257}{30}N$ | $\frac{19}{15}N$ | $\frac{296}{15}N$ | Model 3: $Y_q = -\frac{2}{5},\ Y_l = \frac{1}{10},\ Q_l = \frac{1}{45}(-5Q_{H_1} + 4Q_{H_2})$ |
| $\frac{457}{30}N$ | $\frac{173}{30}N$ | $\frac{271}{15}N$ | $\frac{44}{15}N$ | Model 4: $Y_q = -\frac{2}{5},\ Y_l = \frac{1}{10},\ Q_l = \frac{1}{45}(31Q_{H_1} + 40Q_{H_2})$ |
| $\frac{7}{2}N$ | $\frac{35}{2}N$ | $\frac{19}{3}N$ | $\frac{44}{3}N$ | Model 5: $Y_q = 0,\ Y_l = \frac{1}{2},\ Q_q = \frac{1}{6}(Q_{H_1} + Q_{H_2})$ |
| $\frac{35}{2}N$ | $\frac{7}{2}N$ | $\frac{19}{3}N$ | $\frac{44}{3}N$ | Model 6: $Y_q = 0,\ Y_l = \frac{1}{2},\ Q_q = \frac{5}{6}(Q_{H_1} + Q_{H_2})$ |

Table 5.4: Values of the $U(1)_{\text{extra}}$ charges for the extra triplets and doublets added to the Standard Model spectrum of the $\mu\nu$SSM, for the six solutions of the $[U(1)_{extra}]^3$ anomaly equation.

Summarizing, we have found six interesting models with the following exotic matter: three generations of vector-like color triplets with respect to the SM gauge group (5.21), three generations of $SU(2)_L$ doublets (5.22), and six generations of SM singlets (5.23). The superpotential is given by:

$$\begin{aligned} W &= \epsilon_{ab}(Y_u^{ij}\hat{H}_2^b\hat{Q}_i^a\hat{u}_j^c + Y_d^{ij}\hat{H}_1^a\hat{Q}_i^b\hat{d}_j^c + Y_e^{ij}\hat{H}_1^a\hat{L}_i^b\hat{e}_j^c + Y_\nu^{ij}\hat{H}_2^b\hat{L}_i^a\hat{\nu}_j^c) \\ &- \epsilon_{ab}\lambda^i\hat{\nu}_i^c\hat{H}_1^a\hat{H}_2^b + \epsilon_{ab}(\lambda'^{ijk}\hat{Q}_i^a\hat{L}_j^b\hat{d}_k^c + \lambda'''^{ijk}\hat{L}_i^a\hat{L}_j^b\hat{e}_k^c) \\ &+ \lambda_q^{ijk}\hat{\nu}_i^c\hat{q}_j\hat{q}_k^c + \epsilon_{ab}\lambda_l^{ijk}\hat{\nu}_i^c\hat{l}_j^a(\hat{l}_k^b)^c \end{aligned} \tag{5.31}$$

Let us now make a few comments on the hypercharges of the extra matter. In this model, the hypercharges of the exotic matter lead to non-standard fractional electric charges. This issue has been discussed for example in [121], and references therein. In the case of the exotic triplets, they could form colour-neutral fractionally charged states since the triplets can bind. In principle, the existence of stable charged states could create conflicts with cosmological bounds. Thermal production of these particles would overclose the Universe unless their masses are below a few TeV [122, 123]. In models with non-standard extra triplets, the lightest colour-neutral fractionally charged state will be stable due to electric charge conservation. The estimation of its relic abundance contradicts limits on the existence of fractional charge in matter which is less than $10^{-20}$ per nucleon [123]. Thus, avoiding such fractionally charged states is necessary. A possible mechanism to carry it out is inflation. The inflationary period would dilute these particles. For this to happen, the reheating temperature $T_{RH}$ should be low enough not to produce them again. This reheating temperature must be smaller than $10^{-3}$ times the mass of the particles [124]. In our case, since the exotic triplets have masses of the order of the TeV scale (given by $\lambda_q^{ijk}\nu_i^c$), we should have $T_{RH} < 1$ GeV. This, in principle is possible since the only constraint on this temperature is that it has to be larger than 1 MeV not to spoil the successful nucleosynthesis predictions.

Let us finally recall that R-parity conserving models still need some fine-tuning to agree with the experimental bounds on the proton lifetime since R-parity does not forbid non-renormalizable dimension five operators that break baryon or lepton number, and could produce too fast proton decay if the couplings are of order one [109]. We have checked that in the model analysed here, there are 43 non-renormalizable dimension five B-violating operators allowed by the gauge symmetry of the SM such as $\hat{Q}\hat{Q}\hat{Q}\hat{L}$, $\hat{u}^c\hat{u}^c\hat{d}^c\hat{e}^c$ or $\hat{Q}\hat{Q}\hat{Q}\hat{H}_1$. Nevertheless, all of them are prohibited by the extra $U(1)$. In this sense, the extra $U(1)$ symmetry is more successful than R-parity to protect the proton of decaying. It is then clear that the $\mu\nu$SSM with an extra $U(1)$ is safe from constraints from the non-observation of proton decay at Super-Kamiokande [105].

In Section 5.3 we will study some relevant aspects of the phenomenology of this model.

## 5.3 EW breaking and experimental constraints

In this section we will study the phenomenology of the $U(1)_{\text{extra}}$ $\mu\nu$SSM model presented in Subsection 5.2.2.

The gauge symmetry $SU(3)_C \times SU(2)_L \times U(1)_Y \times U(1)_{extra}$ has to be spontaneously broken to $SU(3)_C \times U(1)_{e.m.}$. To discuss this breaking we have first to calculate the neutral scalar potential, which is the sum of three contributions: F-terms, D-terms and soft terms. Working in the framework of gravity-mediated SUSY breaking, the soft Lagrangian can be written as:

$$\begin{aligned}
\mathcal{L}_{\rm soft} &= \frac{1}{2}(M_3\tilde{\lambda}_3\tilde{\lambda}_3 + M_2\tilde{\lambda}_2\tilde{\lambda}_2 + M_1\tilde{\lambda}_1\tilde{\lambda}_1 + M_1'\tilde{\lambda}_1'\tilde{\lambda}_1' + h.c.) \\
&- \epsilon_{ab}[(A_uY_u)^{ij}H_2^b\tilde{Q}_i^a\tilde{u}_j^c + (A_dY_d)^{ij}H_1^a\tilde{Q}_i^b\tilde{d}_j^c + (A_eY_e)^{ij}H_1^a\tilde{L}_i^b\tilde{e}_j^c \\
&+ (A_\nu Y_\nu)^{ij}H_2^b\tilde{L}_i^a\tilde{\nu}_j^c + (A_{\lambda'}\lambda')^{ijk}\tilde{Q}_i^a\tilde{L}_j^b\tilde{d}_k^c + (A_{\lambda'''}\lambda''')^{ijk}\tilde{L}_i^a\tilde{L}_j^b\tilde{e}_k^c \\
&- (A_\lambda\lambda)^i\tilde{\nu}_i^cH_1^aH_2^b + (A_{\lambda_l}\lambda_l)^{ijk}\tilde{\nu}_i^c\tilde{l}_j^a\tilde{l}_b^{kc} + h.c.] \\
&- [(A_{\lambda_q}\lambda_q)^{ijk}\tilde{\nu}_i^c\tilde{q}_j\tilde{q}_k^c + h.c] - [(M_{\tilde{Q}}^2)^{ij}\tilde{Q}_i^{a*}\tilde{Q}_j^a + (M_{\tilde{u}^c}^2)^{ij}\tilde{u}_i^{c*}\tilde{u}_j^c \\
&+ (M_{\tilde{d}^c}^2)^{ij}\tilde{d}_i^{c*}\tilde{d}_j^c + (M_{\tilde{L}}^2)^{ij}\tilde{L}_i^{a*}\tilde{L}_j^a + (M_{\tilde{e}^c}^2)^{ij}\tilde{e}_i^{c*}\tilde{e}_j^c + M_{H_1}^2H_1^{a*}H_1^a \\
&+ M_{H_2}^2H_2^{a*}H_2^a + (M_{\tilde{\nu}^c}^2)^{ij}\tilde{\nu}_i^{c*}\tilde{\nu}_j^c + (M_{\tilde{s}}^2)^{ij}\tilde{s}_i^*\tilde{s}_j + (M_{\tilde{q}}^2)^{ij}\tilde{q}_i^*\tilde{q}_j \\
&+ (M_{\tilde{q}^c}^2)^{ij}\tilde{q}_i^{c*}\tilde{q}_j^c + (M_{\tilde{l}}^2)^{ij}\tilde{l}_i^*\tilde{l}_j + (M_{\tilde{l}^c}^2)^{ij}\tilde{l}_i^{ac*}\tilde{l}_j^{ac}] \qquad (5.32)
\end{aligned}$$

Once the EW symmetry is spontaneously broken, the neutral scalars develop in general the following VEVs:

$$\langle H_1^0\rangle = v_1, \quad \langle H_2^0\rangle = v_2, \quad \langle\tilde{\nu}_i\rangle = \nu_i \quad \langle\tilde{\nu}_i^c\rangle = \nu_i^c \ .$$

We have checked that the neutral components of the exotic matter do not take VEVs in a wide region of the parameter space, where we will concentrate. In what follows, it will be enough for our purposes to neglect mixing between generations in (5.31) and (5.32), and to assume that only one generation of sneutrinos gets VEVs $\nu$ and $\nu^c$. The extension of the analysis to all generations is straightforward, and the conclusions are similar. The expression of the neutral scalar potential is then given by:

$$\begin{aligned}
< V^0 > &= \frac{1}{8}(g_1^2+g_2^2)(|v_1|^2+|\nu|^2-|v_2|^2)^2 \\
&+ \frac{1}{2}g_1'^2(Q_{H_1}|v_1|^2 + Q_{H_2}|v_2|^2 + Q_L|\nu|^2 + Q_{\nu^c}|\nu^c|^2)^2 \\
&+ |Y_\nu|^2(|v_2|^2|\nu^c|^2 + |v_2|^2|\nu|^2 + |\nu|^2|\nu^c|^2) \\
&+ |\lambda|^2(|v_1|^2|v_2|^2 + |\nu^c|^2|v_2|^2 + |\nu^c|^2|v_1|^2) \\
&+ (-\lambda Y_\nu^* v_1\nu^*|v_2|^2 - \lambda Y_\nu^* v_1\nu^*|\nu^c|^2 + h.c.) \\
&+ M_{\tilde{L}}^2|\nu|^2 + M_{\tilde{\nu}^c}^2|\nu^c|^2 + M_{H_1}^2|v_1|^2 + M_{H_2}^2|v_2|^2 \\
&+ (A_\nu Y_\nu v_2\nu\nu^c - A_\lambda\lambda\nu^c v_1 v_2 + h.c.) \qquad (5.33)
\end{aligned}$$

We also assume, for simplicity, that there is not CP violation in the scalar sector and we take all the parameters and VEVs real in (5.33). The four minimization conditions are:

$$\begin{aligned}
\frac{\partial\langle V^0\rangle}{\partial v_1} &= \frac{1}{4}(g_1^2+g_2^2)(v_1^2+\nu^2-v_2^2)v_1 \\
&+ g_1'^2(Q_{H_1}v_1^2+Q_{H_2}v_2^2+Q_L\nu^2+Q_{\nu^c}\nu^{c2})Q_{H_1}v_1+\lambda^2 v_1(v_2^2+\nu^{c2}) \\
&+ M_{H_1}^2 v_1-\lambda Y_\nu\nu|v_2|^2-\lambda Y_\nu\nu|\nu^c|^2-A_\lambda\lambda\nu^c v_2=0
\end{aligned}$$

$$\begin{aligned}
\frac{\partial\langle V^0\rangle}{\partial v_2} &= -\frac{1}{4}(g_1^2+g_2^2)(v_1^2+\nu^2-v_2^2)v_2 \\
&+ g_1'^2(Q_{H_1}v_1^2+Q_{H_2}v_2^2+Q_L\nu^2+Q_{\nu^c}\nu^{c2})Q_{H_2}v_2+Y_\nu^2 v_2(\nu^2+\nu^{c2}) \\
&+ \lambda^2 v_2(v_1^2+\nu^{c2})+M_{H_2}^2 v_2-2\lambda Y_\nu v_1\nu v_2 \\
&+ A_\nu Y_\nu\nu\nu^c-A_\lambda\lambda\nu^c v_1=0
\end{aligned}$$

$$\begin{aligned}
\frac{\partial\langle V^0\rangle}{\partial \nu^c} &= g_1'^2(Q_{H_1}v_1^2+Q_{H_2}v_2^2+Q_L\nu^2+Q_{\nu^c}\nu^{c2})Q_{\nu^c}\nu^c+Y_\nu^2\nu^c(v_2^2+\nu^2) \\
&+ \lambda^2\nu^c(v_1^2+v_2^2)+M_{\tilde{\nu}^c}^2\nu^c-2\lambda Y_\nu v_1\nu\nu^c \\
&+ A_\nu Y_\nu v_2\nu-A_\lambda\lambda v_1 v_2=0
\end{aligned}$$

$$\begin{aligned}
\frac{\partial\langle V^0\rangle}{\partial \nu} &= \frac{1}{4}(g_1^2+g_2^2)(v_1^2+\nu^2-v_2^2)\nu \\
&+ g_1'^2(Q_{H_1}v_1^2+Q_{H_2}v_2^2+Q_L\nu^2+Q_{\nu^c}\nu^{c2})Q_L\nu+Y_\nu^2\nu(v_2^2+\nu^{c2}) \\
&+ M_{\tilde{L}}^2\nu-\lambda Y_\nu v_1 v_2^2-\lambda Y_\nu v_1\nu^{c2}+A_\nu Y_\nu v_2\nu^c=0 \qquad (5.34)
\end{aligned}$$

Notice that in the last equation in (5.34), $\nu\to 0$ when $Y_\nu\to 0$ and since the Yukawa coupling $Y_\nu$ determines the Dirac mass for the neutrinos, $m_D\equiv Y_\nu v_2$, it has to be very small for reproducing the bounds on neutrino masses. The smallness of the left-handed sneutrino VEVs for a correct description of the neutrino sector in the $\mu\nu$SSM has been numerically proved in [43, 44, 14].

We can now approximate the minimization equations neglecting the values of $\nu$ and $Y_\nu$, and we are left with only three equations. Solving the minimization conditions for the soft masses in terms of the extra charges, coupling constants, VEVs, and the parameters $\lambda$ and $A_\lambda\lambda$, one obtains:

$$\begin{aligned}
M^2_{H_1} &= -\frac{1}{4}(g_1^2+g_2^2)(v_1^2-v_2^2) - g_1'^2(Q_{H_1}v_1^2+Q_{H_2}v_2^2+Q_{\nu^c}\nu^{c2})Q_{H_1} \\
&- \lambda^2(v_2^2+\nu^{c2}) + A_\lambda\lambda\nu^c\frac{v2}{v1} \\
M^2_{H_2} &= \frac{1}{4}(g_1^2+g_2^2)(v_1^2-v_2^2) - g_1'^2(Q_{H_1}v_1^2+Q_{H_2}v_2^2++Q_{\nu^c}\nu^{c2})Q_{H_2} \\
&- \lambda^2(v_1^2+\nu^{c2}) + A_\lambda\lambda\nu^c\frac{v1}{v2} \\
M^2_{\tilde{\nu}^c} &= -g_1'^2(Q_{H_1}v_1^2+Q_{H_2}v_2^2+Q_{\nu^c}\nu^{c2})Q_{\nu^c} - \lambda^2(v_1^2+v_2^2) + A_\lambda\lambda\frac{v_1v_2}{\nu^c}
\end{aligned} \tag{5.35}$$

Note that these equations are equivalent (substituting $\nu^c$ by the VEV of a singlet scalar) to the minimization conditions for U(1)SSM models, where correct EW breaking is known to take place.

On the other hand, the VEVs have to satisfy several phenomenological constraints. First, the mass of the W boson, $M_W = \frac{1}{2}g_2^2(v_1^2+v_2^2+\nu^2)$, is well determined, leading to $(v_1^2+v_2^2) \simeq (174\text{ GeV})^2$ when $\nu$ is neglected. Second, the Z boson of the SM and the Z' boson associated to the $U(1)_{extra}$ are mixed with a mass-squared matrix given by:

$$\begin{pmatrix} M_Z^2 & M_{ZZ'}^2 \\ M_{ZZ'}^2 & M_{Z'}^2 \end{pmatrix} \tag{5.36}$$

where the entries are functions of the VEVs, gauge coupling constants and extra charges:

$$\begin{aligned}
M_Z^2 &= \frac{1}{2}(g_1^2+g_2^2)(v_1^2+v_2^2) \\
M_{Z'}^2 &= 2g_1'^2(Q_{H_1}^2v_1^2+Q_{H_2}^2v_2^2+Q_{\nu^c}^2\nu^{c2}) \\
M_{ZZ'}^2 &= g_1'\sqrt{g_1^2+g_2^2}(-Q_{H_1}v_1^2+Q_{H_2}v_2^2).
\end{aligned} \tag{5.37}$$

Diagonalizing this matrix one obtains the mass eigenstates. The experimental constraints imply the following bound [117] for the mixing parameter:

$$R = \frac{(M_{ZZ'}^2)^2}{M_Z^2M_{Z'}^2} \leq 10^{-3}. \tag{5.38}$$

In addition, the mass of the heaviest eigenstate should be larger than about 600 GeV [116]. If we also ask the heaviest eigenstate to be lighter than

2000 GeV in order not to have a very large fine-tuning (and for the $Z'$ to be discovered at present accelerator experiments), then

$$
\begin{aligned}
(600)^2 \leq & \frac{1}{4}(g_1^2+g_2^2)(v_1^2+v_2^2)+g_1'^2(Q_{H_1}^2v_1^2+Q_{H_2}^2v_2^2+Q_{\nu^c}^2\nu^{c2}) \\
& +[\frac{1}{16}(g_1^2+g_2^2)^2(v_1^2+v_2^2)^2+g_1'^4(Q_{H_1}^2v_1^2+Q_{H_2}^2v_2^2+Q_{\nu^c}^2\nu^{c2})^2 \\
& -\frac{1}{2}(g_1^2+g_2^2)g_1'^2(v_1^2+v_2^2)(Q_{H_1}^2v_1^2+Q_{H_2}^2v_2^2+Q_{\nu^c}^2\nu^{c2}) \\
& +g_1'^2(g_1^2+g_2^2)(-Q_{H_1}v_1^2+Q_{H_2}v_2^2)^2]^{1/2} \leq (2000)^2 \qquad (5.39)
\end{aligned}
$$

From the above equations and Eq. (5.35) it is obvious that the six models found in Section 5.2 give rise to the same phenomenology at low energies, since they only differ in the extra charges and hypercharges of the exotic matter, and this matter does not play any role in the EW breaking.

In order to study the solutions of the equations, we assume the following reasonable values for the parameters: $A_\lambda\lambda = 0.1$ TeV and $\lambda = 0.1, 0.3$. For the sake of definiteness we also take $g_1' = g_1$, together with the extra charges normalization condition $Tr[Y'^2] = Tr[Y^2]$, $1 < \tan\beta = \frac{v_2}{v_1} < 35$, and we work in the parameter space $(\nu^c, \tan\beta)$. Once imposed the experimental constraints on the existence of a new gauge boson $Z'$, we have checked that the effect of the bound on the $Z - Z'$ mixing is more important than the bounds on the mass of the heaviest eigenstate, although it is still possible to find wide allowed regions. The former experimental constraint implies a lower bound on the VEV of the right-handed sneutrino $\nu^c$, depending on the value of $\tan\beta$. In particular, for $\lambda = 0.3$ and $\tan\beta = 1$, $\nu^c$ must be larger than 2 TeV. For increasing values of $\tan\beta$, the lower bound on $\nu^c$ increases since it is more difficult to suppress the $Z - Z'$mixing. For example, for $\tan\beta = 3$ (7), one obtains that $\nu^c$ must be larger than about 4 (4.6) TeV. For $\tan\beta$ larger than 7, the lower bound on $\nu^c$ practically does not vary. Similar results are obtained for $\lambda = 0.1$, although in this case a tachyonic region appears and we always need values of $\nu^c$ larger than 2.5 TeV.

One can translate the constraints on the $Z'$ to the plane $(M_{H_1}^2, M_{H_2}^2)$, finding the allowed region in the parameter space of the soft masses. We show these regions in Figs. 5.3 and 5.4 for $\lambda = 0.1$ and 0.3, respectively.

Once we have shown that the model is phenomenologically viable, let us focus our attention on the neutralino sector. In the $\mu\nu$SSM with an extra U(1) gauge symmetry, the MSSM neutralinos mix with the extra gaugino. The fact that R-parity is broken in this model also produces the mixing of the neutralinos with left- and right-handed neutrinos. Of course, now we have to be sure that one eigenvalue of this matrix is very small, reproducing the experimental results about neutrino masses. In the weak interaction basis

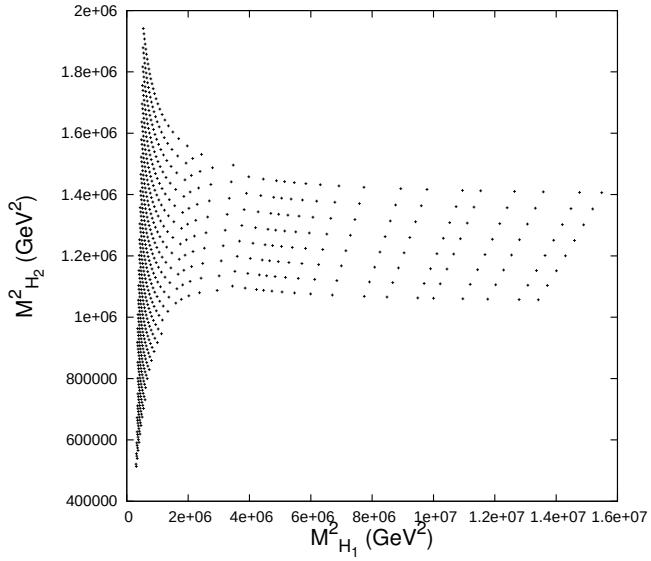


Figure 5.3: Allowed region by the experimental constraints on the $Z'$ in the plane $M^2_{H_1} - M^2_{H_2}$ for $\lambda = 0.1$

defined by $\psi^{0t} = (\tilde{Z}', \tilde{B}^0 = -i\tilde{\lambda}', \tilde{W}_3^0 = -i\tilde{\lambda}_3, \tilde{H}_1^0, \tilde{H}_2^0, \nu^c, \nu)$, the neutral fermion mass terms in the Lagrangian are $\mathcal{L}^{mass}_{neutral} = -\frac{1}{2}(\psi^0)^t \mathcal{M}_n \psi^0 + h.c.$, with $\mathcal{M}_n$ a $7 \times 7$ matrix ($11 \times 11$ if we include all generations of neutrinos),

$$\mathcal{M}_n = \begin{pmatrix} M & m \\ m^t & 0 \end{pmatrix}, \tag{5.40}$$

where

$$M = \begin{pmatrix} M_1' & 0 & 0 & \sqrt{2}g_1' Q_{H_1} v_1 & \sqrt{2}g_1' Q_{H_2} v_2 & \sqrt{2}g_1' Q_{\nu^c} \nu^c \\ 0 & M_1 & 0 & -\frac{1}{\sqrt{2}} g_1 v_1 & \frac{1}{\sqrt{2}} g_1 v_2 & 0 \\ 0 & 0 & M_2 & \frac{1}{\sqrt{2}} g_2 v_1 & -\frac{1}{\sqrt{2}} g_2 v_2 & 0 \\ \sqrt{2}g_1' Q_{H_1} v_1 & -\frac{1}{\sqrt{2}} g_1 v_1 & \frac{1}{\sqrt{2}} g_2 v_1 & 0 & -\lambda \nu^c & -\lambda v_2 \\ \sqrt{2}g_1' Q_{H_2} v_2 & \frac{1}{\sqrt{2}} g_1 v_2 & -\frac{1}{\sqrt{2}} g_2 v_2 & -\lambda \nu^c & 0 & -\lambda v_1 + Y_\nu \nu \\ \sqrt{2}g_1' Q_{\nu^c} \nu^c & 0 & 0 & -\lambda v_2 & -\lambda v_1 + Y_\nu \nu & 0 \end{pmatrix} \tag{5.41}$$

and

$$m^t = (\ \sqrt{2}g_1' Q_\nu \nu\ ,\ -\frac{1}{\sqrt{2}} g_1 \nu\ ,\ \frac{1}{\sqrt{2}} g_2 \nu\ ,\ 0\ ,\ Y_\nu \nu^c\ ,\ Y_\nu v_2\ ). \tag{5.42}$$

Using typical values of the soft gaugino masses, and with values for the rest of parameters in the region allowed by the constraints on the $Z'$, we have checked numerically that correct neutrino masses can easily be obtained, i.e.

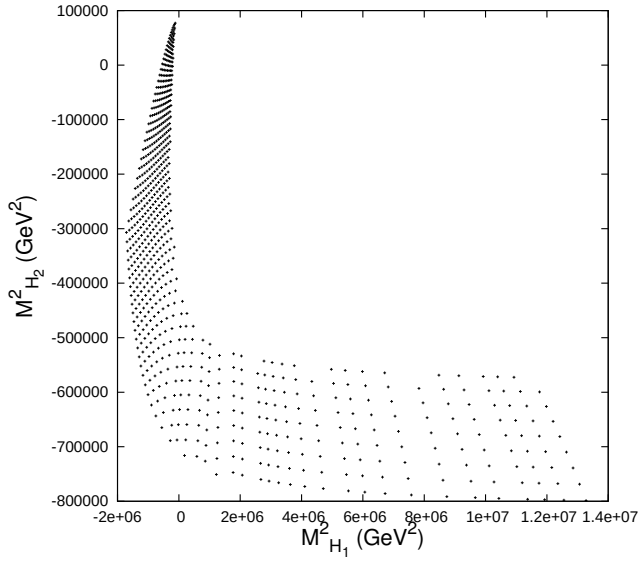


Figure 5.4: Allowed region by the experimental constraints on the $Z'$ in the plane $M^2_{H_1} - M^2_{H_2}$ for $\lambda = 0.3$

once we diagonalize the neutralino mass matrix, one eigenvalue is sufficiently small, of the order of $10^{-2}$ eV. If we include the three generations in the analysis we can obtain different neutrino mass hierarchies playing with the hierarchies in the Dirac masses. For an extensive analysis of the neutrino sector in the $\mu\nu$SSM see Chapter 3. Although such extensive analysis for the case of the neutrino sector in the $\mu\nu$SSM with an extra U(1) is beyond the scope of this Thesis, we can conclude that the neutrino mass generation mechanism works correctly in this model.

We have also performed an estimation of the tree-level upper bound on the lightest Higgs mass in this model. Let us recall that the MSSM has a problem corcerning the mass of the lightest Higgs boson. At tree-level, the mass of the lightest CP-even MSSM Higgs boson is bounded by the mass of the $Z$ gauge boson, $m_h^2 \leq M_Z^2 \cos^2\beta$. This upper bound is considerably smaller than the experimental lower bound from LEP [80], $m_h \geq 114$ GeV, for a SM-like $h^0$. This experimental bound on the lightest Higgs boson mass does not rule out the MSSM because the upper bound can receive large radiative corrections, especially from a heavy scalar top but the agreement with the experimental bound requires certain fine-tuning. The bound on the lightest Higgs boson mass in the case of the NMSSM is given by (5.43) and numerically, can be increased to about 110 GeV for $\lambda$ as large as possible and $\tan\beta \simeq 2$, substantially ameliorating the Higgs mass problem of the MSSM

(here the radiative corrections also help).

Neglecting the small neutrino Yukawa coupling effects, the expression of the upper bound on the lightest Higgs mass in the $\mu\nu$SSM is equivalent to that of the NMSSM, once we define $\lambda^2 = \lambda_1^2 + \lambda_2^2 + \lambda_3^2$, and this is given by the following tree-level expression [40]:

$$m_h^2 \leq M_Z^2(\cos^2 2\beta + \frac{2\lambda^2 \cos^2\theta_W}{g_2^2}\sin^2 2\beta) \tag{5.43}$$

In the case of extra $U(1)$ supersymmetric models, the upper bound receives a positive contribution from the extra $U(1)$ sector that is given by [125]: $2g_1'v^2(Q_{H_2}\cos^2\beta + Q_{H_1}\sin^2\beta)^2$. Adding the two contributions, we can write the tree-level expression on the upper bound to the lightest Higgs mass in the $\mu\nu$SSM with extra $U(1)$ gauge symmetry as:

$$m_h^2 \leq M_Z^2(\cos^2 2\beta + \frac{2\lambda^2 \cos^2\theta_W}{g_2^2}\sin^2 2\beta) + 2g_1'v^2(Q_{H_2}\cos^2\beta + Q_{H_1}\sin^2\beta)^2. \tag{5.44}$$

In the case of the $\mu\nu$SSM, this issue has been analysed in [40] numerically and the upper bound in this model is tipically of the order of that of the NMSSM of about 110 GeV. In the case of the $\mu\nu$SSM with extra $U(1)$ gauge symmetry, we have used (5.44) in order to estimate numerically the upper bound on the lightest Higgs boson mass in this model. It is clear that the numerical value of this bound will depend on the unknown value of the extra gauge coupling constant $g_1'$. Whereas for $g_1' \simeq g_1$ this bound is only raised to 113 GeV, for $g_1' \simeq 2g_1$ it is raised to about 120 GeV. Thus, the addition of an extra $U(1)$ gauge group to the $\mu\nu$SSM has also the nice feature of increasing the upper bound on the lightest Higgs mass leading to a larger window for the discovery of the Higgs at collider experiments.

## 5.4 Conclusions

In this chapter, we have analysed the possibility of extending the gauge symmetry of the $\mu\nu$SSM with an extra $U(1)$ factor. The superpotential of the $\mu\nu$SSM includes R-parity violating terms (there are L-violating terms that are phenomenologically necessary) and, just like the NMSSM, can present a cosmological domain wall problem. One can think that the stability of the proton can be ensured with baryon triality or string theory arguments and that the usual solutions to the domain wall problem present in the NMSSM also work in the case of the $\mu\nu$SSM. In spite of this, we have used an extra $U(1)$ gauge symmetry to forbid dimension 4 and dimension 5 B-violating

operators to ensure the stability of the proton and, at the same time to solve the cosmological domain wall problem. We have searched for consistent models using the anomaly cancellation conditions to constrain the extra charges and selecting which terms are allowed in the superpotential. Exotic matter should be added to the spectrum to cancel all the anomalies and has to be sufficiently massive to have escaped detection. In particular, three generations of vector-like color triplets and $SU(2)_L$ doublets, as well as six SM singlets are needed.

We have analysed the electroweak breaking and the consistency with the experimental bounds on the Z' finding that the model is phenomenologically viable in large regions of the parameter space. We have also studied the neutralino sector of the model. In this model, the MSSM neutralinos mix with left- and right-handed neutrinos and the extra gaugino also mix giving rise to an eleven-states neutralino mass matrix. A complete analysis of the neutrino sector in this model was out of the scope of this work but we have checked numerically that the experimental bound on neutrino masses can be easily reproduced probing that the mechanism of neutrino mass generation works correctly in this model. Finally, we have estimated the upper bound on the lightest Higgs mass in this model finding that it is improved due to the extra $U(1)$ contribution and can be raised to about 120 GeV at the tree-level.

It is clear that to complete the study of the phenomenology of this extension of the $\mu\nu$SSM, much work remains. First, a complete study of the neutrino sector could be carried out. In particular, it would be interesting to reproduce numerically the experimental bounds on the neutrino mass differences and mixing angles, and to explain in an intuitive way how the absence of the effective Majorana mass term and the presence of the extra gaugino affects the seesaw mechanism in this extension compared to the original $\mu\nu$SSM. To carry out a complete study of the vacuum of the model in the general case with three generations of sneutrinos and complex VEVs would also be interesting. The computation of mass matrices and the spectrum would also be welcome. Finally, it would be interesting to study the possible experimental signatures of this extension of the $\mu\nu$SSM. All these issues deserve to be addressed in future works.

# Chapter 6

# Conclusions and Outlook

## 6.1 Conclusions

In this Thesis we have studied the most relevant aspects of the phenomenology of a supersymmetric model called $\mu\nu$SSM because the $\mu$ problem is solved connecting it with $\nu-$ physics. After the introduction presented in Chapter 1, in Chapter 2 we have explained the motivations for going from the SM of particle physics to Supersymmetry and once in SUSY we have explained problems that presents the MSSM and why the $\mu\nu$SSM solves them. After that, we have reviewed the basics of the model.

As neutrino physics is one of the main motivations of the $\mu\nu$SSM, in Chapter 3 we have performed a complete analysis of the neutrino sector of the model at the tree-level based on our results published in [14]. The main conclusion we can extract from this study is that the $\mu\nu$SSM is able to accommodate in a wide region of the parameter space current experimental neutrino data even with a diagonal neutrino Yukawa coupling. The seesaw mechanism is at the TeV scale and is due to the mixing of left- and right-handed neutrinos with the MSSM neutralinos. We have presented an intuitive idea of how the seesaw mechanism works in this model and we have derived approximate analytical equations for the effective neutrino mass matrix. We have also performed a numerical analysis and we have presented our results with plots of the evolution of mass differences, mixing angles and CP phases with the inputs always being into the experimental allowed region.

In this chapter we have also carried out a necessary task that is, to complete the study of the vacuum of the model. We have demonstrated both theoretically and numerically that the vacuum of the $\mu\nu$SSM is in general complex, that is, the VEVs are in general complex. This CP violation arising from the Higgs sector can not explain enterely the CP violation measured

in the quark sector since the CKM matrix would be real if the model is not extended. Nevertheless, extending the Higgs sector with three families of Higgses or extending the quark sector or allowing for explicit CP violation in the quark sector, it is possible to generate the CKM phase. Then, having SCPV in the $\mu\nu$SSM is a nice feature of this model since it can generate CP-violation for the leptonic sector without extending the model and also can solve the SUSY phase problem. The SCPV at the tree-level present in the $\mu\nu$SSM is a very characteristic feature of this model since in general, SUSY models do not present SCPV at the tree-level. We have computed the neutral scalar potential and the minimization equations with complex VEVs and we have performed a numerical analysis of the minimization of the potential finding global minima that break spontaneously CP. Then, we have shown how these CP phases are transmitted to the lepton sector generating the Dirac and Majorana phases of the PMNS matrix. If the Dirac phase would be measured in future experiments, the SCPV origin from the $\mu\nu$SSM could well explain this measure.

We have also discussed the problem of EDMs in the case of SCPV in the $\mu\nu$SSM. The two solutions consisting of internal cancellations or the decoupling of scalar particles are possible to implement in this model. The advantage of SCPV respect to explicit CP violation is that the small CP-phases solution to the EDMs problem is natural since the small CP phases arise from the electroweak breaking, they are not unnaturally small parameters of the Lagrangian.

Since the vacuum of the model and the neutrino sector have been analysed in this Thesis in Chapter 3 and other important topics like gravitino dark matter or baryogenesis have been covered in other works, our next aim was to study in detail the Higgs sector of the model and possible signals at colliders. In Chapter 4 we have presented an analysis on the collider phenomenology of the $\mu\nu$SSM focusing our attention on the Higgs sector. This chapter is based on the results published in [15].

The $\mu\nu$SSM has an extended Higgs sector since sneutrinos are mixed with doublet Higgses. We have described the mixings in the Higgs sector and how to suppress them in order to have light singlets safe from collider constraints or to have the lightest scalar as heavy as possible. For that, relations on the $A_{\lambda_i}$ parameters are derived and it is pointed out that there are also other regions in the parameter space giving rise to small mixings in the Higgs sector.

After that, an overview of the novelties on the decays of the Higgs sector of this model has been provided. To distinguish the $\mu\nu$SSM from other SUSY models, there are two main features. On one hand, the breaking of R-parity implies the decay of the LSP. Displaced vertices are expected on decays of

a Higgs leading to the LSP that subsequently decays. These displaced vertices are typical signals of R-parity breaking models in contrast with missing energy signatures expected in R-parity conserving models. Moreover, the products of the decays of the lightest neutralino can also serve to distinguish the $\mu\nu$SSM from other R-parity breaking models since two-body decays of the lightest neutralino into a Higgs and a neutrino are available in the $\mu\nu$SSM. On the other hand, as we have already said, the mixing of both left- and right-handed sneutrinos with doublet Higgses leads to an extended Higgs sector. Then, more complicated Higgs-to-Higgs cascade decays could be present in this model than in the NMSSM. This fact can also serve to distinguish the $\mu\nu$SSM from other R-parity breaking models as the BRpV model where the Higgs sector does not contain singlets. After presenting the overview on the decays of the Higgs sector, LEP constraints have been discussed in the context of the $\mu\nu$SSM. For that, we have computed the couplings of the Higgs bosons with Z bosons and the sum rules. Also we have reviewed the production mechanims of Higgses at lepton and hadron colliders.

After that, we have provided benchmark points obtained in numerical computations where typical signals of the $\mu\nu$SSM are expected and could arise in the near future at the LHC while all current experimental constraints are satisfied. In particular, we have focused our attention first on the decays of a MSSM-like light Higgs $h_{MSSM}$ with a sizeable branching ratio to two lightest neutralinos. These neutralinos could decay inside the detector leading to displaced vertices. This can be used to distinguish the $\mu\nu$SSM from R-parity conserving models. Besides, the decays can be into a neutrino and an on-shell light singlet pseudoscalar $P$, that subsequently decays into $b\bar{b}$ (or if kinematically forbidden into $\tau^+\tau^-$). Then, the decay $h_{MSSM} \to \tilde{\chi}^0\tilde{\chi}^0 \to 2P2\nu \to 2b2\bar{b}2\nu$ is genuine of the $\mu\nu$SSM. Note that in other R-parity breaking models as the BRpV, there are not singlet Higgses and a lightest neutralino lighter than gauge bosons could decay only through three-body decay processes. Final states with 8 b-jets plus missing energy are possible in situations where singlet-like scalars are produced first by the decay of the neutralino, $h_{MSSM} \to \tilde{\chi}^0\tilde{\chi}^0 \to 2h2\nu \to 4P2\nu \to 4b4\bar{b}2\nu$.

We have also studied a case with a spectrum similar to the one of the MSSM where all CP-even singlet scalars are above 114 GeV and the pseudoscalars are heavier than the neutralinos. Then, the MSSM-like Higgs will decay in a significant ratio to neutralinos, and these will decay only through three-body processes leading to displaced vertices. In another case the neutralino does not play an important role and only Higgs-to-Higgs cascade decays are relevant. Although displaced vertices are not expected, the decays $h_{MSSM} \to 2P \to 2b2\bar{b}$, $h_{MSSM} \to 2h \to 4P \to 4b4\bar{b}$ are possible, allowing to distinguish the $\mu\nu$SSM from other R-parity violating models. Besides,

once a SUSY particle is produced at the collider, decaying into the LSP, the displaced vertex will allow to distinguish the $\mu\nu$SSM from the NMSSM. Finally, we have studied a case where for singlet-like pseudoscalars $P_{1,2}$ the decay into $b\bar{b}$ is kinematically forbidden, but for $P_3$ is allowed. Then, several interesting cascade decays are expected without leading to displaced vertices: $h_{MSSM} \to 2h_1 \to 4P_{1,2} \to 4\tau^+4\tau^-$, $h_{MSSM} \to 2P_3 \to 2b2\bar{b}$. This is a genuine feature of the $\mu\nu$SSM. In addition, the following cascades are possible, with displaced vertices and missing energy: $h_{MSSM} \to \tilde{\chi}^0\tilde{\chi}^0 \to 2P_{1,2}2\nu \to 2\tau^+2\tau^-2\nu$, $h_{MSSM} \to \tilde{\chi}^0\tilde{\chi}^0 \to 2h_{1,2,3}2\nu \to 4P_{1,2}2\nu \to 4\tau^+4\tau^-2\nu$, $h_{MSSM} \to \tilde{\chi}^0\tilde{\chi}^0 \to 2P_32\nu \to 2b2\bar{b}2\nu$. In conclusion, the above discussion gives us the idea that extremely characteristic signals can be expected in certain regions of the parameter space of the $\mu\nu$SSM.

We have also emphasized that in the $\mu\nu$SSM the gravitino could be a viable dark matter candidate, accessible to indirect detection experiments, and without altering the collider phenomenology. In particular, the branching ratio of neutralino into gravitino-photon turns out to be negligible.

The $\mu\nu$SSM solves the $\mu$ problem of the MSSM and generates correct neutrino masses by simply using right-handed neutrino superfields. This mechanism implies that only dimensionless trilinear terms, breaking R-parity, are present in the superpotential. The non-presence in the superpotential of proton decay operators breaking R-parity, a trilinear term generating a domain wall problem, and bilinear terms such as the $\mu$ term and the Majorana masses, can be explained in the $\mu\nu$SSM using string theory arguments, discrete symmetries or non-renormalizable operators. In Chapter 5 we have used a different strategy, namely an extra $U(1)$ gauge symmetry is added to the gauge group of the SM. Since all the fields of the $\mu\nu$SSM can be charged under the extra $U(1)$, all the dangerous operators mentioned above could in principle be forbidden. We have checked that this is precisely the case. For example, dimension four and five baryon number violating operators are forbidden in the superpotential, ensuring the stability of the proton. Chapter 5 is based on [16].

There, we have extensively explained the motivations for extending the gauge group and we have performed the analysis of the anomaly equations to constrain the extra charges, finding that exotic matter should be added to the spectrum. In particular, three generations of vector-like color triplets and $SU(2)_L$ doublets, as well as six SM singlets are needed. We have found a minimal model and we have calculated the extra charges and the hypercharges of all the particles and the numbers of generations of the exotics. Then we have studied the phenomenology of the model found, focusing our attention on the electroweak breaking and the compatibility with the experimental $Z'$ constraints. A lot of phenomenological work remains to study this

extension of the $\mu\nu$SSM but the main conclusions we can extract are that the proton decay issue and the domain wall problem can be solved with this $U(1)$ extension since we have found a unique and minimal model that selects adequately the allowed operators in the superpotential. In a wide region of the parameter space, the constraints on the existence of a new gauge boson $Z'$ can be accommodated and the model presents a correct electroweak breaking. In spite that the complete analysis of the neutrino sector of this extension was out of the scope of this Thesis, we have checked that small neutrino masses compatible with the experimental bounds arise. Another nice feature of this extension is that the upper limit on the lightest Higgs mass is increased opening a larger window to the discovery of the Higgs in accelerator experiments, relaxing the so called little hierarchy problem.

It is clear that, being a relatively new model and due to its complexity, much work remains to complete the study of the phenomenology of the $\mu\nu$SSM. Nevertheless, being a very well motivated model with characteristic features, it deserves to be extensively analysed. This Thesis has covered important parts of the phenomenological study as the neutrino sector, the vacuum, the possibility of SCPV, the collider phenomenology of the Higgs sector or the extra $U(1)$ extension of the gauge group. In all these issues, the $\mu\nu$SSM has been proved to be able to agree with experimental data in relevant parts of the parameter space. If the LHC finds in the near future SUSY particles, the next step would be to try to identify the SUSY model realized in nature. Then, if R-parity violating signals are detected, the $\mu\nu$SSM would be one of the best motivated models for being the correct one.

## 6.2 Outlook

Since the $\mu\nu$SSM is a relatively new model, and for the moment only several works have studied its phenomenology [1, 40, 43, 44, 45, 14, 46, 15, 47, 16, 11, 12, 50], much work has still to be done for having a complete knowledge of the model.

Probably the most important part is a complete exploration of the signals that this model would produce in present and future accelerators. Several works in this area have been already published (see [15] and references along this Thesis), but a SUSY model of the complexity of the $\mu\nu$SSM needs more work in order to do a complete study of the signals that could produce at a collider. There are two issues that could lead to characteristic signals of the $\mu\nu$SSM that can differentiate it among other SUSY models. On the one hand, as R-parity is broken, the study of the decays of the LSP is crucial since the typical SUSY signals of missing energy could not be present. In the

case of neutralino LSP, in [43, 44, 45] the decays of the lightest neutralino were discussed, as well as the correlations of the decay branching ratios with the neutrino mixing angles. A similar study in the case of squark, slepton or sneutrino LSP has not been performed and it would be important since in R-parity breaking models, the LSP can be a charged particle. It is clear that R-parity breaking signals at colliders would be very welcome for the $\mu\nu$SSM but this in principle would not allow to distinguish our model from other R-parity breaking models as the BRpV, except possibly in the $\mu\nu$SSM genuine case of singlino LSP. For the distinction, probably it would be necessary to focus the attention on the Higgs sector. An overview of the phenomenology of the Higgs sector of the $\mu\nu$SSM has been provided in [15]. Different benchmark points with genuine signals of the $\mu\nu$SSM have been presented there, see Chapter 4 of this Thesis. We have focused our attention on the decays of the lightest doublet-like Higgs with a mass of about 120 GeV. It would be also interesting to study the decays of the heavier doublet-like Higgs, where complicate Higgs-to-Higgs decay chains could be important. Studies of the $\mu\nu$SSM with the help of event generators are also necessary.

For the moment, the $\mu\nu$SSM has been only studied within the framework of gravity mediated SUSY breaking. It would be also interesting to study the $\mu\nu$SSM within the framework of gauge mediated SUSY breaking or anomaly mediated SUSY breaking.

The electroweak breaking has been already almost studied, including complex vacua and discarding unphysical or phenomenologically forbidden vacua in the real case. The mass matrices and the spectrum have also been computed, as well as the Landau pole constraints. The neutrino sector has been studied in the literature by different groups (see [14] and references along this Thesis), including tree-level analysis with CP phases and 1-loop analysis. In what concerns the analysis of complex vacua, it would be interesting to study extensions of the $\mu\nu$SSM with SCPV that could generate a complex CKM matrix. In this way all the CP-violation could be originated spontaneously through complex VEVs and could be transmitted to the quark sector extending the Higgs sector with three Higgs families or extending the quark sector having a complex effective CKM matrix. With those extensions the SUSY phase problem would be solved.

The dark matter issue in the $\mu\nu$SSM is highly relevant since the most popular dark matter candidate in SUSY, the lightest neutralino, is excluded because the breaking of R-parity. Gravitino dark matter in the context of the $\mu\nu$SSM has been studied in the literature but for sure, more work has still to be done in this area, including other dark matter candidates as the axion or the axino.

The work performed in Chapter 5 finding an extra $U(1)$ extension of the

$\mu\nu$SSM [16] has opened a new line of research. In this context, it is clear that much phenomenological work has still to be done. In particular, all the phenomenological work carried out for the $\mu\nu$SSM could also be performed for this extension. The complete analysis of the neutrino sector of this new model would be highly relevant and slightly different from the one of the original $\mu\nu$SSM since in the case of the extra $U(1)$ extension, the extra gaugino mix with the neutralinos giving rise to an $11 \times 11$ neutralino mass matrix and in addition, there are not effective Majorana mass terms. A complete analysis of the vacuum would also be welcome, as well as the study of the experimental signals that could produce this new model at colliders.

Finally, let us summarize saying that if the LHC finds SUSY particles and therefore the supersymmetric theory is proved to describe nature at the TeV scale, the next step would be to find which SUSY model is the correct one. And for this, all well motivated SUSY models should be extensively studied. In the case of the $\mu\nu$SSM, while much work has already been done, there remains relevant issues that have to be explored in the near future.

## 6.3 Conclusiones

En esta Tesis hemos estudiado los aspectos más relevantes de la fenomenología de un modelo supersimétrico llamado $\mu\nu$SSM porque resuelve el problema $\mu$ conectando su solución con la física de neutrinos. Después de realizar una breve introducción en el capítulo 1, en el capítulo 2 hemos resumido las razones para pasar desde el SM de Física de Partículas a la Teoría de Supersimetría. Una vez en el contexto de Supersimetría, hemos explicado los problemas que presenta el MSSM y cómo el modelo $\mu\nu$SSM los ataca. A continuación, hemos revisado las claves de este modelo.

Debido a que una de las principales motivaciones del $\mu\nu$SSM es la física de neutrinos, en el Capítulo 3 hemos realizado un análisis completo del sector de neutrinos del modelo a nivel árbol basándonos en los resultados publicados en [14]. La principal conclusión que se puede extraer de este estudio es que el $\mu\nu$SSM es capaz de acomodar en una vasta región del espacio de parámetros los datos experimentales actuales de neutrinos, incluso con un acoplo de Yukawa diagonal. El mecanismo del seesaw se realiza a la escala de energías del TeV gracias a que tanto los neutrinos levógiros como los dextrógiros se mezclan con los neutralinos del MSSM. Hemos explicado de forma intuitiva cómo se realiza el mecanismo del seesaw en este modelo y hemos calculado ecuaciones analíticas aproximadas para la matriz de masa efectiva de neutrinos. También hemos realizado el análisis numérico del sector de neutrinos y hemos presentado nuestros resultados con gráficos de la

evolución de las diferencias de masa, ángulos de mezcla y fases de CP con los parámetros libres del modelo, siempre dentro de la región experimentalmente permitida.

En ese mismo capítulo también hemos realizado una tarea necesaria que consiste en completar el estudio del vacío en este modelo. Hemos demostrado de forma teórica y numérica que, en general, el vacío en el $\mu\nu$SSM es complejo, es decir, los VEVs son en general complejos y a este hecho se le conoce como Violación Espontánea de CP. Esta violación de CP proveniente del sector de Higgs no puede explicar la violación de CP medida en el sector de quarks ya que la matriz CKM sería real si no se extiende de alguna forma el modelo. Sin embargo, extendiendo el sector de Higgs con tres familias de Higgses, o extendiendo el sector de quarks, o permitiendo violación explícita de CP en el sector de quarks, es posible generar la fase de la matriz CKM. Por lo tanto, el hecho de que el $\mu\nu$SSM presente SCPV es una característica con implicaciones positivas ya que este mecanismo puede generar violación de CP en el sector leptónico y también puede resolver el problema de las fases supersimétricas. La SCPV a nivel árbol que presenta el $\mu\nu$SSM es una propiedad muy característica de este modelo ya que, en general, los modelos supersimétricos no presentan SCPV a nivel árbol. Hemos calculado el potencial escalar neutro, las ecuaciones de minimización con VEVs complejos y hemos realizado un estudio numérico de la minimización del potencial, encontrando mínimos globales que violan espontáneamente CP. Seguidamente hemos mostrado cómo se transmiten las fases CP de los VEVs al sector leptónico generando las fases de Dirac y de Majorana de la matriz PMNS. Si se consiguiera medir la fase de Dirac en experimentos futuros, una buena forma de explicar esa violación de CP podría ser a través de SCPV en el modelo $\mu\nu$SSM.

También hemos discutido el problema de los EDMs en el caso del SCPV $\mu\nu$SSM. Las dos soluciones a este problema, cancelaciones internas y desacoplo de las partículas escalares, pueden ser implementadas en este modelo. La ventaja de tener SCPV frente a violación explícita de CP consiste en que la tercera posible solución al problema de los EDMs, fases CP pequeñas, es natural ya que esas fases CP pequeñas provienen de la rotura de la simetría electrodébil, no son parámetros del Lagrangiano arbitrariamente pequeños.

Dado que el vacío y el sector de neutrinos del modelo ya han sido analizados en esta Tesis en el capítulo 3 y otros temas importantes como gravitino candidato a materia oscura o bariogénesis en el $\mu\nu$SSM han sido cubiertos en otros trabajos, nuestro siguiente objetivo ha consistido en el estudio del sector de Higgs y de las posibles señales en experimentos de aceleradores. En el capítulo 4 hemos realizado un análisis de la fenomenología en aceleradores del $\mu\nu$SSM focalizando nuetra atención en el sector de Higgs. Este capítulo

se basa en los resultados publicados en [15].

El $\mu\nu$SSM tiene un sector de Higgs extendido ya que los sneutrinos se mezclan con los dobletes de Higgs. Hemos descrito las mezclas en el sector de Higgs y los mecanismos para suprimirlas para tener singletes ligeros a salvo de las cotas experimentales de colisionadores o para que el escalar más ligero sea lo más pesado posible. Para conseguirlo, hemos deducido relaciones para los parámetros $A_{\lambda_i}$ y sugerido que hay otras regiones en el espacio de parámetros que dan lugar a mezclas pequeñas en el sector de Higgs.

A continuación, hemos resumido las novedades que se producen en los decaimientos del sector de Higgs del modelo. Para distinguir el $\mu\nu$SSM de otros modelos supersimétricos existen dos características principales. Por un lado, la rotura de R-parity implica el decaimiento de la LSP. Por ello, se esperan vértices desplazados en los decays de un Higgs a la LSP, que decae a continuación. Estos vértices desplazados son señales típicas de modelos que rompen R-parity, en contraste con las señales de energía perdida que se esperan en los modelos que conservan R-parity. Además, los productos de los decaimientos del neutralino más ligero pueden servir para distinguir el modelo $\mu\nu$SSM de otros modelos que rompen R-parity ya que en el $\mu\nu$SSM se pueden producir decaimientos a dos cuerpos del neutralino más ligero en un Higgs y un neutrino. Por otra parte, como ya hemos dicho, la mezcla de los sneutrinos dextrógiros y levógiros con los dobletes de Higgs produce un sector de Higgs extendido. Por ello, cascadas Higgs a Higgs más complicadas que las del NMSSM pueden producirse en este modelo. Este hecho puede servir para distinguir el $\mu\nu$SSM de otros modelos que rompen R-parity como el modelo BRpV, en los que el sector de Higgs no contiene singletes. Después de presentar la panorámica general de los decaimientos en el sector de Higgs del $\mu\nu$SSM, hemos analizado las cotas experimentales de LEP en el contexto de este modelo. Para ello hemos calculado los acoplos de los Higgses con los bosones Z y las reglas de adición. También hemos repasado los mecanismos de producción de los Higgses en aceleradores leptónicos y hadrónicos.

A continuación hemos proporcionado puntos de test en el espacio de parámetros obtenidos con computaciones numéricas en los que se esperan señales típicas del $\mu\nu$SSM, que pasan todas las cotas experimentales actuales y que puedan ser detectados pronto en el LHC. En concreto, nos hemos centrado en los decaimientos de un Higgs tipo MSSM, $h_{MSSM}$, con una fracción de decaimiento a dos neutralinos ligeros apreciable. Estos neutralinos pueden decaer dentro del detector produciendo vértices desplazados. Esto se puede usar para distinguir el $\mu\nu$SSM de modelos con R-parity conservada. Además, estos decaimientos pueden ser en un neutrino y un singlete pseudoescalar ligero $P$ en la capa de masas que a continuación decae en $b\bar{b}$ (o si está cinemáticamente prohibido, a $\tau^+\tau^-$). Por tanto, el de-

caimiento $h_{MSSM} \to \tilde{\chi}^0\tilde{\chi}^0 \to 2P2\nu \to 2b2\bar{b}2\nu$ es genuino del $\mu\nu$SSM. Nótese que en otros modelos con rotura de R-parity como el BRpV no hay Higgses singletes y el neutralino más ligero, si es más ligero que los bosones gauge, sólo podría decaer a través de procesos a tres cuerpos. Estados finales con 8 b-jets y energía perdida son posibles en situaciones en las que se producen primero escalares singletes por el decaimiento del neutralino, $h_{MSSM} \to \tilde{\chi}^0\tilde{\chi}^0 \to 2h2\nu \to 4P2\nu \to 4b4\bar{b}2\nu$. También hemos estudiado el caso de un espectro similar al del MSSM, con todos los escalares singletes pares bajo CP por encima de 114 GeV y siendo los pseudoescalares más pesados que los neutralinos. En este caso, el Higgs de tipo MSSM decaerá en una fracción significativa en neutralinos, y éstos decaerán sólo a través de procesos a tres cuerpos dando lugar a vértices desplazados. En otro caso que hemos analizado, el neutralino no juega un papel importante y sólo son relevantes cascadas Higgs a Higgs. Aunque no se esperan vértices desplazados, los decays $h_{MSSM} \to 2P \to 2b2\bar{b}$, $h_{MSSM} \to 2h \to 4P \to 4b4\bar{b}$ son posibles, permitiendo distinguir el $\mu\nu$SSM de otros modelos que violan R-parity. Además, una vez que se produzca una partícula supersimétrica en el colisionador, con su decaimiento a la LSP y su consiguiente vértice desplazado, permitiría distinguir el $\mu\nu$SSM del NMSSM. Finalmente hemos estudiado un caso en el que para los singletes pseudoescalares $P_{1,2}$ el decaimiento a $b\bar{b}$ está cinemáticamente prohibido pero para $P_3$ está permitido. Entonces, varias cascadas interesantes pueden esperarse, sin dejar vértices desplazados: $h_{MSSM} \to 2h_1 \to 4P_{1,2} \to 4\tau^+4\tau^-$, $h_{MSSM} \to 2P_3 \to 2b2\bar{b}$. Este hecho es genuino del $\mu\nu$SSM. Además, las siguientes cascadas con vértices desplazados y energía perdida son posibles: $h_{MSSM} \to \tilde{\chi}^0\tilde{\chi}^0 \to 2P_{1,2}2\nu \to 2\tau^+2\tau^-2\nu$, $h_{MSSM} \to \tilde{\chi}^0\tilde{\chi}^0 \to 2h_{1,2,3}2\nu \to 4P_{1,2}2\nu \to 4\tau^+4\tau^-2\nu$, $h_{MSSM} \to \tilde{\chi}^0\tilde{\chi}^0 \to 2P_32\nu \to 2b2\bar{b}2\nu$. En conclusión, la exposición anterior nos da la idea de que se pueden esperar señales extremadamente características en ciertas regiones del espacio de parámetros del $\mu\nu$SSM.

También hemos apuntado que en el $\mu\nu$SSM, el gravitino puede ser un candidato viable a materia oscura del universo, accesible a experimentos de detección indirecta y sin alterar la fenomenología en aceleradores. En concreto, la fracción de decaimiento del neutralino en gravitino y fotón resulta ser despreciable.

El $\mu\nu$SSM resuelve el problema $\mu$ del MSSM y genera las masas de neutrinos correctas simplemente usando supercampos de neutrinos dextrógiros. Este mecanismo implica que únicamente están presentes en el superpotencial términos trilineales adimensionales que rompen R-parity. La ausencia en el superpotencial de operadores que producen el decaimiento del protón y que violan R-parity, un término trilineal que origina el problema de paredes de dominio y términos bilineales como el término $\mu$ o la masa de Majorana,

puede ser explicada en el $\mu\nu$SSM usando argumentos de teoría de cuerdas, simetrías discretas u operadores no renormalizables. En el Capítulo 5 hemos usado una estrategia distinta, consistente en añadir una simetría gauge $U(1)$ al grupo gauge del SM. Como todos los campos del $\mu\nu$SSM pueden estar cargados bajo el grupo $U(1)$ extra, todos los operadores peligrosos mencionados anteriormente podrían en principio estar prohibidos. Hemos comprobado que eso es posible. Por ejemplo, operadores de dimensión cuatro y cinco que violan número bariónico están prohibidos en el superpotencial, asegurando la estabilidad del protón. El Capítulo 5 se basa en los resultados de [16].

En ese capítulo hemos explicado ampliamente las motivaciones para extender el grupo gauge y hemos analizado las ecuaciones de cancelación de anomalías demostrando que se debe añadir materia exótica al espectro. En concreto, se necesitan añadir tres generaciones de tripletes de color y de dobletes de $SU(2)_L$ así como seis generaciones de singletes bajo el SM. Hemos encontrado un modelo mínimo y hemos calculado las cargas extra e hipercargas de las partículas así como los números de familias de la materia exótica. Una vez encontrado un modelo viable, hemos iniciado el estudio de su fenomenología centrando nuestra atención en la rotura electrodébil y en la compatibilidad con las cotas experimentales sobre la existencia de un nuevo bosón gauge $Z'$. Queda mucho trabajo para estudiar completamente la fenomenología de esta extensión del $\mu\nu$SSM pero la principal conclusión que se puede extraer es que la cuestión de la estabilidad del protón y el problema de las paredes de dominio pueden ser resueltos con esta extensión $U(1)$ extra ya que hemos encontrado una extensión única y mínima que selecciona adecuadamente los operadores permitidos en el superpotencial. Las cotas experimentales sobre el $Z'$ se pueden cumplir en una amplia región del espacio de parámetros y el modelo rompe la simetría electrodébil correctamente. A pesar de que el estudio detallado del sector de neutrinos de esta extensión no ha sido realizado en esta tesis, hemos comprobado que se pueden generar masas de neutrinos pequeñas, compatibles con las cotas experimentales. Otra implicación positiva que presenta la extensión $U(1)$ extra del $\mu\nu$SSM consiste en que la cota superior a la masa del Higgs más ligero se incrementa un poco gracias a la contribución del $U(1)$ extra, ampliando la ventana para la detección del Higgs en experimentos de aceleradores, relajando así el llamado little hierarchy problem.

Está claro que, siendo un modelo relativamente nuevo y debido a su complejidad, queda mucho trabajo por realizar para completar el estudio de la fenomenología del modelo $\mu\nu$SSM y debido a que es un modelo muy bien motivado y con características muy peculiares, es necesario hacerlo. Esta Tesis ha cubierto partes muy importantes del estudio de la fenomenología de este modelo como el sector de neutrinos, el vacío, la posibilidad de SCPV,

la fenomenología en aceleradores del sector de Higgs o la extensión $U(1)$ extra del grupo gauge. En todas estas cuestiones, el modelo $\mu\nu$SSM ha sido capaz de ajustarse a los datos experimentales en partes relevantes del espacio de parámetros. Si el LHC encuentra en un futuro próximo partículas supersimétricas, el siguiente paso sería tratar de identificar qué modelo supersimétrico es el que describe la naturaleza. Entonces, si se detectaran señales de violación de R-parity, el $\mu\nu$SSM sería uno de los modelos mejor motivados y podría ser el correcto.

## 6.4 Trabajo futuro

Debido a que el modelo $\mu\nu$SSM ha sido propuesto hace relativamente poco tiempo y de momento sólo algunos trabajos han estudiado su fenomenología [1, 40, 43, 44, 45, 14, 46, 15, 47, 16, 11, 12, 50], queda mucho trabajo por hacer para obtener un conocimiento completo.

Posiblemente, la parte más importante sería una exploración completa de las señales que dejaría el modelo en aceleradores de partículas presentes y futuros. Algunos trabajos sobre este tema ya han sido publicados (ver [15] y las referencias a lo largo de esta tesis) pero es obvio que un modelo de la complejidad del $\mu\nu$SSM necesita mucho más trabajo para tener completamente analizado el tema de su detección experimental. Hay principalmente dos sectores que pueden proporcionar señales características que permitan distinguir el modelo $\mu\nu$SSM de otros modelos supersimétricos. Por un lado, como R-parity está rota, el estudio de los decaimientos de la partícula supersimétrica más ligera es crucial ya que las señales de energía perdida típicas de supersimetría pueden dejar de estar presentes. Para el caso del neutralino como LSP, en [43, 44, 45] se han estudiado los decaimientos del neutralino más ligero así como las correlaciones de las fracciones de decaimiento con los ángulos de mezcla de neutrinos. No se ha realizado un estudio similar en los casos de squark, slepton o sneutrino como LSP, pero sería muy importante ya que en modelos que rompen R-parity la LSP puede ser una partícula cargada. Está claro que señales de rotura de R-parity en aceleradores serían muy importantes para el $\mu\nu$SSM, pero en principio no permitirían distinguir nuestro modelo de otros modelos que rompen R-parity como el BRpV, salvo posiblemente en el caso genuino del $\mu\nu$SSM con singlino como LSP. Para ello, sería necesario centrar la atención en el sector de Higgs. En [15] se ha expuesto una panorámica de la fenomenología del sector de Higgs en el $\mu\nu$SSM. En esa referencia se han presentado diferentes puntos benchmark con señales genuinas del $\mu\nu$SSM (ver capítulo 4 de esta Tesis). Nos hemos limitado a estudiar los decaimientos del Higgs doblete más ligero con una

masa de unos 120 GeV. Sería interesante estudiar también los decaimientos del Higgs doblete pesado, en los que cascadas complicadas Higgs a Higgs pueden ser importantes. Estudios del $\mu\nu$SSM con generadores de eventos también son necesarios.

Por el momento, el $\mu\nu$SSM sólo ha sido estudiado en el contexto de rotura de supersimetría mediada por gravedad. Sería interesante estudiar el modelo en el contexto de otras teorías de rotura de supersimetría como rotura de supersimetría mediada por interacciones gauge o rotura de supersimetría mediada por anomalías.

La rotura electrodébil en el modelo ya ha sido estudiada en profundidad, incluyendo vacíos con VEVs complejos y descartando vacíos no físicos o fenomenológicamente inaceptables. Las matrices de masa y el espectro ya han sido calculados, así como las restricciones provenientes de polos de Landau. El sector de neutrinos también ha sido estudiado en detalle en la literatura por diferentes grupos (ver [14] y referencias a lo largo de esta Tesis), incluyendo en el análisis fases de violación de CP a nivel árbol y a 1-loop. En lo concerniente al análisis del vacío complejo, sería interesante estudiar extensiones del $\mu\nu$SSM con SCPV que pudieran generar una matriz CKM compleja. De esta forma, toda la violación de CP se originaría de forma espontánea a través de VEVs complejos y podría transmitirse al sector de quarks extendiendo el sector de Higgs con tres generaciones de Higgses o extendiendo el sector de quarks para generar una matriz efectiva CKM compleja. Con estas extensiones el problema de las fases supersimétrico podría quedar resuelto.

La cuestión de la naturaleza de la materia oscura en el $\mu\nu$SSM es muy relevante ya que el mejor candidato a DM en supersimetría, el neutralino más ligero, está excluído por la rotura de R-parity. La cuestión de materia oscura formada por gravitinos en el contexto del $\mu\nu$SSM ha sido estudiada en la literatura, pero seguramente se necesitan realizar más trabajos en este área, incluyendo otros candidatos a materia oscura como el axión o el axino.

El trabajo realizado en el capítulo 5 en el que se encuentra una extensión $U(1)$ extra del $\mu\nu$SSM [16] ha abierto una nueva línea de investigación. En este contexto, está claro que queda todavía mucho trabajo por hacer. En concreto, todo el trabajo fenomenológico que se ha hecho sobre el $\mu\nu$SSM podría hacerse también para esta extensión. El análisis del sector de neutrinos de este nuevo modelo sería muy interesante y diferente del análisis en el $\mu\nu$SSM original ya que en la extensión, al mezclarse el gaugino extra con los neutralinos, la matriz de masa de neutralinos sería una matriz $11 \times 11$. Además, no hay ningún término de masa de Majorana efectivo. Un análisis completo del vacío de este nuevo modelo así como el estudio de las señales características que dejaría en un acelerador de partículas también serían importantes.

Para concluir, resumamos todo lo anterior diciendo que si el LHC consigue detectar partículas supersimétricas demostrando que la supersimetría describe la naturaleza a la escala del TeV, el siguiente paso sería determinar qué modelo supersimétrico es el correcto. Y para ello, todos los modelos supersimétricos consistentes deberían ser estudiados en profundidad. En el caso del $\mu\nu$SSM, aunque ya se ha realizado mucho trabajo, todavía quedan cuestiones relevantes que hay que explorar en un futuro próximo.

# Appendix A

# Mass matrices

In this Appendix we will provide the general mass matrices of the $\mu\nu$SSM except the neutralino and chargino mass matrices that have been already presented in precedent chapters. We will use the indices $i, j, k, l, m = 1, 2, 3$ and $\alpha, \beta, \gamma, \delta = 1, ..., 8$.

## A.1 CP-even neutral scalars

Let us first recall that, due to the breaking of R-parity, the neutral Higgses are mixed with the sneutrinos. The quadratic potential includes

$$V_{\text{quadratic}} = \frac{1}{2}\mathbf{h'}_{\alpha} M^2_{h_{\alpha\beta}} \mathbf{h'}_{\beta} + ... \ , \tag{A.1}$$

where $\mathbf{h'}_{\alpha} = (h_d, h_u, (\widetilde{\nu}^c_i)^R, (\widetilde{\nu}_i)^R)$ is in the unrotated basis, and below we give the expressions for the independent coefficients of $M^2_{h_{\alpha\beta}}$

$$M^2_{h_d h_d} = m^2_{H_d} + \frac{G^2}{4}\{3v_d^2 - v_u^2 + \nu_i\nu_i\} + \lambda_i\lambda_j\nu^c_i\nu^c_j + \lambda_i\lambda_i v_u^2 \ , \tag{A.2}$$

$$\begin{aligned} M^2_{h_u h_u} = m^2_{H_u} + \frac{G^2}{4}(-v_d^2 + 3v_u^2 - \nu_i\nu_i) + \lambda_i\lambda_j\nu^c_i\nu^c_j + \lambda_i\lambda_i v_d^2 \\ -2Y_{\nu_{ij}}\lambda_j v_d \nu_i + Y_{\nu_{ik}}Y_{\nu_{ij}}\nu^c_j\nu^c_k + Y_{\nu_{ik}}Y_{\nu_{jk}}\nu_i\nu_j \ , \end{aligned} \tag{A.3}$$

$$M^2_{h_d h_u} = -a_{\lambda_i}\nu^c_i - \frac{G^2}{2}v_d v_u + 2v_d v_u \lambda_i\lambda_i - (\lambda_k\kappa_{ijk}\nu^c_i\nu^c_j + 2Y_{\nu_{ij}}\lambda_j v_u \nu_i) \ , \tag{A.4}$$

$$M^2_{h_d(\widetilde{\nu}^c_i)^R} = -a_{\lambda_i} v_u + 2\lambda_i\lambda_j v_d \nu^c_j - 2\lambda_k \kappa_{ijk} v_u \nu^c_j - Y_{\nu_{ji}} \lambda_k \nu_j \nu^c_k - Y_{\nu_{jk}} \lambda_i \nu_j \nu^c_k \ , \tag{A.5}$$

$$\begin{aligned} M^2_{h_u(\widetilde{\nu}^c_i)^R} &= -a_{\lambda_i} v_d + a_{\nu_{ji}} \nu_j + 2\lambda_i\lambda_j v_u \nu^c_j - 2\lambda_k \kappa_{ilk} v_d \nu^c_l \\ &\quad + 2Y_{\nu_{jk}} \kappa_{ilk} \nu_j \nu^c_l + 2Y_{\nu_{jk}} Y_{\nu_{ji}} v_u \nu^c_k \ , \end{aligned} \tag{A.6}$$

$$M^2_{h_d(\widetilde{\nu}_i)^R} = \frac{1}{2} G^2 v_d \nu_i - (Y_{\nu_{ij}} \lambda_j v_u^2 + Y_{\nu_{ij}} \lambda_k \nu^c_k \nu^c_j) \ , \tag{A.7}$$

$$M^2_{h_u(\widetilde{\nu}_i)^R} = a_{\nu_{ij}} \nu^c_j - \frac{G^2}{2} v_u \nu_i - 2Y_{\nu_{ij}} \lambda_j v_d v_u + Y_{\nu_{ik}} \kappa_{ljk} \nu^c_l \nu^c_j + 2Y_{\nu_{ij}} Y_{\nu_{kj}} v_u \nu_k \ , \tag{A.8}$$

$$\begin{aligned} M^2_{(\widetilde{\nu}_i)^R(\widetilde{\nu}_j)^R} &= m^2_{\tilde{L}_{ij}} + \frac{G^2}{2} \nu_i \nu_j + \frac{1}{4} G^2 (\nu_k \nu_k + v_d^2 - v_u^2) \delta_{ij} \\ &\quad + Y_{\nu_{ik}} Y_{\nu_{jk}} v_u^2 + Y_{\nu_{ik}} Y_{\nu_{jl}} \nu^c_k \nu^c_l \ , \end{aligned} \tag{A.9}$$

$$\begin{aligned} M^2_{(\widetilde{\nu}_i)^R(\widetilde{\nu}^c_j)^R} &= a_{\nu_{ij}} v_u - Y_{\nu_{ij}} \lambda_k v_d \nu^c_k - Y_{\nu_{ik}} \lambda_j v_d \nu^c_k + 2Y_{\nu_{ik}} \kappa_{jlk} v_u \nu^c_l \\ &\quad + Y_{\nu_{ij}} Y_{\nu_{kl}} \nu_k \nu^c_l + Y_{\nu_{il}} Y_{\nu_{kj}} \nu_k \nu^c_l \ , \end{aligned} \tag{A.10}$$

$$\begin{aligned} M^2_{(\widetilde{\nu}^c_i)^R(\widetilde{\nu}^c_j)^R} &= m^2_{\widetilde{\nu}^c_{ij}} + 2a_{\kappa_{ijk}} \nu^c_k - 2\lambda_k \kappa_{ijk} v_d v_u + 2\kappa_{ijk} \kappa_{lmk} \nu^c_l \nu^c_m \\ &\quad + 4\kappa_{ilk} \kappa_{jmk} \nu^c_l \nu^c_m + \lambda_i \lambda_j (v_d^2 + v_u^2) + 2Y_{\nu_{lk}} \kappa_{ijk} v_u \nu_l \\ &\quad - (Y_{\nu_{kj}} \lambda_i + Y_{\nu_{ki}} \lambda_j) v_d \nu_k + Y_{\nu_{ki}} Y_{\nu_{kj}} v_u^2 + Y_{\nu_{ki}} Y_{\nu_{lj}} \nu_k \nu_l \ . \end{aligned} \tag{A.11}$$

Then the mass eingenvectors are

$$\mathbf{h}_\alpha = R^h_{\alpha\beta} \mathbf{h'}_\beta \tag{A.12}$$

with the diagonal mass matrix

$$(M^{\rm diag}_{h_{\alpha\beta}})^2 = R^h_{\alpha\gamma} M^2_{h_{\gamma\delta}} R^h_{\beta\delta} \ . \tag{A.13}$$

## A.2 CP-odd neutral scalars

In the unrotated basis $\mathbf{P'}_\alpha = \left(P_d, P_u, (\widetilde{\nu}_i^c)^I, (\widetilde{\nu}_i)^I\right)$ we have

$$V_{\text{quadratic}} = \frac{1}{2}\mathbf{P'}_\alpha M^2_{P_{\alpha\beta}} \mathbf{P'}_\beta + ... \tag{A.14}$$

Below we give the expressions for the independent cofficients of $M^2_{P_{\alpha\beta}}$

$$M^2_{P_dP_d} = m^2_{H_d} + \frac{G^2}{4}(v_d^2 - v_u^2 + \nu_i\nu_i) + \lambda_i\lambda_j\nu_i^c\nu_j^c + \lambda_i\lambda_i v_u^2 \ , \tag{A.15}$$

$$\begin{aligned} M^2_{P_uP_u} = m^2_{H_u} + \frac{G^2}{4}(v_u^2 - v_d^2 - \nu_i\nu_i) + \lambda_i\lambda_j\nu_i^c\nu_j^c + \lambda_i\lambda_i v_d^2 \\ -2Y_{\nu_{ij}}\lambda_j v_d\nu_i + Y_{\nu_{ik}}Y_{\nu_{ij}}\nu_k^c\nu_j^c + Y_{\nu_{ik}}Y_{\nu_{jk}}\nu_i\nu_j \ , \end{aligned} \tag{A.16}$$

$$M^2_{P_dP_u} = a_{\lambda_i}\nu_i^c + \lambda_k\kappa_{ijk}\nu_i^c\nu_j^c \ , \tag{A.17}$$

$$M^2_{P_d(\widetilde{\nu}_i^c)^I} = a_{\lambda_i}v_u - 2\lambda_k\kappa_{ijk}v_u\nu_j^c - Y_{\nu_{ji}}\lambda_k\nu_k^c\nu_j + Y_{\nu_{jk}}\lambda_i\nu_k^c\nu_j \ , \tag{A.18}$$

$$M^2_{P_d(\widetilde{\nu}_i)^I} = -Y_{\nu_{ij}}\lambda_j v_u^2 - Y_{\nu_{ij}}\lambda_k\nu_k^c\nu_j^c \ , \tag{A.19}$$

$$M^2_{P_u(\widetilde{\nu}_i^c)^I} = a_{\lambda_i}v_d - a_{\nu_{ji}}\nu_j - 2\lambda_k\kappa_{ilk}v_d\nu_l^c + 2Y_{\nu_{jk}}\kappa_{ilk}\nu_j\nu_l^c \ , \tag{A.20}$$

$$M^2_{P_u(\widetilde{\nu}_i)^I} = -a_{\nu_{ij}}\nu_j^c - Y_{\nu_{ik}}\kappa_{ljk}\nu_l^c\nu_j^c \ , \tag{A.21}$$

$$M^2_{(\widetilde{\nu}_i)^I(\widetilde{\nu}_j)^I} = m^2_{\widetilde{L}_{ij}} + \frac{1}{4}G^2(\nu_k\nu_k + v_d^2 - v_u^2)\delta_{ij} + Y_{\nu_{ik}}Y_{\nu_{jk}}v_u^2 + Y_{\nu_{ik}}Y_{\nu_{jl}}\nu_k^c\nu_l^c \ , \tag{A.22}$$

$$\begin{aligned} M^2_{(\widetilde{\nu}_i)^I(\widetilde{\nu}_j^c)^I} = &- a_{\nu_{ij}}v_u - Y_{\nu_{ik}}\lambda_j v_d\nu_k^c - Y_{\nu_{ij}}Y_{\nu_{lk}}\nu_l\nu_k^c + Y_{\nu_{ik}}Y_{\nu_{lj}}\nu_l\nu_k^c \\ &+ Y_{\nu_{ij}}\lambda_k v_d\nu_k^c + 2Y_{\nu_{il}}\kappa_{jlk}v_u\nu_k^c \ , \end{aligned} \tag{A.23}$$

$$\begin{aligned} M^2_{(\widetilde{\nu}_i^c)^I(\widetilde{\nu}_j^c)^I} = &\ m^2_{\widetilde{\nu}^c_{ij}} - 2a_{\kappa_{ijk}}\nu_k^c + 2\lambda_k\kappa_{ijk}v_dv_u - 2\kappa_{ijk}\kappa_{lmk}\nu_l^c\nu_m^c \\ &+ 4\kappa_{imk}\kappa_{ljk}\nu_l^c\nu_m^c + \lambda_i\lambda_j(v_d^2 + v_u^2) - (Y_{\nu_{ki}}\lambda_j + Y_{\nu_{kj}}\lambda_i)v_d\nu_k \\ &- 2Y_{\nu_{lk}}\kappa_{ijk}v_u\nu_l + Y_{\nu_{ki}}Y_{\nu_{kj}}v_u^2 + Y_{\nu_{li}}Y_{\nu_{kj}}\nu_k\nu_l \ . \end{aligned} \tag{A.24}$$

Then the mass eingenvectors are

$$\mathbf{P}_\alpha = R^P_{\alpha\beta}\mathbf{P'}_\beta \ , \tag{A.25}$$

with the diagonal mass matrix

$$(M^{\text{diag}}_{P_{\alpha\beta}})^2 = R^P_{\alpha\gamma}M^2_{P_{\gamma\delta}}R^P_{\beta\delta} \ . \tag{A.26}$$

## A.3 Charged scalars

Let us first recall that, due to the breaking of R-parity, the charged Higgses are mixed with the charged sleptons. We give here the mass matrix coefficients for the charged scalars which follows from the quadratic term in the potential

$$V_{\text{quadratic}} = \mathbf{S'}^{-}_{\alpha} M^2_{s^{\pm}_{\alpha\beta}} \mathbf{S'}^{+}_{\beta} \ . \tag{A.27}$$

The unrotated charged scalars are $\mathbf{S'}^{+}_{\alpha} = (H_d^+, H_u^+, \tilde{e}_L^+, \tilde{\mu}_L^+, \tilde{\tau}_L^+, \tilde{e}_R^+, \mu_R^+, \tau_R^+)$, and

$$\begin{aligned} M^2_{H_d H_d} &= m^2_{H_d} + \frac{1}{2} g_2^2 ({v_u}^2 - \nu_i \nu_i) + \frac{G^2}{4}(\nu_i \nu_i + v_d^2 - v_u^2) \\ &\quad + \lambda_i \lambda_j \nu_i^c \nu_j^c + Y_{e_{ik}} Y_{e_{jk}} \nu_i \nu_j \end{aligned} \tag{A.28}$$

$$\begin{aligned} M^2_{H_u H_u} &= m^2_{H_u} + \frac{1}{2} g_2^2 (v_d^2 + \nu_i \nu_i) - \frac{G^2}{4}(v_i v_i + v_d^2 - v_u^2) \\ &\quad + \lambda_i \lambda_j \nu_i^c \nu_j^c + Y_{\nu_{ij}} Y_{\nu_{ik}} \nu_j^c \nu_k^c \end{aligned} \tag{A.29}$$

$$M^2_{H_d H_u} = a_{\lambda_i} \nu_i^c + \frac{1}{2} g_2^2 v_d v_u - \lambda_i \lambda_i v_d v_u + \lambda_k \kappa_{ijk} \nu_i^c \nu_j^c + Y_{\nu_{ij}} \lambda_j v_u \nu_i \tag{A.30}$$

$$\begin{aligned} M^2_{\tilde{e}_{L_i} \tilde{e}_{L_j}} &= m^2_{\tilde{L}_{ji}} + \frac{g_2^2}{2}(-\nu_k \nu_k - v_d^2 + v_u^2)\delta_{ij} + \frac{1}{2} g_2^2 \nu_i \nu_j \\ &\quad + \frac{1}{4} G^2 (\nu_k \nu_k + v_d^2 - v_u^2)\delta_{ij} + Y_{\nu_{il}} Y_{\nu_{jk}} \nu_l^c \nu_k^c + Y_{e_{il}} Y_{e_{jl}} v_d^2 \end{aligned} \tag{A.31}$$

$$M^2_{\tilde{e}_{L_i} \tilde{e}_{R_j}} = a_{e_{ij}} v_d - Y_{e_{ij}} \lambda_k v_u \nu_k^c \tag{A.32}$$

$$M^2_{\tilde{e}_{R_j} \tilde{e}_{L_i}} = M^2_{\tilde{e}_{L_i} \tilde{e}_{R_j}} \tag{A.33}$$

$$M^2_{\tilde{e}_{R_i} \tilde{e}_{R_j}} = m^2_{\tilde{e}^c_{ij}} + \frac{g_1^2}{2}(-\nu_k \nu_k - v_d^2 + v_u^2)\delta_{ij} + Y_{e_{ki}} Y_{e_{kj}} v_d^2 + Y_{e_{li}} Y_{e_{kj}} \nu_k \nu_l \tag{A.34}$$

$$M^2_{\tilde{e}_{L_i} H_d} = \frac{g_2^2}{2} v_d \nu_i - Y_{\nu_{ij}} \lambda_k \nu_k^c \nu_j^c - Y_{e_{ij}} Y_{e_{kj}} v_d \nu_k \tag{A.35}$$

$$M^2_{\widetilde{e}_{L_i}H_u} = -a_{\nu_{ij}}\nu^c_j + \frac{g_2^2}{2}v_u\nu_i - Y_{\nu_{ij}}\kappa_{ljk}\nu^c_l\nu^c_k + Y_{\nu_{ij}}\lambda_j v_d v_u - Y_{\nu_{ik}}Y_{\nu_{kj}}v_u\nu_j \tag{A.36}$$

$$M^2_{\widetilde{e}_{R_i}H_d} = -a_{e_{ji}}\nu_j - Y_{e_{ki}}Y_{\nu_{kj}}v_u\nu^c_j \tag{A.37}$$

$$M^2_{\widetilde{e}_{R_i}H_u} = -Y_{e_{ki}}(\lambda_j\nu_k\nu^c_j + Y_{\nu_{kj}}v_d\nu^c_j)\ , \tag{A.38}$$

where $a_{e_{ij}} \equiv (A_eY_e)_{ij}$. Then the mass eigenvectors are

$$\mathbf{S}^{\pm}_{\alpha} = R^{s^{\pm}}_{\alpha\beta}\mathbf{S'}^{\pm}_{\beta}\ , \tag{A.39}$$

with the diagonal mass matrix

$$(M^{\rm diag}_{s^{\pm}})^2_{\alpha\beta} = R^{s^{\pm}}_{\alpha\gamma}M^2_{s^{\pm}_{\gamma\delta}}R^{s^{\pm}}_{\beta\delta}\ . \tag{A.40}$$

## A.4 Squarks

In the unrotated basis, $\widetilde{u'}_i = (\widetilde{u}_{L_i}, \widetilde{u}^*_{R_i})$ and $\widetilde{d'}_i = (\widetilde{d}_{L_i}, \widetilde{d}^*_{R_i})$, we get

$$V_{\rm quadratic} = \frac{1}{2}\widetilde{u'}^{\dagger}M^2_{\widetilde{u}}\ \widetilde{u'} + \frac{1}{2}\widetilde{d'}^{\dagger}M^2_{\widetilde{d}}\ \widetilde{d'}\ , \tag{A.41}$$

where

$$M^2_{\widetilde{q}_{ij}} = \begin{pmatrix} M^2_{\widetilde{q}_{L_iL_j}} & M^2_{\widetilde{q}_{L_iR_j}} \\ M^2_{\widetilde{q}_{R_iL_j}} & M^2_{\widetilde{q}_{R_iR_j}} \end{pmatrix}\ , \tag{A.42}$$

with $\widetilde{q} = (\widetilde{u'}, \widetilde{d'})$. The blocks are different for up and down quarks, and we have

$$\begin{aligned}
M^2_{\widetilde{u}_{L_iL_j}} &= m^2_{\widetilde{Q}_{ij}} + \frac{1}{6}(\frac{3g_2^2}{2} - \frac{g_1^2}{2})(v_d^2 - v_u^2 + \nu_k\nu_k) + Y_{u_{ik}}Y_{u_{jk}}v_u^2\ , \\
M^2_{\widetilde{u}_{R_iR_j}} &= m^2_{\widetilde{u}_{ij}} + \frac{g_1^2}{3}(v_d^2 - v_u^2 + \nu_k\nu_k) + Y_{u_{ki}}Y_{u_{kj}}v_u^2\ , \\
M^2_{\widetilde{u}_{L_iR_j}} &= a_{u_{ij}}v_u - Y_{u_{ij}}\lambda_k v_d\nu^c_k + Y_{\nu_{lk}}Y_{u_{ij}}\nu_l\nu^c_k\ , \\
M^2_{\widetilde{u}_{L_iR_j}} &= m^2_{\widetilde{u}_{R_jL_i}}\ ,
\end{aligned} \tag{A.43}$$

and

$$\begin{aligned} M^2_{\widetilde{d}_{L_i L_j}} &= m^2_{\widetilde{Q}_{ij}} - \frac{1}{6}(\frac{3g_2^2}{2} + \frac{g_1^2}{2})(v_d^2 - v_u^2 + \nu_k\nu_k) + Y_{d_{ik}}Y_{d_{jk}}v_d^2 \\ M^2_{\widetilde{d}_{R_i R_j}} &= m^2_{\widetilde{d}_{ij}} - \frac{g_1^2}{6}(v_d^2 - v_u^2 + \nu_k\nu_k) + Y_{d_{ik}}Y_{d_{jk}}v_d^2 \\ M^2_{\widetilde{d}_{L_i R_j}} &= a_{d_{ij}}v_d - Y_{d_{ij}}\lambda_k v_u \nu_k^c \\ M^2_{\widetilde{d}_{L_i R_j}} &= m^2_{\widetilde{d}_{R_j L_i}} \ , \end{aligned} \tag{A.44}$$

where $a_{u_{ij}} \equiv (A_u Y_u)_{ij}$ and $a_{d_{ij}} \equiv (A_d Y_d)_{ij}$. For the mass state $\widetilde{\mathbf{q}}_i$ we have

$$\widetilde{\mathbf{q}}_i = R^{\widetilde{q}}_{ij}\widetilde{q}_j \ , \tag{A.45}$$

with the diagonal mass matrix

$$(M^{\rm diag}_{\widetilde{q}})^2_{ij} = R^{\widetilde{q}}_{il} M^2_{\widetilde{q}_{lk}} R^{\widetilde{q}}_{jk} \ . \tag{A.46}$$

# Appendix B

# Higgs sector couplings

During this Thesis we have computed the couplings of the Higgs sector of the $\mu\nu$SSM. Here we only present the couplings needed for computing neutral Higgs-to-Higgs decays.

$h_\delta h_\epsilon h_\eta$ :

$$
\begin{aligned}
&\frac{\lambda_i\lambda_j}{\sqrt{2}}[\nu_i^c(\Pi_{\delta\epsilon\eta}^{11(j+2)}+\Pi_{\delta\epsilon\eta}^{22(j+2)})+v_d\Pi_{\delta\epsilon\eta}^{1(i+2)(j+2)}+v_u\Pi_{\delta\epsilon\eta}^{2(i+2)(j+2)}]\\
&+\frac{1}{\sqrt{2}}\lambda_l\lambda_l[v_d\Pi_{\delta\epsilon\eta}^{122}+v_u\Pi_{\delta\epsilon\eta}^{211}]-\frac{1}{\sqrt{2}}\lambda_l\kappa_{ljk}[v_d\Pi_{\delta\epsilon\eta}^{2(j+2)(k+2)}\\
&+v_u\Pi_{\delta\epsilon\eta}^{1(j+2)(k+2)}+2\nu_j^c\Pi_{\delta\epsilon\eta}^{12(k+2)}]\\
&+\sqrt{2}\kappa_{ljk}\kappa_{lbd}[\nu_j^c\Pi_{\delta\epsilon\eta}^{(k+2)(b+2)(d+2)}]+\frac{Y_{\nu_{ij}}Y_{\nu_{kl}}}{\sqrt{2}}[\nu_i\Pi_{\delta\epsilon\eta}^{(j+2)(l+2)(k+5)}+\nu_j^c\Pi_{\delta\epsilon\eta}^{(l+2)(i+5)(k+5)}]\\
&-\frac{1}{\sqrt{2}}Y_{\nu_{ij}}\lambda_k[\nu_i\Pi_{\delta\epsilon\eta}^{1(j+2)(k+2)}+\nu_j^c\Pi_{\delta\epsilon\eta}^{1(k+2)(i+5)}+\nu_k^c\Pi_{\delta\epsilon\eta}^{1(j+2)(i+5)}+v_d\Pi_{\delta\epsilon\eta}^{(j+2)(k+2)(i+5)}]\\
&+\frac{1}{\sqrt{2}}Y_{\nu_{lj}}Y_{\nu_{lm}}[v_u\Pi_{\delta\epsilon\eta}^{2(j+2)(m+2)}+\nu_j^c\Pi_{\delta\epsilon\eta}^{22(m+2)}]\\
&+\frac{1}{\sqrt{2}}Y_{\nu_{il}}Y_{\nu_{jl}}[v_u\Pi_{\delta\epsilon\eta}^{2(i+5)(j+5)}+\nu_i\Pi_{\delta\epsilon\eta}^{22(j+5)}]\\
&-\frac{1}{\sqrt{2}}\lambda_lY_{\nu_{il}}[2v_u\Pi_{\delta\epsilon\eta}^{12(i+5)}+v_d\Pi_{\delta\epsilon\eta}^{22(i+5)}+\nu_i\Pi_{\delta\epsilon\eta}^{122}]\\
&+\frac{1}{\sqrt{2}}\kappa_{ljk}Y_{\nu_{il}}[2\nu_j^c\Pi_{\delta\epsilon\eta}^{2(k+2)(i+5)}+v_u\Pi_{\delta\epsilon\eta}^{(j+2)(k+2)(i+5)}+\nu_i\Pi_{\delta\epsilon\eta}^{2(j+2)(k+2)}]\\
&-\frac{1}{\sqrt{2}}(A_\lambda\lambda)_i\Pi_{\delta\epsilon\eta}^{12(i+2)}+\frac{1}{\sqrt{2}}(A_\nu Y_\nu)_{ij}\Pi_{\delta\epsilon\eta}^{2(i+2)(j+5)}+\frac{1}{3\sqrt{2}}(A_\kappa\kappa)_{ijk}\Pi_{\delta\epsilon\eta}^{(i+2)(j+2)(k+2)}\\
&+\frac{g_1^2+g_2^2}{4\sqrt{2}}[\nu_i\Pi_{\delta\epsilon\eta}^{(i+5)(j+5)(j+5)}+\nu_i\Pi_{\delta\epsilon\eta}^{11(i+5)}-\nu_i\Pi_{\delta\epsilon\eta}^{22(i+5)}\\
&+v_d\Pi_{\delta\epsilon\eta}^{1(i+5)(i+5)}+v_d\Pi_{\delta\epsilon\eta}^{111}-v_d\Pi_{\delta\epsilon\eta}^{122}-v_u\Pi_{\delta\epsilon\eta}^{2(i+5)(i+5)}+v_u\Pi_{\delta\epsilon\eta}^{222}-v_u\Pi_{\delta\epsilon\eta}^{112}]\,, \qquad \text{(B.1)}
\end{aligned}
$$

where $b,d,i,j,k,l,m = 1,2,3$; $\alpha,\beta,\gamma,\delta,\epsilon,\eta = 1,...,8$, and

$$\begin{aligned}\Pi^{\alpha\beta\gamma}_{\delta\epsilon\eta} &= R^h_{\delta\alpha}R^h_{\epsilon\beta}R^h_{\eta\gamma} + R^h_{\delta\alpha}R^h_{\eta\beta}R^h_{\epsilon\gamma} + R^h_{\epsilon\alpha}R^h_{\delta\beta}R^h_{\eta\gamma} \\ &+R^h_{\epsilon\alpha}R^h_{\eta\beta}R^h_{\delta\gamma} + R^h_{\eta\alpha}R^h_{\delta\beta}R^h_{\epsilon\gamma} + R^h_{\eta\alpha}R^h_{\epsilon\beta}R^h_{\delta\gamma}\ .\end{aligned} \tag{B.2}$$

$h_\delta P_\epsilon P_\eta$ :

$$\begin{aligned}
&\frac{\lambda_i\lambda_j}{\sqrt{2}}[\nu^c_i(\Pi^{(j+2)11}_{\delta\epsilon\eta} + \Pi^{(j+2)22}_{\delta\epsilon\eta}) + v_d\Pi^{1(i+2)(j+2)}_{\delta\epsilon\eta} + v_u\Pi^{2(i+2)(j+2)}_{\delta\epsilon\eta}] \\
&+\frac{1}{\sqrt{2}}\lambda_l\lambda_l[v_d\Pi^{122}_{\delta\epsilon\eta} + v_u\Pi^{211}_{\delta\epsilon\eta}] \\
&+\frac{1}{\sqrt{2}}\lambda_l\kappa_{ljk}[v_d(\Pi^{2(j+2)(k+2)}_{\delta\epsilon\eta} - 2\Pi^{(j+2)2(k+2)}_{\delta\epsilon\eta}) + v_u(\Pi^{1(j+2)(k+2)}_{\delta\epsilon\eta} - 2\Pi^{(j+2)1(k+2)}_{\delta\epsilon\eta}) \\
&+2\nu^c_j(\Pi^{(k+2)12}_{\delta\epsilon\eta} - \Pi^{12(k+2)}_{\delta\epsilon\eta} - \Pi^{21(k+2)}_{\delta\epsilon\eta})] \\
&+\sqrt{2}\kappa_{ljk}\kappa_{lbd}[-\nu^c_j\Pi^{(k+2)(b+2)(d+2)}_{\delta\epsilon\eta} + 2\nu^c_j\Pi^{(b+2)(k+2)(d+2)}_{\delta\epsilon\eta}] \\
&-\frac{\lambda_l Y_{\nu_{il}}}{\sqrt{2}}[v_d\Pi^{(i+5)22}_{\delta\epsilon\eta} + \nu_i\Pi^{122}_{\delta\epsilon\eta} + 2v_u\Pi^{21(i+5)}_{\delta\epsilon\eta}] \\
&+\frac{\kappa_{ljk}Y_{\nu_{il}}}{\sqrt{2}}[2\nu^c_j\Pi^{2(k+2)(i+5)}_{\delta\epsilon\eta} + 2\nu^c_j\Pi^{(i+5)2(k+2)}_{\delta\epsilon\eta} - 2\nu^c_j\Pi^{(k+2)2(i+5)}_{\delta\epsilon\eta} + 2v_u\Pi^{(j+2)(i+5)(k+2)}_{\delta\epsilon\eta} \\
&-v_u\Pi^{(i+5)(j+2)(k+2)}_{\delta\epsilon\eta} + 2\nu_i\Pi^{(j+2)2(k+2)}_{\delta\epsilon\eta} - \nu_i\Pi^{2(j+2)(k+2)}_{\delta\epsilon\eta}] \\
&-\frac{Y_{\nu_{ij}\lambda_k}}{\sqrt{2}}[-\nu_i\Pi^{(j+2)(k+2)1}_{\delta\epsilon\eta} + \nu_i\Pi^{(k+2)(j+2)1}_{\delta\epsilon\eta} + \nu_i\Pi^{1(k+2)(j+2)}_{\delta\epsilon\eta} \\
&-\nu^c_j\Pi^{(i+5)(k+2)1}_{\delta\epsilon\eta} - \nu^c_j\Pi^{(k+2)(i+5)1}_{\delta\epsilon\eta} \\
&+\nu^c_j\Pi^{1(k+2)(i+5)}_{\delta\epsilon\eta} - \nu^c_k\Pi^{1(i+5)(j+2)}_{\delta\epsilon\eta} + \nu^c_k\Pi^{(i+5)1(j+2)}_{\delta\epsilon\eta} + \nu^c_k\Pi^{(j+2)1(i+5)}_{\delta\epsilon\eta} - v_d\Pi^{(k+2)(i+5)(j+2)}_{\delta\epsilon\eta} \\
&+v_d\Pi^{(j+2)(k+2)(i+5)}_{\delta\epsilon\eta} + v_d\Pi^{(i+5)(j+2)(k+2)}_{\delta\epsilon\eta}] \\
&+\frac{Y_{\nu_{ij}}Y_{\nu_{kl}}}{\sqrt{2}}[-\nu_i\Pi^{(j+2)(k+5)(l+2)}_{\delta\epsilon\eta} + \nu_i\Pi^{(l+2)(j+2)(k+5)}_{\delta\epsilon\eta} \\
&+\nu_i\Pi^{(k+5)(l+2)(j+2)}_{\delta\epsilon\eta} - \nu^c_j\Pi^{(i+5)(k+5)(l+2)}_{\delta\epsilon\eta} + \nu^c_j\Pi^{(k+5)(i+5)(l+2)}_{\delta\epsilon\eta} + \nu^c_j\Pi^{(l+2)(k+5)(i+5)}_{\delta\epsilon\eta}] \\
&+\frac{Y_{\nu_{lj}}Y_{\nu_{lm}}}{\sqrt{2}}[v_u\Pi^{2(j+2)(m+2)}_{\delta\epsilon\eta} + \nu^c_j\Pi^{(m+2)22}_{\delta\epsilon\eta}] + \frac{Y_{\nu_{il}}Y_{\nu_{jl}}}{\sqrt{2}}[v_u\Pi^{2(i+5)(j+5)}_{\delta\epsilon\eta} + \nu_i\Pi^{(j+5)22}_{\delta\epsilon\eta}] \\
&+\frac{(A_\lambda\lambda)_i}{\sqrt{2}}[\Pi^{(12(i+2))}_{\delta\epsilon\eta} + \Pi^{21(i+2)}_{\delta\epsilon\eta} + \Pi^{(i+2)12}_{\delta\epsilon\eta}] - \frac{(A_\nu Y_\nu)_{ij}}{\sqrt{2}}[\Pi^{2(i+5)(j+2)}_{\delta\epsilon\eta} + \Pi^{(i+5)2(j+2)}_{\delta\epsilon\eta} \\
&+\Pi^{(i+2)2(j+5)}_{\delta\epsilon\eta}] - \frac{(A_\kappa\kappa)_{ijk}}{\sqrt{2}}\Pi^{(i+2)(j+2)(k+2)}_{\delta\epsilon\eta} + \frac{g_1^2+g_2^2}{4\sqrt{2}}[\nu_i\Pi^{(i+5)(j+5)(j+5)}_{\delta\epsilon\eta} + \nu_i\Pi^{(i+5)11}_{\delta\epsilon\eta} \\
&-\nu_i\Pi^{(i+5)22}_{\delta\epsilon\eta} + v_d(\Pi^{1(i+5)(i+5)}_{\delta\epsilon\eta} + \Pi^{111}_{\delta\epsilon\eta} - \Pi^{122}_{\delta\epsilon\eta}) + v_u(\Pi^{222}_{\delta\epsilon\eta} - \Pi^{211}_{\delta\epsilon\eta} - \Pi^{2(i+5)(i+5)}_{\delta\epsilon\eta})]\ ,
\end{aligned} \tag{B.3}$$

where $b,d,i,j,k,l,m = 1,2,3$; $\alpha,\beta,\gamma,\delta = 1,...,8$; $\epsilon,\eta = 1,...,7$, and

$$\Pi^{\alpha\beta\gamma}_{\delta\epsilon\eta} = R^h_{\delta\alpha}(R^P_{\epsilon\beta}R^P_{\eta\gamma} + R^P_{\eta\beta}R^P_{\epsilon\gamma})\ . \tag{B.4}$$

# Bibliography


[1] D. E. López-Fogliani and C. Muñoz, *Phys. Rev. Lett.* **97** (2006) 041801 [arXiv:hep-ph/0508297].

[2] C. Muñoz, unpublished notes (1994).

[3] S. L. Glashow, Nucl. Phys. **22** (1961) 579; M. Gell-Mann, Phys. Lett. **8** (1964) 214; S. Weinberg, Phys. Rev. Lett. **19** (1967) 1264; A. Salam, *In the Proceedings of 8th Nobel Symposium, Lerum, Sweden, 19-25 May 1968, pp 367-377.*

[4] S. Weinberg, Phys. Rev. D **13** (1976) 974; S. Weinberg, Phys. Rev. D **19** (1979) 1277; E. Gildener, Phys. Rev. D **14** (1976) 1667. L. Susskind, Phys. Rev. D **20** (1979) 2619.

[5] For reviews or text books, see for example H.P. Nilles, *Phys. Rep.* **110** (1984) 1; H.E. Haber and G.L. Kane, *Phys. Rep.* **117** (1985) 75; J. Bagger and J. Wess, JHU-TIPAC-9009. *Supersymmetry and Supergravity*, 2nd. edition (Princeton University Press, Princeton, 1992); H. Baer and X. Tata, *Cambridge, UK: Univ. Pr. (2006) 537 p.*

[6] C. Munoz, arXiv:0705.2007 [hep-ph].

[7] S. P. Martin, "A Supersymmetry primer," arXiv:hep-ph/9709356.

[8] J. E. Kim and H. P. Nilles, *Phys. Lett.* **B138** (1984) 150.

[9] Y. Fukuda *al.* [Super-Kamiokande collaboration], *Phys. Rev. Lett.* **81** (1998) 1562 [arXiv:hep-ex/9807003]; Q.R. Ahmad *et al.* [SNO collaboration] , *Phys. Rev. Lett.* **89** (2002) 011301 [arXiv:nucl-ex/0204008]; K. Eguchi *et al.* [KamLAND collaboration], *Phys. Rev. Lett.* **90** (2003) 021802 [arXiv:hep-ex/0212021].

[10] S. Dimopoulos and H. Georgi, Nucl. Phys. B **193** (1981) 150; N. Sakai, Z. Phys. C **11** (1981) 153; N. Sakai and T. Yanagida, Nucl. Phys. B **197**

(1982) 533; H. P. Nilles and S. Raby, Nucl. Phys. B **198** (1982) 102; S. Dimopoulos, S. Raby and F. Wilczek, Phys. Lett. B **112** (1982) 133.

[11] K. Y. Choi, D. E. Lopez-Fogliani, C. Munoz and R. R. de Austri, JCAP **1003** (2010) 028 [arXiv:0906.3681 [hep-ph]].

[12] G. A. Gomez-Vargas, M. Fornasa, F. Zandanel, A. J. Cuesta, C. Munoz, F. Prada, G. Yepes, [arXiv:1110.3305 [astro-ph.HE]].

[13] Z. Maki, M. Nakagawa and S. Sakata, *Prog. Theor. Phys.* **28** (1962) 870.

[14] J. Fidalgo, D. E. Lopez-Fogliani, C. Munoz and R. Ruiz de Austri, JHEP **0908** (2009) 105 [arXiv:0904.3112 [hep-ph]].

[15] J. Fidalgo, D. E. Lopez-Fogliani, C. Munoz and R. R. de Austri, JHEP **1110** (2011) 020 [arXiv:1107.4614 [hep-ph]].

[16] J. Fidalgo and C. Munoz, Submitted to JHEP [arXiv:1111.2836]

[17] H. Fritzsch, P. Minkowski, Phys. Lett. **B62** (1976) 72; P. Minkowski, Phys. Lett. B **67** (1977) 421; R. N. Mohapatra and G. Senjanovic, Phys. Rev. Lett. **44** (1980) 912; T. Yanagida, Conf. Proc. **C7902131** (1979) 95; M. Gell-Mann, P. Ramond and R. Slansky, in *Supergravity*, D. Freedman *et al.*, Editors, North-Holland, Amsterdam (1980); S. Glashow, in *Quarks and Leptons, Cargèse 1979*, M. Lévy *et al.*, Editors, Plenum (1980)

[18] F. Zwicky, Helv. Phys. Acta **6**, 110 (1933); D. N. Spergel *et al.* [WMAP Collaboration], Astrophys. J. Suppl. **170** (2007) 377 [arXiv:astro-ph/0603449].

[19] For reviews see for example E. Farhi and L. Susskind, Phys. Rept. **74** (1981) 277; K. D. Lane, arXiv:hep-ph/9401324.

[20] See e.g.: J. L. Hewett and M. Spiropulu, Ann. Rev. Nucl. Part. Sci. **52** (2002) 397 [arXiv:hep-ph/0205106]; C. Csaki, arXiv:hep-ph/0404096.

[21] For a review see M. Schmaltz, Nucl. Phys. Proc. Suppl. **117** (2003) 40 [arXiv:hep-ph/0210415].

[22] Yu. A. Golfand and E. P. Likhtman, JETP Lett. **13**, 323 (1971) [Pisma Zh. Eksp. Teor. Fiz. **13**, 452 (1971)]; D. V. Volkov and V. P. Akulov, JETP Lett. **16** (1972) 438 [Pisma Zh. Eksp. Teor. Fiz. **16** (1972) 621]; J. Wess and B. Zumino, Nucl. Phys. B **70** (1974) 39; For an historically view of SUSY see "The supersymmetric world: The beginning of the

theory", Eds. G.L. Kane and M. Shifman, World Scientific (2000) 271 p.

[23] E. Witten, Nucl. Phys. B **188** (1981) 513; R. K. Kaul, Phys. Lett. B **109** (1982) 19.

[24] P. Fayet, Phys. Lett. B **64** (1976) 159; P. Fayet, Phys. Lett. B **69** (1977) 489; P. Fayet, Phys. Lett. B **70** (1977) 461.

[25] S. R. Coleman and J. Mandula, Phys. Rev. **159** (1967) 1251.

[26] D. Z. Freedman, P. van Nieuwenhuizen and S. Ferrara, Phys. Rev. D **13** (1976) 3214; S. Deser and B. Zumino, Phys. Lett. B **62** (1976) 335.

[27] For a review, see: C. Muñoz, *Int. J. Mod. Phys.* **A19** (2004) 3093 [arXiv:hep-ph/0309346].

[28] For a review see C. Munoz, arXiv:hep-ph/9709329.

[29] P. Fayet, Nucl. Phys. B **90** (1975) 104; H. P. Nilles, M. Srednicki and D. Wyler, Phys. Lett. B **120** (1983) 346; J. M. Frere, D. R. T. Jones and S. Raby, Nucl. Phys. B **222** (1983) 11; J. P. Derendinger and C. A. Savoy, Nucl. Phys. B **237** (1984) 307; J. R. Ellis, J. F. Gunion, H. E. Haber, L. Roszkowski and F. Zwirner, Phys. Rev. D **39** (1989) 844; M. Drees, Int. J. Mod. Phys. A **4** (1989) 3635; U. Ellwanger, M. Rausch de Traubenberg and C. A. Savoy, Phys. Lett. B **315** (1993) 331 [arXiv:hep-ph/9307322]; P. N. Pandita, Phys. Lett. B **318** (1993) 338; S. F. King and P. L. White, Phys. Rev. D **52** (1995) 4183 [arXiv:hep-ph/9505326]; U. Ellwanger and C. Hugonie, Eur. Phys. J. C **13**, 681 (2000) [arXiv:hep-ph/9812427].

[30] L. J. Hall and I. Hinchliffe, Phys. Lett. B **112** (1982) 351; N. Oshimo and Y. Kizukuri, Prog. Theor. Phys. **71** (1984) 151; A. Aranda and C. D. Carone, Phys. Rev. D **63**, 075012 (2001) [arXiv:hep-ph/0012092]; A. E. Faraggi and M. Thormeier, Nucl. Phys. B **624**, 163 (2002) [arXiv:hep-ph/0109162]; A. Font, L. E. Ibanez and F. Quevedo, Phys. Lett. B **228** (1989) 79; A. H. Chamseddine and H. K. Dreiner, Nucl. Phys. B **447**, 195 (1995) [arXiv:hep-ph/9503454]; C. Coriano, A. E. Faraggi and M. Guzzi, Eur. Phys. J. C **53**, 421 (2008) [arXiv:0704.1256 [hep-ph]]; H. C. Cheng, B. A. Dobrescu and K. T. Matchev, Nucl. Phys. B **543**, 47 (1999) [arXiv:hep-ph/9811316]; J. Erler, Nucl. Phys. B **586**, 73 (2000) [arXiv:hep-ph/0006051]; E. Ma, Phys. Rev. Lett. **89**, 041801 (2002) [arXiv:hep-ph/0201083].

[31] M. Aoki and N. Oshimo, Phys. Rev. Lett. **84**, 5269 (2000) [arXiv:hep-ph/9907481]; M. Aoki and N. Oshimo, Phys. Rev. D **62**, 055013 (2000) [arXiv:hep-ph/0003286];

[32] See e.g., M. Hirsch and J.W.F. Valle, *New J. Phys.* **6** (2004) 76 [arXiv:hep-ph/0405015], and references therein.

[33] M. Hirsch, M.A. Diaz, W. Porod, J.C. Romao and J.W.F. Valle, *Phys. Rev.* **D62** (2000) 113008 [arXiv:hep-ph/0004115], Erratum-ibid. **D65** (2000) 119901.

[34] M. Hirsch, T. Kernreiter, W. Porod, JHEP **0301** (2003) 034. [hep-ph/0211446]; F. de Campos, O. J. P. Eboli, M. B. Magro, W. Porod, D. Restrepo, M. Hirsch, J. W. F. Valle, JHEP **0805** (2008) 048. [arXiv:0712.2156 [hep-ph]].

[35] J. Hisano, T. Moroi, K. Tobe, M. Yamaguchi and T. Yanagida, Phys. Lett. B **357** (1995) 579 [arXiv:hep-ph/9501407]; J. Hisano, T. Moroi, K. Tobe and M. Yamaguchi, Phys. Rev. D **53** (1996) 2442 [arXiv:hep-ph/9510309]; Y. Grossman and H. E. Haber, Phys. Rev. Lett. **78** (1997) 3438 [arXiv:hep-ph/9702421].

[36] For analyses of gravitino dark matter without R-parity, see: F. Takayama and M. Yamaguchi, *Phys. Lett.* **B485** (2000) 388 [arXiv:hep-ph/0005214]; M. Hirsch, W. Porod and D. Restrepo, *J. High Energy Phys.* **03** (2005) 062 [arXiv:hep-ph/0503059].

[37] J. R. Ellis, K. Enqvist, D. V. Nanopoulos, K. A. Olive, M. Quiros and F. Zwirner, Phys. Lett. B **176** (1986) 403; B. Rai and G. Senjanovic, Phys. Rev. D **49**, 2729 (1994) [arXiv:hep-ph/9301240]; S. A. Abel, S. Sarkar and P. L. White, Nucl. Phys. B **454**, 663 (1995) [arXiv:hep-ph/9506359].

[38] S. A. Abel, Nucl. Phys. B **480** (1996) 55 [arXiv:hep-ph/9609323]; C. Panagiotakopoulos and K. Tamvakis, Phys. Lett. B **446**, 224 (1999) [arXiv:hep-ph/9809475].

[39] A. Masiero and J. W. F. Valle, Phys. Lett. B **251** (1990) 273.

[40] N. Escudero, D. E. López-Fogliani, C. Muñoz and R. R. de Austri, *JHEP* **12** (2008) 099 [arXiv:0810.1507 [hep-ph]].

[41] J. R. Espinosa and M. Quiros, Phys. Rev. Lett. **81** (1998) 516 [arXiv:hep-ph/9804235]; Y. Daikoku and D. Suematsu, Prog. Theor. Phys. **104** (2000) 827 [arXiv:hep-ph/0003206];

[42] U. Ellwanger and C. Hugonie, Mod. Phys. Lett. A **22** (2007) 1581 [arXiv:hep-ph/0612133].

[43] P. Ghosh and S. Roy, JHEP **0904** (2009) 069 [arXiv:0812.0084 [hep-ph]].

[44] A. Bartl, M. Hirsch, S. Liebler, W. Porod and A. Vicente, JHEP **0905** (2009) 120 [arXiv:0903.3596 [hep-ph]].

[45] S. Liebler and W. Porod, arXiv:1106.2921 [hep-ph].

[46] P. Ghosh, P. Dey, B. Mukhopadhyaya and S. Roy, JHEP **1005** (2010) 087 [arXiv:1002.2705 [hep-ph]].

[47] P. Bandyopadhyay, P. Ghosh and S. Roy, arXiv:1012.5762 [hep-ph].

[48] Y. Farzan and J.W.F. Valle, *Phys. Rev. Lett.* **96** (2006) 011601 [arXiv:hep-ph/0509280].

[49] B. Mukhopadhyaya and R. Srikanth, *Phys. Rev.* **D74** (2006) 075001 [arXiv:hep-ph/0605109].

[50] D. J. H. Chung and A. J. Long, Phys. Rev. D **81** (2010) 123531 [arXiv:1004.0942 [hep-ph]].

[51] C. Munoz, arXiv:0909.5140 [hep-ph].

[52] F. J. Botella, G. C. Branco, M. Nebot and M.N. Rebelo, *Nucl. Phys.* **B 725** (2005) 155 [arXiv:hep-ph/0502133].

[53] B. Aubert *et al.* [BaBar Collaboration], Phys. Rev. Lett. **93** (2004) 131801 [arXiv:hep-ex/0407057].

[54] Y. Chao *et al.* [Belle Collaboration], Phys. Rev. Lett. **93**, 191802 (2004) [arXiv:hep-ex/0408100]; K. Abe *et. al.* [Belle Collaboration], arXiv:hep-ex/0411049.

[55] O. Lebedev, *Phys. Lett.* **B452** (1999) 294 [arXiv:hep-ph/9812501]; G.C. Branco, F. Kruger, J.C. Romao and A.M. Teixeira, *JHEP* **07** (2001) 027 [arXiv:hep-ph/0012318].

[56] H. Georgi, *Hadronic J.* **1** (1978) 155; M.A.B. Beg and H.-S. Tsao, *Phys. Rev. Lett.* **41** (1978) 278; R.N. Mohapatra and G. Senjanovic, *Phys. Lett.* **79B** (1978) 283; G. Segre and H.A. Weldon, *Phys. Rev. Lett.* **42** (1979) 1191; S. Barr and P. Langacker, *Phys. Rev. Lett.* **42** (1979) 1654; A. Nelson, *Phys. Lett.* **136B** (1984) 165; S.M. Barr, *Phys. Rev. Lett.* **53**

(1984) 329; *Phys. Rev.* **D30** (1984) 1805; S.M. Barr and A. Zee, *Phys. Rev. Lett.* **55** (1985) 2253; L. Lavoura, *Phys. Lett.* **B400** (1997) 152 [arXiv:hep-ph/9701221].

[57] G. C. Branco, D. Emmanuel-Costa and J.C. Romao, *Phys. Lett.* **B639** (2006) 661 [arXiv:hep-ph/0604110].

[58] A. Doff, C.A. de S.Pires and P.S. Rodrigues da Silva, *Phys. Rev.* **D74** (2006) 015014 [arXiv:hep-ph/0604021]; N. Sahu and S. Uma Sankar, *Nucl. Phys.* **B724** (2005) 329 [arXiv:hep-ph/0501069].

[59] See for example, H. Cheng, *Phys. Rept.* **158** (1988) 1; S.M. Barr and G. Segrè, *Phys. Rev.* **D48** (1993) 302; K.S. Babu and S.M. Barr, *Phys. Rev. Lett.* **72** (1994) 2831; G. C. Branco and R.N. Mohapatra, Phys. Lett. **B643** (2006) 115 [arXiv:hep-ph/0607271]; T. Ibrahim and P. Nath, *Rev. Mod. Phys.* **80** (2008) 577 [arXiv:0705.2008[hep-ph]], and references therein.

[60] N. Escudero, C. Muñoz and A.M. Teixeira, *Phys. Rev.* **D73** (2006) 055015 [arXiv:hep-ph/0512046].

[61] S. Abel and C. Muñoz, *JHEP* **02** (2003) 010 [arXiv:hep-ph/0212258]; N. Escudero, C. Muñoz and A.M. Teixeira, *JHEP* **07** (2006) 041 [arXiv:hep-ph/0512301].

[62] G. Branco, *Phys. Rev. Lett.* **44** (1980) 504; *Phys. Rev.* **D22** (1980) 201.

[63] M. Masip and A. Rasin, *Phys. Rev.* **D52** (1995) 3768 [arXiv:hep-ph/9506471]; *Nucl. Phys.* **B460** (1996) 449 [arXiv:hep-ph/9508365].

[64] M. Masip and A. Rasin, *Phys. Rev.* **D58** (1998) 035007 [arXiv:hep-ph/9803271].

[65] J. C. Romao, *Phys. Lett* **B287** (1986) 331.

[66] S. W. Ham, S. K. Oh and D. Son, *Phys. Rev.* **D66** (2002) 015008 [arXiv:hep-ph/0110183].

[67] G.L. Fogli, E. Lisi, A. Marrone, A. Melchiorri, A. Palazzo, A. M. Rotunno, P. Serra, J. Silk and A. Slosar, *Phys. Rev.* **D78** (2008) 033010 [arXiv:0805.2517 [hep-ph]], T. Schwetz, M. Tortola and J. W. F. Valle, New J. Phys. **13** (2011) 063004 [arXiv:1103.0734 [hep-ph]].

[68] S. F. King, arXiv:0712.1750 [physics.pop-ph].

[69] S. Antusch, J. Kersten, M. Lindner, M. Ratz and M. A. Schmidt, *JHEP* **03** (2005) 024 [arXiv:hep-ph/0501272].

[70] V. Barger, P. Huber, D. Marfatia and W. Winter, *Phys. Rev.* **D76** (2007) 053005 [arXiv:hep-ph/0703029]; H. Nunokawa, S. J. Parke and J.W.F. Valle, *Prog. Part. Nucl. Phys.* **60** (2008) 338 [arXiv:0710.0554[hep-ph]].

[71] D. Ayres *et al.* [NOvA collaboration], arXiv:hep-ex/0210005; arXiv:hep-ex/0503053.

[72] K. Hagiwara, N. Okamura and K.-i Senda, *Phys. Rev.* **D76** (2007) 093002 [arXiv:hep-ph/0607255].

[73] V. Barger, S. L. Glashow, P. Langacker and D. Marfatia, *Phys. Lett.* **B540** (2002) 247 [arXiv:hep-ph/0205290].

[74] J. R. Ellis, S. Ferrara and D. V. Nanopoulos, Phys. Lett. B **114** (1982) 231; J. Polchinski and M. B. Wise, Phys. Lett. B **125** (1983) 393; M. Dugan, B. Grinstein and L. J. Hall, Nucl. Phys. B **255** (1985) 413.

[75] Y. Kizukuri and N. Oshimo, Phys. Rev. D **45** (1992) 1806; Y. Kizukuri and N. Oshimo, Phys. Rev. D **46** (1992) 3025.

[76] T. Ibrahim and P. Nath, Phys. Rev. D **57** (1998) 478 [Erratum-ibid. D **58** (1998 ERRAT,D60,079903.1999 ERRAT,D60,119901.1999) 019901] [arXiv:hep-ph/9708456]; M. Brhlik, G. J. Good and G. L. Kane, Phys. Rev. D **59** (1999) 115004 [arXiv:hep-ph/9810457]; A. Bartl, T. Gajdosik, W. Porod, P. Stockinger and H. Stremnitzer, Phys. Rev. D **60** (1999) 073003 [arXiv:hep-ph/9903402].

[77] M. Frank, K. Huitu and T. Ruppell, Eur. Phys. J. C **52** (2007) 413 [arXiv:0705.4160 [hep-ph]].

[78] LEP Higgs Working Group, LHWG Note/2002-02.

[79] L.J. Hall and M. Suzuki, *Nucl. Phys.* **B231** (1984) 419; I.H. Lee, *Phys. Lett.* **B138** (1984) 121, *Nucl. Phys.* **B246** (1984) 120; S. Dawson, *Nucl. Phys.* **B261** (1985) 297.

[80] G. Abbiendi *et al.*, LEP Working Group for Higgs Boson Searches, *Phys. Lett.* **B565** (2003) 61 [arXiv:hep-ex/0306033].

[81] G. Abbiendi *et al.* [OPAL Collaboration], *Eur. Phys. J.* **C37** (2004) 49 [arXiv:hep-ex/0406057].

[82] G. Abdallah *et al.* [DELPHI Collaboration], *Eur. Phys. J.* **C38** (2004) 1 [arXiv:hep-ex/0410017].

[83] R. Dermisek and J. F. Gunion, *Phys. Rev.* **D73** (2006) 111701 [hep-ph/0510322], *Phys. Rev. Lett.* **95** (2005) 041801 [hep-ph/0502105].

[84] G. Abbiendi *et al.* [OPAL Collaboration], *Eur. Phys. J.* **C27** (2003) 311 [arXiv:hep-ex/0206022].

[85] G. Abbiendi *et al.* [OPAL Collaboration], *Eur. Phys. J.* **C27** (2003) 483 [arXiv:hep-ex/0209068].

[86] S. Schael *et al.* [ALEPH Collaboration], *JHEP* **05** (2010) 049 [arXiv:1003.0705 [hep-ex]].

[87] K. Hagiwara *et al.*, *Phys. Rev.* **D66** (2002) 010001; J. Abdallah *et al.* [DELPHI Collaboration], *Eur. Phys. J.* **C31** (2004) 421 [arXiv:hep-ex/0311019]; G. Abbiendi *et al.* [OPAL Collaboration], *Eur. Phys. J.* **C35** (2004) 1 [arXiv:hep-ex/0401026].

[88] C. Panagiotakopoulos and A. Pilaftsis, *Phys. Rev.* **D63** (2001) 055003 [arXiv:hep-ph/0008268].

[89] S. W. Ham, H. Genten, B. R. Kim and S. K. Oh, *Phys. Lett.* **B383** (1996) 179 [arXiv:hep-ph/9606361].

[90] U. Ellwanger and C. Hugonie, *Comput. Phys. Commun.* **175** (2006) 290 [arXiv:hep-ph/0508022].

[91] W. Porod, *Comput. Phys. Commun.* **153** (2003) 275 [arXiv:hep-ph/0301101].

[92] J. Abdallah *et al.*, LEP SUSY Working Group, http://lepsusy.web.cern.ch/lepsusy/

[93] K. Nakamura *et al.* [Particle Data Group], J. Phys. G **37** (2010) 075021.

[94] D. Buskulic *et al.* [ALEPH Collaboration], *Phys. Lett.* **B313** (1993) 312.

[95] LEP Higgs Working Group, LHWG Note 2001-06, arXiv:hep-ex/0107032.

[96] G. Abbiendi *et al.* [OPAL Collaboration], *Phys. Lett.* **B597** (2004) 11 [arXiv:hep-ex/0312042].

[97] LEP Higgs Working Group, LHWG Note 2001-07, arXiv:hep-ex/0107034.

[98] A. Belyaev, J. Pivarski, A. Safonov, S. Senkin, A. Tatarinov, Phys. Rev. **D81** (2010) 075021. [arXiv:1002.1956 [hep-ph]].

[99] M. Spira, [hep-ph/9510347].

[100] W. B. Atwood *et al.* [LAT Collaboration], Astrophys. J. **697** (2009) 1071 [arXiv:0902.1089 [astro-ph.IM]].

[101] See e.g.: W. Buchmuller, L. Covi, K. Hamaguchi, A. Ibarra and T. Yanagida, JHEP **0703** (2007) 037 [arXiv:hep-ph/0702184], and references therein.

[102] G. F. Giudice, R. Rattazzi, Phys. Rept. **322** (1999) 419-499. [hep-ph/9801271].

[103] L. E. Ibanez and G. G. Ross, Phys. Lett. B **260** (1991) 291; L. E. Ibanez and G. G. Ross, Nucl. Phys. B **368** (1992) 3; H. K. Dreiner, C. Luhn and M. Thormeier, Phys. Rev. D **73**, 075007 (2006) [arXiv:hep-ph/0512163].

[104] J. A. Casas, E. K. Katehou and C. Munoz, Nucl. Phys. B **317** (1989) 171; J. A. Casas and C. Munoz, Phys. Lett. B **212** (1988) 343.

[105] K. Kobayashi *et al.* [Super-Kamiokande Collaboration], Phys. Rev. D **72** (2005) 052007 [arXiv:hep-ex/0502026].

[106] F. Zwirner, Phys. Lett. B **132** (1983) 103; S. Dawson, Nucl. Phys. B **261** (1985) 297; R. Barbieri and A. Masiero, Nucl. Phys. B **267** (1986) 679; S. Dimopoulos and L. J. Hall, Phys. Lett. B **207** (1988) 210; V. D. Barger, G. F. Giudice and T. Han, Phys. Rev. D **40** (1989) 2987; R. M. Godbole, P. Roy and X. Tata, Nucl. Phys. B **401** (1993) 67 [arXiv:hep-ph/9209251]; G. Bhattacharyya and D. Choudhury, Mod. Phys. Lett. A **10** (1995) 1699 [arXiv:hep-ph/9503263].

[107] For reviews, see G. Bhattacharyya, Nucl. Phys. Proc. Suppl. **52A** (1997) 83 [arXiv:hep-ph/9608415]; H. K. Dreiner, arXiv:hep-ph/9707435; B. Allanach *et al.* [R parity Working Group Collaboration], arXiv:hep-ph/9906224; B. C. Allanach, A. Dedes and H. K. Dreiner, Phys. Rev. D **69** (2004) 115002 [Erratum-ibid. D **72** (2005) 079902] [arXiv:hep-ph/0309196]; M. Chemtob, Prog. Part. Nucl. Phys. **54** (2005) 71 [arXiv:hep-ph/0406029].

[108] R. Barbier *et al.*, arXiv:hep-ph/9810232; R. Barbier *et al.*, Phys. Rept. **420** (2005) 1 [arXiv:hep-ph/0406039].

[109] S. Weinberg, Phys. Rev. D **26** (1982) 287; J. R. Ellis, D. V. Nanopoulos and K. Tamvakis, Phys. Lett. B **121** (1983) 123; J. R. Ellis, J. S. Hagelin, D. V. Nanopoulos and K. Tamvakis, Phys. Lett. B **124** (1983) 484; R. Harnik, D. T. Larson, H. Murayama and M. Thormeier, Nucl. Phys. B **706**, 372 (2005) [arXiv:hep-ph/0404260].

[110] R. Kallosh, A. D. Linde, D. A. Linde and L. Susskind, Phys. Rev. D **52** (1995) 912 [arXiv:hep-th/9502069].

[111] LEPSUSYWG, ALEPH, DELPHI,L3 and OPAL experiments, note LEPSUSYWG/01-03.1(http://lepsusy.web.cern.ch/lepsusy/Welcome.html)

[112] G. F. Giudice and A. Masiero, Phys. Lett. B **206** (1988) 480.

[113] E. J. Chun, J. E. Kim and H. P. Nilles, Nucl. Phys. B **370** (1992) 105; J. A. Casas and C. Munoz, Phys. Lett. B **306** (1993) 288 [hep-ph/9302227].

[114] H. Georgi and S. Weinberg, Phys. Rev. D **17** (1978) 275; R. N. Mohapatra and D. P. Sidhu, Phys. Rev. D **18** (1978) 856; V. D. Barger and R. J. N. Phillips, Phys. Rev. D **18** (1978) 775; A. Davidson, Phys. Rev. D **20** (1979) 776; T. G. Rizzo, Phys. Rev. D **21** (1980) 1214; A. Masiero, Phys. Lett. B **93** (1980) 295; F. del Aguila and A. Mendez, Nucl. Phys. B **189** (1981) 212; S. M. Barr, Phys. Lett. B **128** (1983) 400.

[115] D. Suematsu and Y. Yamagishi, Int. J. Mod. Phys. A **10** (1995) 4521 [arXiv:hep-ph/9411239]; M. Cvetic and P. Langacker, Phys. Rev. D **54** (1996) 3570 [arXiv:hep-ph/9511378]; P. Langacker and J. Wang, Phys. Rev. D **58**, 115010 (1998) [arXiv:hep-ph/9804428]; H. C. Cheng, B. A. Dobrescu and K. T. Matchev, Phys. Lett. B **439** (1998) 301 [arXiv:hep-ph/9807246]; D. A. Demir, Phys. Rev. D **59** (1999) 015002 [arXiv:hep-ph/9809358]; J. Erler, P. Langacker and T. j. Li, Phys. Rev. D **66**, 015002 (2002) [arXiv:hep-ph/0205001].

[116] F. Abe *et al.* [CDF Collaboration], Phys. Rev. Lett. **79** (1997) 2192.

[117] G. C. Cho, Mod. Phys. Lett. A **15**, 311 (2000) [arXiv:hep-ph/0002128].

[118] M. Cvetic, D. A. Demir, J. R. Espinosa, L. L. Everett and P. Langacker, Phys. Rev. D **56** (1997) 2861 [Erratum-ibid. D **58** (1998) 119905] [arXiv:hep-ph/9703317].

[119] H. S. Lee, K. T. Matchev and T. T. Wang, Phys. Rev. D **77** (2008) 015016 [arXiv:0709.0763 [hep-ph]].

[120] See e.g.: M. Chemtob and P. Hosteins, Eur. Phys. J. C **68** (2010) 539 [arXiv:0909.4497 [hep-ph]], and references therein.

[121] C. Munoz, JHEP **0112** (2001) 015 [arXiv:hep-ph/0110381].

[122] S. Davidson, B. Campbell and D. C. Bailey, Phys. Rev. D **43** (1991) 2314; S. Chang, C. Coriano and A. E. Faraggi, Nucl. Phys. B **477**, 65 (1996) [arXiv:hep-ph/9605325].

[123] For a review, see, M. L. Perl, P. C. Kim, V. Halyo, E. R. Lee, I. T. Lee, D. Loomba and K. S. Lackner, Int. J. Mod. Phys. A **16**, 2137 (2001) [arXiv:hep-ex/0102033].

[124] D. J. H. Chung, E. W. Kolb and A. Riotto, Phys. Rev. D **60** (1999) 063504 [arXiv:hep-ph/9809453].

[125] D. E. Morrissey and J. D. Wells, Phys. Rev. D **74** (2006) 015008 [arXiv:hep-ph/0512019].